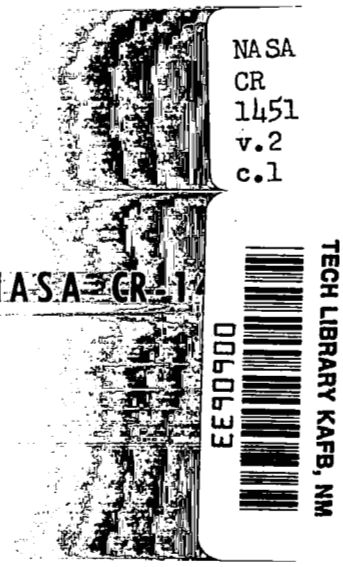

NASA CONTRACTOR REPORT

NASA CR-1452

ALTERNATOR AND VOLTAGE REGULATOR-EXCITER FOR A BRAYTON CYCLE SPACE POWER SYSTEM

II - Unbalanced Electromagnetic Forces

by J. E. Greenwell, E. F. Russell, and L. J. Yeager

Prepared by
GENERAL ELECTRIC COMPANY
Erie, Pa.
for Lewis Research Center

NATIONAL AERONAUTICS AND SPACE ADMINISTRATION • WASHINGTON, D. C. • MAY 1970

1. Report No.	2. Government Accession No.	3. Recipient's Catalog No.
NASA CR-1452		

4. Title and Subtitle	5. Report Date
ALTERNATOR AND VOLTAGE REGULATOR-EXCITER FOR A BRAYTON CYCLE SPACE POWER SYSTEM II - UNBALANCED ELECTROMAGNETIC FORCES	May 1970
	6. Performing Organization Code
7. Author(s) J. E. Greenwell, E. F. Russell, L. J. Yeager	8. Performing Organization Report No. A69-003 Vol. II
9. Performing Organization Name and Address General Electric Co. Erie, Pennsylvania	10. Work Unit No.
	11. Contract or Grant No. NAS 3-6013
	13. Type of Report and Period Covered Contractor Report
12. Sponsoring Agency Name and Address National Aeronautics and Space Administration Washington, D.C. 20546	14. Sponsoring Agency Code

15. Supplementary Notes

16. Abstract

The unbalanced magnetic forces in a homopolar inductor alternator due to rotor eccentricity were determined both analytically and experimentally. Analytic expressions consisting of cosinusoidal terms are given for forces in the X and Y axes of the stator. Forces were measured through the use of specially constructed end shields instrumented with strain gages. Output from the gages was displayed on an oscilloscope in the form of a Lissajous pattern. A correlation between measured and predicted forces is given.

17. Key Words (Suggested by Author(s))	18. Distribution Statement
	Unclassified - unlimited

19. Security Classif. (of this report)	20. Security Classif. (of this page)	21. No. of Pages	22. Price*
Unclassified	Unclassified	167	$3.00

*For sale by the Clearinghouse for Federal Scientific and Technical Information Springfield, Virginia 22151

TABLE OF CONTENTS

SECTION I

FOREWORD

The research described herein, which was conducted by General Electric Company of Erie, Pennsylvania under subcontract to Pratt and Whitney Aircraft Division of United Aircraft Corporation, was performed under NASA contract NAS 3-6013. The Project Manager for NASA was Mr. Henry B. Tryon, Space Power Systems Division, Lewis Research Center. The report was originally issued as General Electric report A69-003 Vol. II.

SECTION II

SUMMARY

The Brayton Cycle turboalternator will run on gas bearings, the design of which depends to a large extent on the unbalanced electromagnetic forces existing in the alternator as a result of eccentricity between the rotor and stator. Due to conflicting literature on the subject, and a need to have good design data, an analytical and experimental bearing force program was initiated to determine the nature and magnitude of the forces.

The analytical results consisted of equations made up of cosinusoidal terms for an X-axis and Y-axis fixed on the stator. The Y-axis equation produced a DC component and a large 2 per revolution term for the balanced load cases, and higher harmonic terms for the single phase loading and single phase short circuit cases. Similar terms appeared in the X-axis equation, but no DC component existed. Saturation reduced the force magnitude as expected. Forces predicted from the above equations were modified by dividing by the number of stator circuits to reflect a circuit effect.

Forces were measured through the use of specially constructed end shields instrumented with strain gages in both the X and Y axes. Output from the gages was passed through appropriate electronic equipment and displayed on an oscilloscope as a Lissajous pattern. The alternator was driven by an induction motor. The alternator and the motor were flange mounted onto a test stand which was isolated from surrounding vibration by vibration mounts.

The nature of the measured forces was as predicted, but the magnitude was significantly less. Further testing at the no load case revealed that the force reducing effect of the stator circuits and possibly the amortisseur winding was about twice as great as assumed. Differential saturation of the opposing stator teeth produced further reduction which, when factored in with the above circuit effect gave reasonable correlation between measured and predicted forces for the balanced load and single phase loading cases. The Lissajous pattern for the single phase short circuit case was very complex reflecting the higher harmonic content predicted, but the magnitude was significantly less due to time variant saturation and the aforementioned factors.

Recommendations for future work include investigations into stator circuit effect, amortisseur effect, and time variant saturation.

SECTION III

INTRODUCTION

The work covered in this report was done under subcontract PWASC 6013-2 to Pratt & Whitney Aircraft who served as Prime Contractor to NASA for contract NAS3-6013. NASA has envisioned the future need for large blocks of power for space applications, and one of the energy conversion schemes being investigated is the Brayton Cycle which includes rotating machinery as shown in Figure 1. This turboalternator uses argon gas as the working fluid and runs on hydrodynamic gas bearings to provide long life and eliminate the problem of working fluid contamination that would exist if conventional oil lubricated bearings were used. Since gas bearings have limited ability to carry large radial loads and operate with extremely small radial clearances, it became important to determine the nature and magnitude of the radial electromagnetic load for proper bearing design and to avoid bearing instability.

The alternator, in the turboalternator package, is capable of exerting very high radial forces due to unbalanced magnetic forces in the air gap if not designed properly.

With the centerline of the alternator rotor coincident with the centerline of its stator (uniform air gap), the unbalanced radial magnetic force should be zero. As the rotor is displaced from the stator centerline, the air gaps become unequal and the resulting changes in flux density cause the magnetic forces between rotor and stator to become unbalanced. The force between rotor and stator becomes higher on the side with small air gap and high flux density and lower on the side with the greater gap. The result is a net unbalanced radial force in the general direction of the rotor displacement. In order to more properly define the force, the problem was attacked from two directions, analytically and experimentally.

The analytical study produced equations which describe the force under various conditions of alternator loading and eccentricity direction. These equations contain the effects of rotor pole saliency, stator slotting, amortisseur slotting, armature reaction, and magnetic saturation. They are in the form of Fourier series which can readily be introduced as input to gas bearing stability computer programs. The effects of stator circuits and amortisseur reaction were not included in the analysis, but are recommended for future study; especially the stator circuits which appear to have a stronger force reducing capability than assumed.

In the experimental program, the Alternator Research Package was equipped with specially designed endshields and anti-friction bearings so that the bearing reactions could be measured. The forces developed at the air gap could then be calculated by moment summation. The endshields had necked-down portions which support the bearing housings. Strain gages on these supports gave an electrical readout of instantaneous bearing reactions. The alternator was driven from a separate induction motor rather than a turbine. Four sets of bearing housings were made. By changing bearing housings, the eccentricity of rotor with respect to stator could be varied from essentially zero to .006" (out of a .040" nominal air gap). Tests were staged by loading the alternator

at different KVA power outputs, different power factors and with balanced and unbalanced loads and shorts.

Detailed descriptions of the analytical procedure and experimental testing can be found in Sections IV and VII. The various Appendices cover related tests, analysis of problems encountered during the course of the testing, the actual test data, analytical derivations, and computer programs developed for the analysis.

BRAYTON CYCLE TURBOALTERNATOR
NAS 3-6013

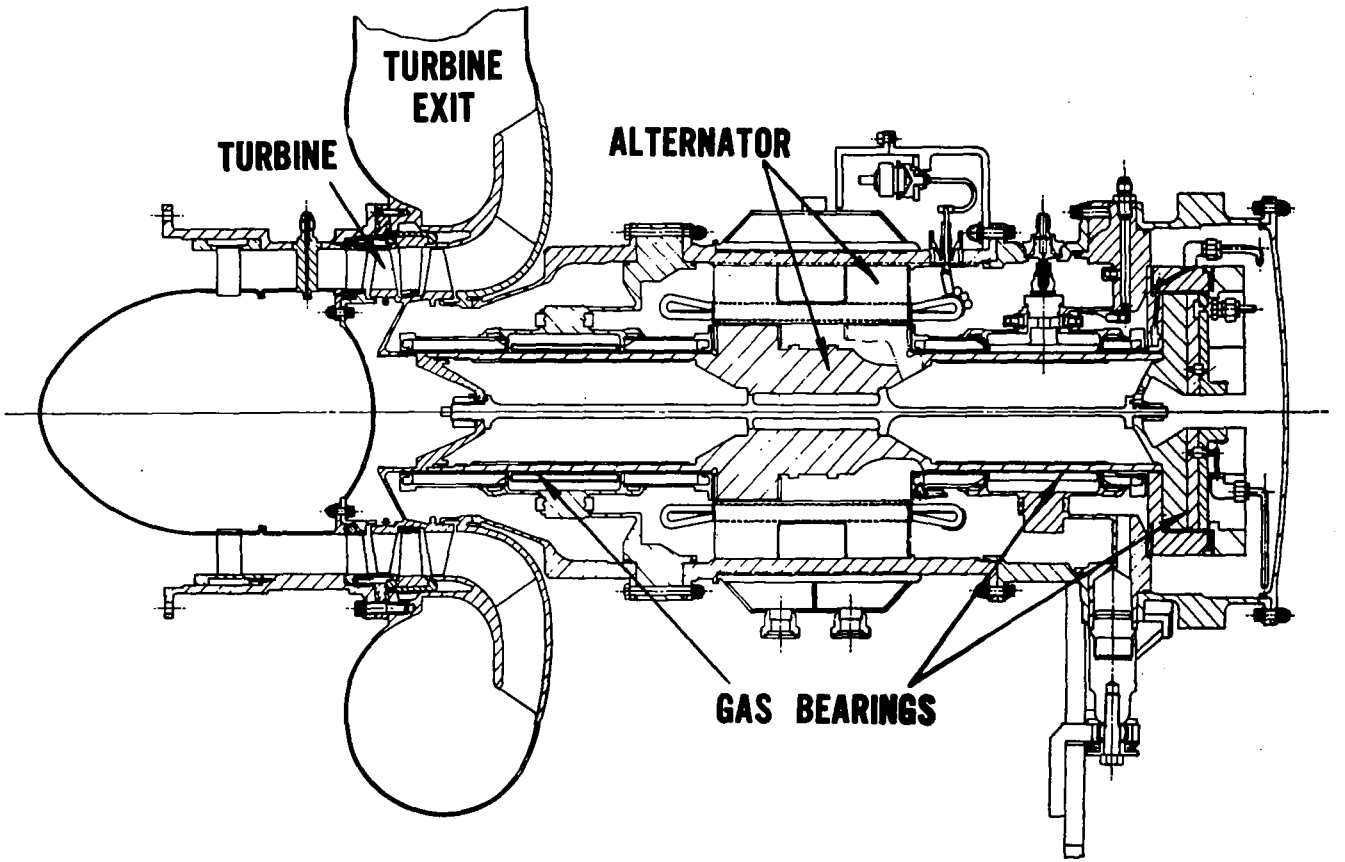

FIGURE 1

SECTION IV

Origin of the Force and Analytical Development

The likelihood of building a machine with a perfectly concentric rotor and stator is very small. The problem might be compared to that of placing a steel ball exactly between the poles of a horseshoe magnet so that it won't move when all restraint is taken away.

Consider the sketch below:

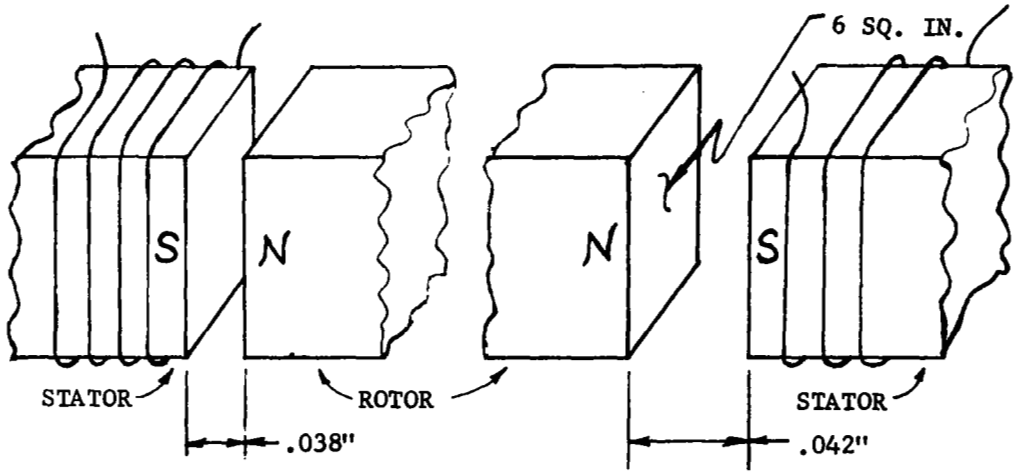

Assume that the above figure represents a .002" "error" in manufacturing so that one pole of the rotor on one end is closer to the stator than the other. For the above figure let the exciting magnetomotive force (MMF) be 635 amp turns and the surface area of each pole 6 sq. inches.

It can be shown that

$$F = \int \frac{\mathcal{B}^2}{72} dA$$

For the left gap

$$P_1 = \frac{\mu A}{1} = \frac{3.19 \times 6}{.038} = 505$$

$$\emptyset = P_1 \times MMF = 505 \times 635 = 320,675$$

$$\mathcal{B} = \frac{\emptyset}{A} = \frac{320,675}{6} = 53,500$$

Where:

F = Force in pounds

$\mathcal{B}$ = Flux density in K LINE/IN^2

A = Area in sq. inches

μ = Permeability of medium

l = Magnetic path length in inches

P_l = Permeance

ϕ = Flux in lines

$$F = \frac{28.6 \times 10^8 \times 6}{72 \times 10^6} = 237 \text{ lbs.}$$

For the right hand gap

$P_r = 455$

$\mathcal{B} = 48{,}100$ lines/in^2

$F = 193$ lbs. (right side)

This can be pictured vectorially as

or

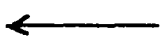

44 lbs.

So a shift of .002" in the spacing of the example gives a net 44 lb. pull to the left. This pull then arises from the difference in flux densities of the unequal air gaps which result from tolerance in the manufacturing process and assembly.

The 44 pounds of this example is roughly equivalent to the Brayton Cycle F_y calculated force of Fig. 3, Section VI when operating at 15 KVA, 8 P.F without a circuit reducing effect. The MMF of 635, the pole area of 6 in^2, and the air gap of .038" correspond to the Brayton Cycle Alternator for the stated load condition. Factoring in a circuit effect of 2 reduces the force to 22 pounds.

Since the two stator circuits are connected in parallel, a circulating current will flow reducing the flux and thus the force at the smaller gap and increasing these at the larger gap, yeilding a net reduction.

Analytical Development

The bearing forces experienced in an alternator are somewhat more complex than the previous example. The mmf's in an alternator stator are moving in time and space. If the load is balanced, the fundamental mmf is moving in synchronism with the rotor while the harmonics rotate backward or forward at some speed other than synchronous. If the load is unbalanced, large mmf waves moving in the backward direction (as referred to the rotor) are generated.

All of these interacting mmf's impressed across saturable steel and a changing air gap cause a non-uniformly distributed flux wave across the rotor poles. This flux wave modulated by the stator and rotor slot permeances is predictable. In most cases, the center or peak of the armature mmf's is out of line with the rotor direct axis and results in a maximum force displaced from the center of the rotor pole and the point of minimum air gap. Under unbalanced conditions, the angle between minimum air gap and maximum force may even be shifting with time.

Saturation further clouds the force picture. The ampere turns of mmf (both field and armature reaction) are relatively fixed in magnitude at a given point. The effective ampere turns varies as a function of the location around the machine while the permeance is also varying with location. Because of these factors the ratio between ampere turns in the iron and ampere turns in the gap varies from point to point around the machine.

The Brayton Cycle Bearing Force Analytical Study centers around the type of eccentricity shown below. The sketch represents an axial view of one end of the alternator and shows the stator bore and rotor outline.

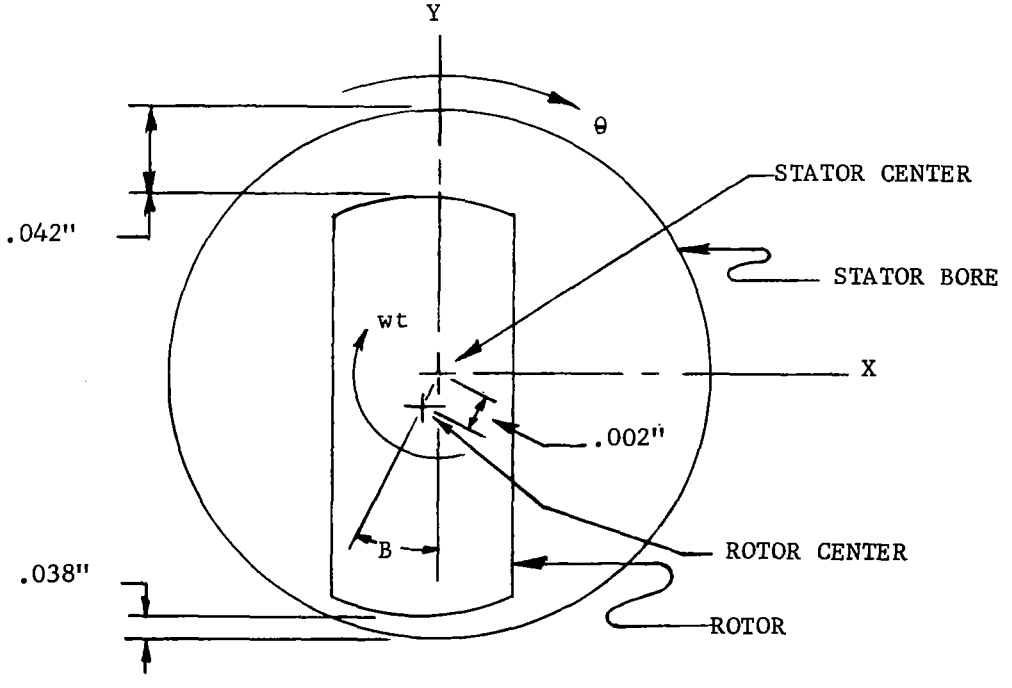

Illustrated:

Case where B = o, eccentricity = 0.002"*

All angles positive clockwise from Y axis (B from neg Y - axis)

The analytical development begins with the equation:

$$F = \int \frac{\mathcal{B}^2}{72} da \qquad \text{Eq \#1}$$

Where F is directed radially outward

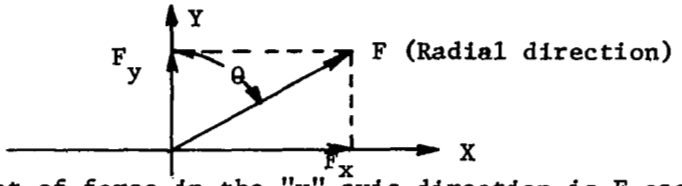

and the component of force in the "y" axis direction is F cos θ and the component of force in the "x" axis direction is F sin θ, as shown above.

In equation #1

$\mathcal{B}^2$ = (gap flux density)^2 -- and -- Eq #2

$\mathcal{B}_{gap} = \mu$ (mmf gap) X (P_{gap}) Eq #3

where P_{gap} is a <u>per unit</u> permeance
for example, permeance is defined by the following equation:

$$\text{Permeance} = \frac{\mu A}{L} \qquad \text{Eq \#4}$$

where A = Cross sectional area perpendicular to flux
L = Length of flux path
μ = Permeability of medium

rearranging Eq #4 results in:

$$P = \text{per unit permeance} = \frac{\text{Permeance}}{\mu A} = \frac{1}{L} \qquad \text{Eq \#5}$$

The modulated per unit gap permeance is expressed as:

$$P_{gap} = P_{rotor} \times P_{stator} \times P_{eccentricity}$$

and the ampere turns of mmf are:

$$\text{mmf gap} = \text{mmf}_{ac} + AT_{dc} = \text{mmf}\ (\theta, \text{wt}, \phi) + AT_{dc}. \qquad \text{Eq \#6}$$

where: θ = mech angle ϕ = power angle

The rotor permeance is in two parts, the amortisseur and main saliency, so that $P_{rotor} = P_{amort} + P_{main\ saliency}$. Eq. #7

* B is defined as the angle between the negative Y axis and the line connecting the rotor magnetic center with stator magnetic center. It is measured in a clockwise direction in radians.

The following analytical development deals with the reciprical of the gap as the permeance of the machine.

The rotor gap representation and permeance expression is obtained by a Fourier analysis of the rotor using the following saliency representation:

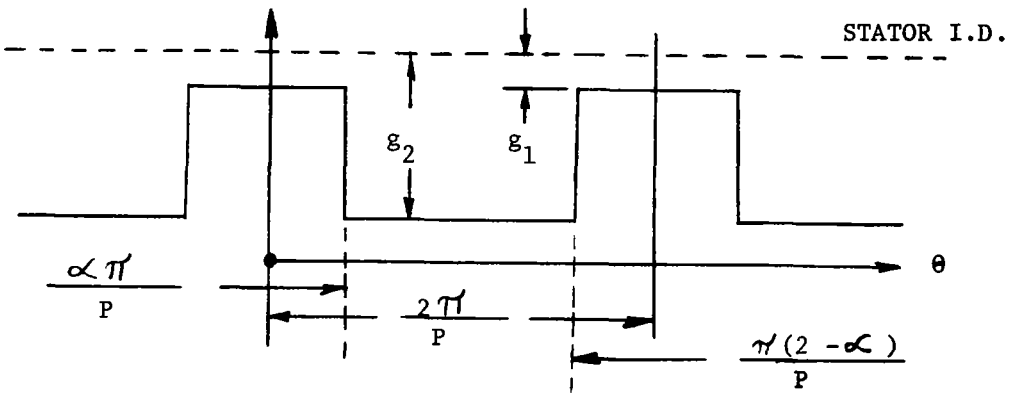

P = pole
α = per unit pole arc
g_1 = gap over pole
g_2 = gap over saliency

From the Fourier analysis, (See Section IX) the D-C or constant term is:

$$P_o = \left(\frac{\alpha}{g_1} + \frac{1-\alpha}{g_2}\right) \qquad \text{Eq \#8}$$

and the main permeance harmonics are:

$$P_n = \frac{2}{n\pi}\left(\frac{1}{g_1} - \frac{1}{g_2}\right) \sin n\pi\alpha \qquad \text{Eq \#9}$$

where n represents the harmonic number.

Combining these gives the total rotor main saliency permeance expression

$$P_{\text{main saliency}} = \left(\frac{\alpha}{g_1} + \frac{1-\alpha}{g_2}\right) + \sum \frac{2}{n\pi}\left(\frac{1}{g_1} - \frac{1}{g_2}\right) \sin n\pi\alpha (\cos (n\rho (\theta - wt))) \qquad \text{Eq \#10}$$

The amortisséur permeance is given by a similar expression

$$P_{amort} = P_{An} \cos (nN_A (\theta - wt)) \qquad \text{Eq \#11}$$

where N_A = effective amortisseur slots = 50

The stator slot permeance expression is

$$P_S = P_{Sn} \cos (n N_S \theta) \qquad \text{Eq \#12}$$

where N_S = 48 stator slots

and P_{An}, P_{Sn} are coefficients for amortisseur and stator slot harmonic permeance taken from a paper by Freeman. (1)

For the Brayton Cycle, the coefficients are:

Stator slots	Amortisseur Slots
$P_{S1} = +.09 \times P_o$	$P_{A1} = .022 \times P_o$
$P_{S2} = -.058 \times P_o$	$P_{A2} = -.017 \times P_o$
$P_{S3} = +.039 \times P_o$	$P_{A3} = .013 \times P_o$
$P_{S4} = -.024 \times P_o$	$P_{A4} = -.010 \times P_o$
$P_{S0} = 1.0$	$P_{A0} = 1.0$

and P_o is the average permeance of the gap over the rotor poles. It is also possible to express eccentricity as a permeance. This has been done so that the only terms in the expression for flux density are permeance and mmf.

The permeance expression representing eccentricity is:

$$P_{ecc} = 1 - \frac{\delta}{g} \cos (\theta - B). \qquad \text{Eq \#13}$$

The current in the stator winding and field coil can be expressed as a series of turns times current as a function of position and time. For most conditions the series is:

$$mmf_n = M K_{pn} K_{dn} \cos (n p (\theta - wt + \pi - \psi_e)) + AT_{dc} \qquad \text{Eq \#14}$$

K_{pn} = pitch factor $\qquad$ K_{dn} = distribution factor

where M is a constant containing the currents and number of turns.

From the various permeances and the mmf expression, a complete expression for B can be written.

(1) The Calculation of Harmonics Due to Slotting in the Flux Density Waveform in Dynamo Electric Machines, IEE paper #523U, June 1962, Dr. Freeman.

Then substituting Equations 10, 11, 12, 13 and 14 into Equation #3 yields:

$$\frac{B}{\mu} = \left\{\left[P_o + \sum \frac{2}{n\pi} \sin \alpha n\pi \left(\frac{1}{g_1} - \frac{1}{g_2}\right) \cos\left(n\rho(\theta - wt)\right)\right.\right.$$

$$\left. + P_A \cos n_a (N_A (\theta - wt))\right] \times \left[P_S \cos n_s N_S \theta\right] \times \left[\left(1 - \frac{\delta}{g} \cos(\theta - B)\right] \times\right.$$

$$\left.\left[M K_{pn} K_{dn} \sum \cos\left(n\rho(\theta - wt + \pi - \psi_e)\right) + AT_{dc}\right]\right\} \qquad \text{Eq. \#15}$$

With n an unlimited variable this equation takes on rather large proportions. For the analytical study, n was limited to significant values for each permeance and resulted in an expression for B of approximately 8000 terms. * Since force is proportional to B^2 the 8000 terms B expression must be squared. To keep track of the terms, the notation

$$B_{x_1 x_2 x_3 x_4 x_5} \qquad \text{Eq. \#16}$$

was introduced.

The x's represent rotor, stator, amortisseur, eccentricity, and MMF harmonic numbers respectively.

The following example shows how a force arises from a given set of permeance harmonics. Choose the case $B_{10000} \times B_{10011}$ which is one of the cross product terms of the B^2 expression. The first B is made up of the rotor fundamental permeance and zero order permeance or MMF terms, the second is made up of the rotor fundamental, eccentricity fundamental, MMF fundamental, and zero order terms for the stator and amortisseur permeance.

$$B_{10000} = \mu P_1 \cos 2(\theta - wt)(AT_{dc}) \qquad \text{Eq. \#18}$$

$$B_{10011} = \frac{-\delta}{g} \mu P_1 M K_{p1} K_{d1} \frac{1}{4}\left[\cos(-\theta + B - \pi + \psi_e) + \right.$$

$$\cos(3\theta - 4wt + B + \pi - \psi_e) + \cos(\theta - B - \pi + \psi_e) \qquad \text{Eq. \#19}$$

$$\left. + \cos(5\theta - 4wt - B + \pi - \psi_e)\right]$$

After multiplying $B_{10000} \times B_{10011}$ the product expands to:

* The harmonics used were $-5 \rightarrow 0 \rightarrow 5$ for the rotor, $-2 \rightarrow 0 \rightarrow +2$ for the stator $-2 \rightarrow 0 \rightarrow 2$ for the amortisseur, $0 \rightarrow 1$ for eccentricity and through the 13th for MMF.

$$B^2 = \frac{\mu P_1 (ATdc)\left(\frac{d}{g}\right) \mu P_1 M K_{P_1} K_{d_1}}{4} \Big\{ 1/2 \cos(2\theta - 2wt + \theta - B + \pi - \psi_e) \quad \text{Eq \#20}$$

$$* + 1/2 \cos(2\theta - 2wt - \theta + B - \pi + \psi_e)$$

$$* + 1/2 \cos(2\theta - 2wt - 3\theta + 4wt - B - \pi + \psi_e)$$

$$+ 1/2 \cos(2\theta - 2wt + 3\theta - 4wt + B + \pi - \psi_e)$$

$$* + 1/2 \cos(2\theta - 2wt - \theta + B + \pi - \psi_e)$$

$$+ 1/2 \cos(2\theta - 2wt + \theta - B - \pi + \psi_e) \Big\}$$

This multiplied by cos θ to denote direction and integrated over 2π results in

$$Fy = -2.09 \cos(-2wt + B - \pi + \psi_e) \quad \text{Eq \#21}$$

$$- 4.18 \cos(2wt - B - \pi + \psi_e)$$

Note we could have predicted that only the terms marked with * would integrate to other than zero[1] since they have an angle which contains ± θ which when combined with the cos θ (direction term) cancels to eliminate θ from the integral.

There are other considerations in this force. For example, each term of the rotor permeance is reduced in magnitude and shifted in space to reflect saturation in both the rotor and stator teeth. Saturation is calculated as a function of time and mechanical angle for each operating condition. To accomplish this the flux wave in the alternator is analyzed to yield permeance harmonic coefficients which alter the unsaturated rotor permeance harmonic coefficients before bearing force is calculated. At the same time, the angle ψ_e associated with mmf, the exact value of ATdc as seen at the air gap, and fringing between the rotor poles is calculated and introduced in the mmf or permeance series.

Unbalanced electrical loading on the stator terminals introduces negative and zero sequence currents leading to additional armature reaction terms rotating opposite to the rotor at the same speed or standing still in mechanical position. The mmf's are handled by adding two additional sets of terms to the mmf term already containing the positive sequence current and ATdc. (See Equation #14)

The Brayton Cycle's multicircuit stator winding reduces magnetic bearing force. Windings 180 mechanical degrees apart are connected in parallel so that if they have unequal induced voltages a circulating current flows tending to offset the effect of differing permeances. This effect is dependent on speed and the relative reactance and resistance of the machine. As speed is increased, the force drops sharply to a reduced level and remains essentially constant with further speed increase. For the Brayton Cycle generator, the breakoff point is about 300 rpm with force relatively constant in the 300 - 12000 rpm range.

(1) See Section XI for more detailed analytical development.

Computer Approach

The Fourier approach to the problem allows a direct force expression to be calculated that gives harmonic content, space angles and time angles. However it involves a large number of very similar multiplications and integrations. If each of the $\mathfrak{B}$ terms were integrated for each of six cases 384 million integrations would be necessary, followed by a summing up of all the terms alike in time and space. For this reason, the entire problem has been computerized. The computer decks perform the following operations:

(1) Compute saturation, ATdc, ψ e.

(2) Compute series for permeance and mmf

(3) Compute expression for $\mathfrak{B}$

(4) Compute expression for $\mathfrak{B}^2$

(5) Eliminate terms which will integrate to zero

(6) Integrate $\mathfrak{B}^2$

(7) Combine force terms to simplest expression

The program is broken down into several decks interconnected by magnetic tapes.

SECTION V

NOMENCLATURE - ANALYTICAL STUDY

A	Area in square inches of magnetic surface
AT_{dc}	Amp turns of d.c. excitation/stator half
B	Mechanical reference angle of minimum air gap (radians)
D	Air gap diameter (inches)
F	Force (pounds)
g	Air gap length (inches)
I	Amps
K	Appropriate constant
L	Period length (radians)
l	Length of magnetic path (inches)
M or MMF	Armature ampere turn series
mmf	Magneto motive force
N_A	Number of amortisseur slots (effective)
n_a	Amortisseur harmonic order number
n_e	Eccentricity harmonic order number
n_r	Rotor saliency harmonic order number
N_S	Number of stator slots
n_s	Slot (Stator) harmonic order number
P	Main electromagnetic poles
P.U..	Per unit
R	Resistance
V	Volts
w	Mechanical angular velocity (radians/sec)
t	Time (seconds)
X	AC reactance
$\emptyset$	Flux or phases
θ	Mechanical position angle (radians)
P_a	Amortisseur slotting permeance (per unit)
P_e	Eccentricity effective permeance (per unit)
$\mathcal{B}$	Flux density (lines or kilo lines per square inch)
ρ	Pairs of poles
α	Per unit pole arc
μ	Permeativity of air in English units (1/313)
ψ_e	Power angle (radians)
δ	Radially measured eccentricity (inches)
P_r	Rotor saliency permeance (per unit)
P_s	Stator slotting permeance (per unit)

SECTION VI

RESULTS

This Results Section contains both analytical and experimental data which are presented in the following order:

A. Form and Significance of Equations

B. Summary of Analytical Results

C. Summary of Experimental Results (Tables II and III)

D. Experimental and Analytical Correlation

E. Conclusion and Recommendations

A. Form and Significance of Equations

The results of the analytical study are a set of force equations describing radial magnetic bearing force. The force equations are in terms of a cartesian coordinate system fixed in the magnetic center of one stator perpendicular to the axis of the rotor shaft as indicated in Figure 2. For each defined load condition of the machine, a radial magnetic force is represented by six multi term equations. The six equations describe Fy, Fx, $\frac{dFy}{dB}$, $\frac{dFx}{dB}$, $\frac{dFy}{\delta}$, $\frac{dFx}{\delta}$. For example, below is the equation for Fy with the machine operating at 11.25 KVA.

$$
\begin{aligned}
Fy = {} & -.06 \cos(2\,wt - B + 5\phi) - 12.045 \cos(2\,wt - B + \phi) \\
& -25.395 \cos(B) - 0.03 \cos(B - 5\phi) \\
& -0.03 \cos(B + 5\phi) - 9.81 \cos(13 + \phi) \\
& -9.77 \cos(B - \phi) - 20.69 \cos(2\,wt - B) \\
& -4.97 \cos(2\,wt - B - \phi) - 0.04 \cos(2\,wt - B - 2\phi) \\
& -0.67 \cos(B + 2\phi) - 1.31 \cos(2\,wt - B + 2\phi) \\
& -0.7 \cos(B - 2\phi) \text{ pounds}
\end{aligned}
$$

where:

Fy = Force in Y direction (pounds)
w = mechanical angular velocity
t = time (seconds)
B = mechanical angle between negative Y - axis and direction of eccentricity (radians)
f = eccentricity (inches)
$\phi = \pi$ - Power Angle

Power Angle = Electrical angle (radians) between load current and direct axis magnetizing current

Assuming that the force is inversely proportional to the number of circuits, the equation shown on the previous page can be divided by 2 and then represents a 10.0 pound dc force with a two per revolution cosinusoidal peak of 17.50 pounds. For this case $\phi = \pi - 0.625$ radians, indicating that the maximum force occurs slightly off center from the minimum air gap point.

B. Summary of Analytical Results

Table I summarizes the analytical calculations. To compare these forces with measured values, Fx and Fy must be reflected to the bearings from the stator center, and then added vectorially to obtain a magnitude and angle.

The following comments can be made concerning the analytical results:

(1) With balanced full load (15 KVA, 0.8 PF),the radial magnetic bearing force appearing at the air gap in the Brayton Cycle alternator is about 10 lbs/mil of eccentricity.

(2) The major force as defined by $(\vec{F_x} + \vec{F_y})$ is two per rev. and unidirectional in nature.

(3) The results of saturation tend to lower the overall magnetic force about 18% at full load.

(4) All the results correspond to the six load cases and all are at 2.0 mils (.002") of radial eccentricity with B=0, i.e., the rotor displaced straight down .002".

(5) The analytical results are for one end of the machine, assuming the rotor is symmetrical about its center in any place perpendicular to the shaft.

(6) The analytical results do not account for any mechanical unbalance or the effects of gravity.

(7) The six cases investigated were:

Case 1. The machine is at 15 KVA 0.8 PF lagging balanced 3ϕ load.

Case 2. The machine is at 11.25 KVA 0.8 PF lagging balanced 3ϕ load.

Case 3. The machine is at no load with field excited.

Case 4. The machine is under a 3ϕ short circuit condition.

Case 5. The machine has a 3.33 KVA, 1.0 PF load on one phase only (L-N). The other phases are open.

Case 6. The machine is running as per Case 1 and one phase is shorted to neutral.

(8) For these cases, the machine consists of the alternator and voltage regulator exciter, with excitation being determined by the regulator. Graphs of the force for the six cases are shown in Figures 3, 4, 5, 6, 7 and 8. The equations from which the graphs were plotted are given in Section VIII.

C. Summary of Experimental Results

A summary of experimental results is given in Tables II and III. Table II is for the opposite drive end of the alternator and Table III for the drive end. All values represent the maximum force observed and its angle relative to the eccentricity direction. Results were obtained from the Lissajous patterns given in Section X. Data was taken on the test setup shown in Figure 9, and recorded at a speed of 3000 rpm for the reasons presented in Section XIII.

D. Experimental and Analytical Correlation

Table IV shows the correlation obtained between analytical and experimental data. The analytical results of Table I were reflected to the bearings as shown in Section XIV and then multiplied by 3 to reflect a 0.006" eccentricity. (See 4 below for validity.) Results obtained are shown in the 2nd column of Table IV. Column 3 shows the modified results factoring in the greater circuit effect obtained experimentally and differential saturation. (See 1 and 8 below and also Section XIV.) The following comments can be made regarding the data as presented in these Results and the experimental data of Section X.

1. Magnitude

Experimental results show significantly less force than analytical calculations. Exacting comparisons were made on the no load case, and indicate that the force reducing effect of stator circuits is greater than assumed. Differential saturation of the opposing stator teeth also reduces the force and contributes to the difference as does different Carter's coefficients.

2. Harmonic Content

The analytic expressions agree well with the experimental results in harmonic content and proportions of DC and time variant forces for the balanced load cases. An exception is the three-phase short circuit where a fairly constant force was predicted but experimental data shows a time variant existing. The complex nature of the unbalanced load cases was verified, although it is difficult to identify the contributing harmonics in the experimental data.

3. Time & Space Angles

The analytical prediction of the maximum forces occurring off center from the minimum air gap and having components 90 mechanical degrees away from the minimum air gap point were proven correct.

4. Linearity of Force with Eccentricity

The analytical expression for force (Eq's 20 and 21) implies that force is directly proportional to eccentricity. Figure 10 is a plot of the data given in Table II and shows excellent agreement with the analytical prediction. However, when the other bearing data of Table III was plotted in Figure 11, agreement was poor. No explanation is known as to why the .004" eccentricity points measured lower than expected.

5. Effect of Negative and Zero Sequence Currents

The analytical expression for unbalanced load was rather complex with counter rotating harmonic terms resulting in time variant saturation. Experimental data bears out the complex nature of the unbalanced forces, especially that of the single phase short circuit under load conditions. (See Section X.) Despite this complexity, a reasonable comparison was made for the unbalanced single phase loading case (Table IV). Although negative and zero sequence reactances were used with alternator test data to obtain the positive, negative, and zero sequence currents for the single phase short circuit analysis, a fuller understanding of the amortisseur reaction effect on the force is needed.

6. Saturation

The analytical results reflect the effect of uniform saturation on opposing stator teeth, but not the differential effect noted in (1) above and covered in Section XIV. Time variant saturation for the single phase short circuit case was handled indirectly as given in Section VIII and may represent the main reason for the large discrepancy between the analytical and experimental results. However, Section X, Figures V-9, V-33, V-16, V-40, V-23 and V-47 show the very complex Lissajous pattern and represent a very formidable analytical problem. Time variant saturation could be factored into the present analysis but only with a major effort.

7. Excitation

The calculations for saturation necessarily include power angle, mmf harmonics, permeance harmonics, and excitation requirements. These calculations have been borne out experimentally.

8. Multicircuit Winding and Variation of Force with Speed

As noted in (1), a force reducing factor of 2 was applied to the analytical results since the Brayton Cycle Alternator has 2 circuits. Figure 12 gives the experimental results at no load obtained by varying the speed from zero (0) to 3000 rpm. Note that the force is reduced by about 4 to 1 and that it stays relatively constant above 300 rpm. At this speed the machine reactance predominates over its resistance, and since reactance is directly proportional to speed, it holds the flux and thus the force constant as speed increases. Induced voltage in the amortisseur winding would also reduce the force and might explain the large reduction factor.

9. "One Per Rev" Force

The analytical study indicated that no forces would occur at the generator mechanical fundamental speed. Some force did occur at the mechanical fundamental frequency which may be attributed to differences in the mechanical structure of the rotor poles, but this force was very small.

10. Cogging Torques

Cogging torque was briefly evaluated analytically and found to be small in comparison with the radial components of force. No experimental work was done on this aspect of magnetic force.

11. Transients

No transient cases were analyzed or experimentally measured. The analysis implies that high forces could be encountered if armature reaction was suddenly reduced allowing full field to be momentarily applied across the air gap. However, stator tooth saturation would put an upper limit on the force.

E. Conclusions and Recommendations

The following conclusions can be drawn from the study:

1. It is possible to derive analytical expressions that properly describe the nature of the unbalanced magnetic force.

2. The force can be measured by the use of strain-gages on specially designed end shields.

3. The measured forces were significantly less in magnitude than the analytical predictions. A larger than expected force reducing effect from stator circuits and differential saturation are believed to be the main causes of the difference.

4. The single phase short circuit case produced the most complex Lissajous pattern and reflected the time variant saturation and amortisseur reaction which are present during this type of operation.

5. The effect of stator or amortisseur slotting is small.

Recommendations for future work include the following:

1. Investigate the effect of circuits on the force.

2. Factor differential saturation and different Carter's coefficients into the present analysis.

3. Investigate the effect of amortisseur reaction during unbalanced load conditions.

4. Investigate the feasibility of factoring time variant saturation into the present analysis.

SUMMARY OF ANALYTICAL RESULTS

FOR .002" ECCENTRICITY*

Power Factor	Load	F Max	Fx Max	Fy Max	Fx Ave	Fy Ave	Angle between Force Center Line and Min Air Gap
0.8	Balanced 15 KVA (Unsaturated)	24.5	-***	24.5	-***	13.5	18°
0.8	Balanced 15 KVA (Saturated)	21.94	8.5	20.2	0.0	11.44	18°
0.8	Balanced 11.25 KVA	19.04	7.5	17.5	0.0	10.01	10°
-	No Load with Excitation	15.0	6.0	13.75	0.0	7.64	0°
1.0	3.33 KVA 1Ø	17.84	9.0	15.4	0.0	7.86	23°
-	3Ø Short	13.09	0.0	13.09	0.0	13.09	-**
0.8 (before short)	3Ø Full Load 1Ø Short	54.0	-***	54.0	-***	33.4	43°

These results are in terms of force in the x and y directions at the center of the armature stack.

* Eccentricity is distance in inches between rotor center and stator magnetic center. Minimum air gap is in the y axis.

** This is a d.c. force with no associated angle.

*** Calculated (Section VIII) but not reduced to a final force.

TABLE I

EXPERIMENTAL BEARING LOADING
(MAGNITUDE & DIRECTION RELATIVE TO ECCENTRICITY DIRECTION)
AT OPPOSITE DRIVE END OF ALTERNATOR

Eccentricity* (Inches)		Power Factor	No Load-No Field	3.33** KVA Single Phase	11.25 KVA 3-Phase	15 KVA 3-Phase	15 KVA 3-Phase, then 1-Phase Shorted	15 KVA 3-Phase, then 3-Phase Shorted
Ref.	Act.							
0	.0009	1	2.0 lb/$_{+106^\circ}$	1.8 lb/$_{+96^\circ}$	1.5 lb/$_{+56^\circ}$	N.A.	N.A.	N.A.
0.002	.0025	1	1.5 lb/$_{-169^\circ}$	3.0 lb/$_{-19^\circ}$	3.0 lb/$_{+1^\circ}$	N.A.	N.A.	N.A.
0.002	.0025	0.8 (lagging)	Not Applicable	N.A.	3.2 lb/$_{-39^\circ}$	3.5 lb/$_{-29^\circ}$	6.5 lb/$_{-29^\circ}$	4.0 lb/$_{-4^\circ}$
0.004	.0048	1	2.5 lb/$_{+67^\circ}$	7.1 lb/$_{+17^\circ}$	8.0 lb/$_{-3^\circ}$	N.A.	N.A.	N.A.
0.004	.0048	0.8 (lagging)	Not Applicable	N.A.	8.1 lb/$_{-3^\circ}$	1.0 lb/$_{+2^\circ}$	11.2 lb/$_{-13^\circ}$	12.2 lb/$_{+2^\circ}$
0.006	.0063	1	1.2 lb/$_{-123^\circ}$	9.1 lb/$_{-13^\circ}$	10.8 lb/$_{-13^\circ}$	N.A.	N.A.	N.A.
0.006	.0063	0.8 (lagging)	Not Applicable	N.A.	11.8 lb/$_{-18^\circ}$	14.2 lb/$_{-23^\circ}$	14.9 lb/$_{-23^\circ}$	16.0 lb/$_{-8^\circ}$

*Eccentricity is defined here as the displacement of the rotor center from the stator center. (total indicator reading would be twice the eccentricity)

**The other two phases are on open circuit.

TABLE II

EXPERIMENTAL BEARING LOADING

(MAGNITUDE & DIRECTION RELATIVE TO ECCENTRICITY DIRECTION)

AT DRIVE END OF ALTERNATOR

Eccentricity* (Inches)		Power Factor	No Load-No Field	3.33** KVA Single Phase	11.25 KVA 3-Phase	15 KVA 3-Phase	15 KVA 3-Phase, then 1-Phase Shorted	15 KVA 3-Phase, then 3-Phase Shorted
Ref.	Act.							
0	.0005	1	2.5 lb/$_{+150^\circ}$	2.2 lb/$_{+170^\circ}$	2.1 lb/$_{-120^\circ}$	N.A.	N.A.	N.A.
0.002	.002	1	1.8 lb/$_{-180^\circ}$	2.0 lb/$_{0^\circ}$	2.8 lb/$_{0^\circ}$	N.A.	N.A.	N.A.
0.002	.002	0.8 (lagging)	Not Applicable	N.A.	3.5 lb/$_{0^\circ}$	3.0 lb/$_{-35^\circ}$	4.5 lb/$_{+5^\circ}$	4.0 lb/$_{-10^\circ}$
0.004	.0041	1	1.2 lb/$_{-173^\circ}$	2.8 lb/$_{+7^\circ}$	3.2 lb/$_{-3^\circ}$	N.A.	N.A.	N.A.
0.004	.0041	0.8 (lagging)	Not Applicable	N.A.	4.0 lb/$_{-7^\circ}$	4.8 lb/$_{+7^\circ}$	8.2 lb/$_{+25^\circ}$	7.3 lb/$_{+5^\circ}$
0.006	.0063	1	2.2 lb/$_{+72^\circ}$	7.0 lb/$_{-8^\circ}$	9.0 lb/$_{+12^\circ}$	N.A.	N.A.	N.A.
0.006	.0063	0.8 (lagging)	Not Applicable	N.A.	9.2 lb/$_{+7^\circ}$	11.8 lb/$_{+3^\circ}$	15.0 lb/$_{+12^\circ}$	13.1 lb/$_{-10^\circ}$

*Eccentricity is defined here as the displacement of the rotor center from the stator center. (total indicator reading would be twice the eccentricity)

**The other two phases are on open circuit.

TABLE III

ANALYTICAL AND EXPERIMENTAL CORRELATION*

.006" ECCENTRICITY

	Experimental (Data from Table II except for NL point)	Analytical	Modified Analytical**
No Load with 2.7 amps Excitation	9	32	11.7
15 KVA, .8 PF	14.2	47.4	17.3
3.33 KVA, Single phase	9.1	40.0	14.6

* Data presented is maximum force occurring at the bearings and is in pounds.

** Reflects a 4:1 rather than a 2:1 circuit effect and factors in differential saturation. Latter was calculated for No Load case and same reduction applied to other two cases.

TABLE IV

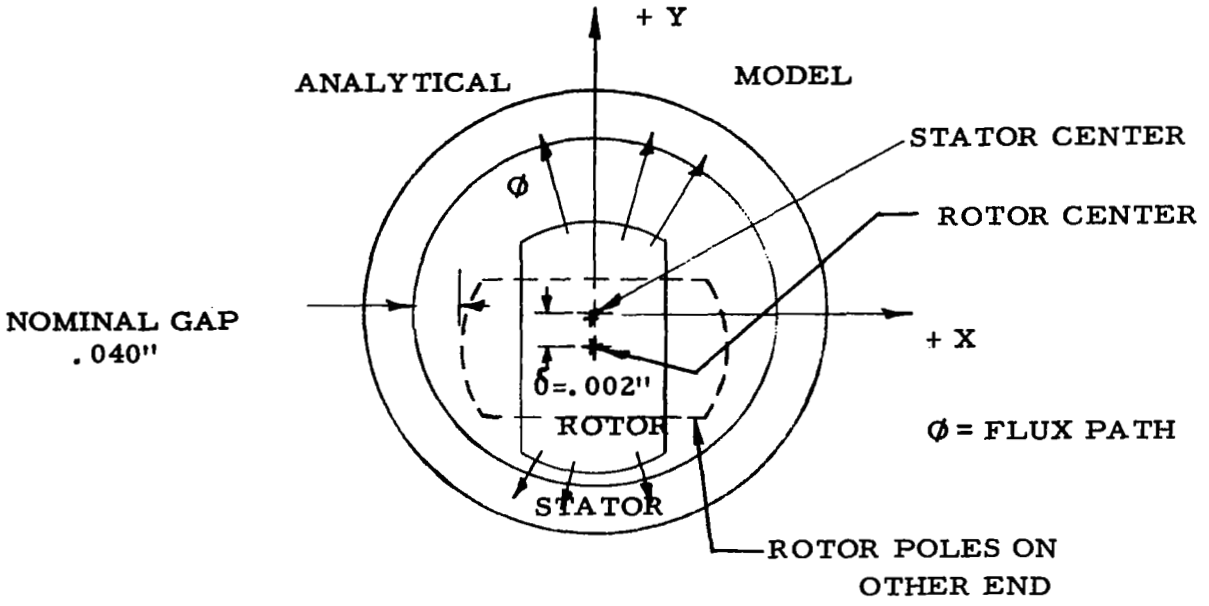

END VIEW

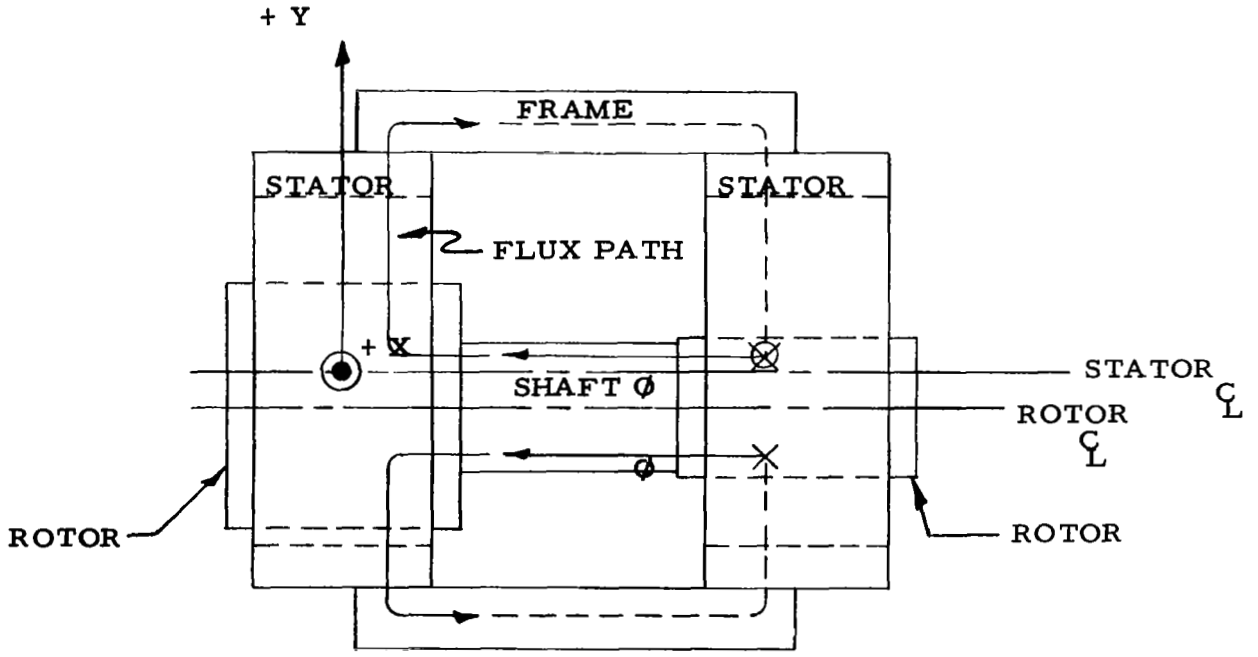

SIDE VIEW

FIGURE 2

BRAYTON CYCLE ALTERNATOR

CALCULATED RADIAL MAGNETIC FORCE *

15 KVA, .8 P. F. 120/208 VOLTS, 400 CPS, 0.002 " ECCENTRICITY

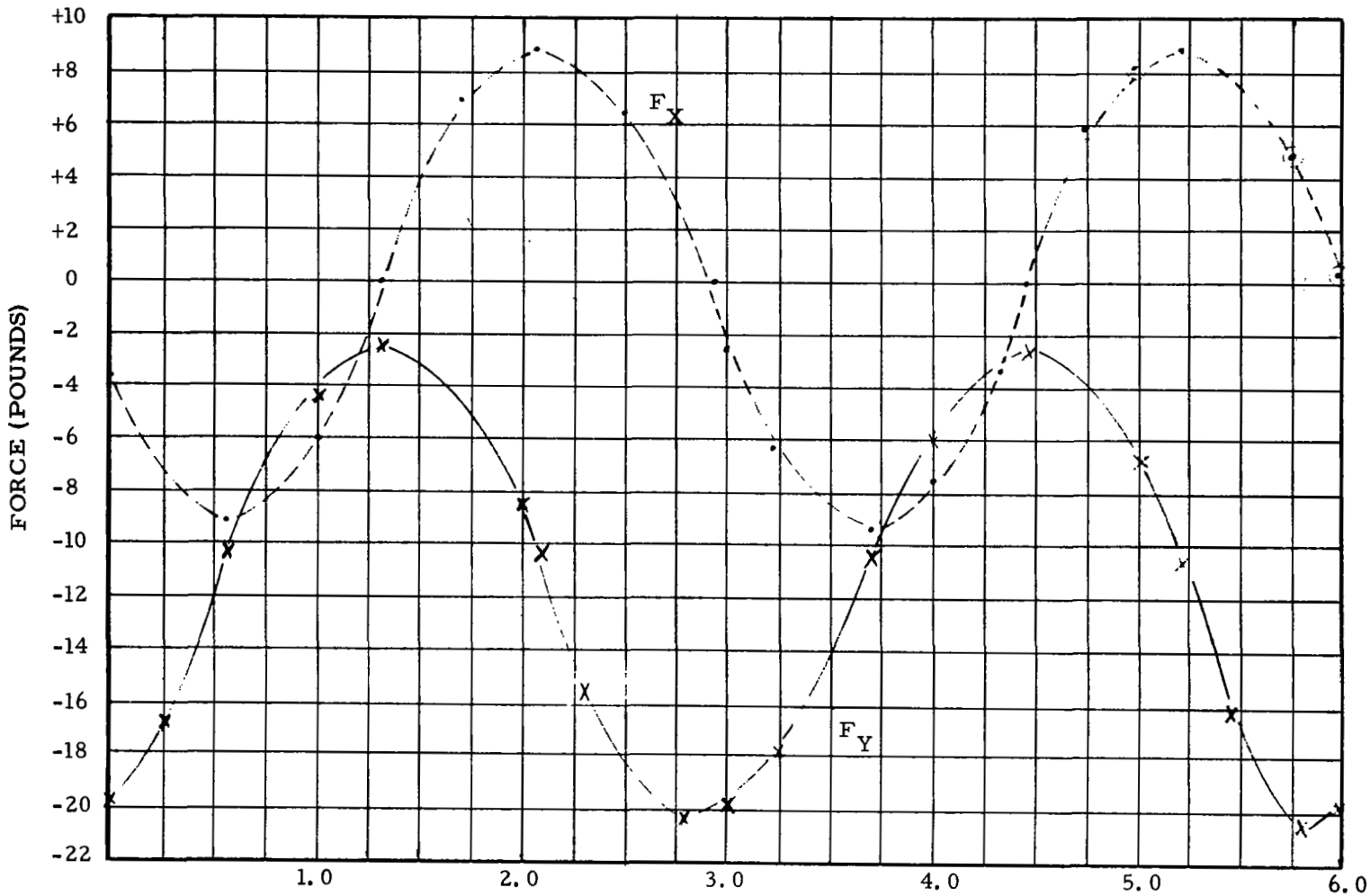

* DIVIDED BY TWO TO REFLECT CIRCUIT EFFECT

FIGURE 3

BRAYTON CYCLE ALTERNATOR

CALCULATED RADIAL BEARING FORCE *

11.25 KVA, 120/208 VOLTS, 400 CPS, 0.002" ECCENTRICITY

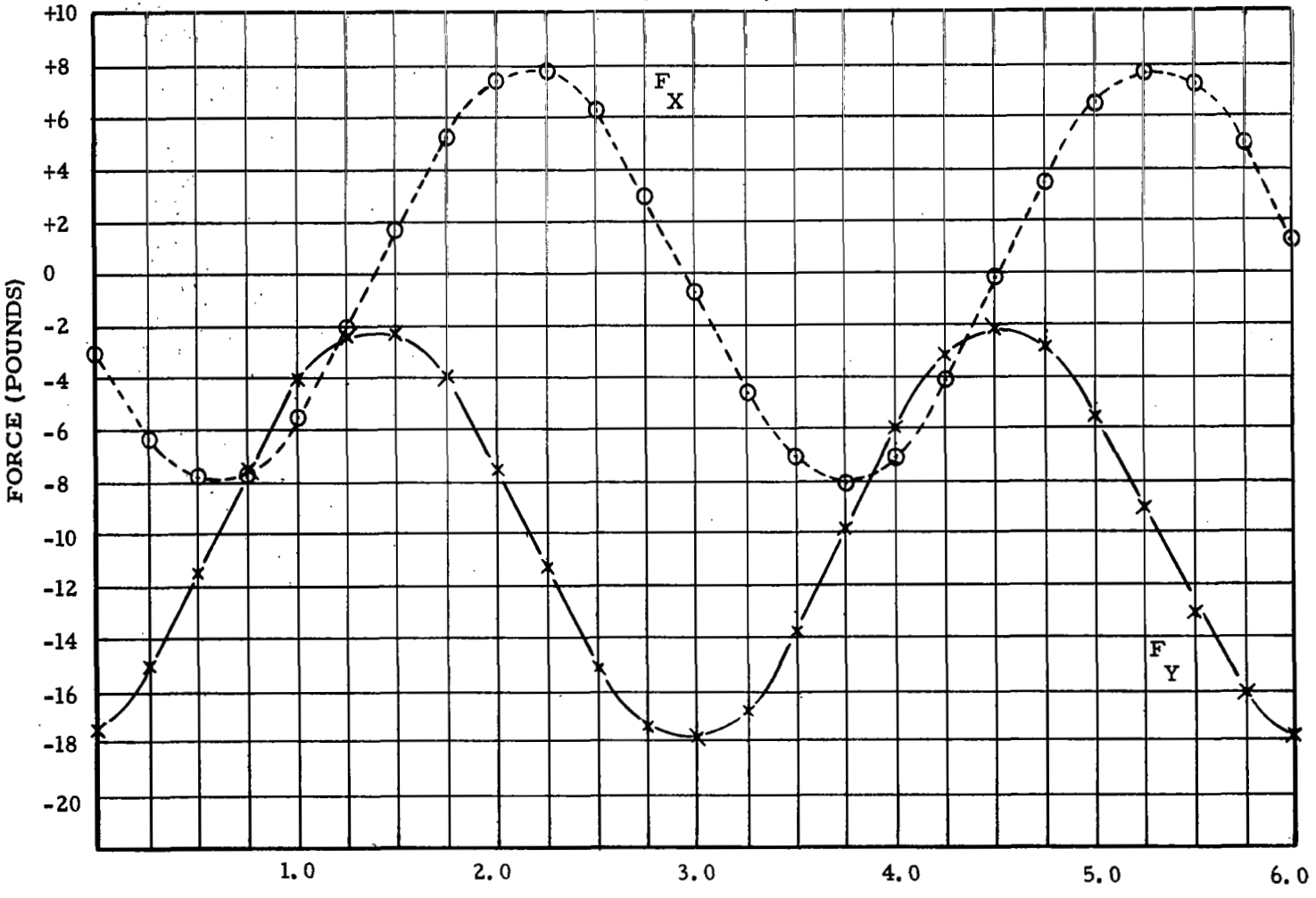

* DIVIDED BY TWO TO REFLECT CIRCUIT EFFECT

FIGURE 4

BRAYTON CYCLE ALTERNATOR

CALCULATED RADIAL BEARING FORCE *

NO LOAD, 120/208 VOLTS, 400 CPS, 0.002" ECCENTRICITY

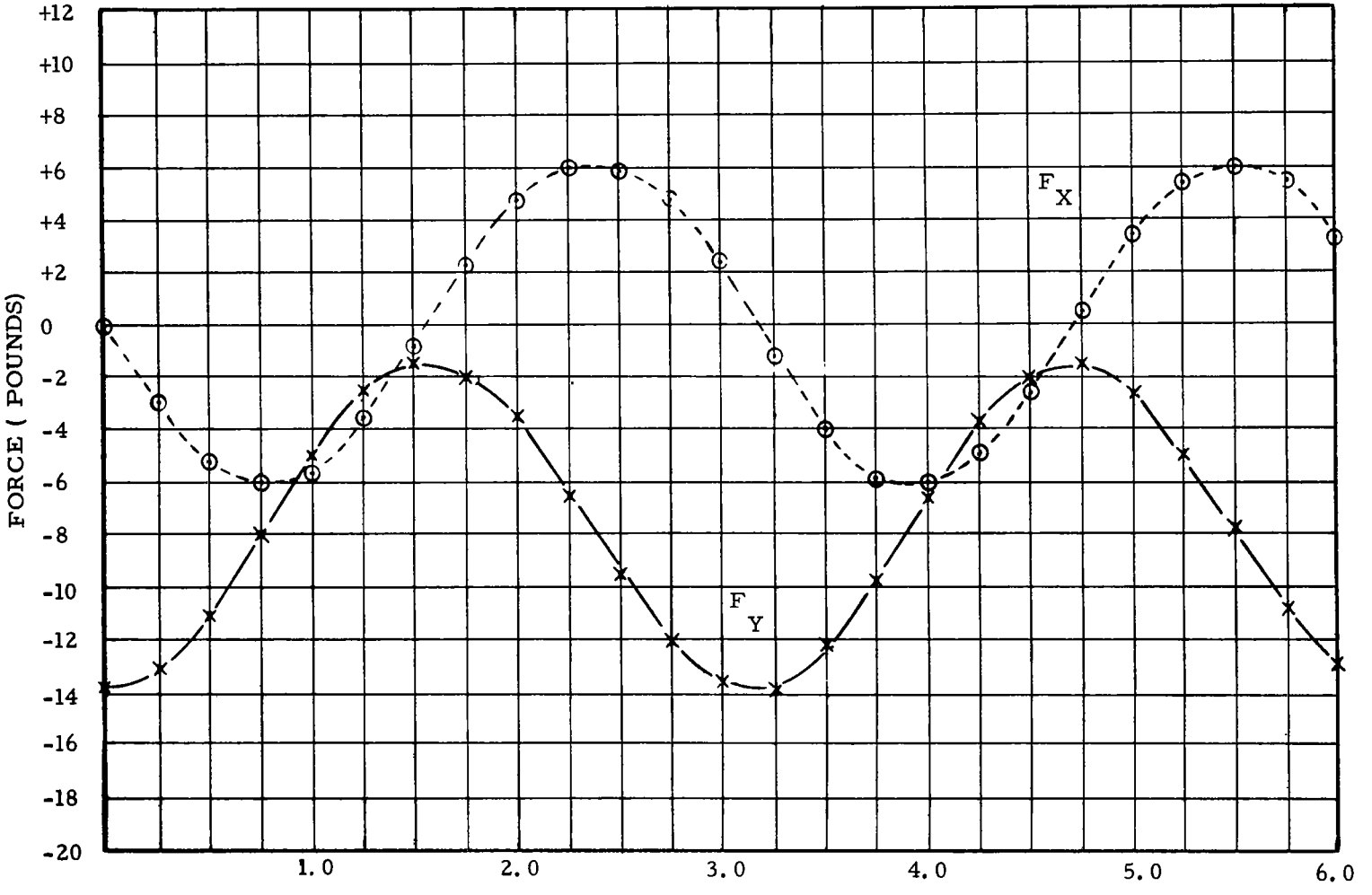

* DIVIDED BY TWO TO REFLECT CIRCUIT EFFECT

FIGURE 5

BRAYTON CYCLE ALTERNATOR

CALCULATED RADIAL BEARING FORCE *

3 PHASE BALANCED SHORT CIRCUIT - .002 ECCENTRICITY

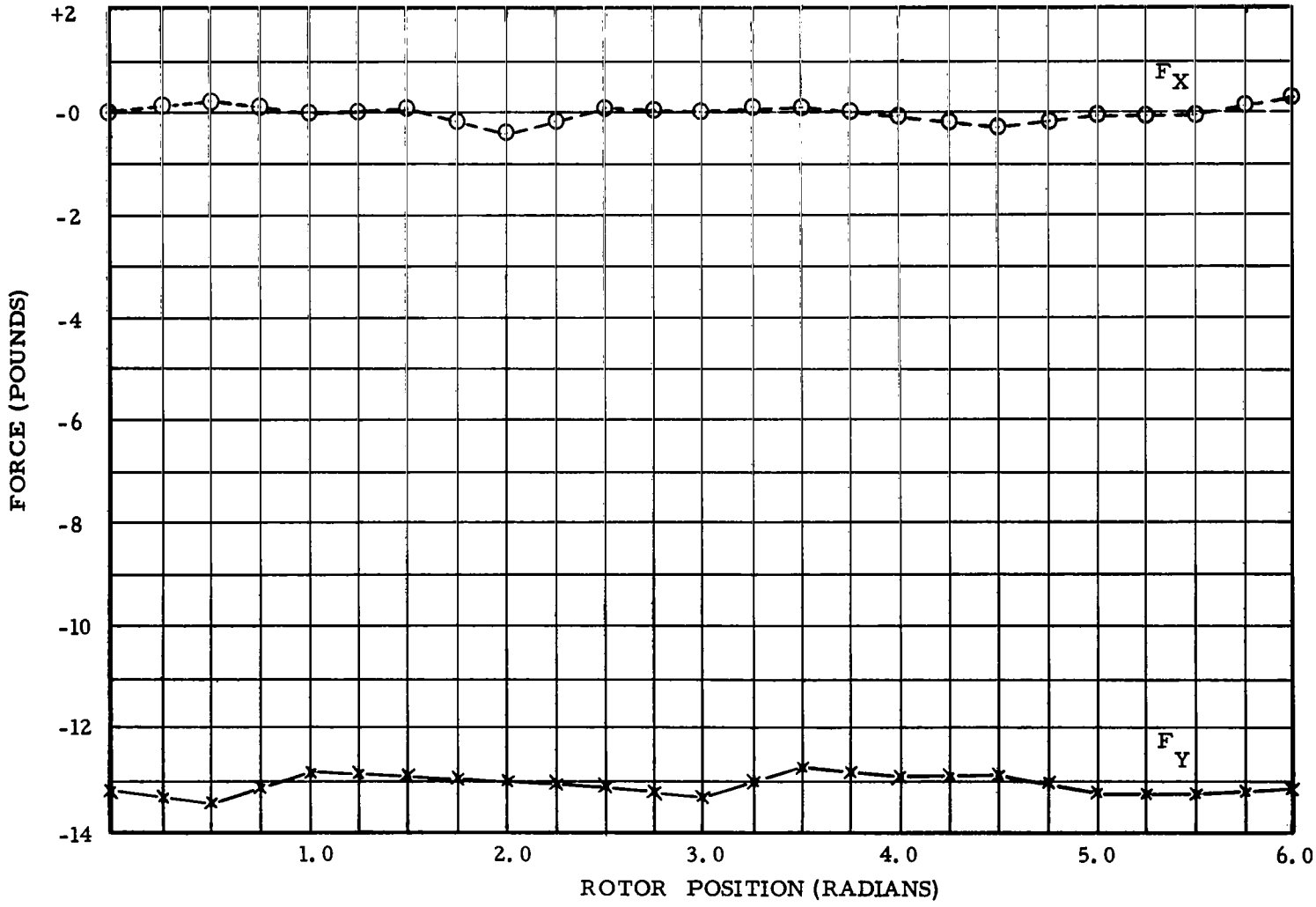

* DIVIDED BY TWO TO REFLECT CIRCUIT EFFECT

FIGURE 6

BRAYTON CYCLE ALTERNATOR
CALCULATED RADIAL MAGNETIC FORCE*
3.33 KVA, 1.0 P. F. SINGLE PHASE LOAD-0.002"ECCENTRICITY

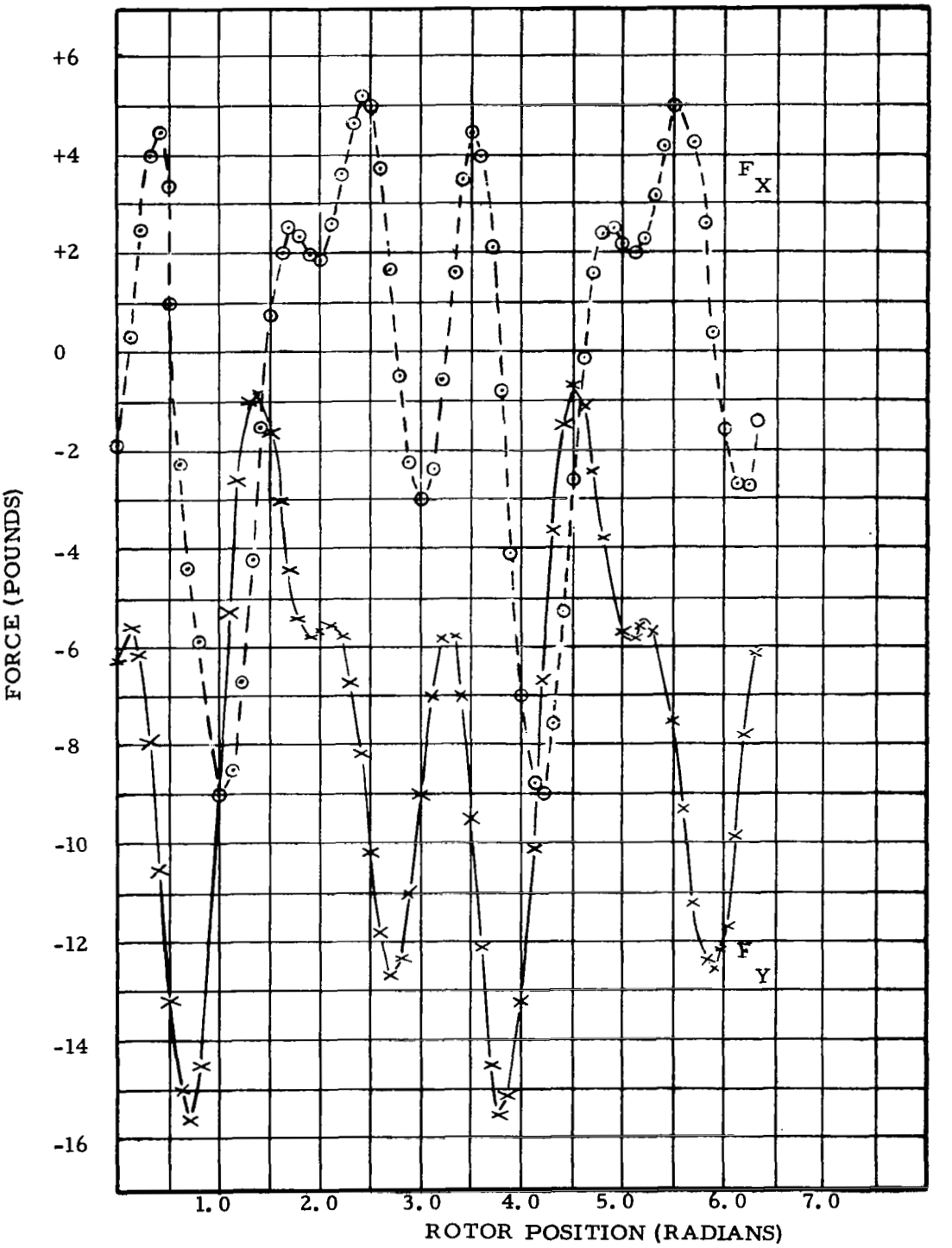

* DIVIDED BY TWO TO REFLECT CIRCUIT EFFECT

FIGURE 7

BRAYTON CYCLE ALTERNATOR

CALCULATED RADIAL MAGNETIC FORCE *

SINGLE PHASE SHORT WITH 15 KVA, .8 P. F. APPLIED - 0.002" ECCENTRICITY

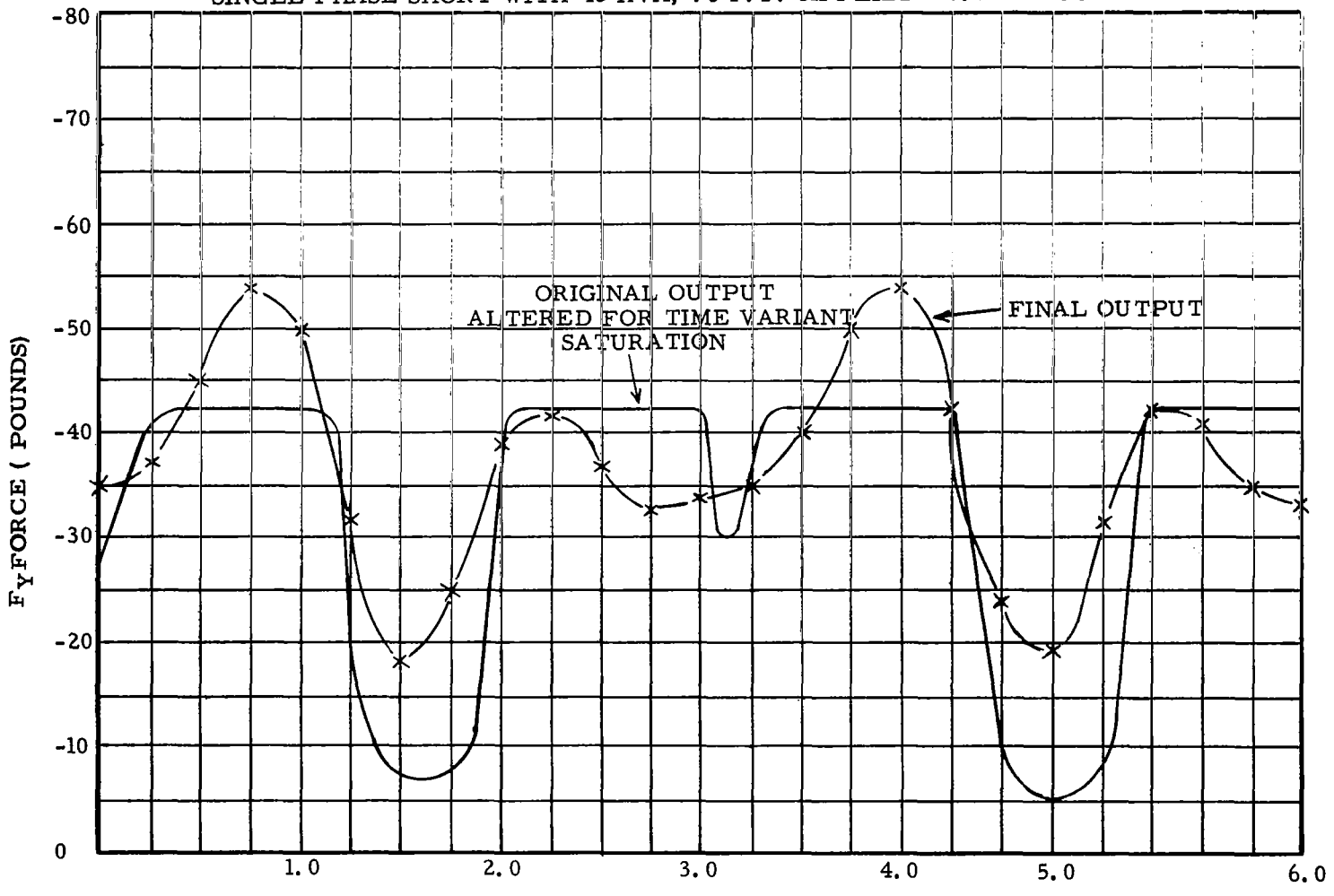

* DIVIDED BY TWO TO REFLECT CIRCUIT EFFECT

FIGURE 8

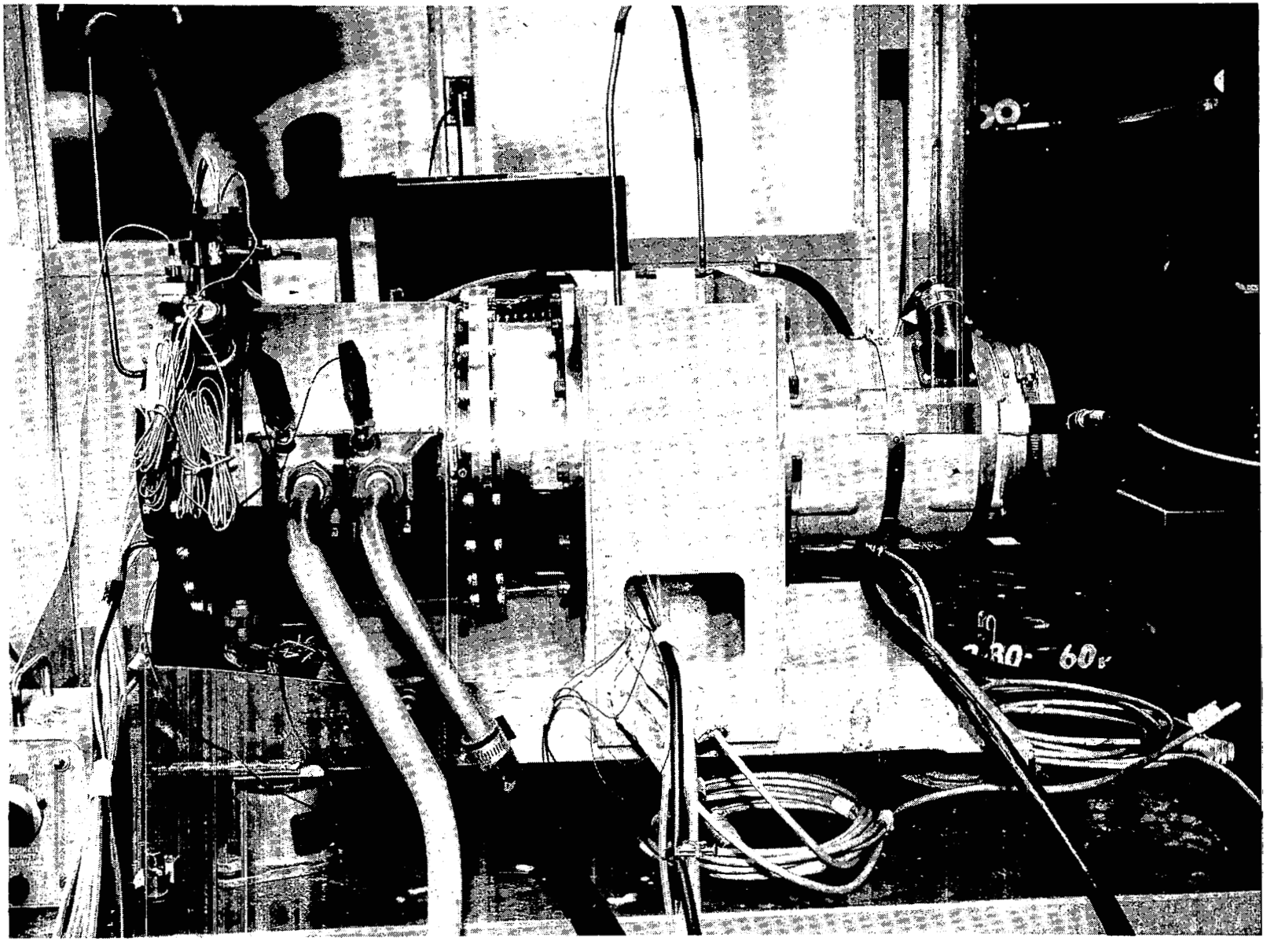

ALTERNATOR AND DRIVE MOTOR FOR BEARING FORCE TESTING

BRAYTON CYCLE ALTERNATOR

TABLE II DATA -- OPPOSITE DRIVE END

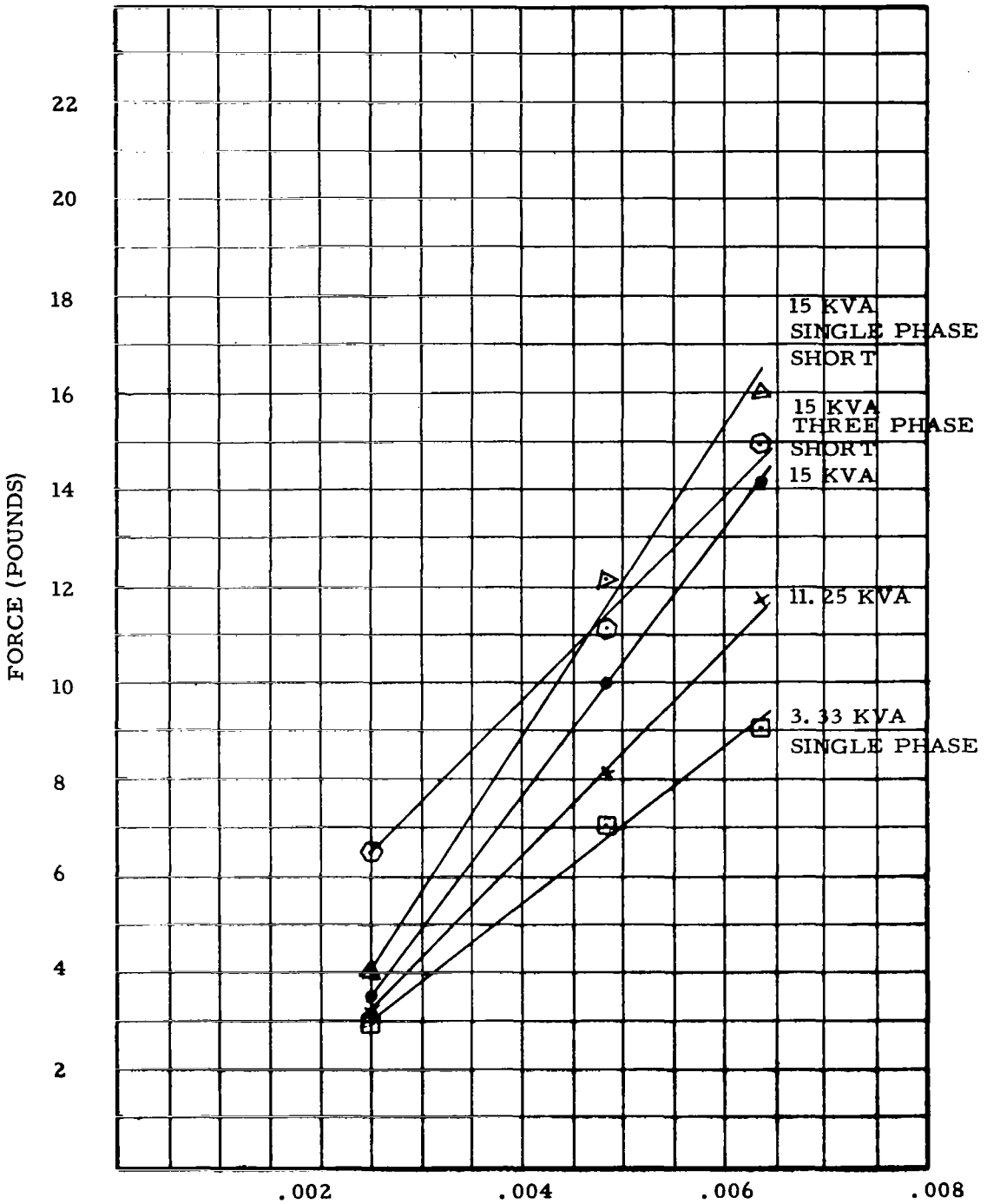

FIGURE 10

BRAYTON CYCLE ALTERNATOR

TABLE III DATA --- DRIVE END

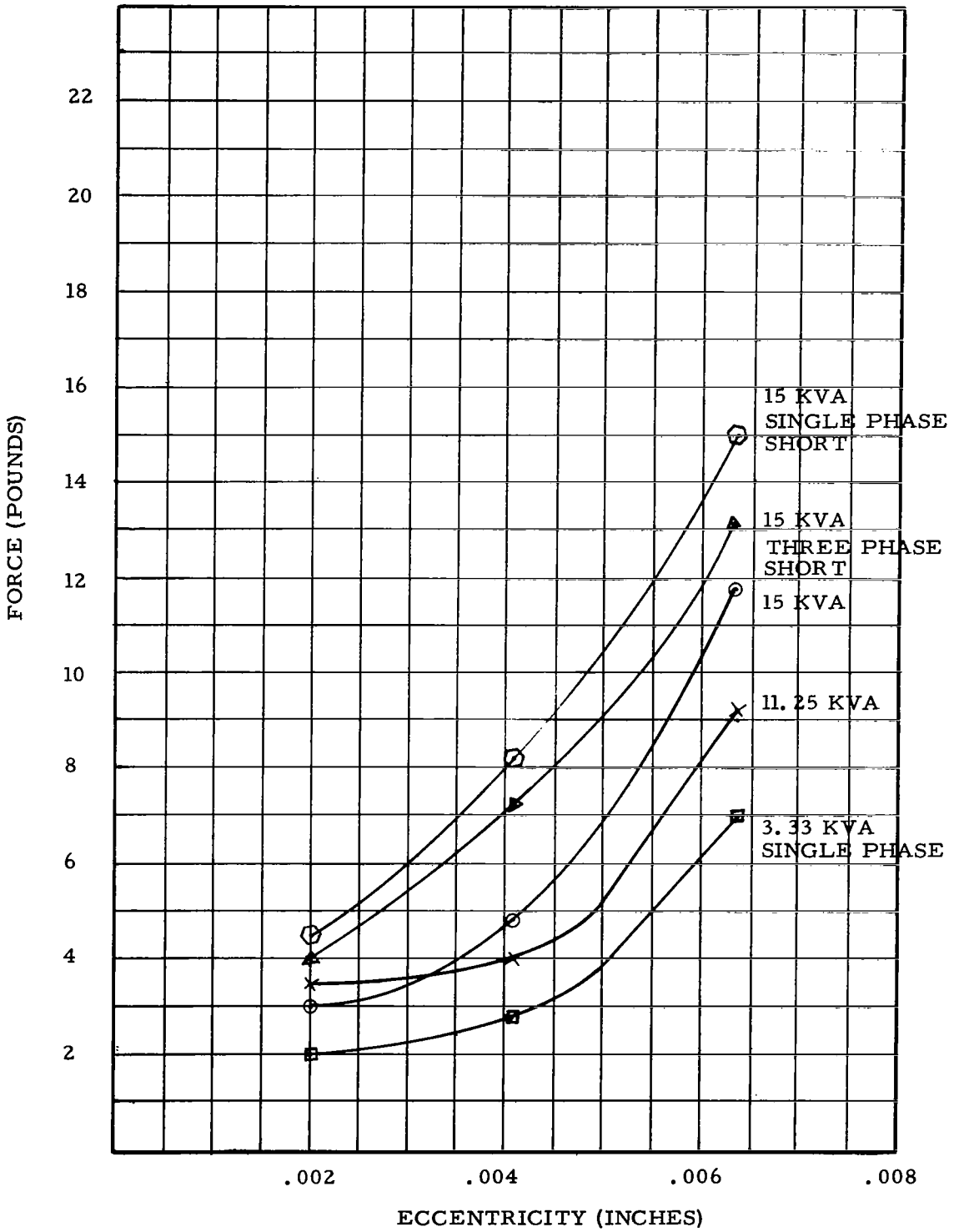

FIGURE 11

BRAYTON CYCLE ALTERNATOR

MEASURED RADIAL MAGNETIC FORCE-DRIVE END*

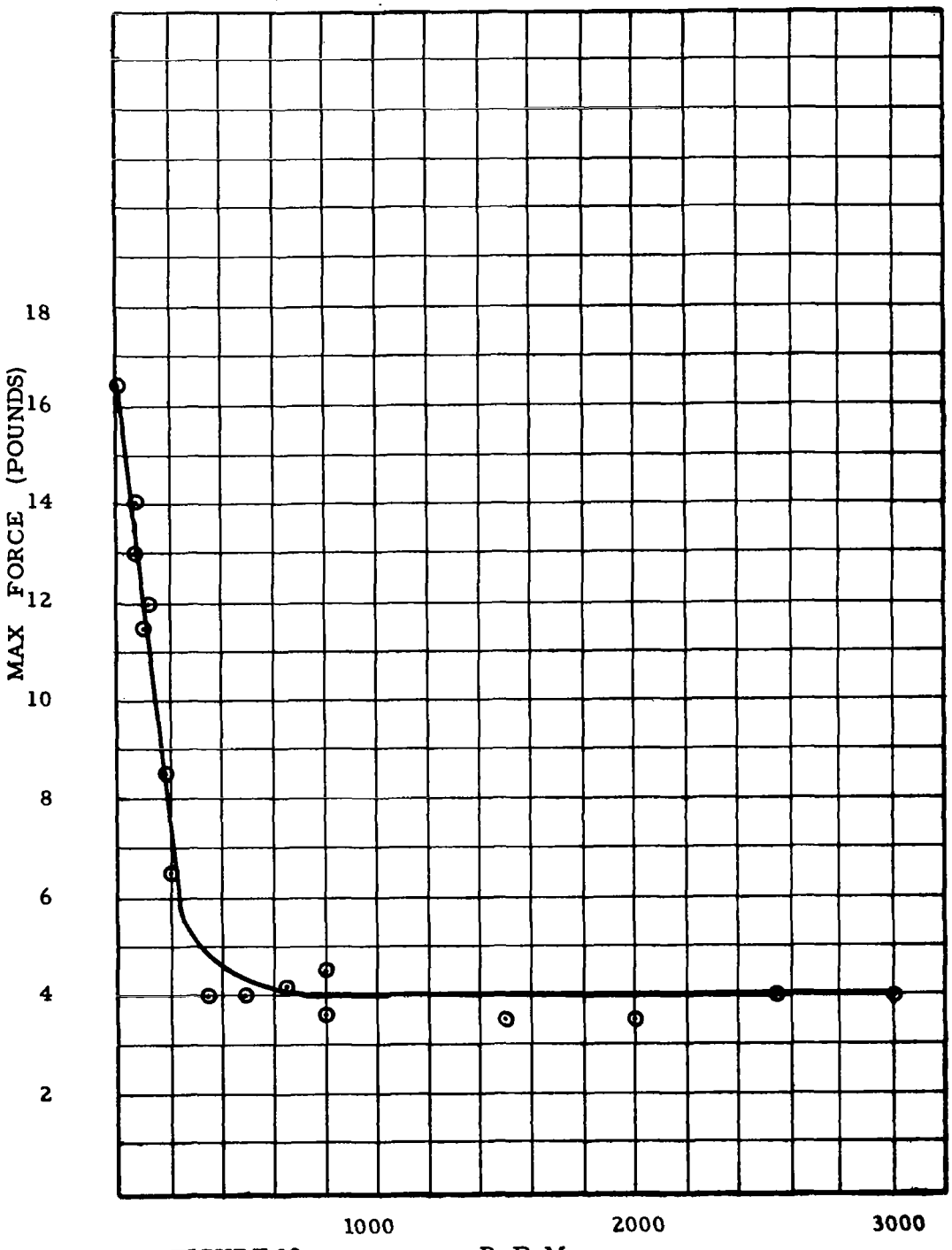

FIGURE 12

* NO LOAD 2.7 FIELD AMPS
0.004" ECCENTRICITY

SECTION VII

TEST APPARATUS AND TEST METHODS

The Brayton Cycle alternator used in the bearing force measurement tests consisted of stator wound S/N BC-374-318 and the rotor from the in-house alternator research package.

This rotor had small diameter shaft extensions suitable for use with anti-friction bearings, and can be seen in Figure 13. The bearings used were MRC R type bearings which had a reduced shoulder and a large number of balls for increased radial stiffness. The bearings had phenolic cages and the inner races were made to ABEC-9 tolerances and the outer races to ABEC-7 tolerances to eliminate as much as possible any contribution of the bearings to rotating unbalance. The bearings were preloaded axially with about 80 pounds of force to eliminate any radial play and to increase their radial stiffness.

The test stand in which the alternator was mounted is shown in Figures 14 and 15. The alternator was flange mounted and its opposite drive end stabilized by an additional bracket. The alternator was driven by a small induction motor, which is also flange mounted and can be seen on the opposite face of the test stand. The torque of the drive motor was transmitted through a Thomas Flexible Coupling which can be seen in Figure 14. The very long center portion of this coupling allows a relatively great off-center displacement of the alternator rotor without incurring high bending forces in the alternator shaft.

The test stand was mounted on rubber isolation mounts which had a resonant frequency in the below ten cycles per second range. The Brayton Cycle alternator was water-cooled, using the same cooling passages that will be used in the eventual application. Additional cooling water was piped to the face of each of the bearing housings of the alternator. Other water was directed to the transducer arms to stabilize their temperature (see Section XII). The induction motor (to the right in Figure 14) was air-cooled with a cooling arrangement which was added later and therefore does not show in this picture. At the extreme right end of the induction motor can be seen the disc and magnetic pickup with which timing information was generated for use in data acquisition and reduction.

Since the Brayton Cycle alternator was to be driven at exactly 3000 RPM by an induction motor, and the induction motor had some speed regulation due to slip, it was necessary to have a variable frequency drive to power this setup. A schematic of the power flow and the many units involved is shown in the sketch in Figure 16. Working backward from the Brayton Cycle, the sketch shows that the Brayton Cycle alternator is driven by an induction motor which is in turn driven by an alternator. The rotational speed of this alternator must vary to make up for the slip involved at different loads in the induction motor. This alternator was therefore driven by a DC motor and that DC motor in turn driven by an adjustable voltage power supply, which, in this case, was a motor-generator set. This motor-generator set had an induction motor and a DC generator. This setup worked very smoothly and was wonderfully flexible, but did have the disadvantage of having a fair amount of speed regulation as loads were changed. If

a load were suddenly applied as in the short circuit tests, there would be a fair amount of speed change in the whole setup and, of course, particularly in the Brayton Cycle alternator. This was overcome by setting the no load speed or the pre-short speed at some higher value and letting the whole setup sag down to the 3000 RPM figure after the load was applied. The field winding of the Brayton Cycle alternator was powered from a battery which, of course, had no ripple current to add more confusion to the data.

An extensive description of the force transducer design and the accompanying system is given in Section XII. Basically, forces were measured by measuring the force between the bearing housings and the stator by mounting the bearing housings in very thin arms which were then strain gaged. The output of the strain gages then gave an indication of the bearing forces involved.

The decision was made during the course of these tests to run all of the tests at 3000 RPM rather than the 12,000 RPM figure originally specified in the contract. Some of the many reasons for making this decision and the supporting data are shown and discussed in Section XIII.

Figure 17 is a schematic of the system used to acquire the data presented in this report. The bearing force transducers were arranged in such a way that they gave a "X" and "Y" component of the force felt at the bearing housing. Both the "X" and the "Y" force components were fed into strain gage amplifiers, in this case, Tektronix "Q" units. The output of the strain gage amplifiers and the timing information were all recorded on magnetic tape. All of the data recorded was monitored on an oscilloscope.

The eccentricity of the Brayton Cycle alternator rotor with respect to its stator was adjusted by using one of four sets of bearing housings. One of these sets of bearing housings was ground with the ID concentric to its OD and each of the other sets were ground with the ID eccentric to the OD by .002", .004", and .006".

Once the Brayton Cycle alternator was set up with some particular amount of eccentricity, a test cycle could begin. A complete series of tests would be taken under all of the specified load conditions while taking force data at one end of the alternator. The "X" component of force, the "Y" component of force and timing information would all be recorded simultaneously on magnetic tape. Before each series of tests would start, a calibrating signal generated in each of the strain gage amplifiers was also recorded on tape. This calibrating signal was used to set the gain for all subsequent treatment of data, thus eliminating a great deal of confusion and worry about phase inversion and proper amounts of amplication. Each of the required tests (load conditions) would be staged and recorded in turn. After a complete series of tests was run, taking data at one end of the alternator, the whole series of tests would be repeated while data was taken at the other end of the alternator. When data from each end of the alternator was complete, the alternator would be removed from the test setup and the bearing housing for the next eccentricity condition installed.

A schematic of the data reduction setup used is shown in Figure 18. Earlier tests disclosed that there was a great deal of mechanical noise being sensed by the force transducers at frequencies above about 300 cycles per second (see Section XIII). Running the tests at 3000 RPM allowed the first three harmonics of pole frequency to be examined (100, 200 and 300 cycles per second) and the mechanical noise occurring at higher frequencies to be filtered out.

When making Lissajous figures, plotting X force versus Y force, filters were set to pass all frequencies below 300 cycles and attenuate frequencies above 300 cycles at the rate of 32 DB per octave. The DC portion of force was passed with additional low pass filters, since the variable frequency filters did not have this capability. To make a clean Lissajous figure, it was necessary to display the data acquired during only one revolution of the Brayton Cycle alternator. This was done by using the timing trace to brighten the scope beam for only the time required to display one revolution. Some of the higher frequency mechanical noise still coming through the filter would cause the oscilloscope to display multiple (but quite similar) images which were more difficult to interpret than the single revolution trace.

To set up the proper amplification and phase relation to the filter network, the calibrating signal generated in the two Q units was used. After the filters were set, the oscilloscope amplifiers were adjusted to give the proper beam deflection during the display of the calibrating signal. The attenuation of the various filters was corrected by using a calibrated voltage source at the particular frequency involved.

The Lissajous figures, having been treated with a filter which was set for a low pass of 300 cycles, had some phase shift involved in the two and three hundred cycle portion. The types of filters we were forced to use did have an effect on phase near the set frequency. This phase shift has little effect on the basic shape of the Lissajous figures.

When X force versus time or Y force versus time data was to be displayed and recorded, the filtering arrangement was used in a different manner. In this case, it was desired to generate a trace that would be useful in comparing analytically generated force predictions with experimental data. In this case, it was important that there be no phase shift existing and that the phase relationships between pole frequency and the second and third harmonic of pole frequency be preserved without distortion. To do this, the DC portion of the force was passed with a separate low pass network and the information at pole frequency (100 cycles per second) was added to this. The filters were set with both high pass and low pass at 100 cycles per second, creating a band pass filter. The filters attenuated at the rate of 32 DB per octave on each side of the desired frequency. Using the filters in this fashion generated no phase shift, since they were symmetrical about the frequency of interest. This procedure was repeated with the filters set to pass 200 and 300 cps to obtain information at the second and third harmonic of pole frequency.

None of the tests were taken by running the Brayton Cycle alternator to a temperature equilibrium because it was felt that this would accomplish no real purpose. For each of the load conditions, there would be a different temperature distribution established in the machine. Any temperature effect on the resistance of amortisseur or armature windings would be different for each of these cases and the data would be as much in error having run the alternator to one highly variable temperature equilibrium as to run it to a variable transient condition. This allowed a great savings in time over running to temperature equilibrium. The data resulting from this series of tests probably is of an accuracy that would mask any of these temperature effects.

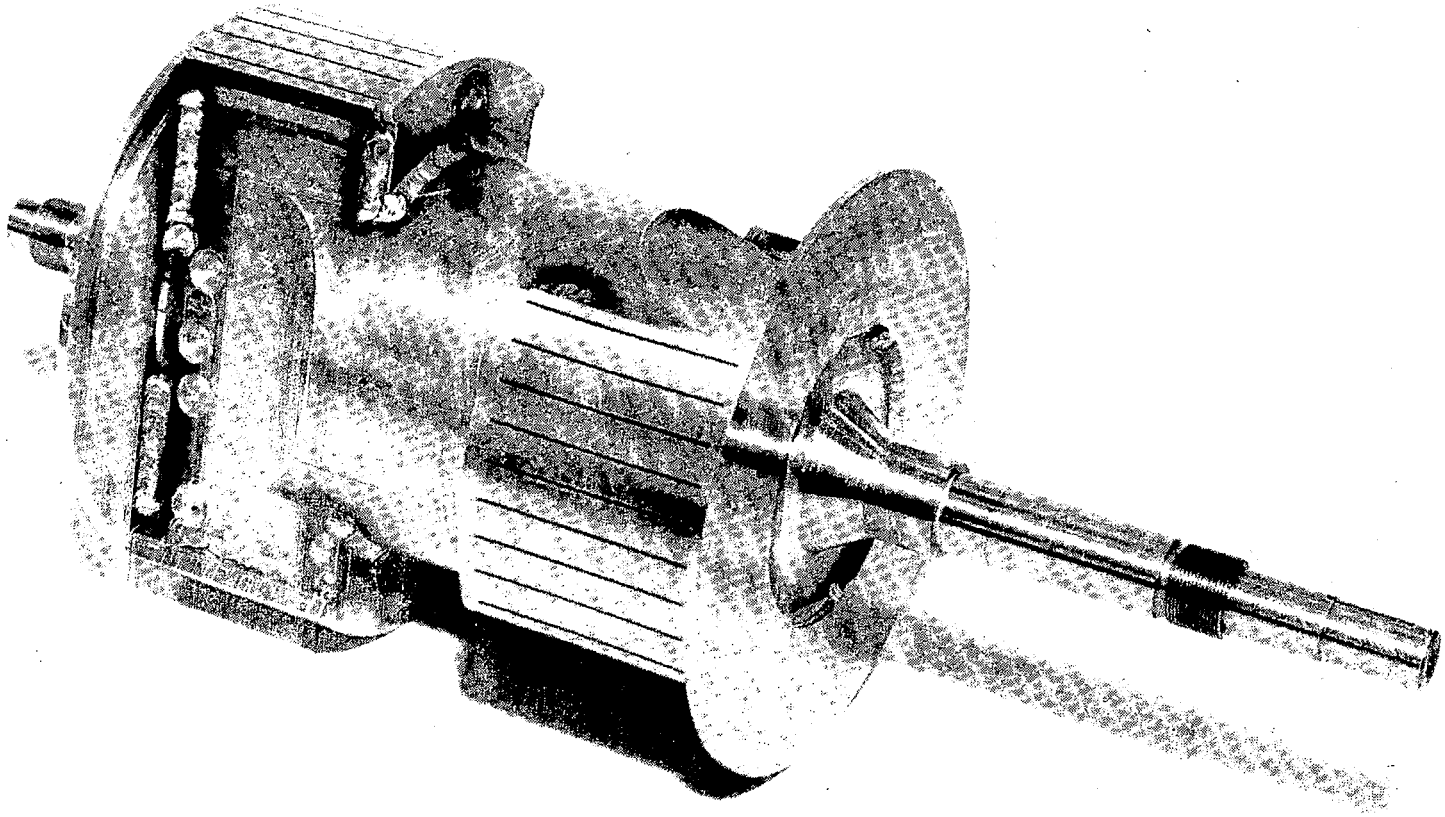

ARP BRAYTON CYCLE ROTOR

FIGURE 13

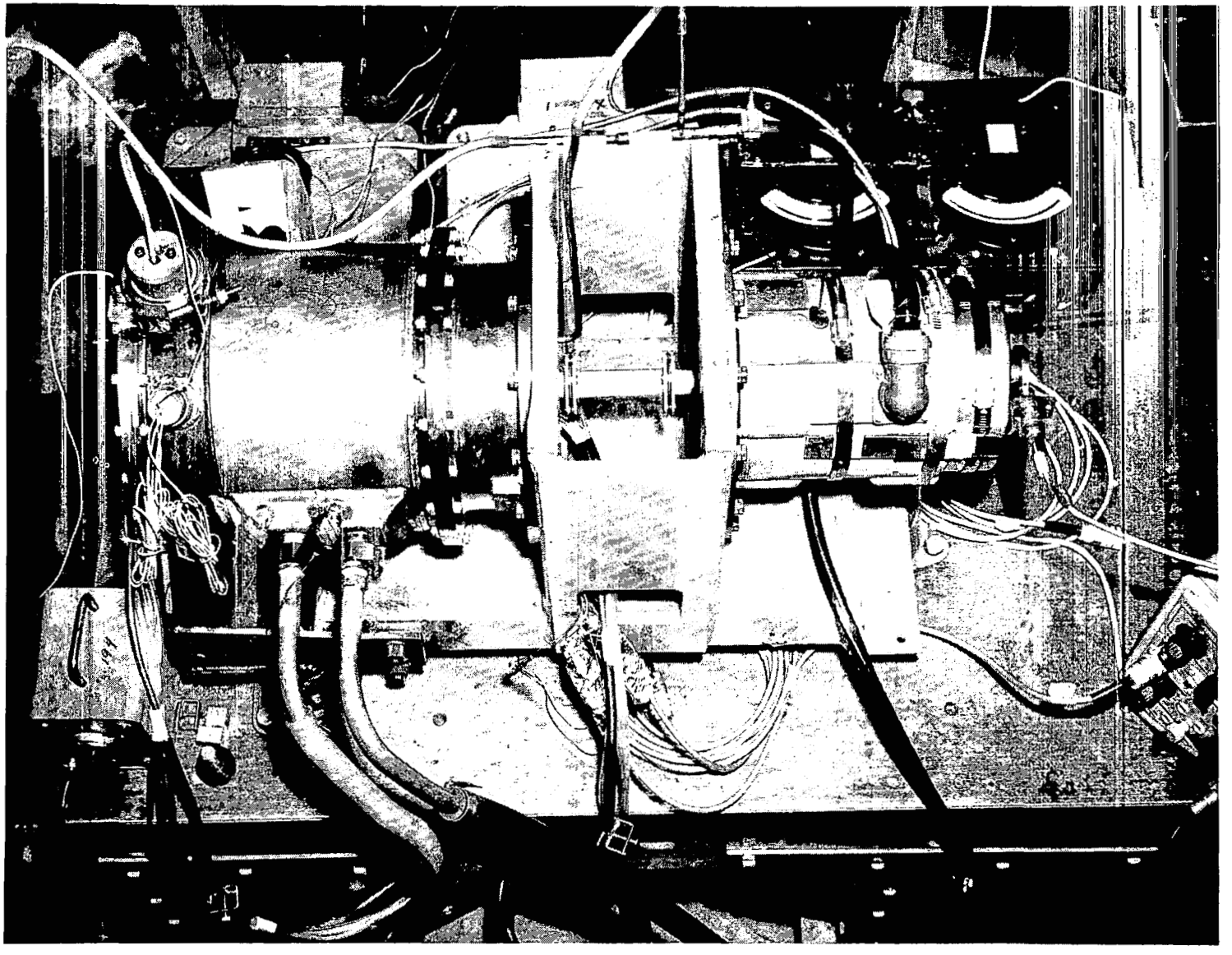

BEARING FORCE TEST RIG-ALTERNATOR AND DRIVE MOTOR

FIGURE 14

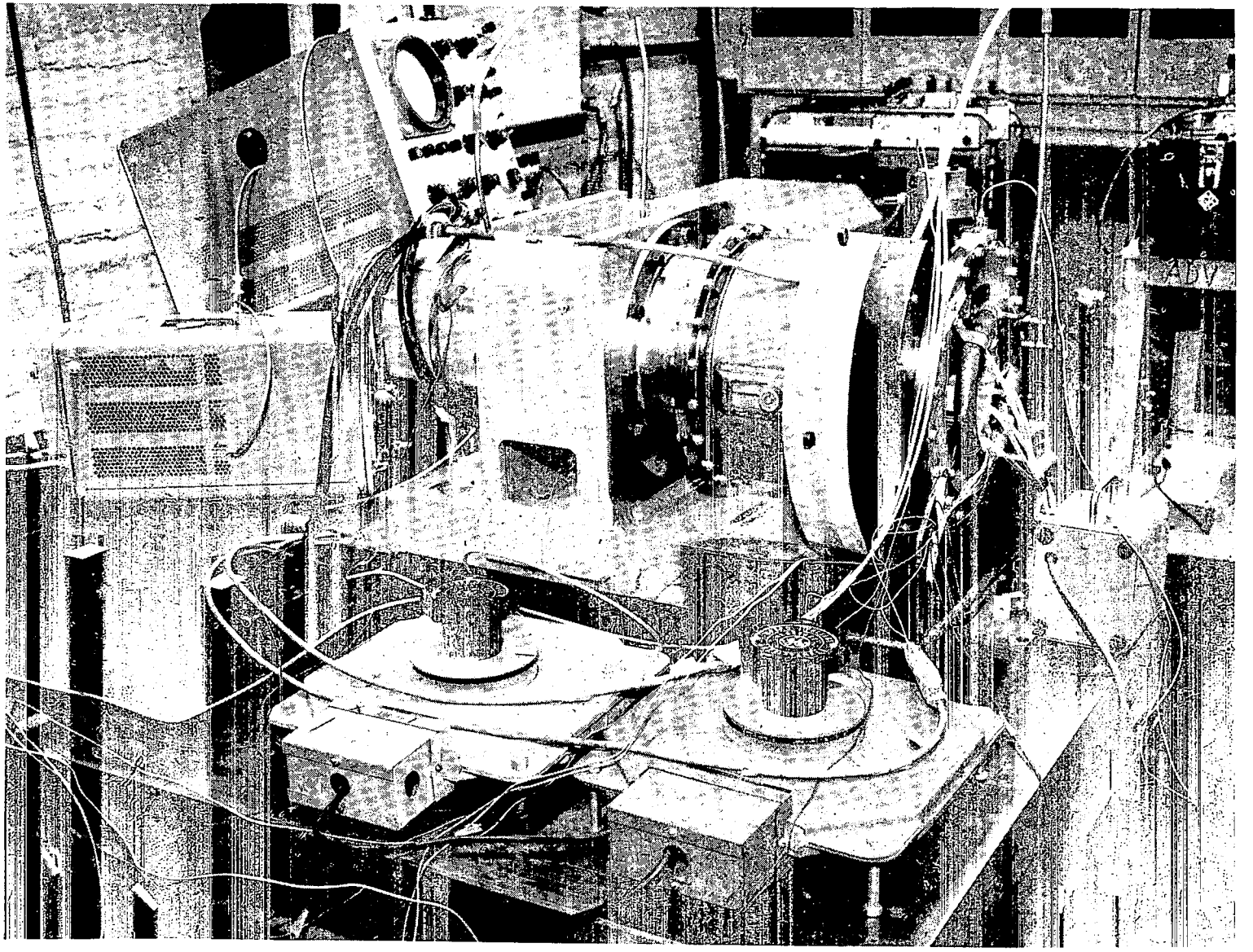

BEARING FORCE TEST RIG ALTERNATOR, DRIVE MOTOR, AND TEST APPARATUS

FIGURE 15

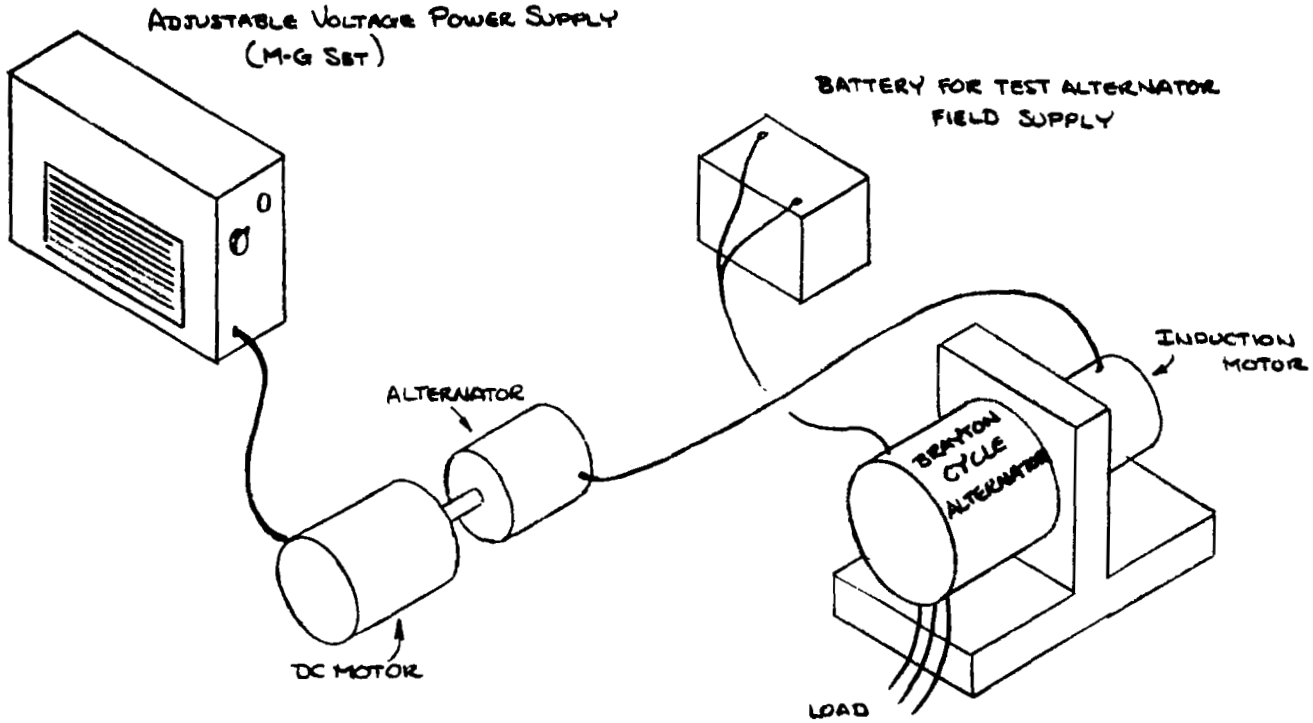

SCHEMATIC - TEST SET UP FOR DRIVING BRAYTON CYCLE ALTERNATOR

FIGURE 16

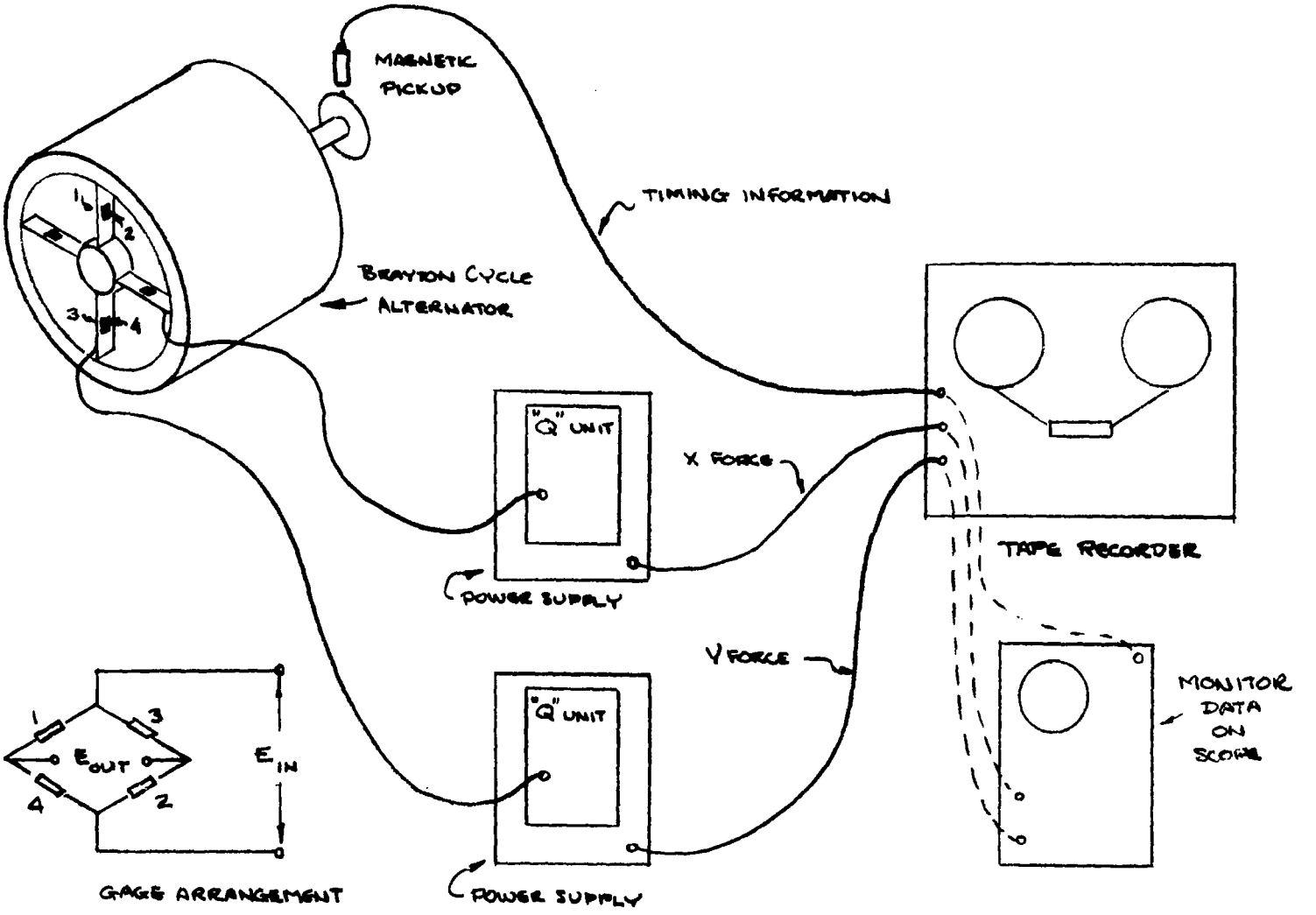

DATA ACQUISITION

FIGURE 17

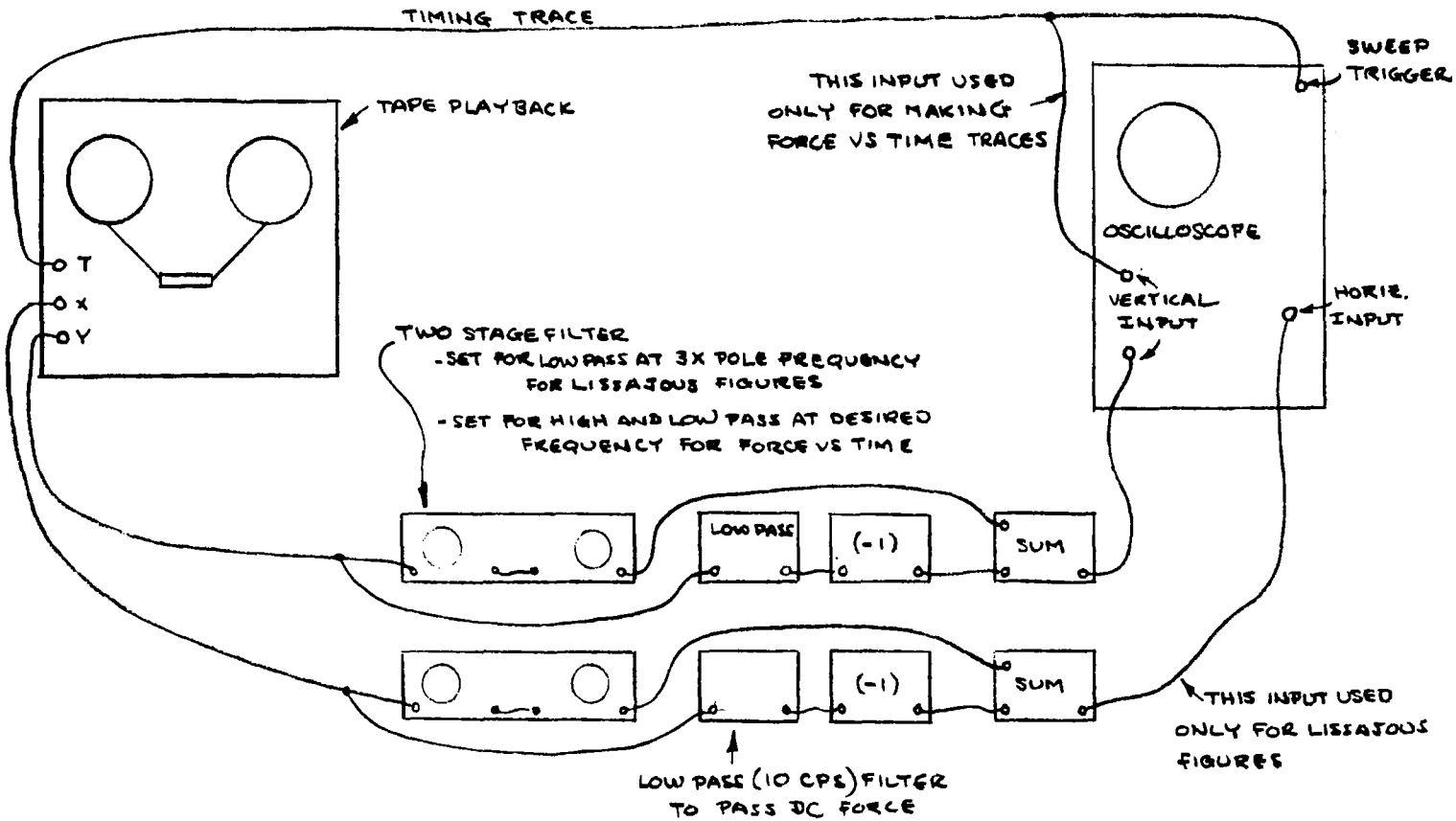

DATA REDUCTION

FIGURE 18

SECTION VIII

Complete Analytical Expressions

Case — Page

Each Case is Broken Down Into

(a) Force in the Y-direction (pounds)
(b) Rate of change of force in the Y direction with respect to eccentricity (pounds/inch)
(c) Rate of change of force in the Y direction with respect to eccentricity angle (pounds/radian)
(d) Force in the X-direction
(e) Rate of change of force in the X direction with respect to eccentricity (pounds/inch).
(f) Rate of change of force in the X direction with respect to eccentricity angle (pounds/radian)
(g) Definition of terms for the above expressions.

CASE I UNSATURATED
15 KVA, 0.8 PF BALANCED LOAD

The analytical expression for the radial bearing force on one end of the Brayton Cycle Alternator when operating at 15 KVA, .8 PF lagging, balanced load is given below. An eccentricity of .002" has been used in arriving at the force coefficients. These expressions are for the unsaturated case. The effect of saturation is to decrease the bearing force. Since the Brayton Cycle Alternator has two (2) circuits in the stator windings, the calculated forces have been divided by two (2) and the given expression reflects this division. All harmonic forces less than 0.1 pounds have been neglected. The co-ordinate system is fixed in the stator.

A. Force in the Y direction (pounds)

$$
\begin{aligned}
F_y = \quad & -.67 \cos(2\omega t - B + 5\phi) - .24 \cos(2\omega t - B + 7\phi) \\
& -20.950 \cos(2\omega t - B + \phi) - 37.15 \cos(B) \\
& -.845 \cos(B - 5\phi) - .22 \cos(B - 4\phi) \\
& -.845 \cos(B + 5\phi) - 17.115 \cos(B + \phi) \\
& -.5 \cos(2\omega t - B - 5\phi) - 17.215 \cos(B - \phi) \\
& -35.025 \cos(2\omega t - B) - 8.87 \cos(2\omega t - B - \phi) \\
& +.26 \cos(2\omega t - B + 4\phi) - .275 \cos(2\omega t - B - 2\phi) \\
& -1.345 \cos(B + 2\phi) - 2.28 \cos(2\omega t - B + 2\phi) \\
& +1.425 \cos(B - 2\phi) - .11 \cos(B + 4\phi)
\end{aligned}
$$

B. Rate of change of F_y with respect to eccentricity (pounds/inch)

$$
\begin{aligned}
\frac{dF_y}{d\delta} = \quad & -335.0 \cos(2\omega t - B + 5\phi) - 120.0 \cos(2\omega t - B + 7\phi) \\
& -10{,}475.0 \cos(2\omega t - B + \phi) - 18{,}575.0 \cos(B) \\
& -422.5 \cos(B - 5\phi) - 110.0 \cos(B - 4\phi) \\
& -422.5 \cos(B + 5\phi) - 8{,}557.5 \cos(B + \phi) \\
& -250.0 \cos(2\omega t - B - 5\phi) - 8{,}607.5 \cos(B - \phi) \\
& -17{,}512.5 \cos(2\omega t - B) - 4{,}435.0 \cos(2\omega t - B - \phi) \\
& +130.0 \cos(2\omega t - B + 4\phi) - 137.5 \cos(2\omega t - B - 2\phi) \\
& -672.5 \cos(B + 2\phi) - 1{,}140.0 \cos(2\omega t - B + 2\phi) \\
& -712.5 \cos(B - 2\phi) - 55.0 \cos(B + 4\phi)
\end{aligned}
$$

C. Rate of change of F_y with respect to eccentricity angle (pounds/radian)

$$
\begin{aligned}
\frac{dF_y}{dB} = \quad & -.67 \sin(2\omega t - B + 5\phi) - .24 \sin(2\omega t - B + 7\phi) \\
& -20.950 \sin(2\omega t - B + \phi) + 37.15 \sin(B) \\
& +.845 \sin(B - 5\phi) + .22 \sin(B - 4\phi) \\
& +.845 \sin(B + 5\phi) + 17.115 \sin(B + \phi) \\
& -.5 \sin(2\omega t - B - 5\phi) + 17.215 \sin(B - \phi) \\
& -35.025 \sin(2\omega t - B) - 8.87 \sin(2\omega t - B - \phi) \\
& +.26 \sin(2\omega t - B + 4\phi) - .275 \sin(2\omega t - B - 2\phi) \\
& +1.345 \sin(B + 2\phi) - 2.28 \cos(2\omega t - B + 2\phi) \\
& +1.425 \sin(B - 2\phi) + .11 \sin(B + 4\phi)
\end{aligned}
$$

D. Force in the X direction (pounds)

$F_x =$ -.67 sin (2wt-B+5Ø) -.24 sin (2wt-B+7Ø)
-20.950 sin (2wt-B+Ø) -37.15 sin (B)
-.845 sin (B-5Ø) -.22 sin (B-4Ø)
-.845 sin (B+5Ø) -17.115 sin (B+Ø)
-.5 sin (2wt-B-5Ø) -17.215 sin (B-Ø)
-35.025 sin (2wt-B) -8.87 sin (2wt-B-Ø)
+.26 sin (2wt-B+4Ø) -.275 sin (2wt-B-2Ø)
-1.345 sin (B+2Ø) -2.28 sin (2wt-B+2Ø)
-1.425 sin (B-2Ø) -.11 sin (B+4Ø)

E. Rate of change of F_x with respect to eccentricity (pounds/inch)

$\frac{dF_x}{d\delta} =$ -335.0 sin (2wt-B+5Ø) -120.0 sin (2wt-B+7Ø)
-10,475.0 sin (2wt-B+Ø) -18,575.0 sin (B)
-422.5 sin (B-5Ø) -110.0 sin (B-4Ø)
-422.5 sin (B+5Ø) -8,557.5 sin (B+Ø)
-250.0 sin (2wt-B-5Ø) -8,607.5 sin (B-Ø)
-17,512.5 sin (2wt-B) -4,435.0 sin (2wt-B-Ø)
+130.0 sin (2wt-B+4Ø) -137.5 sin (2wt-B-2Ø)
-672.5 sin (B+2Ø) -1,140.0 sin (2wt-B+2Ø)
-712.5 sin (B-2Ø) -55.0 sin (B+4Ø)

F. Rate of change of F_x with respect to eccentricity angle (pounds/radian)

$\frac{dF_x}{dB}$ +.67 cos (2wt-B+5Ø) +.24 cos (2wt-B+7Ø)
+20.950 cos (2wt-B+Ø) -37.15 cos (B)
-.845 cos (B-5Ø) -.22 cos (B-4Ø)
-.845 cos (B+5Ø) -17.115 cos (B+Ø)
+.5 cos (2wt-B-5Ø) -17.215 cos (B-Ø)
+35.025 cos (2wt-B) +8.87 cos (2wt-B-Ø)
-.26 cos (2wt-B+4Ø) +.275 cos (2wt-B-2Ø)
-1.345 cos (B+2Ø) +2.28 cos (2wt-B+2Ø)
-1.425 cos (B-2Ø) -.11 cos (B+4Ø)

G. Definition of terms in above expressions

t = time (secs)
w = mechanical angular velocity (1256 radians/sec)
B = mechanical angle between Y axis and direction of eccentricity (radians)
δ = eccentricity (inches)
Ø = π - power angle (radians)
Power Angle = Electrical angle between load current and direct axis magnetizing current (use.6 radians)

CASE I SATURATED
15 KVA, 0.8 PR BALANCED LOAD

The analytical expression for the radial bearing force on one end of the Brayton Cycle Alternator when operating at 15 KVA, .8 PF lagging, balanced load are given below. An eccentricity of .002" has been used in arriving at the force coefficients. These expressions are for the saturated case. The effect of saturation is to decrease the bearing force. Since the Brayton Cycle Alternator has two (2) circuits in the stator windings, the calculated forces have been divided by two (2) and the given expression reflects this division. All harmonic forces less than 0.1 pounds have been neglected. The co-ordinate system is fixed in the stator.

A. Force in the Y direction pounds

$$F_y = -.045 \cos(2\omega t - B + 5\phi) - 18.25 \cos(2\omega t - B + \phi)$$
$$-35.14 \cos(B) - 0.11 \cos(B - 5\phi) - 0.11 \cos(B + 5\phi)$$
$$-14.88 \cos(B + \phi) - 14.82 \cos(B - \phi)$$
$$-28.62 \cos(2\omega t - B) - 7.62 \cos(2\omega t - B - \phi)$$
$$+0.04 \cos(2\omega t - B + 4\phi) - 0.07 \cos(2\omega t - B - 2\phi)$$
$$-1.18 \cos(B + 2\phi) - 2.28 \cos(2\omega t - B + 2\phi)$$
$$-1.24 \cos(B - 2\phi)$$

B. Rate of change of F_y with respect to eccentricity (pounds/inch)

$$\frac{dF_y}{d\delta} = -22.5 \cos(2\omega t - B + 5\phi) - 9125.0 \cos(2\omega t - B + \phi)$$
$$-17570.0 \cos(B) - 55.0 \cos(B - 5\phi) - 55.0 \cos(B + 5\phi)$$
$$-7440.0 \cos(B + \phi) - 7410.0 \cos(B - \phi)$$
$$-14310.0 \cos(2\omega t - B) - 3810.0 \cos(2\omega t - B - \phi)$$
$$+20.0 \cos(2\omega t - B + 4\phi) - 35.0 \cos(2\omega t - B - 2\phi)$$
$$-590.0 \cos(B + 2\phi) - 1140.0 \cos(2\omega t - B + 2\phi)$$
$$-620.0 \cos(B - 2\phi)$$

C. Rate of change of F_y with respect to eccentricity angle (pounds/radian)

$$\frac{dF_y}{d\beta} = -.045 \sin(2\omega t - B + 5\phi) - 18.25 \sin(2\omega t - B + \phi)$$
$$+35.14 \sin(B) + 0.11 \sin(B - 5\phi) + 0.11 \sin(B + 5\phi)$$
$$+14.88 \sin(B + \phi) + 14.82 \sin(B - \phi)$$

$-28.62 \sin (2\,wt - B) - 7.62 \sin (2\,wt - B - \phi)$

$+0.04 \sin (2\,wt - B + 4\phi) - 0.07 \sin (2\,wt - B - 2\phi)$

$+ 1.18 \sin (B + 2\phi) - 2.28 \sin (2\,wt - B + 2\phi)$

$+1.24 \sin (B - 2\phi)$

D. Force in the X direction (pounds)

$$F_x = -.045 \sin (2\,wt - B + 5\phi) - 18.25 \sin (2\,wt - B + \phi)$$
$$-35.14 \sin (B) - 0.11 \sin (B - 5\phi) - 0.11 \sin (B + 5\phi)$$
$$-14.88 \sin (B + \phi) - 14.82 \sin (B - \phi)$$
$$-28.62 \sin (2\,wt - B) - 7.62 \sin (2\,wt - B - \phi)$$
$$+0.04 \sin (2\,wt - B + 4\phi) - 0.07 \sin (2\,wt - B - 2\phi)$$
$$-1.18 \sin (B + 2\phi) - 2.28 \sin (2\,wt - B + 2\phi)$$
$$-1.24 \sin (B - 2\phi)$$

E. Rate of change of F_x with respect to eccentricity (pounds/inch)

$$\frac{dF_x}{d\delta} = -22.5 \sin (2\,wt - B + 5\phi) - 9125.0 \sin (2\,wt - B + \phi)$$
$$-17570.0 \sin (B) -55.0 \sin (B - 5\phi) - 55.0 \sin (B + 5\phi)$$
$$-7440.0 \sin (B + \phi) - 7410.0 \sin (B - \phi)$$
$$-14310,0 \sin (2\,wt - B) - 3810.0 \sin (2\,wt - B - \phi)$$
$$+20.0 \sin (2\,wt - B + 4\phi) - 35.0 \sin (2\,wt - B - 2\phi)$$
$$-590.0 \sin (B + 2\phi) - 1140.0 \sin (2\,wt - B + 2\phi)$$
$$-620.0 \sin (B - 2\phi)$$

F. Rate of change of F_x with respect to eccentricity angle (pounds/radian)

$$\frac{dF_x}{dB} = +.045 \cos (2\,wt - B + 5\phi) + 18.25 \cos (2\,wt - B + \phi)$$
$$-35.14 \cos (B) - 0.11 \cos (B-5\phi) - 0.11 \cos (B + 5\phi)$$
$$-14.88 \cos (B + \phi) - 14.82 \cos (B - \phi)$$
$$+28.62 \sin (2\,wt - B) + 7.62 \cos (2\,wt - B - \phi)$$
$$-0.04 \cos (2\,wt - B + 4\phi) + 0.07 \cos (2\,wt - B - 2\phi)$$

$$-1.18 \cos (B + 2\phi) + 2.28 \cos (2 wt - B + 2\phi)$$

$$-1.24 \cos (B - 2\phi)$$

G. Definitions same as unsaturated Case I except use

$$\phi = 2.5646 \text{ or } (\pi - 0.577 \text{ radians})$$

CASE II
11.25 KVA 0.8 PF BALANCED LOAD

The analytical expression for the radial bearing force on one end of the Brayton Cycle Alternator when operating at 11.25 KVA, .8 PF lagging, balanced load given below. An eccentricity of .002" has been used in arriving at the force coefficients. Since the Brayton Cycle Alternator has two (2) circuits in the stator windings, the calculated forces have been divided by two (2) and the given expression reflects this division. The co-ordinate system is fixed in the stator.

A. Force in the Y direction (pounds)

$$F_y = -.06 \cos(2\omega t - B + 5\phi) - 12.045 \cos(2\omega t - B + \phi) - 25.395 \cos(B) - 0.03 \cos(B - 5\phi) - 0.03 \cos(B + 5\phi) - 9.81 \cos(B + \phi) - 9.77 \cos(B - \phi) - 20.69 \cos(2\omega t - B) - 4.97 \cos(2\omega t - B - \phi) - 0.04 \cos(2\omega t - B - 2\phi) - .67 \cos(B + 2\phi) - 1.31 \cos(2\omega t - B + 2\phi) - .7 \cos(B - 2\phi)$$

B. Rate of change of F_y with respect to eccentricity (pounds/inch)

$$\frac{dF_y}{d\epsilon} = -30.0 \cos(2\omega t - B + 5\phi) - 6{,}022 \cos(2\omega t - B + \phi) - 12{,}697.5 \cos(B) - 15 \cos(B - 5\phi) - 15 \cos(B + 5\phi) - 4{,}905.0 \cos(B + \phi) - 4{,}885.0 \cos(B - \phi) - 10{,}348 \cos(2\omega t - B) - 2{,}485.0 \cos(2\omega t - B - \phi) - 20.0 \cos(2\omega t - B - 2\phi) - 332.5 \cos(B + 2\phi) - 655.0 \cos(2\omega t - B + 2\phi) - 350.0 \cos(B - 2\phi)$$

C. Rate of change of F_y with respect to eccentricity angle (pounds/radian).

$$\frac{dF_y}{dB} = -.06 \sin(2\omega t - B + 5\phi) - 12.045 \sin(2\omega t - B + \phi) + 25.395 \sin(B) + 0.03 \sin(B - 5\phi) + 0.03 \sin(B + 5\phi) + 9.81 \sin(B + \phi) + 9.77 \sin(B - \phi) - 20.69 \sin(2\omega t - B) - 4.97 \sin(2\omega t - B - \phi) - 0.04 \sin(2\omega t - B - 2\phi) + .67 \sin(B + 2\phi) - 1.31 \sin(2\omega t - B + 2\phi) + .70 \sin(B - 2\phi)$$

D. Force in the X direction (pounds)

F_x = -.06 sin (2wt-B+5Ø)
-12.045 sin (2wt-B+Ø) -25.935 sin (B)
-0.03 sin (B-5Ø)
-0.03 sin (B+5Ø) -9.81 sin (B+Ø)
-9.77 sin (B-Ø)
-20.69 sin (2wt-B) -4.97 sin (2wt-B-Ø)
-0.04 sin (2wt-B-2Ø)
-.67 sin (B+2Ø) -1.31 sin (2wt-B+2Ø)
-.70 sin (B-2Ø)

E. Rate of change of F_x with respect to eccentricity (pounds/inch).

$\frac{dF_x}{d\delta}$ = -30. sin (2wt-B+5Ø)
-6,022 sin (2wt-B+Ø) -12,697.0 sin (B)
-15.0 sin (B-5Ø)
-15.0 sin (B+5Ø) -4,905.0 sin (B+Ø) - 4,885 sin (B-Ø)
-10,348 sin (2wt-B) -2,485.0 sin (2wt-B-Ø)
-20.0 sin (2wt-B-2Ø)
-332.5 sin (B+2Ø) -655.0 sin (2wt-B+2Ø)
-350.0 sin (B-2Ø)

F. Rate of change of F_x with respect to eccentricity angle (pounds/radian)

$\frac{dF_x}{dB}$ = +0.06 cos (2wt-B+5Ø)
+12.045 cos (2wt-B+Ø) -25.395 cos (B)
-0.03 cos (B-5Ø)
-0.03 cos (B+5Ø) -9.81 cos (B+Ø)
-9.77 cos (B-Ø)
+20.69 cos (2wt-B) +4.97 cos (2wt-B-Ø)
+0.04 cos (2wt-B-2Ø)
-.67 cos (B+2Ø) +1.31 cos (2wt-B+2Ø)
-.70 cos (B-2Ø)

G. Definition of terms in above expressions

t= time (secs)
w= mechanical angular velocity (1256 radians/sec)
B= mechanical angle between Y axis and direction of eccentricity (radians)
δ= eccentricity (inches)
Ø= π -power angle (radians)
Power Angle = electrical angle between load current and direct axis magnetizing current (use .625 radians)

CASE III NO LOAD

The following force expression is for the no load case where the machine is operating at 120 V L-N balanced 3Ø with no armature current.

A. $F_y =$

$$\begin{aligned}&-0.08 \cos (B-\phi) -7.65 \cos (B)\\&-0.10 \cos (B+\phi) -0.03 \cos (2wt-B-\phi)\\&-6.17 \cos (2wt-B) -0.13 \cos (2wt-B+\phi)\end{aligned}$$

B. $\frac{dF_y}{d\delta} =$

$$\begin{aligned}&-40.0 \cos (B-\phi) -3,825.0 \cos (B)\\&-50.0 \cos (B+\phi) -15.0 \cos(2wt -B-\phi)\\&-3085.0 \cos (2wt-B) -65.0 \cos (2wt-B+\phi)\end{aligned}$$

C. $\frac{dF_y}{dB} =$

$$\begin{aligned}&+0.08 \sin (B-\phi) +7.65 \sin (B)\\&+0.10 \sin (B+\phi) -0.03 \sin (2wt-B-\phi)\\&-6.17 \sin (2wt-B) -0.13 \sin (2wt-B+\phi)\end{aligned}$$

D. F_x

$$\begin{aligned}&-0.08 \sin (B-\phi) -7.65 \sin (B)\\&-0.10 \sin (B+\phi) -0.03 \sin (2wt-B-\phi)\\&-6.17 \sin (2wt-B) -0.13 \sin (2wt-B+\phi)\end{aligned}$$

E. $\frac{dF_x}{d\delta} =$

$$\begin{aligned}&-40.0 \sin (B-\phi) -3,825.0 \sin (B)\\&-50.0 \sin (B+\phi) -15.0 \sin (2wt-B-\phi)\\&-3085.0 \sin (2wt-B) -65.0 \sin (2wt-B+\phi)\end{aligned}$$

F. $\frac{dF_x}{dB} =$

$$\begin{aligned}&-0.08 \cos (B-\phi) -7.65 \cos (B)\\&-0.10 \cos (B+\phi) +0.03 \cos (2wt-B-\phi)\\&+6.17 \cos (2wt-B) +0.13 \cos (2wt-B+\phi)\end{aligned}$$

G. Definition of terms in above expressions

t = time (secs)
w = mechanical angular velocity (1256 radians/sec)
B = mechanical angle between Y axis and direction of eccentricity (radians)
= eccentricity (inches)
Ø = - power angle (radians)
Power Angle = electrical angle between load current and direct axis magnetizing current (use 1.505 radians).

CASE IV

3 Phase Balanced Short Circuit

The analytical expression for the radial bearing force on one end of the Brayton Cycle Alternator when operating at a 3 phase balanced short circuit condition is given below. An eccentricity of .002" has been used in arriving at the force coefficients. Since the Brayton Cycle Alternator has two (2) circuits in the stator winding, the calculated forces have been divided by two (2) and the given expression reflects this division. The co-ordinate system is fixed in the stator.

A. F_y =

-0.02 cos (-B+6Ø) -155.87 cos (B-Ø)
-22.89 cos (B-2Ø) - 0.53 cos (B-4Ø)
-1.19 cos (B-5Ø) - 0.56 cos (B-6Ø)
-0.12 cos (B-7Ø) -280.72 cos (B)
-155.94 cos (B+Ø) -22.01 cos (B+2Ø)
-0.29 cos (B+4Ø) -1.19 cos (B+5Ø)
-0.52 cos (B+6Ø) -0.12 cos (B+7Ø)
-87.31 cos (2wt-B-Ø) -4.00 cos (2wt-B-2Ø)
-0.52 cos (2wt-B-4Ø) -0.69 cos (2wt-B-5Ø)
-0.18 cos (2wt-B-6Ø) +0.02 cos (2wt-B-7Ø)
-232.62 cos (2wt-B) -183.04 cos (2wt-B+Ø)
-39.20 cos (2wt-B+2Ø) +0.36 (2wt-B+4Ø)
-0.80 cos (2wt-B+5Ø) -0.98 cos (2wt-B+6Ø)
-0.37 cos (2wt-B+7Ø) -0.06 cos (2wt-B+8Ø)
+0.02 cos (2wt+B-7Ø) +0.01 cos (4wt-B+7Ø)
+0.01 cos (4wt+B7Ø) +0.01 cos (6wt-B-4Ø)
+0.01 cos (6wt+B+4Ø) +0.02 cos (8wt-B-4Ø)
+0.02 cos (8wt-B-5Ø) +0.02 cos (8wt+B+4Ø)
+0.02 cos (8wt+B+5Ø) +0.03 cos (10wt-B-5Ø)
+0.01 cos (10wt-B-6Ø) +0.03 cos (10wt+B+5Ø)
+0.01 cos (10wt+B+6Ø) -0.04 cos (12wt-B-4Ø)
+0.02 cos (12wt-B-6Ø) -0.04 cos (12wt+B+4Ø)
+0.02 cos (12wt+B+6Ø) -0.08 cos (14wt-B-4Ø)
-0.08 cos (14wt-B-5Ø) -0.08 cos (14wt+B+4Ø)
-0.08 cos (14wt+B+5Ø) -0.12 cos (16wt-B-4Ø)
-0.16 cos (16wt-B-5Ø) -0.04 cos (16wt-B-6Ø)
-0.12 cos (16wt+B+4Ø) -0.16 cos (16wt+B+5Ø)
-0.04 cos (16wt+B+6Ø) -0.08 cos (18wt-B-4Ø)
-0.24 cos (18wt-B-5Ø) -0.08 cos (18wt-B-6Ø)
-0.08 cos (18wt+B+4Ø) -0.24 cos (18wt+B+5Ø)
-0.08 cos (18wt+B+6Ø) -0.04 cos (20wt-B-4Ø)
-0.16 cos (20wt-B-5Ø) -0.12 cos (20wt-B-6Ø)
-0.04 cos (20wt+B+4Ø) -0.16 cos (20wt+B+5Ø)
-0.12 cos (20wt+B+6Ø) -0.08 cos (22wt-B-5Ø)
-0.08 cos (22wt-B-6Ø) -0.08 cos (22wt+B+5Ø)
-0.08 cos (22wt+B+6Ø) +0.02 cos (24wt-B-4Ø)
-0.04 cos (24wt-B-6Ø) +0.02 cos (24wt+B+4Ø)
-0.04 cos (24wt+B+6Ø) +0.01 cos (26wt-B-4Ø)
+0.03 cos (26wt-B-5Ø) +0.01 cos (26wt+B+4Ø)
+0.03 cos (26wt+B+5Ø) +0.02 cos (28wt-B-5Ø)
+0.02 cos (28wt-B-6Ø) +0.02 cos (28wt+B+5Ø)
+0.02 cos (28wt+B+6Ø) +0.01 cos (30wt-B-6Ø)
+0.01 cos (30wt+B+6Ø) -0.20 cos (46wt-B)
-0.24 cos (46wt-B+Ø) - 0.04 cos (46wt-B+2Ø)
-0.16 cos (48wt+B-Ø) -0.48 cos (48wt+B)
-0.16 cos (48wt+B+Ø) - 0.24 cos (50wt-B-Ø)
-0.42 cos (50wt-B) -0.24 cos (50wt-B+Ø)
-0.08 cos (98wt-B-Ø) -0.12 cos (98wt-B)

B. Rate of change of F_y with respect to eccentricity (pounds/inch)

$$\frac{dF_y}{d\delta} =$$

$$
\begin{aligned}
&-10 \cos(-B+6\phi) - 77{,}935 \cos(B-\phi) \\
&-11{,}445 \cos(B-2\phi) - 265 \cos(B-4\phi) \\
&-595 \cos(B-5\phi) - 280 \cos(B-6\phi) \\
&-60 \cos(B-7\phi) - 140{,}360 \cos(B) \\
&-77{,}970 \cos(B+\phi) - 11{,}005 \cos(B+2\phi) \\
&-145 \cos(B+4\phi) - 595 \cos(B+5\phi) \\
&-260 \cos(B+6\phi) - 60 \cos(B+7\phi) \\
&-43{,}655 \cos(2\omega t-B-\phi) - 2000 \cos(2\omega t-B-2\phi) \\
&-260 \cos(2\omega t-B-4\phi) - 345 \cos(2\omega t-B-5\phi) \\
&-90 \cos(2\omega t-B-6\phi) + 10 \cos(2\omega t-B-7\phi) \\
&-116{,}310 \cos(2\omega t-B) - 94{,}020 \cos(2\omega t-B+\phi) \\
&-19{,}600 \cos(2\omega t-B+2\phi) + 180 \cos(2\omega t-B+4\phi) \\
&-400 \cos(2\omega t-B+5\phi) - 490 \cos(2\omega t-B+6\phi) \\
&-185 \cos(2\omega t-B+7\phi) - 30 \cos(2\omega t-B+8\phi) \\
&+10 \cos(2\omega t+B-7\phi) + 5 \cos(4\omega t-B+7\phi) \\
&+5 \cos(4\omega t+B-7\phi) + 5 \cos(6\omega t-B-4\phi) \\
&+5 \cos(6\omega t+B+4\phi) + 10 \cos(8\omega t-B-4\phi) \\
&+10 \cos(8\omega t-B-5\phi) + 10 \cos(8\omega t+B+4\phi) \\
&+10 \cos(8\omega t+B+5\phi) + 15 \cos(10\omega t-B-5\phi) \\
&+5 \cos(10\omega t-B-6\phi) + 15 \cos(10\omega t+B+5\phi) \\
&+5 \cos(10\omega t+B+6\phi) - 20 \cos(12\omega t-B-4\phi) \\
&+10 \cos(12\omega t-B-6\phi) - 20 \cos(12\omega t+B+4\phi) \\
&+10 \cos(12\omega t+B+6\phi) - 40 \cos(14\omega t-B-4\phi) \\
&-40 \cos(14\omega t-B-5\phi) - 40 \cos(14\omega t+B+4\phi) \\
&-40 \cos(14\omega t+B+5\phi) - 60 \cos(16\omega t-B-4\phi) \\
&-80 \cos(16\omega t-B-5\phi) - 20 \cos(16\omega t-B-6\phi) \\
&-60 \cos(16\omega t+B+4\phi) - 80 \cos(16\omega t+B+5\phi) \\
&-20 \cos(16\omega t+B+6\phi) - 40 \cos(18\omega t-B-4\phi) \\
&-120 \cos(18\omega t-B-5\phi) - 40 \cos(18\omega t-B-6\phi) \\
&-40 \cos(18\omega t+B+4\phi) - 120 \cos(18\omega t+B+5\phi) \\
&-40 \cos(18\omega t+B+6\phi) - 20 \cos(20\omega t-B-4\phi) \\
&-80 \cos(20\omega t-B-5\phi) - 60 \cos(20\omega t-B-6\phi) \\
&-20 \cos(20\omega t+B+4\phi) - 80 \cos(20\omega t+B+5\phi) \\
&-60 \cos(20\omega t+B+6\phi) - 40 \cos(22\omega t-B-5\phi) \\
&-40 \cos(22\omega t-B-6\phi) - 40 \cos(22\omega t+B+5\phi) \\
&-40 \cos(22\omega t+B+6\phi) + 10 \cos(24\omega t-B-4\phi) \\
&-20 \cos(24\omega t-B-6\phi) + 10 \cos(24\omega t+B+4\phi) \\
&-20 \cos(24\omega t+B+6\phi) + 5 \cos(26\omega t-B-4\phi) \\
&+15 \cos(26\omega t-B-5\phi) + 5 \cos(26\omega t+B+4\phi) \\
&+15 \cos(26\omega t+B+5\phi) + 10 \cos(28\omega t-B-5\phi) \\
&+10 \cos(28\omega t-B-6\phi) + 10 \cos(28\omega t+B+5\phi) \\
&+10 \cos(28\omega t+B+6\phi) + 5 \cos(30\omega t-B-6\phi) \\
&+5 \cos(30\omega t+B+6\phi) - 100 \cos(46\omega t-B) \\
&-120 \cos(46\omega t-B+\phi) - 20 \cos(46\omega t-B+2\phi) \\
&-80 \cos(48\omega t+B-\phi) - 240 \cos(48\omega t+B) \\
&-80 \cos(48\omega t+B+\phi) - 120 \cos(50\omega t-B-\phi) \\
&-210 \cos(50\omega t-B) - 120 \cos(50\omega t-B+\phi) \\
&-40 \cos(98\omega t-B-\phi) - 60 \cos(98\omega t-B)
\end{aligned}
$$

C. Rate of change of F_y with respect to eccentricity angle (pounds/radian).

$$\frac{dF_y}{dB} =$$

-0.02 sin (-B+6Ø) +155.87 sin (B-Ø)
+22.89 sin (B-2Ø) +0.53 sin (B-4Ø)
+1.19 sin (B-5Ø) +0.56 sin (B-6Ø)
+0.12 sin (B-7Ø) +280.72 sin (B)
+155.94 sin (B+Ø) +22.02 sin (B+2Ø)
+0.29 sin (B+4Ø) +1.19 sin (B+5Ø)
+0.52 sin (B+6Ø) +0.12 sin (B+7Ø)
-87.31 sin (2wt-B-Ø) -4.00 sin (2wt-B-2Ø)
-0.52 sin (2wt-B-4Ø) -0.69 sin (2wt-B-5Ø)
-0.18 sin (2wt-B-6Ø) +0.02 sin (2wt-B-7Ø)
-232.62 sin (2wt-B) -188.04 sin (2wt-B+Ø)
-39.20 sin (2wt-B+2Ø) +0.36 sin (2wt-B+4Ø)
-0.80 sin (2wt-B+5Ø) -0.98 sin (2wt-B+6Ø)
-0.37 sin (2wt-B+7Ø) -0.06 sin (2wt-B+8Ø)
-0.02 sin (2wt+B7Ø) +0.01 sin (4wt-B+7Ø)
-0.01 sin (4wt+B-7Ø) +0.01 sin (6wt-B-4Ø)
-0.01 sin (6wt+B+4Ø) +0.02 sin (8wt-B-4Ø)
+0.02 sin (8wt-B-5Ø) -0.02 sin (8wt+B+4Ø)
-0.02 sin (8wt+B+5Ø) +0.03 sin (10wt-B-5Ø)
+0.01 sin (10wt-B-6Ø) -0.03 sin (10wt+B+5Ø)
-0.01 sin (10wt+B+6Ø) -0.04 sin (12wt-B-4Ø)
+0.02 sin (12wt-B-6Ø) +0.04 sin (12wt+B+4Ø)
-0.02 sin (12wt+B+6Ø) - 0.08 sin (14wt-B-4Ø)
-0.08 sin (14wt-B-5Ø) +0.08 sin (14wt+B+4Ø)
+0.08 sin (14wt+B+5Ø) -0.12 sin (16wt-B-4Ø)
-0.16 sin (16wt-B-5Ø) -0.04 sin (16wt-B-6Ø)
+0.12 sin (16wt+B+4Ø) +0.16 sin (16wt+B+5Ø)
+0.04 sin (16wt+B+6Ø) -0.08 sin (18wt-B-4Ø)
-0.24 sin (18wt-B-5Ø) -0.08 sin (18wt-B-6Ø)
+0.08 sin (18wt+B+4Ø) +0.24 sin (18wt+B+5Ø)
+0.08 sin (18wt+B+6Ø) -0.04 sin (20wt-B-4Ø)
-0.16 sin (20wt-B-5Ø) -0.12 sin (20wt-B-6Ø)
+0.04 sin (20wt+B+4Ø) +0.16 sin (20wt+B+5Ø)
+0.12 sin (20wt+B+6Ø) -0.08 sin (22wt-B-5Ø)
-0.08 sin (22wt-B-6Ø) +0.08 sin (22wt+B+5Ø)
+0.08 sin (22wt+B+6Ø) +0.02 sin (24wt-B-4Ø)
-0.04 sin (24wt-B-6Ø) -0.02 sin (24wt+B+4Ø)
+0.04 sin (24wt+B+6Ø) +0.01 sin (26wt-B-4Ø)
+0.03 sin (26wt-B-5Ø) -0.01 sin (26wt+B+4Ø)
-0.03 sin (26wt+B+5Ø) +0.02 sin (28wt-B-5Ø)
+0.01 sin (28wt-B-6Ø) -0.02 sin (28wt+B+5Ø)
-0.01 sin (28wt+B+6Ø) +0.01 sin (30wt-B-6Ø)
-0.01 sin (30wt+B+6Ø) -0.20 sin (46wt-B)
-0.24 sin (46wt-B+Ø) -0.04 sin (46wt-B+2Ø)
+0.16 sin (48wt+B-Ø) +0.48 sin (48wt+B)
+0.16 sin (48wt+B+Ø) -0.24 sin (50wt-B-Ø)
-0.42 sin (50wt-B) -0.24 sin (50wt-B+Ø)
-0.08 sin (98wt-B-Ø) -0.12 sin (98wt-B)

D. Force in the X direction (pounds)

F_x = repeat all of A. (force in Y direction) except replace each cosine (cos) by sine (sin).

E. Rate of change of F_x with respect to eccentricity (pounds/inch).

$\frac{dF_x}{d\delta}$ = repeat all of B. ($dF_y/d\delta$) except replace all cosines by sines.

F. Rate of change of F_x with respect to eccentricity angle (pounds/radian)

$\frac{dF_x}{dB}$ = Repeat all of C (dF_y/dB) except replace all sines by cosines and change the sign of each term. ie if there is a "+" in C replace it by "-" and visa versa.

G. Definition of terms

t = time (seconds)

w = mechanical angular velocity (1256 radians/sec)

B = mechanical angle between Y axis and direction of eccentricity (radians)

δ = eccentricity (inches)

ϕ = π'-power angle (radians)

Power Angle = electrical angle between load current and direct axis magnetizing current (use 0.0 radians)

CASE V

3.33 KVA 1.0 PF 1 Phase Only
Other 2 Phases Open Circuited

The analytical expression for the radial bearing force on one end of the Brayton Cycle alternator when operating at 3.33 KVA unity power factor with the load connected from one phase to neutral is given below.

An eccentricity of .002" has been used in arriving at the force coefficients. Since the Brayton Cycle Alternator has two (2) circuits in the stator windings, the calculated forces have been divided by two (2) and the given expression reflects this division. The coordinate system is fixed in the stator.

A. Force in the Y direction (pounds)

$$F_y = -7.88 \cos(B) - 1.49 \cos(2\omega t - B - \phi) - 4.41 \cos(2\omega t - B) - 0.38 \cos(2\omega t + B + \phi) - 1.43 \cos(4\omega t - B - \phi) - 0.59 \cos(4\omega t - B + \phi) - 0.04 \cos(B + 2\phi) - 1.93 \cos(4\omega t + B - \phi) - 2.68 \cos(4\omega t + B + \phi) - 2.67 \cos(6\omega t - B + \phi) - 0.45 \cos(6\omega t + B + \phi) - 0.07 \cos(8\omega t + B - 2\phi) - 0.12 \cos(8\omega t + B + 2\phi)$$

B. Rate of change of F_y with respect to eccentricity (pounds/inch)

$$\frac{dF_y}{d\delta} = -3940 \cos(B) - 745 \cos(2\omega t - B - \phi) - 2205 \cos(2\omega t - B) - 190 \cos(2\omega t + B + \phi) - 715 \cos(4\omega t - B - \phi) - 295 \cos(4\omega t - B + \phi) - 20 \cos(B + 2\phi) - 965 \cos(4\omega t + B - \phi) - 1340 \cos(4\omega t + B + \phi) - 1335 \cos(6\omega t - B + \phi) - 225 \cos(6\omega t + B + \phi) - 35 \cos(8\omega t + B - 2\phi) - 60 \cos(8\omega t + B + 2\phi)$$

C. Rate of change of F_y with respect to eccentricity angle (pounds/radian).

$$\frac{dF_y}{dB} = +7.88 \sin(B) - 1.49 \sin(2\omega t - B - \phi) - 4.41 \sin(2\omega t - B) + 0.38 \sin(2\omega t + B + \phi) - 1.43 \sin(4\omega t - B - \phi) - 0.59 \sin(4\omega t - B + \phi) + 0.04 \sin(B + 2\phi) + 1.93 \sin(4\omega t + B - \phi) + 2.68 \sin(4\omega t + B + \phi) - 2.67 \sin(6\omega t - B + \phi) + 0.45 \sin(6\omega t + B + \phi) + 0.07 \sin(8\omega t + B - 2\phi) + 0.12 \sin(8\omega t + B + 2\phi)$$

D. Force in the X direction (pounds)

$$F_x = -7.88 \sin(B) - 1.49 \sin(2\omega t - B - \phi) - 4.41 \sin(2\omega t - B) - 0.38 \sin(2\omega t + B + \phi) - 1.43 \sin(4\omega t - B - \phi) - 0.59 \sin(4\omega t - B + \phi) - 0.04 \sin(B + 2\phi) - 1.93 \sin(4\omega t + B - \phi) - 2.68 \sin(4\omega t + B + \phi) - 2.67 \sin(6\omega t - B + \phi) - 0.45 \sin(6\omega t + B + \phi) - 0.07 \sin(8\omega t + B - 2\phi) - 0.12 \sin(8\omega t + B + 2\phi)$$

E. Rate of change of F_x with respect to eccentricity (pounds/inch)

$$\frac{dF_x}{d\delta} =$$

-3940 sin (B)-745 sin (2wt-B-Ø)
-2205 sin (2wt-B)-190 sin (2wt+B+Ø)
-715 sin (4wt-B-Ø)-295 sin (4wt-B+Ø)
-20 sin (B+2Ø) -965 sin (4wt+B-Ø)
-1340 sin (4wt+B+Ø) -1335 sin (6wt-B+Ø)
-225 sin (6wt+B+Ø) -35 sin (8wt+B-2Ø)
-60 sin (8wt+B+2Ø)

F. Rate of change of F_x with respect to eccentricity angle (pounds/radian)

$$\frac{dF_x}{dB} =$$

-7.88 cos (B)+1.49 cos (2wt-B-Ø)
+4.41 cos (2wt-B) -0.38 cos (2wt+B+Ø)
+1.43 cos (4wt-B-Ø) +0.59 cos (4wt-B+Ø)
-0.04 cos (B+2Ø) -1.93 cos (4wt+B-Ø)
-2.68 cos (4wt+B+Ø) +2.67 cos (6wt-B+Ø)
-0.45 cos (6wt+B+Ø) -0.07 cos (8wt+B-2Ø)
-0.12 cos (8wt+B+2Ø)

G. Definition of terms in above expression

t=time (seconds)
w=mechanical angular velosity (1256 radians/sec)
B=mechanical angle between Y axis and direction of eccentricity (radians)
=eccentricity (inches)
Ø=π-power angle (radians)
power angle=elec. angle between load current and direct axis magnetizing current (use 1.042 radians)

CASE VI

Single Phase Short

The analytical expression for the radial force on one end of the Brayton Cycle alternator when operating at 15 KVA, 0.8 PF, 3 phase and a short between one line and ground is given below. An eccentricity of .002" has been used in arriving at the force coefficients. Since the Brayton Cycle alternator has two (2) circuits in the stator winding, the calculated forces have been divided by two (2) and the given expressions reflect this division. The coordinate system is fixed in the stator.

A. Force in the Y direction (pounds)

F_y =

+.7088 cos (-B-Ø-X1) +.8447 cos (-B-Ø+X2)
-.3485 cos (-B-Ø) -.649 cos (-B-X1)
-.0808cos (-B+X2) -5.634 cos (-B)
+.0689 cos (-B+Ø-X1) -.0275 cos (-B+Ø)
+.0689 cos (B-Ø+X1) -.055 cos (B-Ø)
-1.529 cos (B-X1) - 1.697 cos (B-X2)
-.1909 cos (B-X3) - 1.577 cos (B+X1)
-1.646 cos (B+X2) -.1909 cos (B+X3)
-32.749 cos (B) +.8447 cos (B+Ø-X2)
+.7797 cos (B+Ø+X1) +.572 cos (B+Ø)
-.0832 cos (2wt-B-Ø-X1-0.2886) - .0698 cos (2wt-B-Ø-X2-0.2886)
-.0528 cos (2wt-B-Ø+X1-0.2886) - .0898 cos (2wt-B-Ø+X2-0.2886)
-1.444 cos (2wt-B-Ø-0.2886) -.2209 cos (2wt-B-X1-0.2886)
-.2264 cos (2wt-B-X2-0.2886) - .0284 cos (2wt-B-X3-0.2886)
-.2098 cos (2wt-B+X1-0.2886) - .2383 cos (2wt-B+X2-0.2886)
-0284 cos (2wt-B+X3-0.2886) - 3.489 cos (2wt-B-0.2886)
+.0344 cos (2wt-B+Ø-X1-0.2886) - .0059 cos (2wt-B+Ø+X2-0.2886)
-.0135 cos (2wt-B+Ø-0.2886) - .1132 cos (2wt+B-Ø-X2-0.2886)
-.0650 cos (2wt+B-Ø+X1-0.2886) - .0177 cos (2wt+B-Ø-0.2886)
-Ø119 cos (2wt+B-X2-0.2886) - .0111 cos (2wt+B+X1-0.2886)
-1.592 cos (2wt+B-0.2886) + .0120 cos (2wt+B+Ø-X2-0.2886)
+.0112 cos (2wt+B+Ø+X1-0.2886) - .1795 cos (2wt+B+Ø)
-.218 cos (4wt-B-Ø-X1+4.05) -.235 cos (4wt-B-Ø+X2+4.05)
-.727 cos (4wt-B-Ø+4.05) -.01 cos (4wt-B-2Ø-X1+4.05)
-.011 cos (4wt-B-2Ø+X2+4.05) -.798 cos (4wt-B-2Ø+4.05)
-.032 cos (4wt-B-X1+4.05) - .041 cos (4wt-B+X2+4.05)
-.350 cos (4wt-B+4.05) - .345 cos (4wt-B+Ø-X1+4.05)
-.412 cos (4wt-B+Ø+X2+4.05) - .057 cos (4wt-B+Ø+4.05)
-.246 cos (4wt+B-Ø-X1+4.05) -.635 cos (4wt+B-Ø-X2+4.05)
-.551 cos (4wt+B-Ø+X1+4.05) -.266 cos (4wt+B-Ø+X2+4.05)
-5.293 cos (4wt+B-Ø+4.05) +.006 cos (4wt+B+X1+4.05)
-.050 cos (4wt+B+4.05) -.249 cos (4wt+B+Ø-X1+4.05)
-.509 cos (4wt+B+Ø-X2+4.05) - .472 cos (4wt+B+Ø+X1+4.05)
-.269 cos (4wt+B+Ø+X2+4.05) - 6.001 cos (4wt+B+Ø+4.05)
-.0657 cos (6wt-B-Ø-X1+1.66) - .0701 cos (6wt-B-Ø+X2+1.66)
-.0928 cos (6wt-B-Ø+1.66) - .0194 cos (6wt-B-2Ø-X1+1.66)

-.0197 cos (6wt-B-2Ø+X2+1.66)
+.2772 cos (6wt-B+1.66)
-.5572 cos (6wt-B+Ø-X1+1.66) - .2370 cos (6wt-B+Ø-X2+1.66)
-.2194 cos (6wt-B+Ø+X1+1.66) - .6016 cos (6wt-B+Ø+X2+1.66)
-5.363 cos (6wt-B-Ø+1.66)
-.2248 cos (6wt+B-Ø-X2+1.66) - .2079 cos (6wt+B-Ø+X1+1.66)
-.8823 cos (6wt+B-Ø+1.66)
+0.3011 cos (6wt+B+1.66)
-.4299 cos (6wt+B+Ø-X2+1.66) - .3993 cos (6wt+B+Ø+X1+1.66)
-.3454 cos (6wt+B+Ø+1.66) -.0229 cos (6wt+B+2Ø-X2+1.66)
-.0213 cos (6wt+B+2Ø+X1+1.66) - .1674 cos (6wt+B+2Ø+1.66)

B. Rate of change of F_y with respect to eccentricity (pounds/inch)

$$\frac{dF_y}{d\epsilon} =$$

+354.4 cos (-B-Ø-X1) +422.35 cos (-B-Ø+X2)
-174.25 cos (-B-Ø) - 32.45 cos (-B-X1)
-40.4 cos (-B+X2) -2817.0 cos (-B)
+34.45 cos (-B+Ø-X1) -13.75 cos (-B+Ø)
+34.45 cos (B-Ø+X1) -27.5 cos (B-Ø)
-764.5 cos (B-X1) -848.5 cos (B-X2)
-95.45 cos (B-X3) -788.5 cos (B+X1)
-823.0 cos (B+X2) - 95.45 cos (B+X3)
-16,374.5 cos (B) + 422.35 cos (B+Ø-X2)
+389.85 cos (B+Ø+X1) + 286.0 cos (B+Ø)
-41.6 cos (2wt-B-Ø-X1-0.2886) - 34.9 cos (2wt-B-Ø-X2-0.2886)
-26.4 cos (2wt-B-Ø+X1-0.2886) - 44.9 cos (2wt-B-Ø+X2-0.2886)
-722 cos (2wt-B-Ø-0.2886) - 110.45 cos (2wt-B-X1-0.2886)
-113.2 cos (2wt-B-X2-0.2886) - 14.2 cos (2wt-B-X3-0.2886)
-104.9 cos (2wt-B+X1-0.2886) - 119.15 cos (2wt-B+X2-0.2886)
-14.2 cos (2wt-B+X3-0.2886) - 1,744.5 cos (2wt-B-0.2886)
+17.2 cos (2wt-B+Ø-X1-0.2886) - 2.95 cos (2wt-B+Ø+X2-0.2886)
-6.75 cos (2wt-B+Ø-0.2886) - 56.6 cos (2wt+B+Ø-X2-0.2886)
-32.5 cos (2wt+B-Ø+X1-0.2886) - 8.85 cos (2wt+B-Ø-0.2886)
-5.95 cos (2wt+B-X2-0.2886) - 5.55 cos (2wt+B+X1-0.2886)
-796.0 cos (2wt+B-0.2886) +6.0 cos (2wt+B+Ø-X2-0.2886)
+5.6 cos (2wt+B+Ø+X1-0.2886)- 89.75 cos (2wt+B+Ø-0.2886)
-109 cos (4wt-B-Ø-X1+4.05) - 117.5 cos (4wt-B-Ø+X2+4.05)
-363.5 cos (4wt-B-Ø+4.05) - 5.0 cos (4wt-B-2Ø-X1+4.05)
-5.5 cos (4wt-B-2Ø+X2+4.05) - 399 cos (4wt-B-2Ø+4.05)
-16 cos (4wt-B-X1+4.05) - 20.5 cos (4wt-B+X2+4.05)
-175 cos (4wt-B+4.05) - 172.5 cos (4wt-B+Ø-X1+4.05)
-206 cos (4wt-B+Ø+X2+4.05) - 28.5 cos (4wt-B+Ø+4.05)
-123 cos (4wt+B-Ø-X1+4.05) - 317.5 cos (4wt+B-Ø-X2+4.05)
-275.5 cos (4wt+B-Ø+X1+4.05) - 133 cos (4wt+B-Ø+X2+4.05)
-2646.5 cos (4wt+B-Ø+4.05) +3.0 cos (4wt+B+X1+4.05)
-25 cos (4wt+B+4.05) - 124.5 cos (4wt+B+Ø-X1+4.05)
-254.5 cos (4wt+B+Ø-X2+4.05) - 236 cos (4wt+B+Ø+X1+4.05)
-134.5 cos (4wt+B+Ø+X2+4.05) - 3,000.5 cos (4wt+B+Ø+4.05)
-32.85 cos (6wt-B-Ø-X1+1.66) - 35.05 cos (6wt-B-Ø+X2+4.05)
-46.4 cos (6wt-B-Ø+1.66) - 9.7 cos (6wt-B-2Ø-X1+1.66)
-9.85 cos (6wt-B-2Ø+X2+1.66)
+138.6 cos (6wt-B+1.66)

-278.6 cos (6wt-B+Ø-X1+1.66) - 118.5 cos (6wt-B+Ø-X2+1.66)
-109.7 cos (6wt-B+Ø+X1+1.66) - 300.8 cos (6wt-B+Ø+X2+1.66)
-2681.5 cos (6wt-B+Ø+1.66)
-112.4 cos (6wt+B-Ø-X2+1.66) - 103.95 cos (6wt+B-Ø+X1+1.66)
-441.15 cos (6wt+B-Ø+1.66)
+150.55 cos (6wt+B+1.66)
-214.95 cos (6wt+B+Ø-X2+1.66) - 199.65 cos (6wt+B+Ø+X1+1.66)
-172.7 cos (6wt+B+Ø+1.66) - 11.45 cos (6wt+B+2Ø-X2+1.66)
-10.65 cos (6wt+B+2Ø+X1+1.66) - 83.7 cos (6wt+B+2Ø+1.66)

C. Rate of change of F_y with respect to eccentricity angle (pounds/radian).

$$\frac{dF_y}{dB} =$$

+.7088 sin (-B-Ø-X1) +.8447 sin (-B-Ø+X2)
-.3485 sin (-B-Ø) - .0649 sin (-B-X1)
-.0808 sin (-B+X2) - 5.634 sin (-B)
+.0689 sin (-B+Ø-X1) -.0275 sin (-B+Ø)
+1.529 sin (B-X1) +.055 sin (B-Ø)
-.0689 sin (B-Ø+X1) +1.697 sin (B-X2)
+.1909 sin (B-X3) +1.577 sin (B+X1)
+1.646 sin (B+X2) +.1909 sin (B+X3)
+32.749 sin (B) - .8447 sin (B+Ø-X2)
-.7797 sin (B+Ø+X1) -.572 sin (B+Ø)
-.0832 sin (2wt-B-Ø-X1-0.2886) - .0698 sin (2wt-B-Ø-X2-0.2886)
-.0528 sin (2wt-B-Ø+X1-0.2886) - .0898 sin (2wt-B-Ø+X2-0.2886)
-1.444 sin (2wt-B-Ø-0.2886) - .2209 sin (2wt-B-X1-0.2886)
-.2264 sin (2wt-B-X2-0.2886) - .0204 sin (2wt-B-X3-0.2886)
-.2098 sin (2wt-B-X1-0.2886) - .2383 sin (2wt-B+X2-0.2886)
-.0284 sin (2wt-B+X3-0.2886) - 3.489 sin (2wt-B-0.2886)
+.0344 sin (2wt-B+Ø-X1-0.2886) - .0059 sin (2wt-B+Ø+X2-0.2886)
-.0135 sin (2wt-B+Ø-0.2886) +.1132 sin (2wt+B-Ø-X2-0.2886)
+.065 sin (2wt+B-Ø+X1-0.2886) +.0177 sin (2wt+B-Ø-0.2886)
+.0119 sin (2wt+B-X2-0.2886) +.0111 sin (2wt+B+X1-0.2886)
+1.592 sin (2wt+B-0.2886) -.012 sin (2wt+B+Ø-X2-0.2886)
-.0112 sin (2wt+B+Ø+X1-0.2886) +.1795 sin (2wt+B+Ø-0.2886)
-.218 sin (4wt-B-Ø-X1+4.05) - .235 sin (4wt-B-Ø+X2+4.05)
-.727 sin (4wt-B-Ø+4.05) - .01 sin (4wt-B-2Ø-X1+4.05)
-.011 sin (4wt-B-2Ø+X2+4.05) - .798 sin (4wt-B-2Ø+4.05)
-.032 sin (4wt-B-X1+4.05) - .041 sin (4wt-B+X2+4.05)
-.350 sin (4wt-B+4.05) - .345 sin (4wt-B+Ø-X1+4.05)
-.412 sin (4wt-B+Ø+X2+4.05) - .057 sin (4wt-B+Ø+4.05)
+.246 sin (4wt+B-Ø-X1+4.05) + .635 sin (4wt+B-Ø-X2+4.05)
+.551 sin (4wt+B-Ø+X1+4.05) + .266 sin (4wt+B-Ø+X2+4.05)
+5.293 sin (4wt+B-Ø+4.05) - .006 sin (4wt+B+X1+4.05)
+.050 sin (4wt+B+4.05) + .249 sin (4wt+B+Ø-X1+4.05)
+.509 sin (4wt+B+Ø-X2+4.05) +.472 sin (4wt+B+Ø+X1+4.05)
+.269 sin (4wt+B+Ø-X2+4.05) +6.001 sin (4wt+B+Ø+4.05)
-.0657 sin (6wt-B-Ø-X1+1.66) - .0701 sin (6wt-B-Ø+X2+1.66)
-.0928 sin (6wt-B-Ø+1.66) -.0194 sin (6wt-B-2Ø-X1+1.66)
-.0197 sin (6wt-B-2Ø+X2+1.66)
+.2772 sin (6wt-B+1.66)

-.5572 sin (6wt-B+ϕ-X1+1.66) - .237 sin (6wt-B+ϕ-X2+1.66)
-.2194 sin (6wt-B+ϕ+X1+1.66) - .6016 sin (6wt-B+ϕ+X2+1.66)
-5.363 sin (6wt-B-ϕ+1.66)
+.2248 sin (6wt+B-ϕ-X2+1.66) +.2079 sin (6wt+B-ϕ+X1+1.66)
+.8823 sin (6wt+B-ϕ+1.66)
-.3011 sin (6wt+B+1.66)
+.4299 sin (6wt+B+ϕ-X2+1.66) +.3993 sin (6wt+B+ϕ+X1+1.66)
+.3454 sin (6wt+B+ϕ+1.66) +.0229 sin (6wt+B+2ϕ-X2+1.66)
+.0213 sin (6wt+B+2ϕ+X1+1.66) +.1674 sin (6wt+B+2ϕ+1.66)

D. Force in the X direction (pounds)

F_x = repeat all of A. (force in Y direction) except replace each cosine (cos) by sine (sin).

E. Rate of change of F_x with respect to eccentricity (pounds/inch).

$\frac{dF_x}{d\,\sigma}$ = repeat all of B. (dF_y /dσ) except replace all cosines by sines.

F. Rate of change of F_x with respect to eccentricity angle (pound/radian).

$\frac{dF_x}{dB}$ = Repeat all of C. (dF_y /dB) except replace all sines by cosines and change the sign of each term. ie, if there is a "+" in C replace it by "-" and visa versa.

G. Definition of terms in above expression

t = time (seconds)
w = mechanical angular velosity (1256 radians/sec)
B = mechanical angle between y axis and direction of eccentricity (radians)
σ = eccentricity (inches)
ϕ = - power angle (radians)
Power angle = electrical angle between load current and direct axis magnetizing current (use -,.018 radians).

X1 = A->B phase relation use (2.30 radians)
X2 = B->C phase relation use (4.33 radians)
X3 = A->C phase relation use (6.64 radians)

SECTION IX

Derivation of Analytical Expressions

Derivations for Permeance and MMF

As previously mentioned (Eq. #1) the magnetic force is given by:

$$F = K\int \mathcal{B}^2 dA \text{ where } K = \frac{1}{72} \text{ for } \mathcal{B} \text{ in kilolines per square inch.}$$

Since $B = \mu P \times MMF$ (See Eq. #3) the derivations are given for representations of p and MMF. Each of these is derived as an infinite series and then truncated at appropriate harmonics. In both cases, the reference of the series is fixed in the stator at a point referred to the minimum air gap by angle B. Mechanical angles, wt, are used throughout while electrical displacement, ψ_e, is the generator torque angle in mechanical radians.

Fundamental permeance is defined as $(\mu A/\ell)$ where μ is the medium permeability, A is the area, and ℓ is gap or path length. If A is considered to be one square inch, and μ is divided out as a constant multiplier, the unitized permeance becomes $(1/\ell)$ or the reciprocal of the air gap length. The permeance series can then be described as mechanical gap.

The rotor, air gap, stator and eccentricity combine to present a non-uniform air gap due to slotting and eccentricity. The rotor moving past the stator presents a modulated permeance which is again modulated by eccentricity if eccentricity is present. A truncated Fourier cosine series written for rotor and amortisseur, stator, and air gap eccentricity, has been used to represent the physical picture in the machine. These three permeances multiplied together represent the modulated permeance of the machine as functions of time, mechanical eccentricity angle and their magnitudes.

The rotor can be represented as in the sketch below:

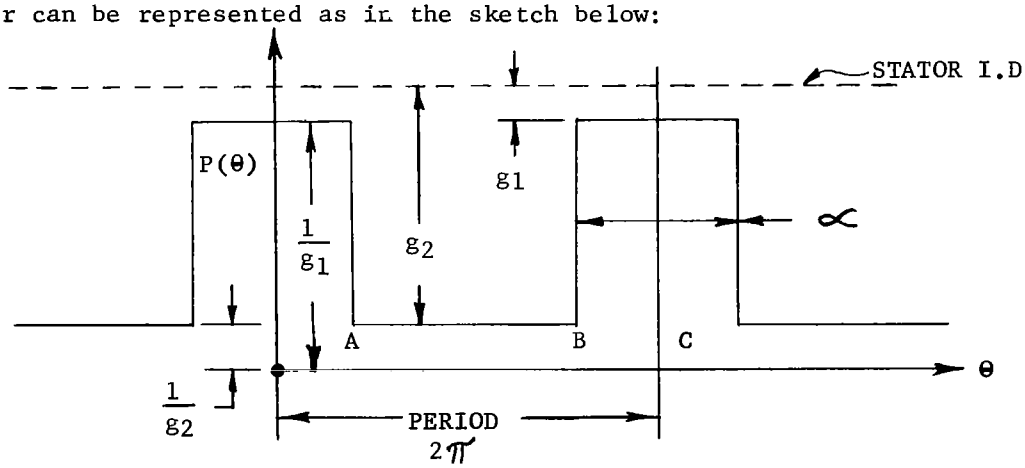

Point A $= \frac{2\pi\alpha}{2} = \pi\alpha$ radians Eq. #22

The saliency angle between poles is:

Angle $= 2\pi(1-\alpha)$ radians Eq. #23

And therefore Point B and Point C become:

Point B = $\pi(2-\alpha)$ Eq. #24

Point C = $2\pi D/P$ Eq. #25

The rotor permeance can be represented by a Fourier Series of the following form:

$$f(x) = a_o + \sum_{n=1}^{\infty} a_n \cos nx \qquad \text{Eq. \#26}$$

where the coefficients are given by:

$$a_o = \frac{1}{L} \int_o^L f(x)dx \qquad \text{Eq. \#27}$$

$$a_n = \frac{2}{L} \int_o^L f(x) \cos (nx)\, dx \qquad \text{Eq. \#28}$$

By letting $L = 2\pi$ and $f(x) = P(\theta)$, Eq. #28 can be expanded to:

$$a_n = \frac{1}{\pi} \int_o^{\pi\alpha} g_1 \cos(n\theta)\, d\theta + \frac{1}{\pi} \int_{\pi\alpha}^{\pi(2-\alpha)} \frac{1}{g_2} \cos(n\theta)\, d\theta$$

$$+ \frac{1}{\pi} \int_{\pi(2-\alpha)}^{2\pi} \frac{1}{g_1} \cos(n\theta)\, d\theta \qquad \text{Eq. \#30}$$

Performing the integration yields:

$$a_n = \left(\frac{1}{g_1} - \frac{1}{g_2}\right) \frac{2}{n\pi} \quad \text{Sin } n\pi\alpha$$

Using a_n to write the main rotor permeance in the form of Eq. #10 gives:

$$P_n = a_n \cos(n\rho(\theta - wt)) \qquad \text{Eq. \#31}$$

where an angle (wt) is included in the argument of this expression if the rotor is viewed as starting at some point where the direct axis and reference center don't coincide.

Applying the above coefficient formulas to the Brayton Cycle Alternator where $g_1 = .04"$ and $g_2 = 1.0$:

$P_0 = 8.90$ Eq. #32

$P_1 = 12.82$ Eq.#33

$P_2 = 5.82$ Eq.#34

$P_3 = 0.750$ Eq.#35

$P_4 = -3.42$ Eq. #36

$P_5 = -2.035$ Eq. #37

Amortisseur and Stator Slots

Amortisseur and stator slotting could be handled like the rotor saliency, but this would lead to higher permeance modulation than is actually seen by the machine. The amortisseur slot sketch below explains this to a degree.

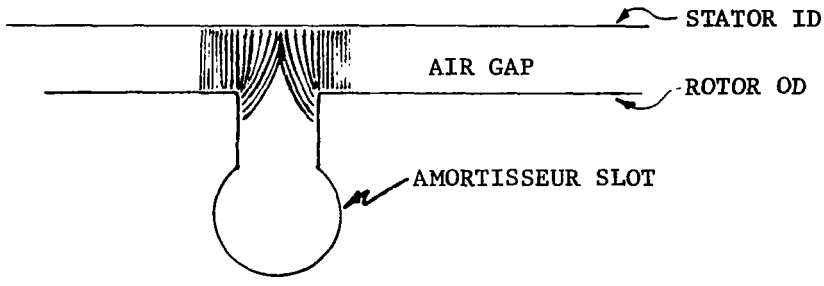

Very little flux actually links the bottom of the slot so a strictly mechanical representation of the permeance would be misleading. Dr. Freeman in his IEE Paper #523U, June 1962, "The Calculation of Harmonics, Due to Slotting, in the Flux-Density Waveform of a Dynamo-Electric Machine" solves a more exact case.

He transforms the above sketch to a form as shown below:

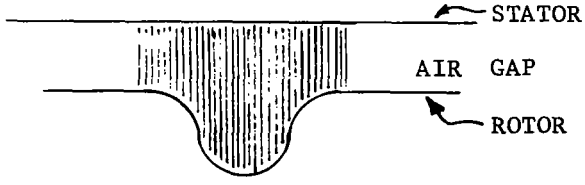

with a similar representation for the stator slots.

This can be represented by a cosine series of the general form taken by the rotor saliency and some average permeance, so that for the amortisseur:

$$P_{amort.} = \gamma P_o \cos (n(N_A\theta - N_A \text{ wt})) + 1 \qquad \text{Eq. \#38}$$

where γ is taken from Freeman's graphs as functions of machine parameters, and N_A is the number of slots.

Although there are only eighteen physical amortisseur slots in one end of the Brayton Cycle machine, this is equivalent to fifty amortisseur slots, if they are continued through the region of rotor slots.

$\therefore \quad N_A = 50$

The only difference between the stator and amortisseur slotting is the number of slots, time as a variable and slightly different coefficients due to a different slot opening. The stator slotting permeance can be represented by the cosine series.

$$P_{stator} = 1 + (\gamma \cos (N_s \theta)) \qquad \text{Eq. \#39}$$

where $N_s = 48$ slots

Eccentricity

Eccentricity can be viewed as a permeance since it is a change in gap that, in effect, modulates the machine permeance.

Consider the rotor as a cylinder within another cylinder (the stator) as below:

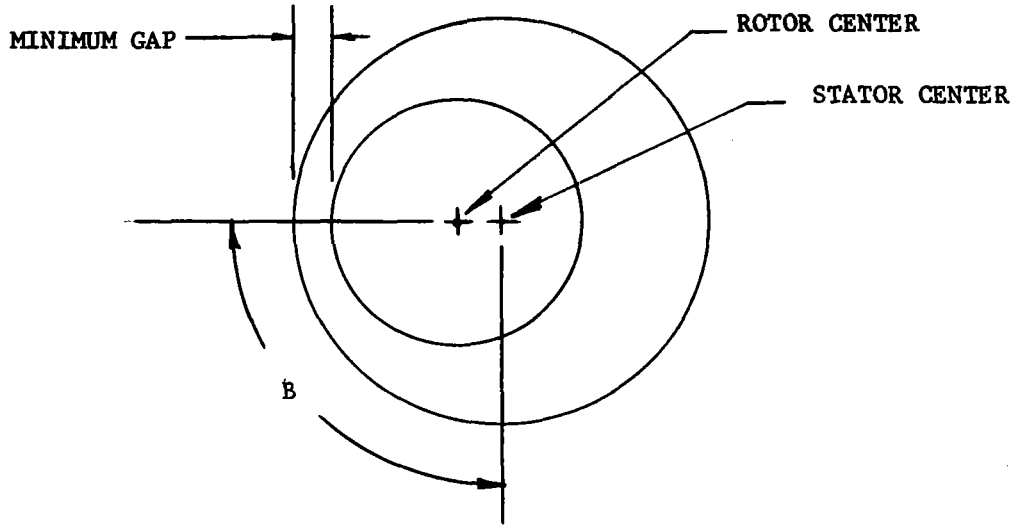

The eccentricity permeance can be represented by an equation of the form:

$$P_e = P_{eo} + P_{e1} \cos (\theta - B) + P_{e2} \cos 2(\theta - B) + - - - \qquad \text{Eq. \#40}$$

where: $P_{eo} = 1$

$P_{e1} = \delta/g$

$P_{e2} = (\delta/g)^2$

δ = eccentricity (in.)

g = gap (in.)

For the Brayton Cycle Alternator gap of 0.04" and an eccentricity of 0.002", $P_{e1} >> P_{e2}$ and harmonics higher than the first can be neglected. Eccentricity permeance is then:

$$P_e = 1 - \frac{\delta}{g} \cos(\theta - B) \qquad \text{Eq. \#41}$$

The rotor, amortisseur, stator, and eccentricity expressions can be combined to form a complete expression for the machine permeance (except for end effects). This expression doesn't account for fringing of the main rotor poles or saturation both of which are corrected for in the computer deck.

The rotor pole permeance and amortisseur permeances are combined to represent the total rotor permeance since the two represent one component which cannot modulate itself. This is then modulated by both the eccentricity and stator slotting. The complete expression is as written below:

$$P_{gap} = (P_R + P_A) \times P_S \times P_E \qquad \text{Eq. \#42}$$

These are all infinite series truncated to reasonable accuracy by limiting the number of harmonics to the fifth, second, second, and fundamental respectively representing nearly 99% of the total permeance.

MMF

Since force is dependent on (Flux density)^2, and Flux density is dependent on MMF and Permeance, a complete description of MMF is required. (See Eq's #1, #3).

The MMF expression needed is one that describes the total ampere turns impressed across the gap at a given condition as functions of time, mechanical angle, electrical angle, and current. If the machine is operating with a balanced three-phase load, the winding coil pitch is 2/3 pitch as in the Brayton Cycle and there are an integral number of stator slots per pole, then the MMF can be expressed as a cosine series containing only odd nontriplen harmonics. The general term in this series is shown below:

$$MMF = \frac{2qM\psi}{n\pi} K_{pn} K_{dn} \cos(n p (\theta - wt + \pi - \psi_e)) \qquad \text{Eq. \#43}$$

where n = harmonic number
$M = \sqrt{2} \times T \times I$
T = turns per coil
I = amps/line/circuits
ψ = slots/phase belt
q = phase belts/pole
ψ_e = power angle

and K_{pn} = pitch factor for the n^{th} harmonic;

and K_{dn} = distribution factor for the n^{th} harmonic

This expresses the time variant MMF. To complete the expression the field excitation (AT_{dc}) for one end of the machine must be added to Eq. #43. The complete expression gives a gap MMF as shown below at t = 0.

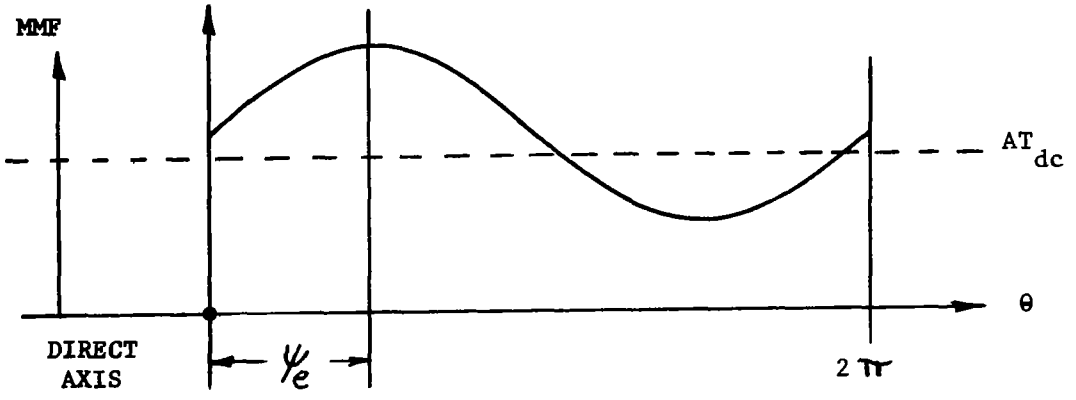

The above expression does not express the picture that is present if the machine load is unbalanced. When the load is unbalanced, each phase will be at different current values and the amortisseur circuit will have current flowing due to backward rotating and standing MMF waves. The complete MMF expression must then contain the forward, backward, and standing MMF waves due to the unbalanced line currents, amortisseur currents and AT_{dc}.

By solving the circuit below which contains the positive, negative, and zero sequence impedances of the alternator, forward, backward, and zero sequence currents can be found:

$R_L + jX_L$ = Load impedance

$R_0 + jX_0$ = Zero sequence impedance

$R_2 + jX_2$ = Negative sequence impedance

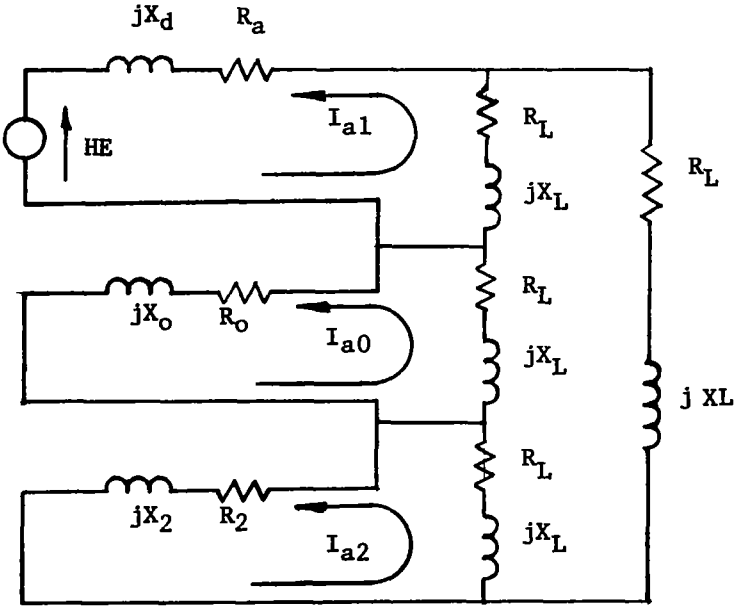

The sequence current components reflect the amortisseur attenuation of the backward and standing fields relative to the positive sequence field. These currents (Ia, Iao, Ia2) can then be operated on by the vector operators, $\vec{a}$ and $\vec{a}^2$, to form correct expressions for the phase currents due to unbalanced conditions.

The MMF[3] can then be expressed by the terms below:

$$MMF = 3/2\ F_{max} \cos (n(\theta - wt + \pi - \psi_e)$$
$$+ 1/2\ F_{max} \cos (n(\theta + wt + \pi - \psi_e)$$
$$+ 1/2\ F_{max} \cos (n(\theta + wt + \pi - \psi_e + A - 240^o)$$
$$+ 1/2\ F_{max} \cos (n(\theta + wt + \pi - \psi_e + B - 480^o) + AT_{dc} \qquad \text{Eq. \#44}$$

This represents two sets of counter rotating current vectors including all machine effects. This might be pictured as below:

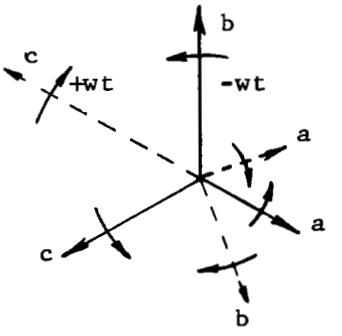

In general:

$$F_{max} = \left(\frac{4}{\pi}\right) \frac{K_{pn} K_{dn}}{poles} (IN) \qquad \text{Eq. \#45}$$

A and B represent the displacement from 120° time space vector current relationship.

3 Concordia, "Synchronous Machines"

Saturation

The rotor permeance expression as derived is correct only if no saturation occurs in the rotor. It also ignores the fact that fringing takes place near the pole tips and further implies no stator saturation. If the flux density and distribution in the gap is known, it can be Fourier analyzed and a more correct rotor permeance expression realized. This technique is illustrated in the following paragraphs.

An air gap MMF can be obtained using the previously derived MMF expression. (Eq. #43). This MMF expression is then evaluated at increments around the periphery of the air gap to describe the MMF on a point by point basis over a pair of poles and 48 equally spaced points equal to 360 degrees.

To use this MMF to obtain flux an expression for reluctance is necessary. The reluctances of the stator and rotor teeth and slots can be represented by the electrical equivalent circuit shown below. The impedances of the iron portions will be nonlinear due to saturation. The reluctances are determined on a point-by-point basis.

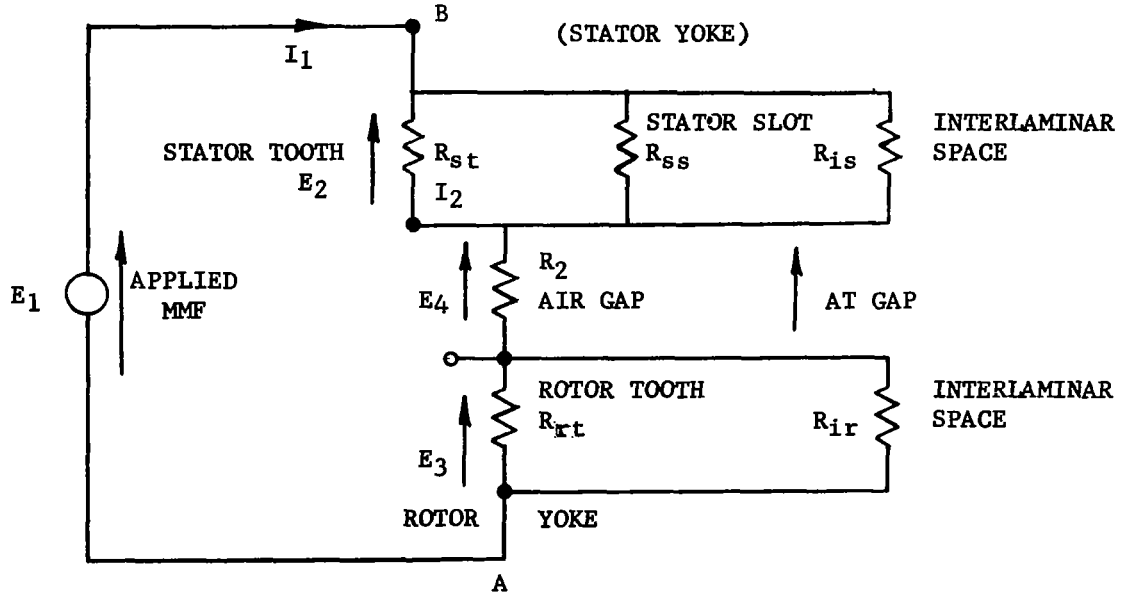

By assuming a flux density (current) between points A&B, a given ampere turn drop (voltage) can be calculated for the circuit with the aid of steel magnetization tables and physical dimensions of the slot, lamination, stacking factor, and tooth length (stator and rotor). The drop across the stator tooth, stator slot, air gap and rotor tooth can thus be found. The sum of these drops

is the applied MMF, and the gap density is the result of the applied MMF at the given point. This process of assuming a flux density and computing MMF is repeated until a graph of MMF vs. B gap is obtained over a reasonable range of densities. For the Brayton Cycle, B ranges from 0 to 150 KL/inch^2 in 80 steps.

Figure 19 shows the MMF around the gap for a pair of poles and Figure 20 shows gap density vs. applied MMF.

A picture of gap density around the pair of poles is now drawn by taking the MMF at a point (Figure 19) and reading a resultant gap density (Figure 20). This process is completed around the 360^o electrical degrees for 48 points and results in Figure 21.

Figure 20 is only used over the pole region. The slot portion of Figure 21 (points 9 to 39) is calculated by two methods and the higher resultant density is used (pessimistic value in saliency) in the calculations.

Method #1 assumes a flux path between pole tip and stator as the sketch below shows:

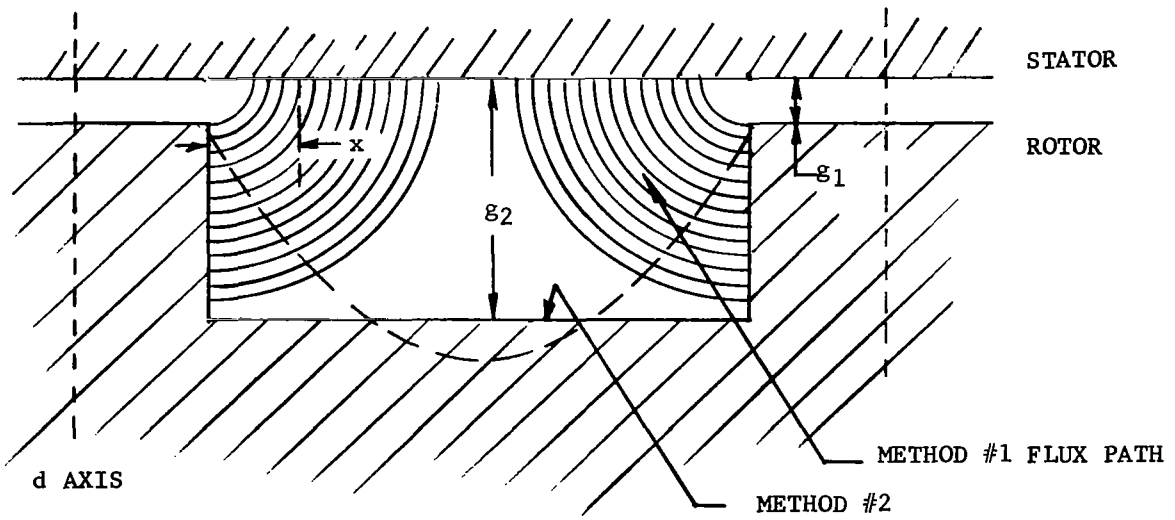

This method gives a gap that accounts well for fringing at the pole tips by calculating gap length g as a quarter circle.

However it is unrealistic near the center region of the slot. Method #2 simply assumes a constant gap (g_2) as shown in the sketch and is used when the resultant permeance is higher than that of Method #1.

The combination of the two saliency methods and the pole saturation method gives the complete picture of the density shown in Figure 21.

MMF VS THETA

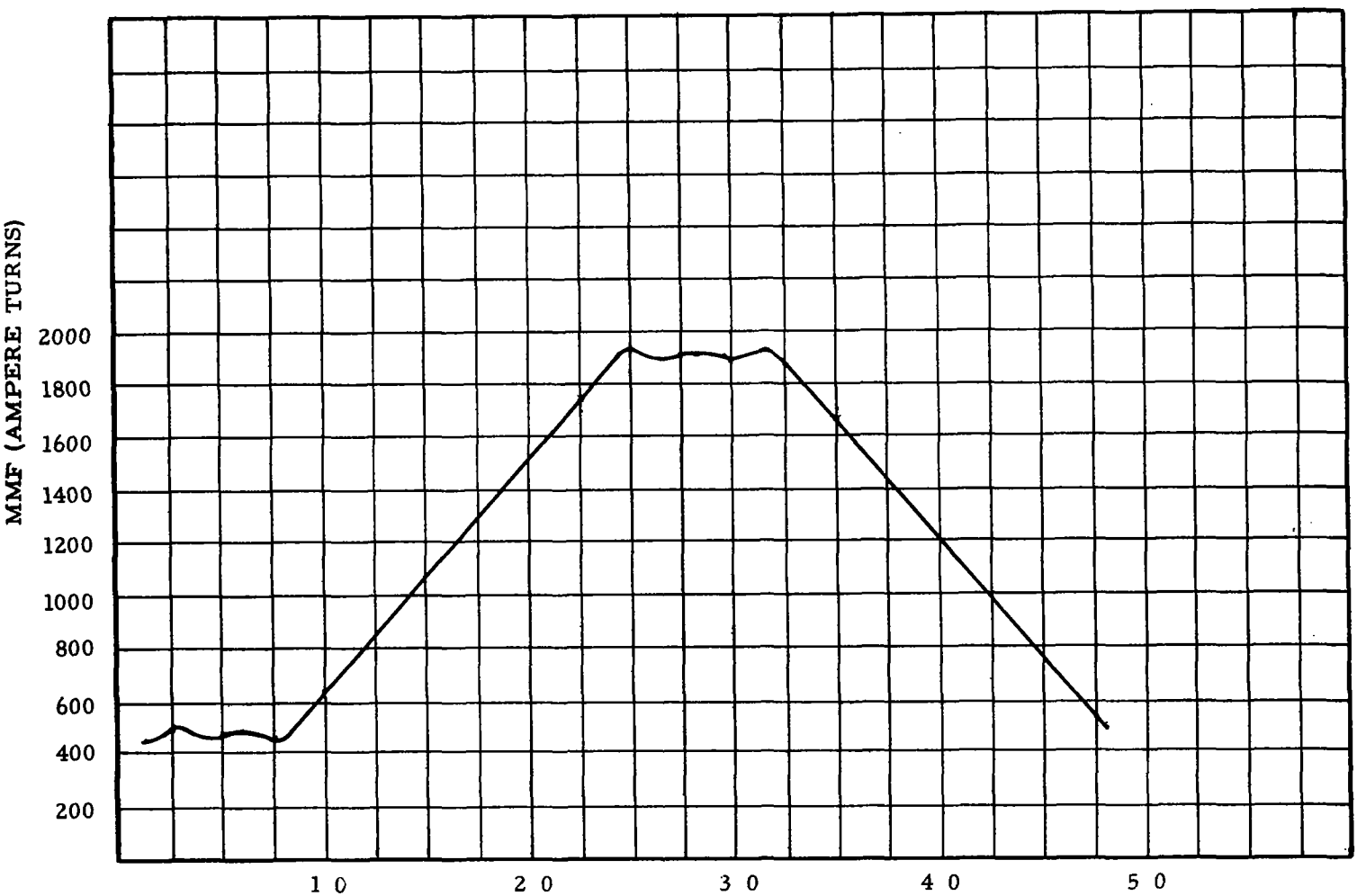

FIGURE 19

AIR GAP FLUX DENSITY VS MMF

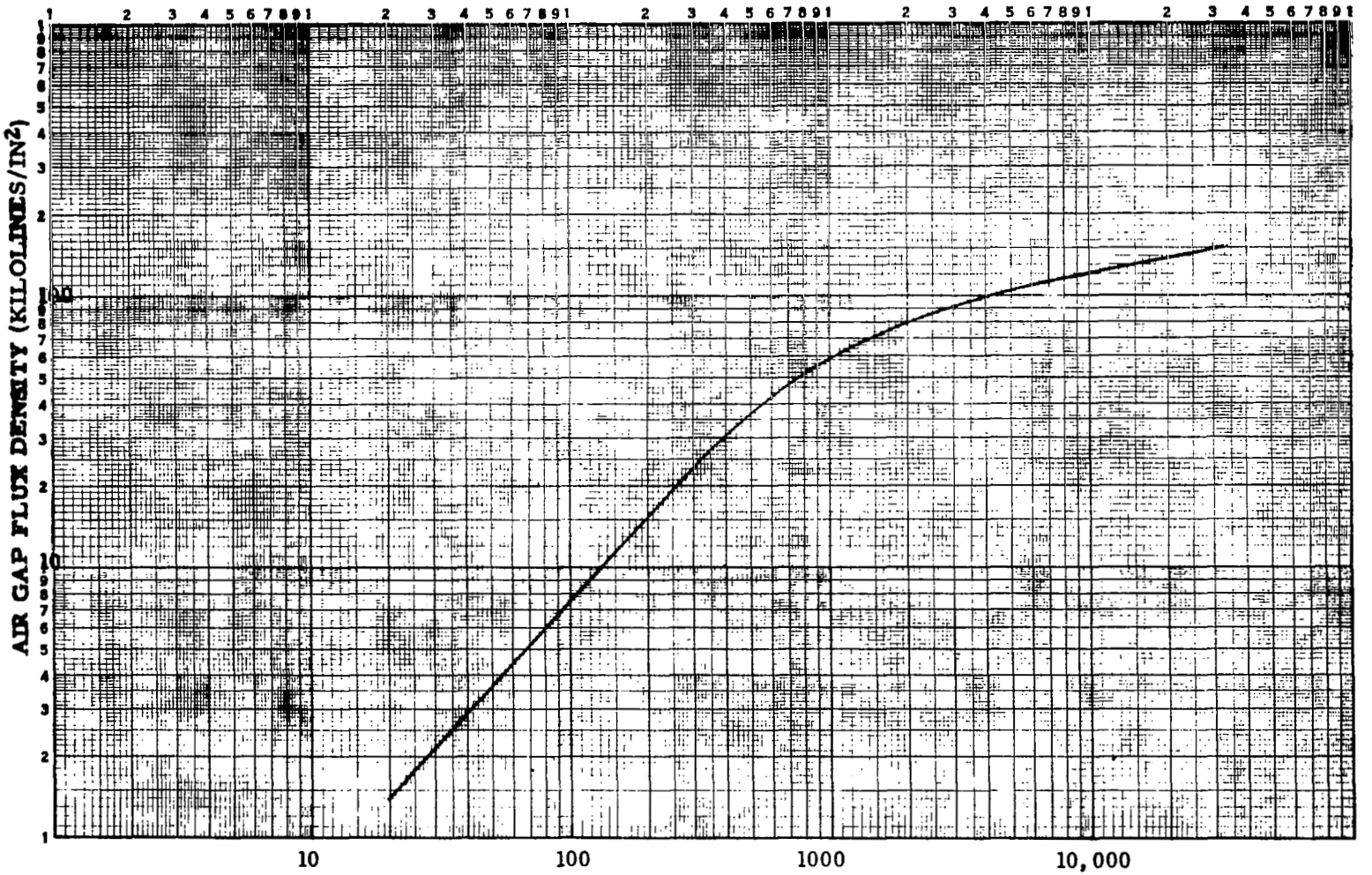

FIGURE 20

AIR GAP FLUX DENSITY VS THETA

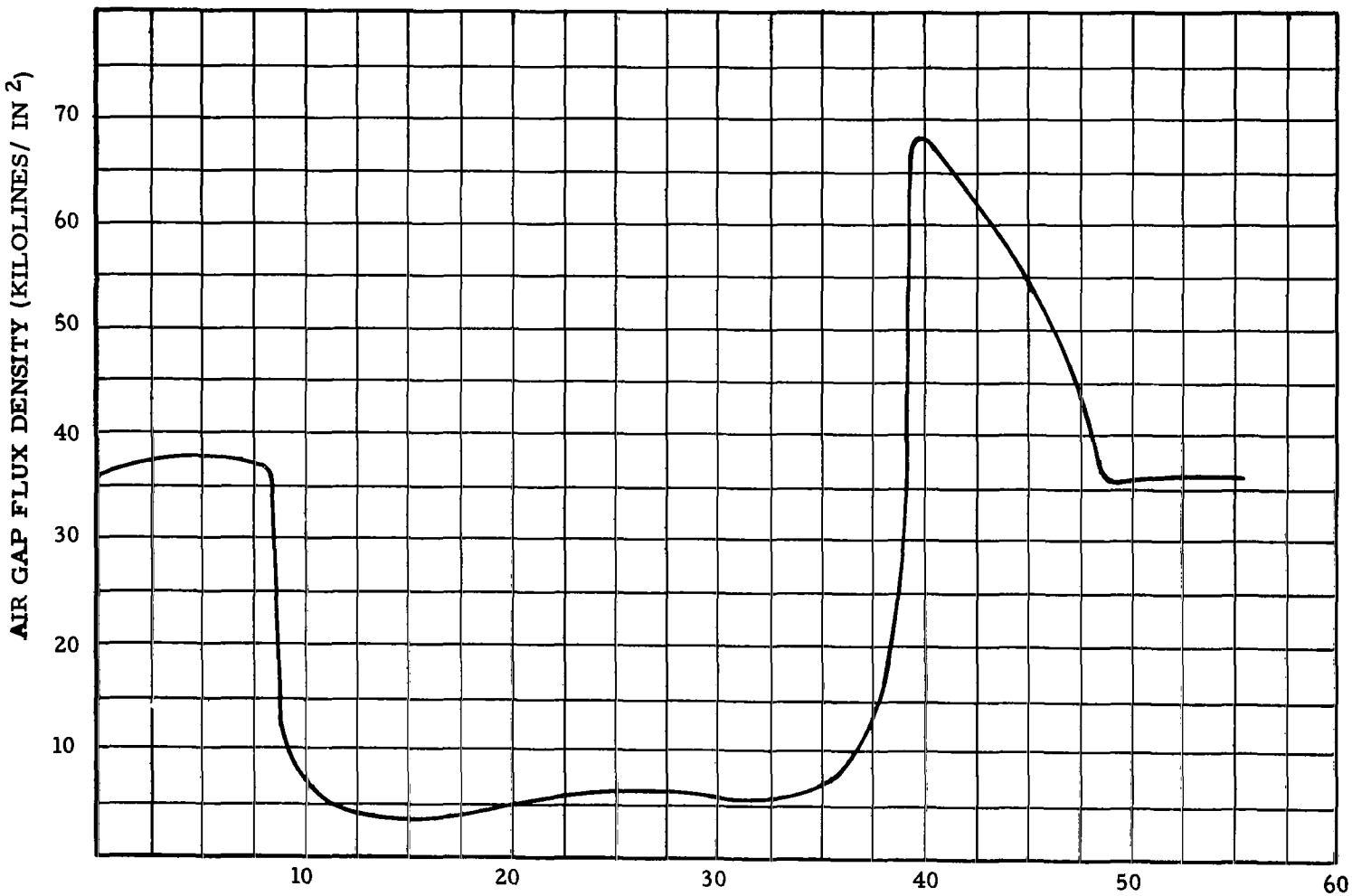

FIGURE 21

Note that Figure 21 goes from direct axis to direct axis so the left hand region of the figure corresponds to the leading pole tip and the right hand region to the trailing edge of the next pole tip. The trailing edge is at a higher flux density and therefore is more saturated, which reflects as a lower permeance level.

Figure 21 is Fourier analyzed to give the angle between the direct axis and the flux fundamental. This angle is directly related to ψ_e and therefore the power factor and the assumed $*\psi_e$. If the calculated angle does not check with the angle based on the assumed ψ_e, ψ_e is changed and the process repeated over again until an exact ψ_e is arrived at based on the power factor and the assumed AT_{DC}.

Since the Fourier analysis gives the fundamental AC flux, ϕ_{ac}, the induced voltage, E_i can also be claculated using the following equation (Faraday's Law):

$$E_i = 4.44 \; f \; T_{ie} \; \phi_{ac} \; X \; 10^{-5}$$

where: f = frequency (cps)
T_{ie} = effective turns per phase

The above calculated E_i is then compared with the E_i determined from terminal condition of the alternator using the following vector diagram.

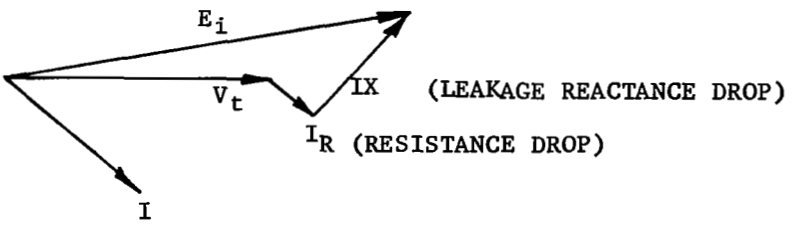

If the two E_i's do not check, then the AT_{DC} is adjusted and the calculation on ψ_e and E_i are repeated until the values are within 0.5% of each other.

Now that the value and shape of the gap flux is known, it follows that the gap permeance is also known, and can be Fourier analyzed to determine the average and first five harmonic terms.**

Each of these harmonics can be compared with the unsaturated rotor expression, and a correction factor determined to make the original rotor expression reflect the saturation in the alternator rotor and stator. These correction factors are determined in the computer program. They are necessary since the original gap flux expression is not in a form that can be used to obtain $\vec{B}$ terms computable with the Force Calculation Program.

Figure 22 shows the relation between saturated and unsaturated permeance. Note how the fringing is apparent in the saturated case.

* An assumed ψ_e must be used to begin the iteration process.
** The original permeance expression neglecting saturation utilized five harmonics.

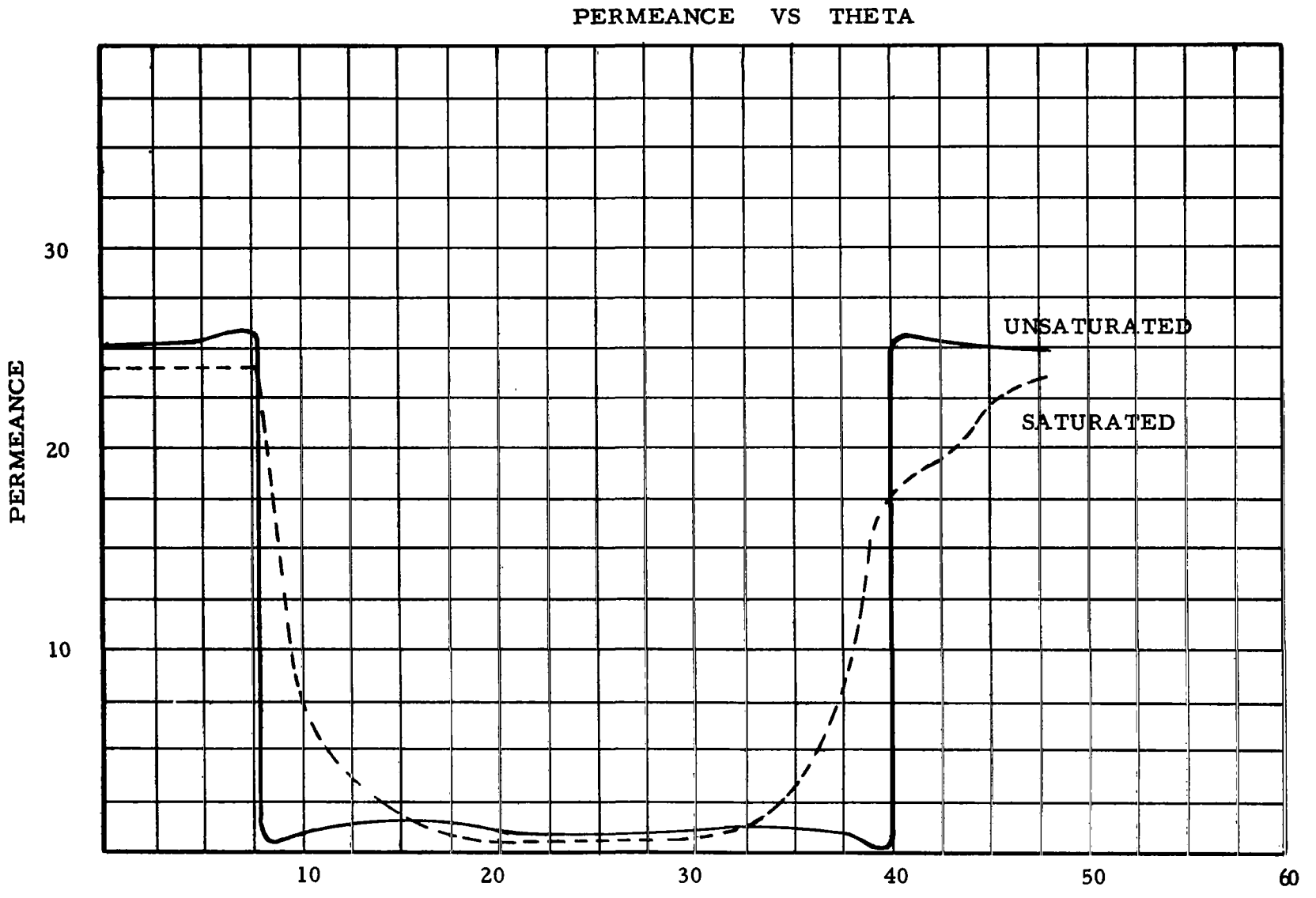
PERMEANCE VS THETA
PERMEANCE
30
20
10
UNSATURATED
SATURATED
10
20
30
40
50
60
POSITION POINTS (7.5 ELECTRICAL DEGREES PER POINT)

FIGURE 22

Figures 19 through 22 were taken directly from the computer output. The program uses the iterative process described above and arrives at saturation excitation and the alternator power angle.

The process used for calculating saturation, is sufficient for all cases except where the generator is operating at 15 KVA balanced load with a short applied from line to neutral on one phase.

The reason the saturation calculation is not sufficient is because only average saturation at a given point around the machine is considered whereas the saturation is really time variant.

When the excitation is high and the load unbalanced, the backward and standing MMF waves are interacting with the forward and AT_{dc} MMF's to form radically varying total MMF across the rotor, gap, stator magnetic path at a given point in time and space. Saturation as a function of rotor position does not show the heavy saturation that takes place when AT_{dc} is not being opposed by the armature reactions combined waves.

This specific case of unbalanced loading was first analyzed in the same manner as the other five cases then adjusted by placing limits on the maximum force. The limits were determined from the maximum flux density that the steel could support.

The following flow chart type of representation illustrates how the analytical force was arrived at for this case.

As with the other cases differential saturation was not considered.

ORIGINAL CALCULATION

FOR CASE SIX

(Short 1θ, 5 KVA in each of two remaining phases)

Test Results

From Test Results, terminal currents, and voltages

I_1, I_2, I_3,

V_1, V_2, V_3

AT_{DC}

Symmetrical Component Analysis

I_1, $\angle\phi_1$, V_1

I_2, $\angle\phi_2$, V_2

I_0, $\angle\phi_0$, V_0

Forward Rotating Components Only

Saturation Program

AT_{DC}, $\angle\phi_1$, I_1, V_1
K1, K2, K3, K4, K5, K6 for P0, P1, P2, P3, P4, P5, where Pr = nth harmonic rotor permeance and K = adjustment for saturation in path from STATOR YOKE TO ROTOR YOKE

Force Calculation Program

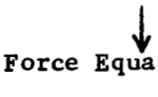

Force Equations (Too High).

Basically the force calculation was done as the other cases (1 to 5) except that only the forward rotating quantities were used to calculate saturation.

Test data was used in a symetrical component analysis to determine correct input data to the Saturation Program (DC3015-0-0). Data from both the Saturation Program and the symetrical component analysis is required to calculate force. The Saturation Program adjusts permeance, the symetrical component analysis mmf.

MMF's SEEN BY ROTOR

1. Forward Rotating MMF (Positive Sequence)

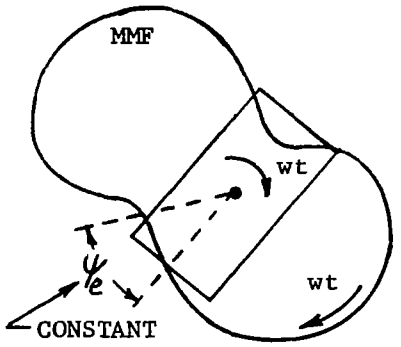

Always moves with the rotor and has the same displacement from peak to MMF to a point on rotor.

2. D. C. Excitation is seen as a constant and has no reference angle since it is of uniform magnitude around the gap.

3. Backward Rotating MMF (Negative Sequence)

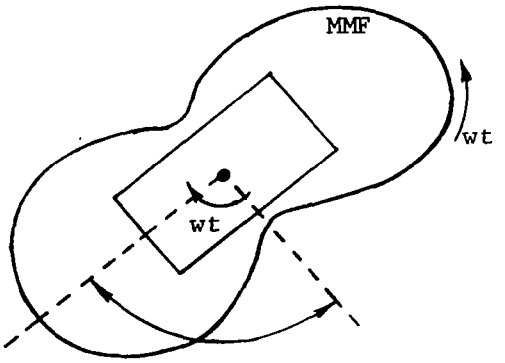

Moves at rotor speed but in opposite direction; looks like 2 wt to a rotor pole.

4. Standing wave MMF (Zero Sequence)

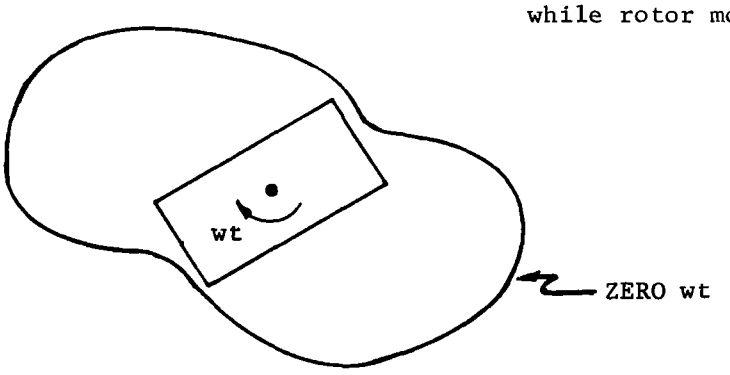

MMF Stands still and pulsates in magnitude while rotor moves past it.

Combining these MMF's results in Exhibit A on the following page. As the sketch indicates, the much higher MMF peaks result in large time variant saturation parameters.

EFFECT OF TIME VARIANT SATURATION

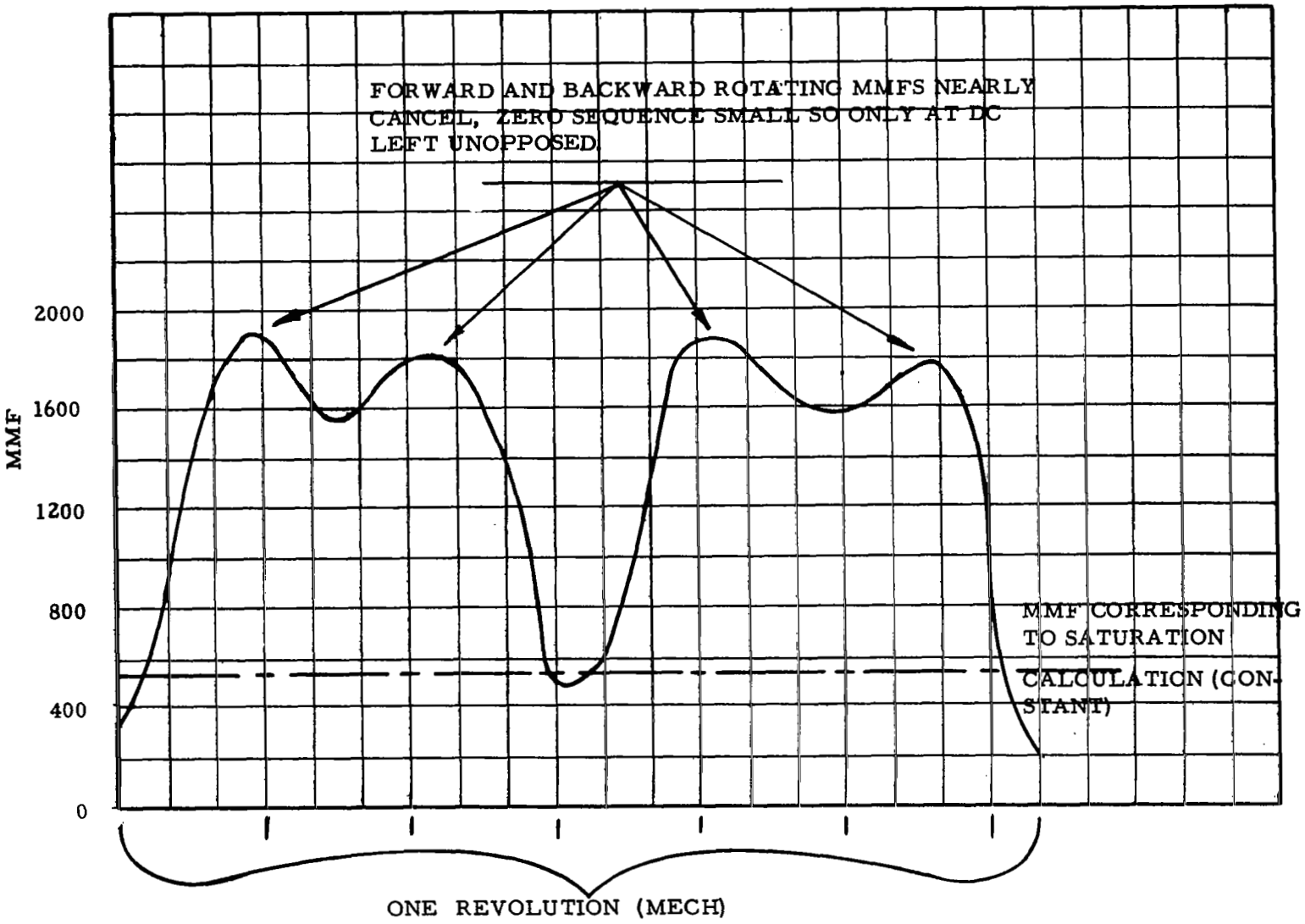

EXHIBIT A

An adjustment was made on the original force calculation for case six to account for the high levels of time variant saturation.

ADJUSTMENT FOR CASE SIX

Terminal Conditions
From Test Including I_f — This sets the ground rules for the maximum mmf available in the alternator.

↓

Graph of Gap Density
vs. Total Amp Turns — This combined with the terminal conditions above yield the maximum gap density.

↓

Calc. Max. Possible Force — i.e., based on the miximum gap density a maximum force was calculated.

↓

Place Limits on Original
Force Equation consisting of maximum force calculated above.

↓

Fourier Analysis of New
Limited Force so that the force limits are in terms like the calculated harmonic and steady state force.

↓

New Coefficient for each
harmonic in Force Expression

↓

Computer program ← Old Harmonic Coefficients from original calculation
to adjust each old coefficient
so that the total is within the
new boundry conditions

↓

→ New Force equation of exactly the same Form as originally but with adjusted coefficients for each term.

Derivation of Criterion for Integrating to a Force

In the analytical development section, it was pointed out that actual integration of all the terms is unnecessary because many will go to zero. A criterion was established and computerized to select only the terms that would integrate to a force.

Equation 15 (below):

$$\frac{\mathcal{B}}{\mu} = \left\{\left[P_o + \sum \frac{2}{n\pi} \sin\alpha(n\pi(\frac{1}{g_1} - \frac{1}{g_2}) \cos(n\rho(\theta - wt))\right.\right.$$
$$\left.+ P_A \cos n_a (N_A(\theta - wt))\right] X \left[P_S \cos n_s N_S\theta\right] X \left[(1 - \frac{\delta}{g} \cos(\theta - B)\right] X$$
$$\left.\left[M K_{pn} K_{dn} \sum \cos(n\rho(\theta - wt + \pi - \psi_e)) + AT_{dc}\right]\right\} \qquad \text{Eq. \#15}$$

can be viewed as:

$$\frac{\mathcal{B}}{\mu} = \left\{\left[P_o + K_1 \cos(n\rho(\theta - wt)) + K_2 \cos(N_A(\theta - wt))\right] X\right.$$
$$\left.\left[K_3 \cos n N_S\theta\right] X \left[K_4 \cos(\theta - B)\right] X \left[K_5 \cos n\rho(\theta - wt + \pi - \psi_e) + K_6\right]\right\}$$

where the K's represent the various permeance and MMF coefficients in Eq. #15. This can be further reduced by performing the indicated multiplications. This gives the form

$$\frac{\mathcal{B}}{\mu} = P_o K_3 \cos n N_S\theta + P_o K_4 \cos(\theta - B) + \ldots.$$
$$+ K_5K_1 \cos(n\rho(\theta - wt)) \cos(n\rho(\theta - wt + \pi - \psi_e)) + \ldots.$$

which when further reduced by the identity in Eq. #50b and letting all the K's and P_o be a constant $\mathcal{P}$ and omitting terms containing no cosines results in Eq. #46 where terms of the form $n_x N_x$ are represented by N_x.

$$\frac{\mathcal{B}_{x1x2x3x4x5}}{\mu} = \mathcal{P} \cos(\pm N_R\rho\theta \pm N_S\theta \pm N_A\theta + N_E\theta$$
$$\pm N_{mmf}\rho\theta \pm N_R Wt - N_A Wt$$
$$\pm N_{mmf}\rho Wt \pm \pi \pm \psi_e \pm B) \qquad \text{Eq. \#46}$$

Each of these can be represented in a simpler fashion by combining all the θ coefficients to a and wt coefficients to b.

$$\mathcal{B}_{x1x2x3x4x5} = \mathcal{P}\cos(a\theta + bwt + \pi - \psi_e + B) \qquad \text{Eq. \#47}$$

Since two terms are necessary to form $\mathcal{B}^2$, let c be like a and d like b then

$$\mathcal{B}_{x1x2x3x4x5} = \mathcal{P} \cos (a\theta + b) \text{ or } \mathcal{P} \cos (c\theta + d) \qquad \text{Eq. \#48}$$

Then any force term can be represented by substituting the above in Eq. #1.

$$F = K\int_{c}^{2\pi} \mathcal{P} \cos (a\theta + b)\ \mathcal{P} \cos (c\theta + d)\, d\theta \qquad \text{Eq. \#49}$$

where K is a constant.

To give this force a sense of direction either cos θ or sin θ must be included in the integral and act as a multiplier for the other* cosine terms.

We can write the following expression for a force in the "y" direction.

$$FY = K\mathcal{P}^2 (\cos(a\theta + b) \cos (c\theta + d) \cos\theta)\, d\theta \qquad \text{Eq. \#50}$$

Looking just at

$$\cos (a\theta + b) \cos (c\theta + d) \cos\theta$$

And expanding by the identity

$$\cos\alpha \cos B = 1/2 \cos (\alpha + B) + 1/2 \cos (\alpha - B) \qquad \text{Eq. \#50b}$$

Indicates that

$$\cos (a\theta + b) \cos (c\theta + d) \cos\theta =$$

$$1/2 \cos ((a + 1)\theta + b) \cos (c\theta + d) + 1/2 \cos ((a-1)\theta + b) \cos (c\theta + d)$$

which can be further expanded to:

$$= 1/4 \cos ((a + 1 + c)\theta + b + d)$$

$$+ 1/4 \cos ((a + 1 - c)\theta + b - d)$$

$$+ 1/4 \cos ((a - 1 + c)\theta + b + d)$$

$$+ 1/4 \cos ((a - 1 - c)\theta + b + d) \qquad \text{Eq. \#51}$$

It can be shown that $\int_{c}^{2\pi} \cos n\theta = 0$

Therefore:

$$a + 1 + c = 0 \qquad \text{Eq. \#52}$$
$$a + 1 - c = 0 \qquad \text{Eq. \#53}$$
$$a - 1 + c = 0 \qquad \text{Eq. \#54}$$
$$a - 1 - c = 0 \qquad \text{Eq. \#55}$$

in Eq. #51 will integrate to a non zero value of force.

Since the Brayton Cycle machine has an even number of amortisseur slots, stator slots, and poles, the only terms that can be combined and integrated to a force are those where one $\mathcal{B}$ term contains eccentricity and one $\mathcal{B}$ term contains only other coefficients. The eccentricity term contains an odd

* The force in Eq. #1 is radially outward, therefore; $F_y = F_{\cos\theta}$ and $F_x = F_{\sin\theta}$.

θ which will combine with the direction sine or cosine θ to form some argument with a 0 for the θ coefficient as in Eq's. 52, 53, 54, 55.

The following is an example of one $(\mathcal{B})^2$ term integrated to a force. The first term contains average or dc permeance and the fundamental of armature reaction. The second term contains the fundamental rotor permeance, eccentricity and the MMF fundamental.

$$\begin{aligned}\mathcal{B}_{00001} \times \mathcal{B}_{10011} = 1/8\ K &\cos(2\theta - 2\,wt + \pi - \psi_e + \theta - B + \pi - \psi_e) \\ &+ \cos(2\theta - 2\,wt + \pi - \psi_e - \theta + \pi + \psi_e) \\ &+ \cos(2\theta - 2\,wt + \pi - \psi_e - 3\theta + 4\,wt - B - \pi + \psi_e) \\ &+ \cos(2\theta - 2\,wt + \pi - \psi_e + 3\theta - 4\,wt + b + \pi - \psi_e) \\ &+ \cos(2\theta - 2\,wt + \pi - \psi_e - \theta + B + \pi - \psi_e) \\ &+ \cos(2\theta - 2\,wt + \pi - \psi_e + \theta - B - \pi + \psi_e)\end{aligned} \qquad \text{Eq. \#56}$$

Where $K = \frac{-\delta \mu^2}{g} P_0 \mathcal{P}_M^2$

Eliminating the terms that don't differ by unity gives.

$$\mathcal{B}_{00001} \times \mathcal{B}_{10011} = \frac{K}{8} \left(\cos(\theta - 2\,wt + B - 2\psi_e) + 2\cos(-\theta + 2\,wt - B)\right) \qquad \text{Eq. \#57}$$

Integrating:

$$F(y) = -.932 \cos(2\,wt - B + 2\psi_e) - 1.864 \cos(-2\,wt + B) \qquad \text{Eq. \#58}$$

This force has two permutations as follows:

$\mathcal{B}_{000001} \times \mathcal{B}_{10011}$ is equivalent to

$\mathcal{B}_{10001} \times \mathcal{B}_{00011}$

Thus only one integration is necessary to find four forces arising from two sets of $\mathcal{B}$ Terms.

By predicting the terms that may be combined to exactly the same force the total number of terms that must be integrated is cut in half. An elaborate bookkeeping scheme in the computer program accomplishes this by generating the flux density terms in a specific order.

The net result of the several million possible terms in the force equation is a few hundred terms of actual force. Those with like angular arguments are combined by the computer. The final computer output also contains expressions for the derivations of force with respect to eccentricity and eccentricity angle B.

SECTION X

EXPERIMENTAL DATA

"Table" of Contents - Where to Find the Polaroid Photos of Oscilloscope Traces of Bearing Force for Various Test Conditions. **No load at 2.7 field amperes is given in photo V-49.**

Page No. DE/Page No. ODE

Eccentricity (nominal)	P. F.	No Load No Field	3.33 KVA Single Phase	11.25 KVA 3 Phase	15 KVA 3 Phase	15 KVA 3 Phase, then 1 Phase Shorted	15 KVA 3 Phase, then 3 Phase Shorted
0	1	88/112	89/113	90/114	---	---	---
.002"	1.0	91/115	92/116	93/117	---	---	---
.002"	.08 lag	---	---	94/118	95/119	96/120	97/121
.004"	1.0	98/122	99/123	100/124	---	---	---
.004"	.08 lag	---	---	101/125	102/126	103/127	104/128
.006"	1.0	105/129	106/130	107/131	---	---	---
.006"	.08 lag	---	---	108/132	109/133	110/134	111/135

FORCES EXERTED ON THE BEARINGS OF THE BRAYTON CYCLE ALTERNATOR

Eccentricity: Zero

Equivalent Load Condition: No load, no field

Location: DE bearing

RPM: 3000

Force Scale: 5 pounds per centimeter radial or vertical

Time Scale: One revolution between timing marks

Top of Alternator

Left Side of Alternator

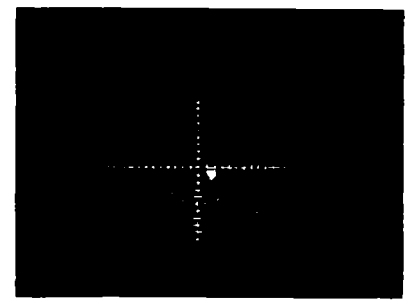

Poler Plot of Bearing Forces

X Forces vs. Time

Y Forces vs. Time

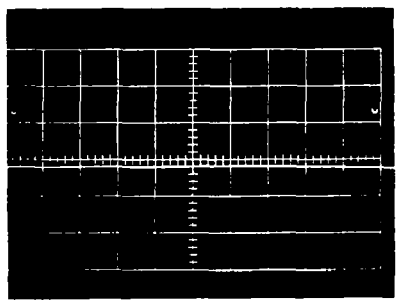

dc force plus 100 cps component

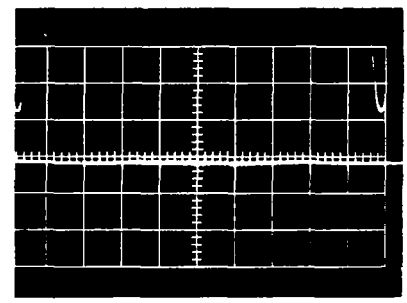

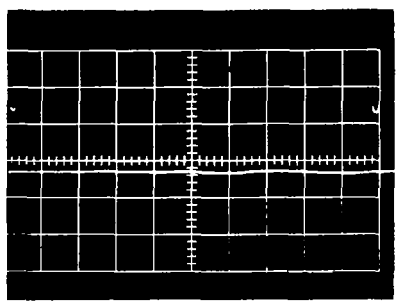

dc force plus 200 cps component

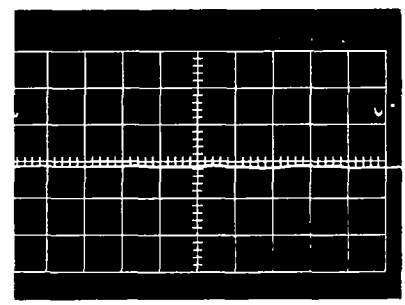

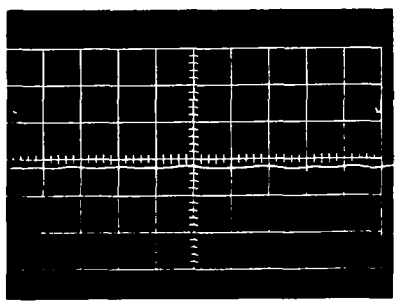

dc force plus 300 cps component

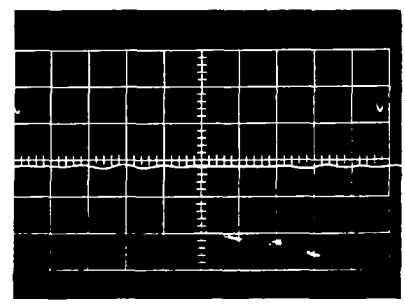

FORCES EXERTED ON THE BEARINGS OF THE BRAYTON CYCLE ALTERNATOR

Eccentricity: Zero

Equivalent Load Condition: 3.33 KVA [illegible] P.F. [illegible] ϕ

Location: DE bearing

RPM: 7600

Force Scale: 5 pounds per centimeter radial or vertical

Time Scale: One revolution between timing marks

Top of Alternator

Left Side of Alternator

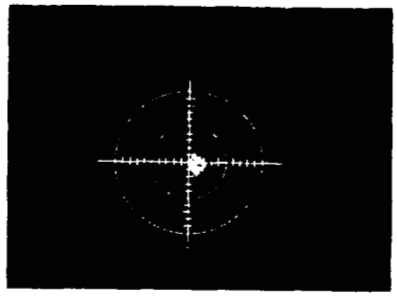

+Y↑

+X→

Polar Plot of Bearing Forces

X Forces vs. Time

Y Forces vs. Time

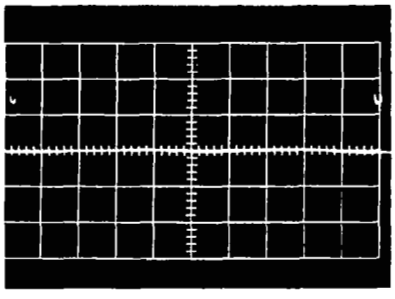

+X↑

+Y↑

dc force plus 100 cps component

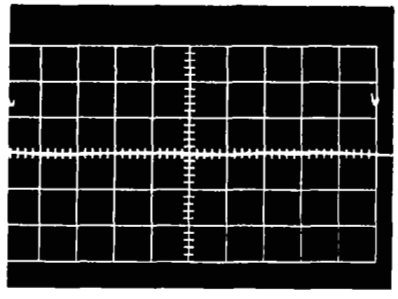

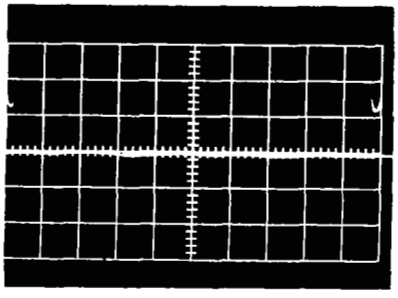

dc force plus 200 cps component

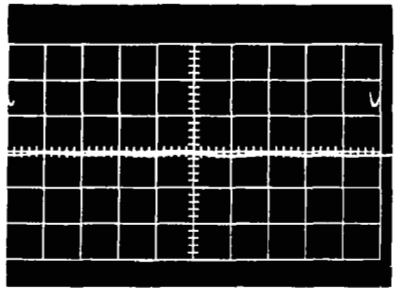

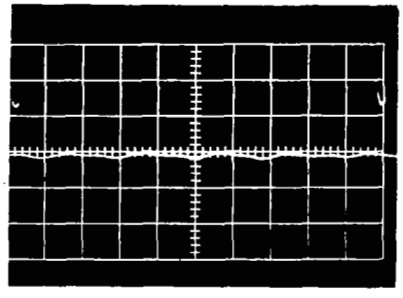

dc force plus 300 cps component

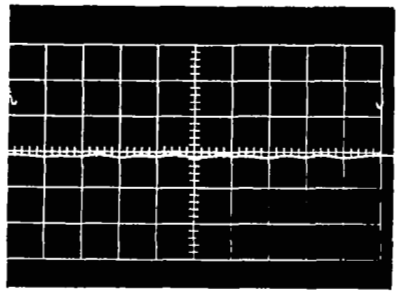

Eccentricity: Zero

Equivalent Load Condition: 11.25 KVA 1.0 P.F. 3 ϕ

Location: DE bearing

RPM: 3000

Force Scale: 5 pounds per centimeter radial or vertical

Time Scale: One revolution between timing marks

Top of Alternator

Left Side of Alternator

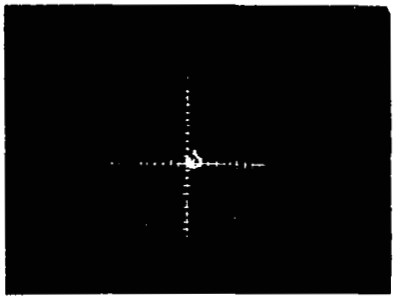

+Y↑

+X→

Polar Plot of Bearing Forces

X Forces vs. Time

Y Forces vs. Time

+X↑

+Y↑

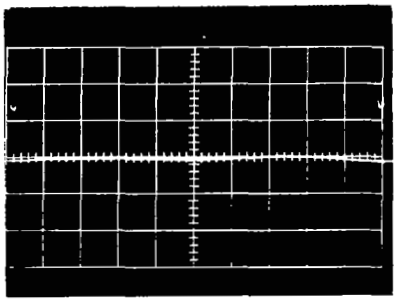

dc force plus 100 cps component

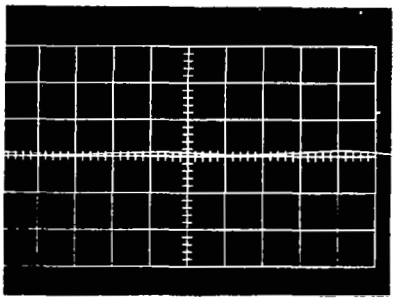

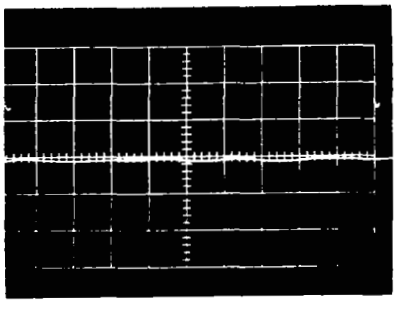

dc force plus 200 cps component

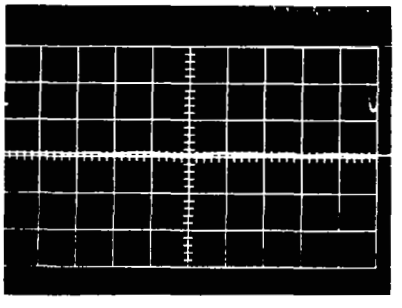

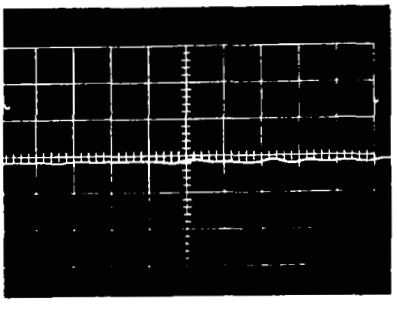

dc force plus 300 cps component

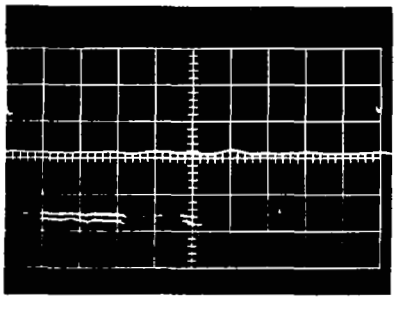

FORCES EXERTED ON THE BEARINGS OF THE BRAYTON CYCLE ALTERNATOR

Eccentricity: .002 in. toward bottom of generator

Equivalent Load Condition: No load, no field

Location: DE bearing

RPM: 3000

Force Scale: 5 pounds per centimeter radial or vertical

Time Scale: One revolution between timing marks

Top of Alternator

Left Side of Alternator

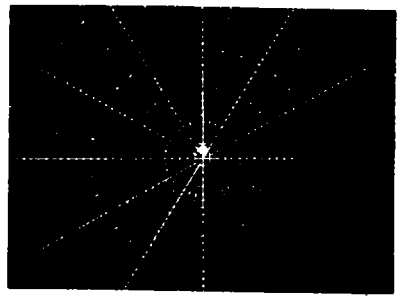

+Y↑

+X→

Polar Plot of Bearing Forces

X Forces vs. Time

Y Forces vs. Time

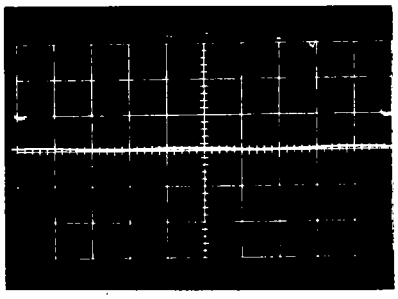

+X↑

dc force plus 100 cps component

+Y↑

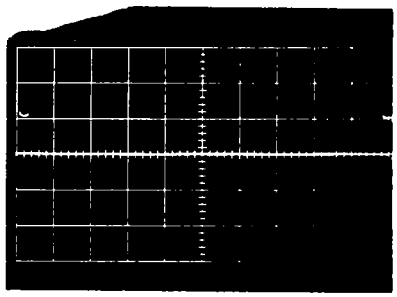

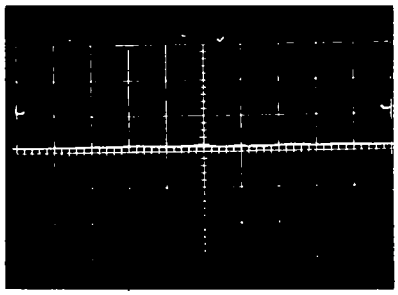

dc force plus 200 cps component

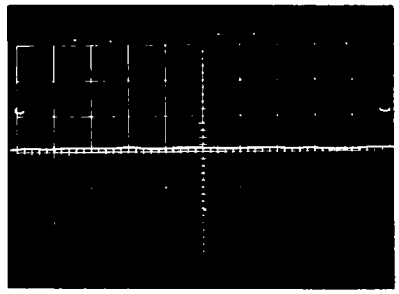

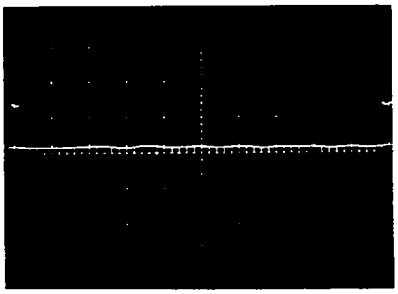

dc force plus 300 cps component

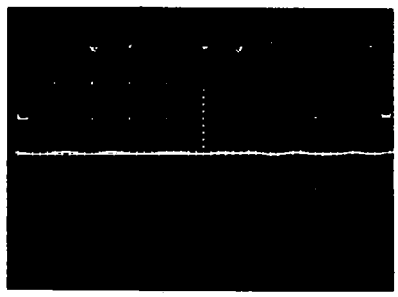

FORCES EXERTED ON THE BEARINGS OF THE BRAYTON CYCLE ALTERNATOR

Eccentricity: .002 in. toward bottom of generator

Equivalent Load Condition: 3.33 KVA 1.0 P.F. 1 ϕ

Location: DE bearing

RPM: 3000

Force Scale: 5 pounds per centimeter radial or vertical

Time Scale: One revolution between timing marks

Top of Alternator

Left Side of Alternator

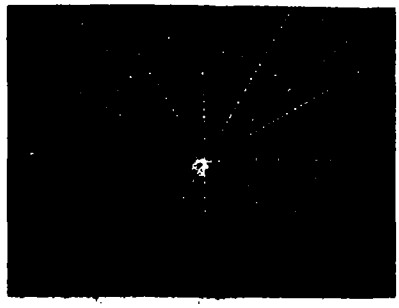

+Y

+X

Polar Plot of Bearing Forces

X Forces vs. Time

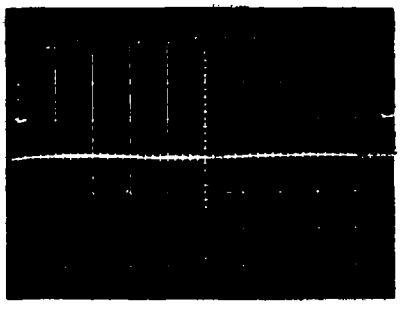

+X

dc force plus 100 cps component

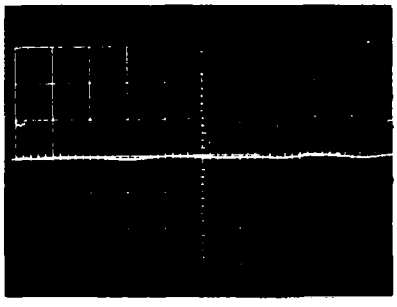

dc force plus 200 cps component

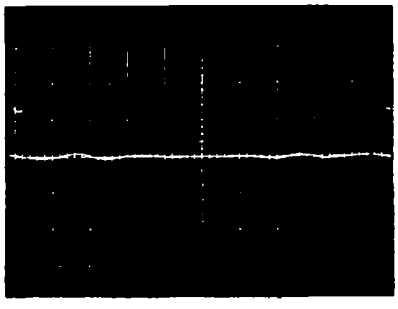

dc force plus 300 cps component

+Y

Y Forces vs. Time

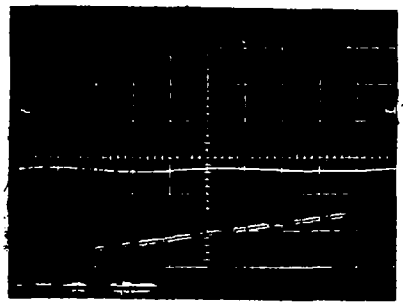

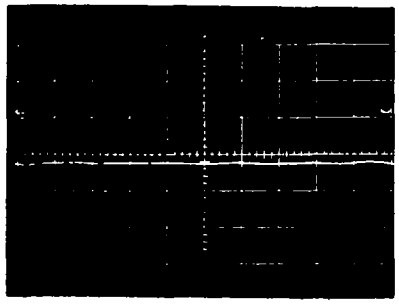

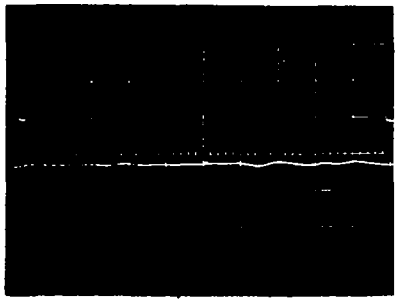

FORCES EXERTED ON THE BEARINGS OF THE BRAYTON CYCLE ALTERNATOR

Eccentricity: .002 in. toward bottom of generator

Equivalent Load Condition: 11.25 KVA 1.0 P.F. 3 ϕ

then ϕ shorted

Location: DE bearing

RPM: 3000

Force Scale: 5 pounds per centimeter radial or vertical

Time Scale: One revolution between timing marks

Top of Alternator

Left Side of Alternator

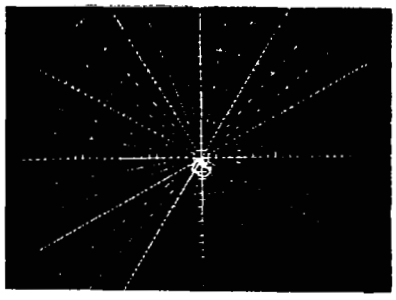

+Y

+X

Polar Plot of Bearing Forces

X Forces vs. Time

Y Forces vs. Time

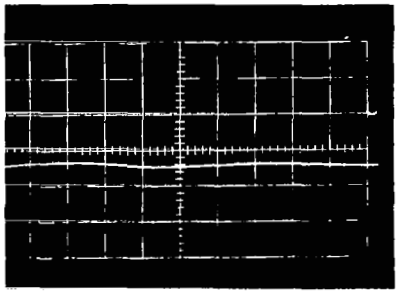

+X

dc force plus 100 cps component

+Y

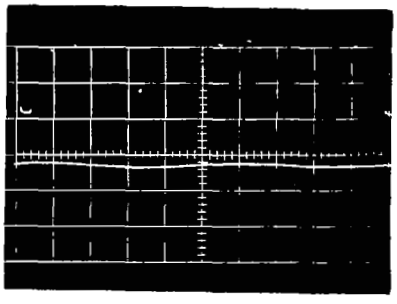

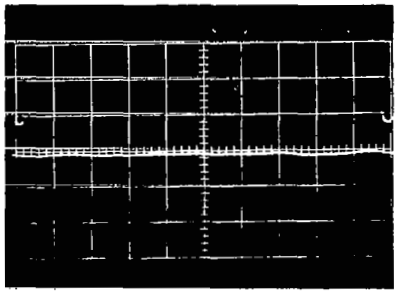

dc force plus 200 cps component

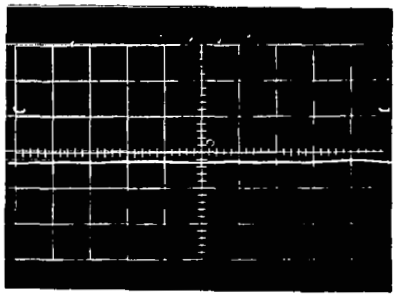

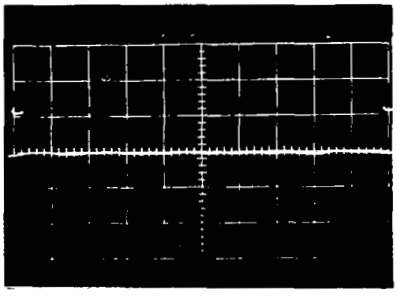

dc force plus 300 cps component

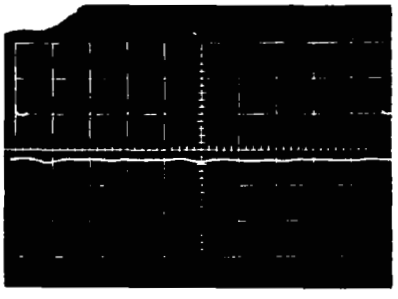

FORCES EXERTED ON THE BEARINGS OF THE BRAYTON CYCLE ALTERNATOR

Eccentricity: .002 in. toward bottom of generator

Equivalent Load Condition: 11.25 KVA 0.8 P.F. 3 ϕ

Location: DE bearing

RPM: 3000

Force Scale: 5 pounds per centimeter radial or vertical

Time Scale: One revolution between timing marks

Top of Alternator

Left Side of Alternator

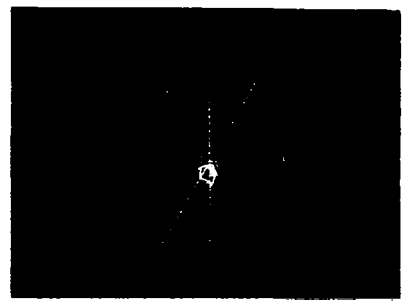

+Y

+X

Polar Plot of Bearing Forces

X Forces vs. Time

Y Forces vs. Time

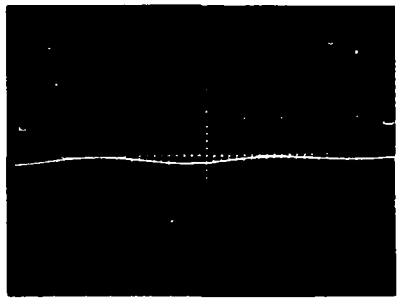

+X

+Y

dc force plus 100 cps component

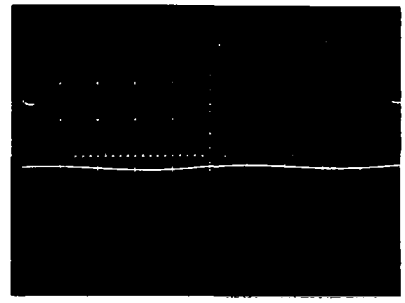

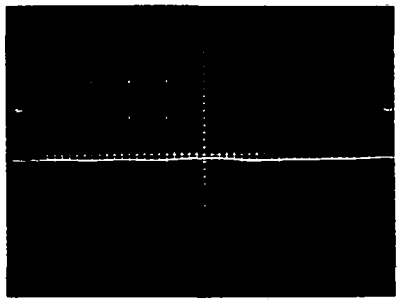

dc force plus 200 cps component

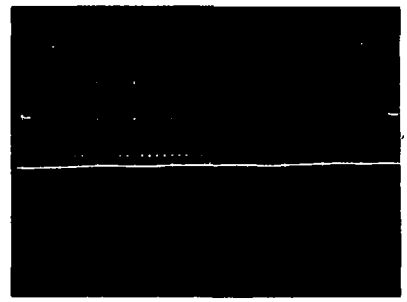

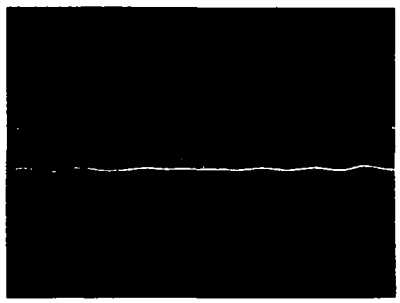

dc force plus 300 cps component

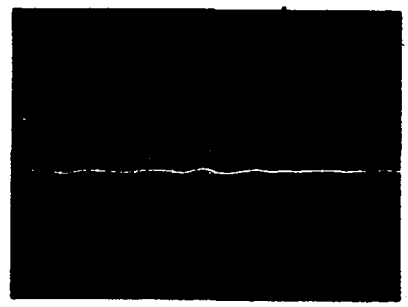

FORCES EXERTED ON THE BEARINGS OF THE BRAYTON CYCLE ALTERNATOR

Eccentricity: .002 in. toward bottom of generator

Equivalent Load Condition: 15 KVA 0.6 P.F. 3 ϕ

Location: DE bearing

RPM: 3000

Force Scale: 5 pounds per centimeter radial or vertical

Time Scale: One revolution between timing marks

Top of Alternator

Left Side of Alternator

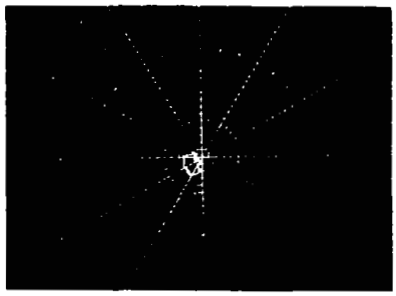

+Y↑

+X→

Polar Plot of Bearing Forces

X Forces vs. Time

Y Forces vs. Time

+X↑

+Y↑

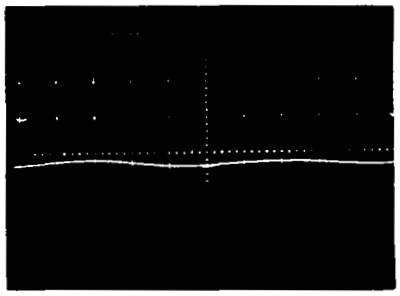

dc force plus 100 cps component

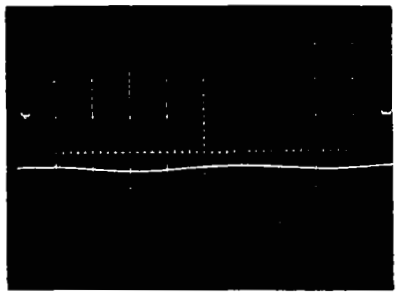

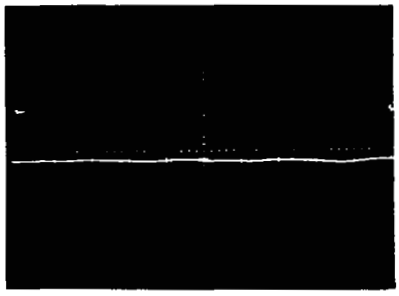

dc force plus 200 cps component

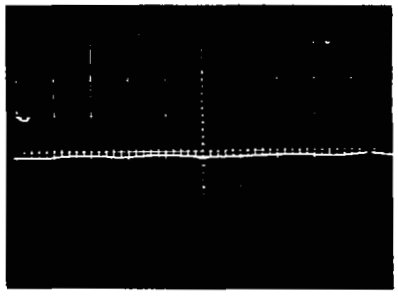

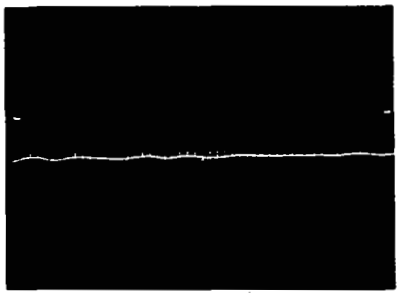

dc force plus 300 cps component

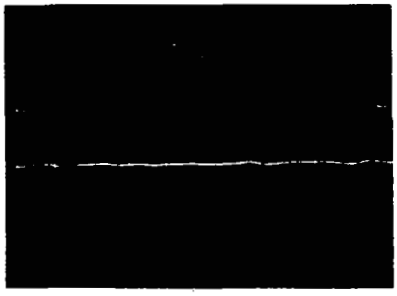

FORCES EXERTED ON THE BEARINGS OF THE BRAYTON CYCLE ALTERNATOR

Eccentricity: .002 in. toward bottom of generator

Equivalent Load Condition: 15 KVA 0.8 P.F. 3ϕ

then 1ϕ shorted

Location: DF bearing

RPM: 7000

Force Scale: 5 pounds per centimeter radial or vertical

Time Scale: One revolution between timing marks

Top of Alternator

Left Side of Alternator

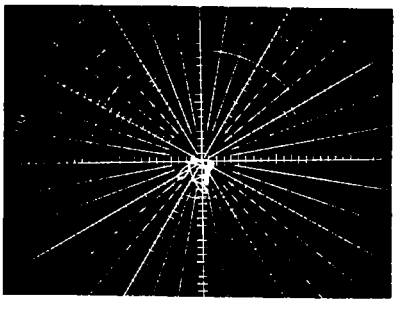

+Y↑

+X→

Polar Plot of Bearing Forces

X Forces vs. Time

Y Forces vs. Time

+X↑

+Y↑

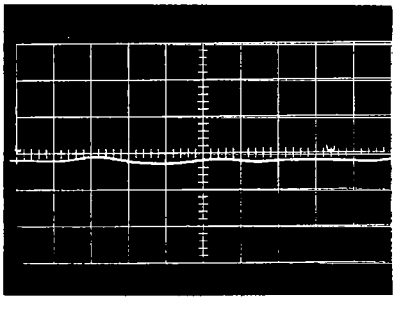

dc force plus 175 cps component

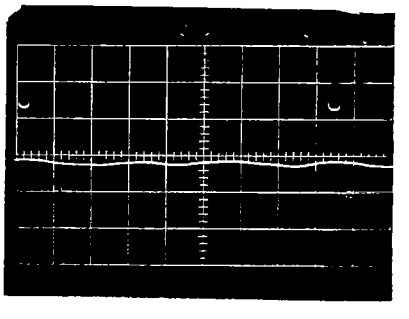

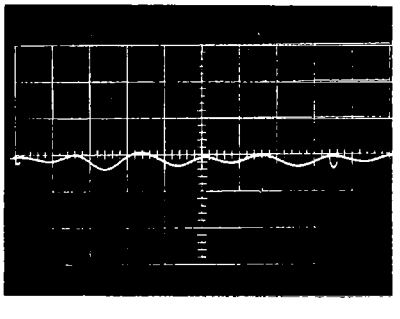

dc force plus 230 cps component

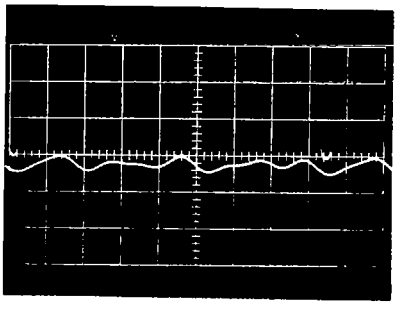

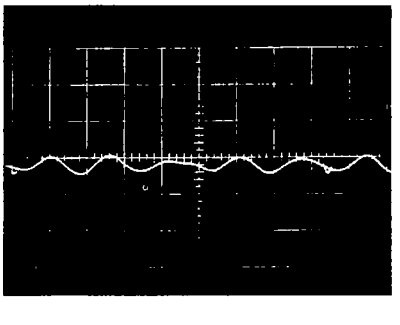

dc force plus 345 cps component

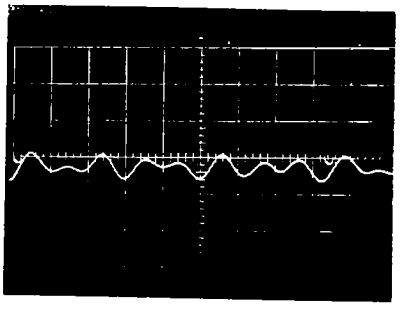

FORCES EXERTED ON THE BEARINGS OF THE BRAYTON CYCLE ALTERNATOR

Eccentricity: .002 in. toward bottom of generator

Equivalent Load Condition: 15 KVA 0.8 P.F. 3 ϕ

then 3 ϕ shorted

Location: DE bearing

RPM: 3000

Force Scale: 5 pounds per centimeter radial or vertical

Time Scale: One revolution between timing marks

Top of Alternator

Left Side of Alternator

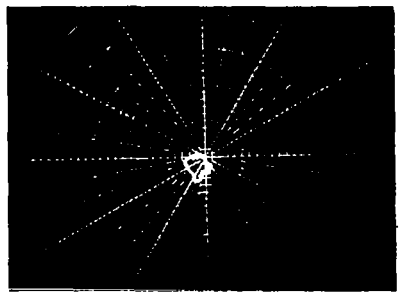

+Y↑

+X→

Polar Plot of Bearing Forces

X Forces vs. Time

Y Forces vs. Time

+X↑

+Y↑

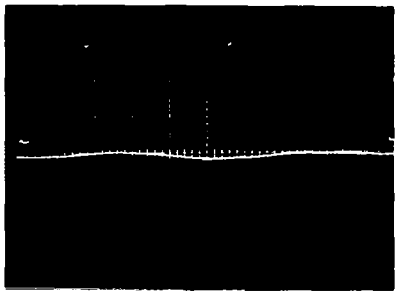

dc force plus 100 cps component

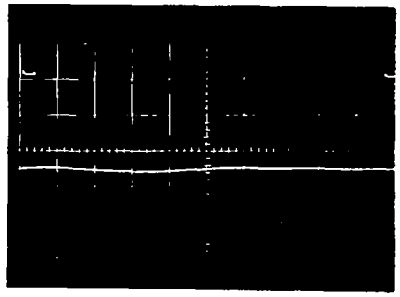

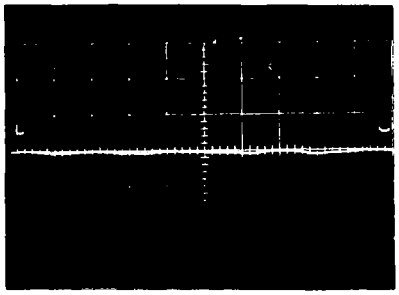

dc force plus 200 cps component

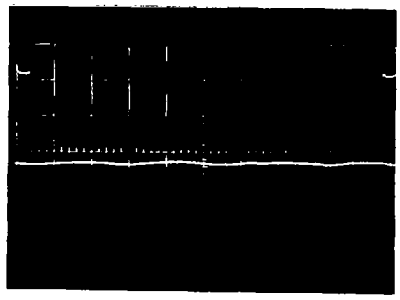

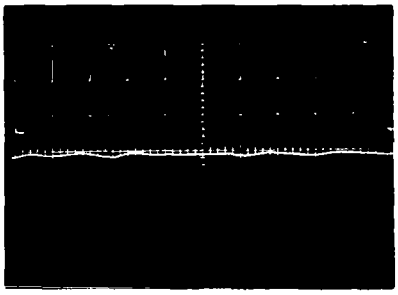

dc force plus 300 cps component

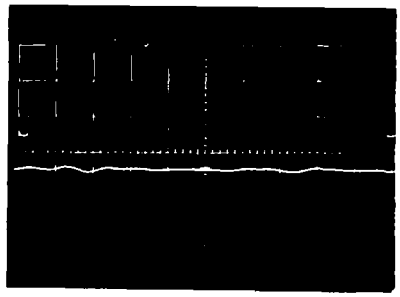

FORCES EXERTED ON THE BEARINGS OF THE BRAYTON CYCLE ALTERNATOR

Eccentricity: .[illegible] in. toward bottom of generator

Equivalent Load Condition: [illegible]

Location: [illegible] bearing

RPM:

Force Scale: [illegible] pounds per centimeter radial or vertical

Time Scale: One revolution between timing marks

Top of Alternator

Left Side of Alternator

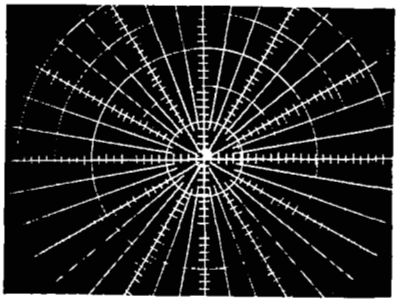

-Y↑

+X→

Polar Plot - Bearing Forces

X Forces vs. Time

Y Forces vs. Time

+X↑

+Y↑

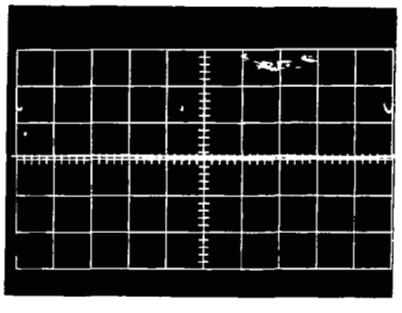

dc force plus 100 cps component

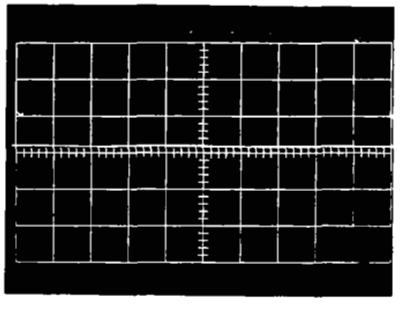

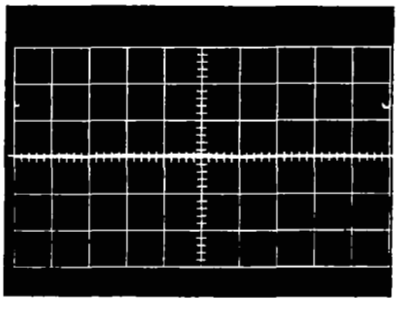

dc force plus 200 cps component

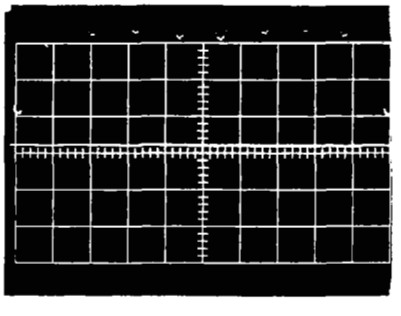

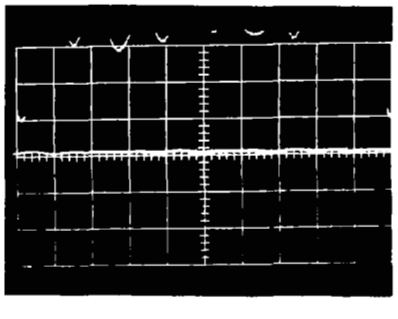

dc force plus 300 cps component

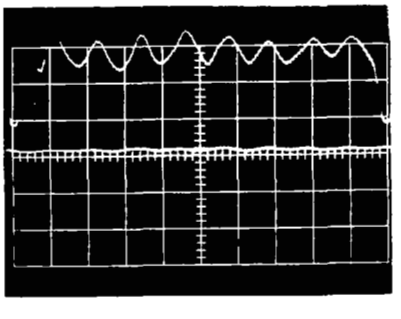

FORCES EXERTED ON THE BEARINGS OF THE BRAYTON CYCLE ALTERNATOR

Eccentricity: .044 in. toward bottom of generator

Equivalent Load Condition: 3.33 KVA 1.0 P.F. 1ϕ

Location: DE bearing

RPM: 3000

Force Scale: 5 pounds per centimeter radial or vertical

Time Scale: One revolution between timing marks

Top of Alternator

Left Side of Alternator

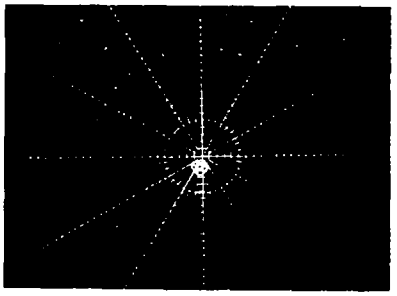

+Y↑

+X→

Polar Plot of Bearing Forces

X Forces vs. Time

Y Forces vs. Time

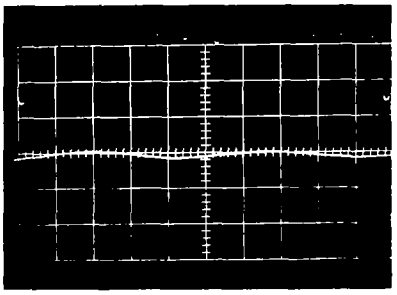

+X↑

+Y↑

dc force plus 100 cps component

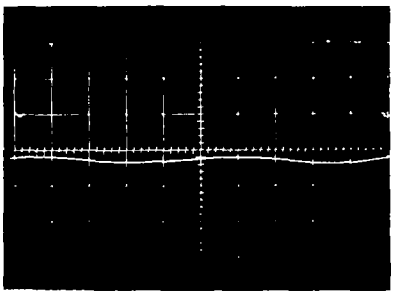

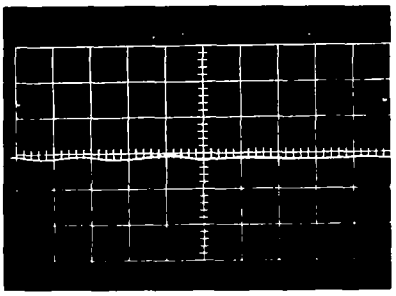

dc force plus 200 cps component

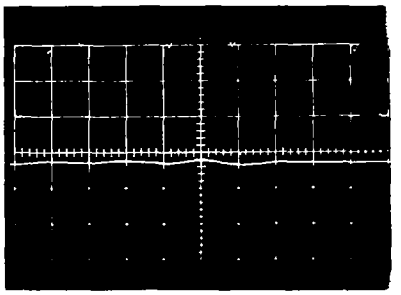

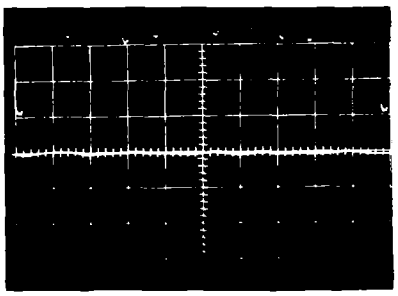

dc force plus 300 cps component

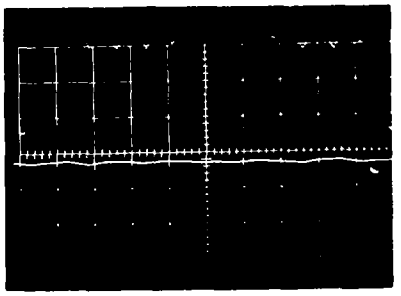

Eccentricity: .004 in. toward bottom of generator

Equivalent Load Condition: 11.25 KVA 1.0 P.F. 3ϕ

Location: DE bearing

RPM: 3000

Force Scale: 5 pounds per centimeter radial or vertical

Time Scale: One revolution between timing marks

Top of Alternator

Left Side of Alternator

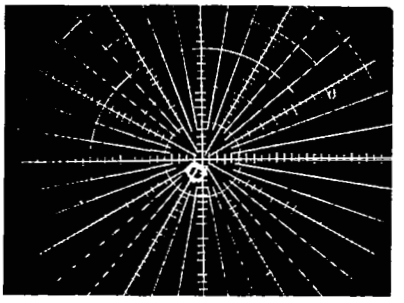

+Y↑

+X→

Polar Plot of Bearing Forces

X Forces vs. Time

Y Forces vs. Time

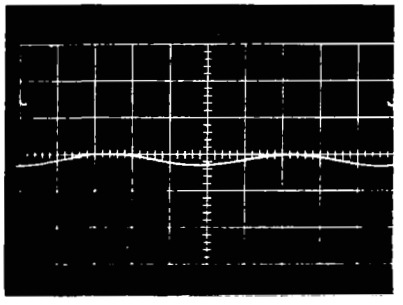

+X↑

dc force plus 100 cps component

+Y↑

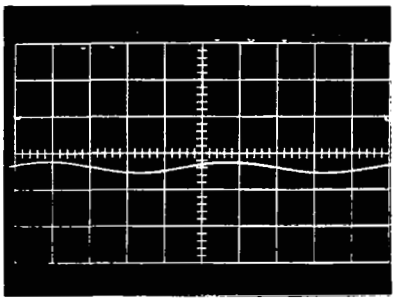

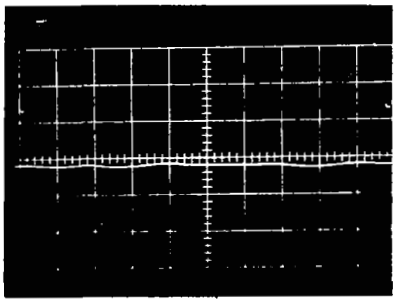

dc force plus 200 cps component

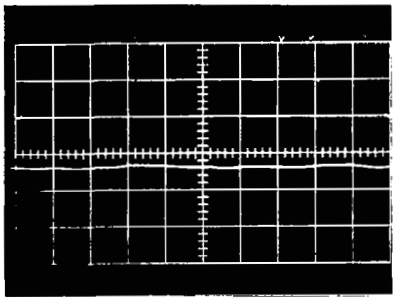

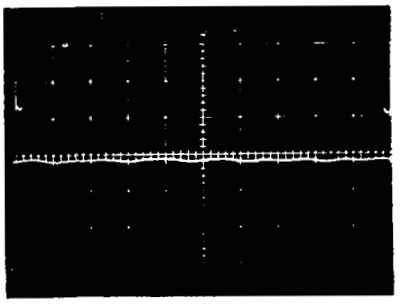

dc force plus 300 cps component

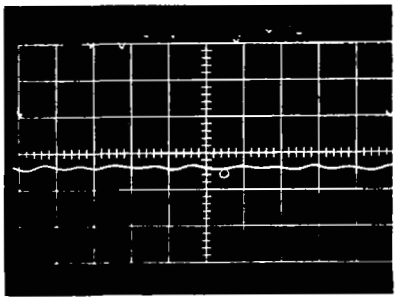

FORCES EXERTED ON THE BEARINGS OF THE BRAYTON CYCLE ALTERNATOR

Eccentricity: .004 in. toward bottom of generator

Equivalent Load Condition: 11.25 KVA 0.8 P.F. 3 ϕ

Location: DE bearing

RPM: 3000

Force Scale: 5 pounds per centimeter radial or vertical

Time Scale: One revolution between timing marks

Top of Alternator

Left Side of Alternator

+Y↑

+X→

Polar Plot of Bearing Forces

X Forces vs. Time

Y Forces vs. Time

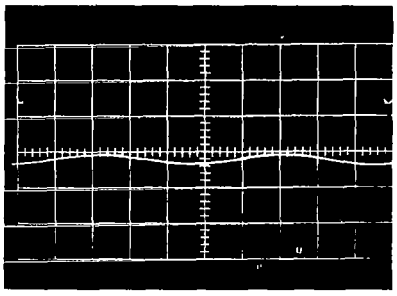

+X↑

dc force plus 100 cps component

+Y↑

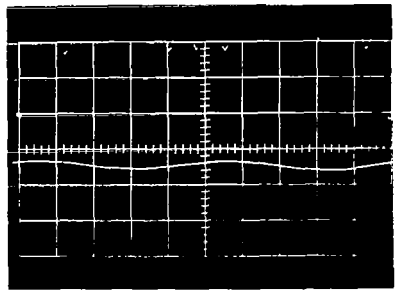

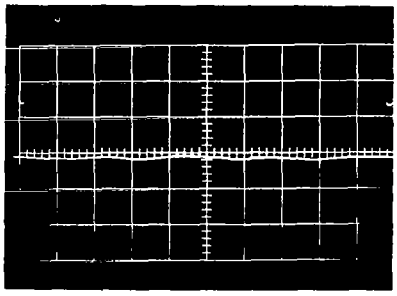

dc force plus 200 cps component

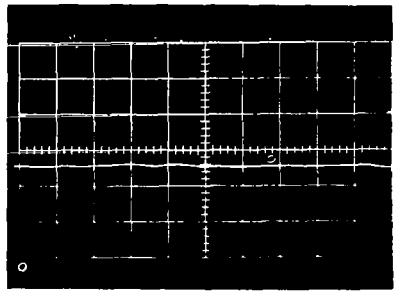

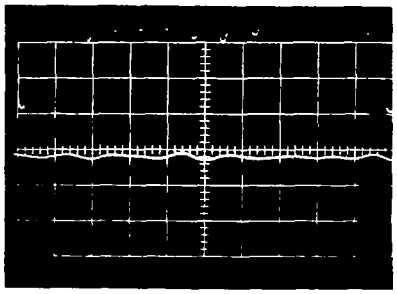

dc force plus 300 cps component

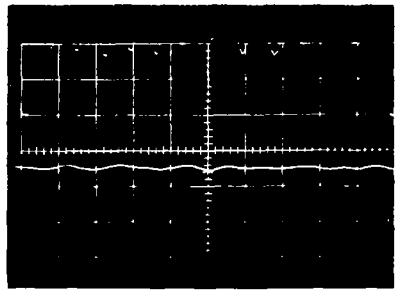

FORCES EXERTED ON THE BEARINGS OF THE BRAYTON CYCLE ALTERNATOR

Eccentricity: .004 in. toward bottom of generator

Equivalent Load Condition: 15 KVA 0.8 P.F. 3 ϕ

Location: DE bearing

RPM: 3000

Force Scale: 5 pounds per centimeter radial or vertical

Time Scale: One revolution between timing marks

Top of Alternator

Left Side of Alternator

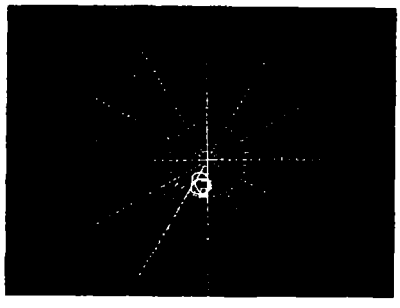

+Y↑

+X→

Polar Plot of Bearing Forces

X Forces vs. Time

Y Forces vs. Time

+X↑

+Y↑

dc force plus 100 cps component

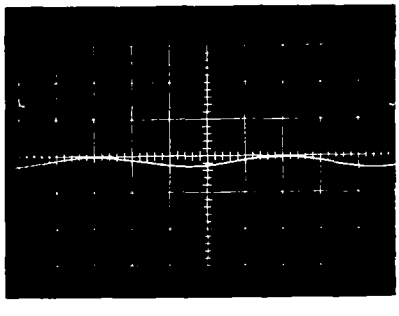

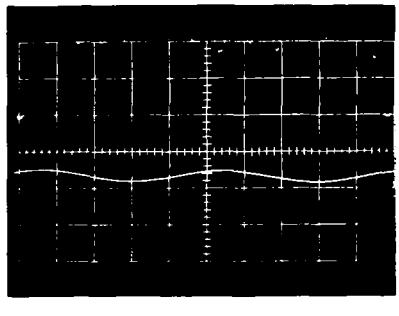

dc force plus 200 cps component

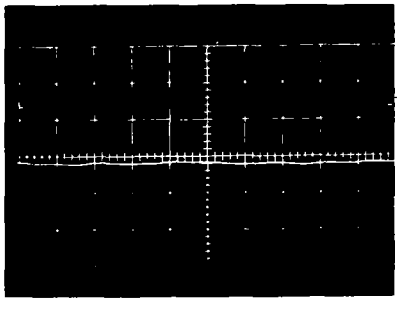

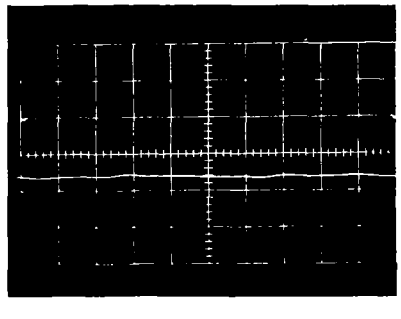

dc force plus 300 cps component

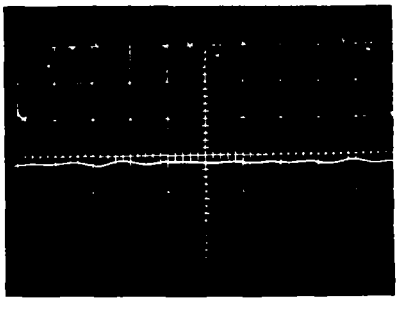

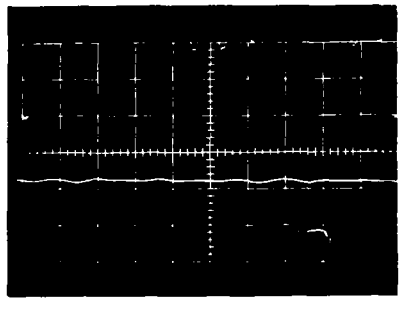

FORCES EXERTED ON THE BEARINGS OF THE BRAYTON CYCLE ALTERNATOR

Eccentricity: .004 in. toward bottom of generator

Equivalent Load Condition: 15 KVA 0.8 P.F. 3ϕ

then 1 ϕ shorted

Location: DE bearing

RPM: 3450

Force Scale: 5 pounds per centimeter radial or vertical

Time Scale: One revolution between timing marks

Top of Alternator

Left Side of Alternator

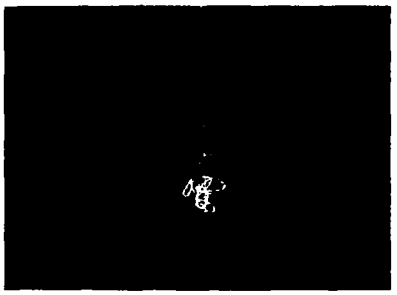

+Y↑

+X→

Polar Plot of Bearing Forces

X Forces vs. Time

Y Forces vs. Time

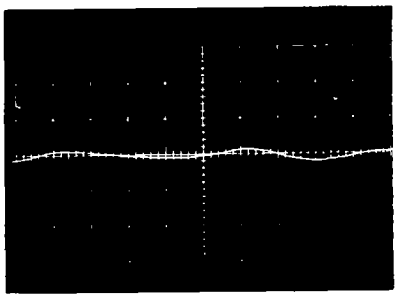

+X↑

+Y↑

dc force plus 115 cps component

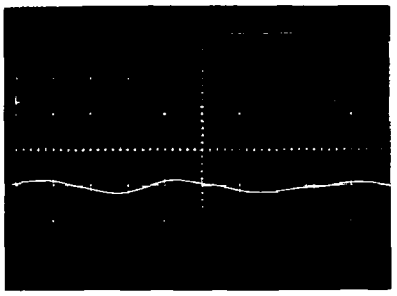

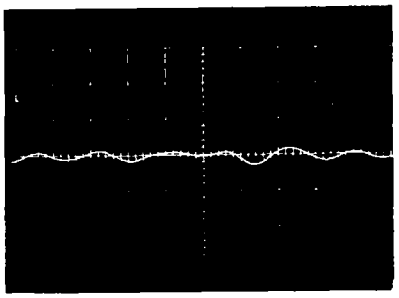

dc force plus 230 cps component

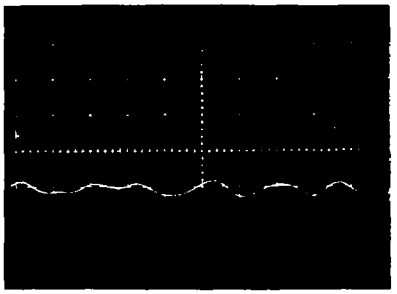

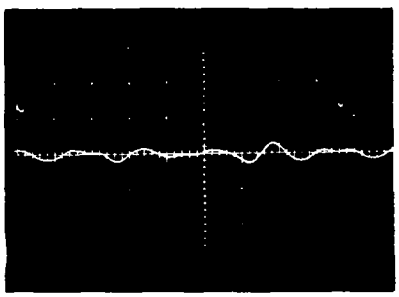

dc force plus 345 cps component

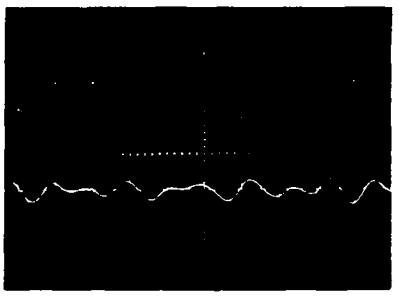

FORCES EXERTED ON THE BEARINGS OF THE BRAYTON CYCLE ALTERNATOR

Eccentricity: .004in. toward bottom of generator

Equivalent Load Condition: 15 KVA 0.8 P.F. 3ϕ

then 3 ϕ shorted

Location: DE bearing

RPM: 3000

Force Scale: 5 pounds per centimeter radial or vertical

Time Scale: One revolution between timing marks

Top of Alternator

Left Side of Alternator

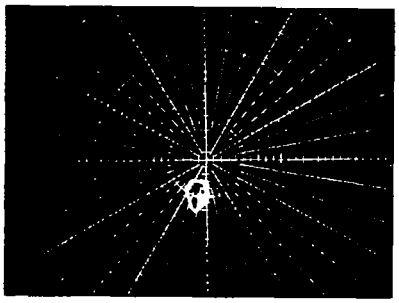

+Y↑

+X→

Polar Plot of Bearing Forces

X Forces vs. Time

Y Forces vs. Time

+X↑

+Y↑

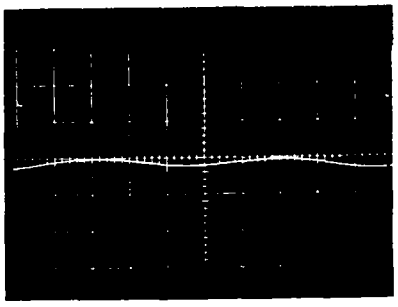

dc force plus 100 cps component

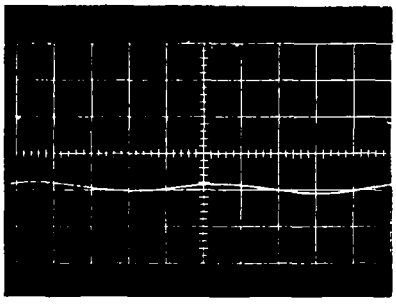

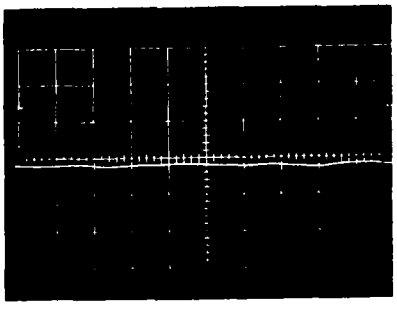

dc force plus 200 cps component

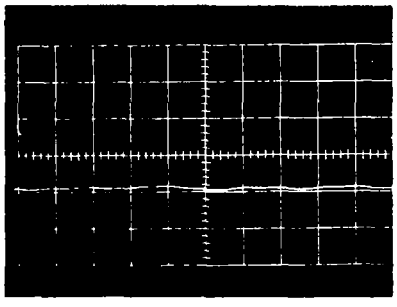

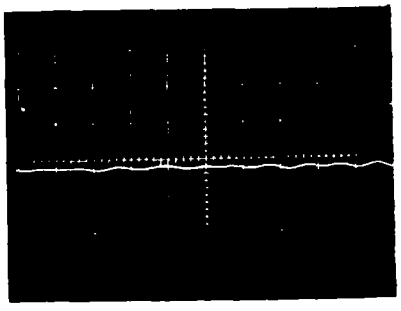

dc force plus 300 cps component

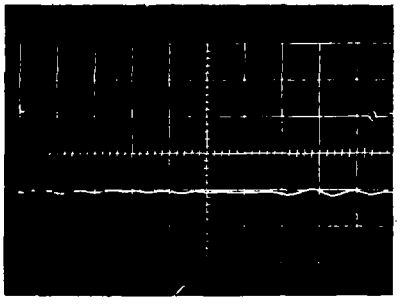

FORCES EXERTED ON THE BEARINGS OF THE BRAYTON CYCLE ALTERNATOR

Eccentricity: .006 in. toward bottom of generator

Equivalent Load Condition: No load, no field

Location: DE bearing

RPM: 4000

Force Scale: 5 pounds per centimeter radial or vertical

Time Scale: One revolution between timing marks

Top of Alternator

Left Side of Alternator

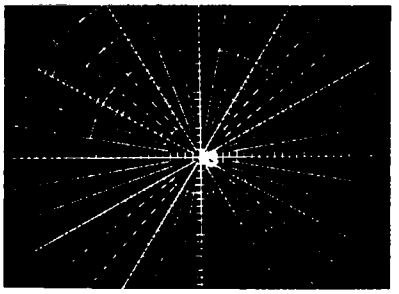

+Y↑

+X→

Polar Plot of Bearing Forces

X Forces vs. Time

Y Forces vs. Time

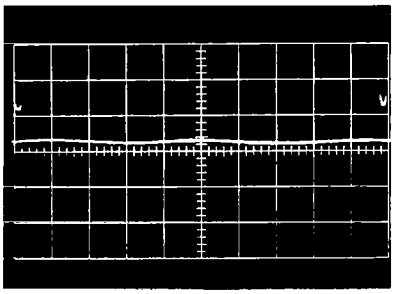

+X↑

dc force plus 100 cps component

+Y↑

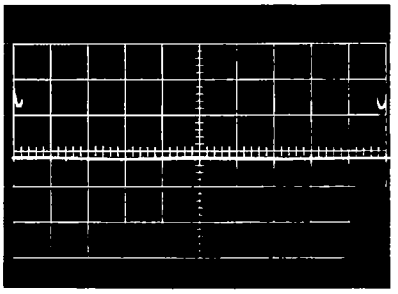

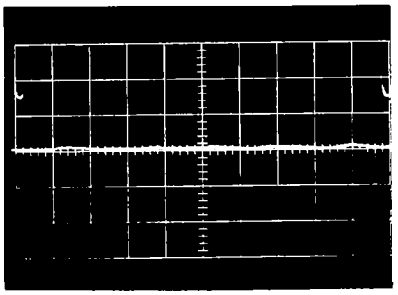

dc force plus 200 cps component

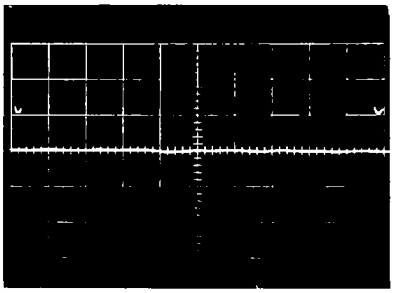

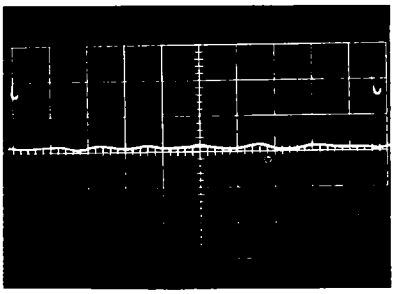

dc force plus 300 cps component

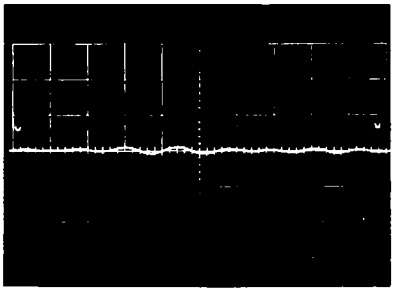

FORCES EXERTED ON THE BEARINGS OF THE BRAYTON CYCLE ALTERNATOR

Eccentricity: .006 in. toward bottom of generator

Equivalent Load Condition: 3.33 KVA 1.0 P.F. 1♦

Location: DE bearing

RPM: 3000

Force Scale: 5 pounds per centimeter radial or vertical

Time Scale: One revolution between timing marks

Top of Alternator

Left Side of Alternator

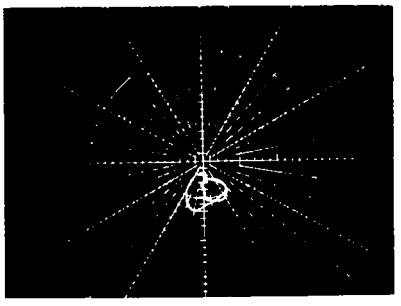

+Y↑

+X→

Polar Plot of Bearing Forces

X Forces vs. Time

Y Forces vs. Time

+X↑

+Y↑

dc force plus 100 cps component

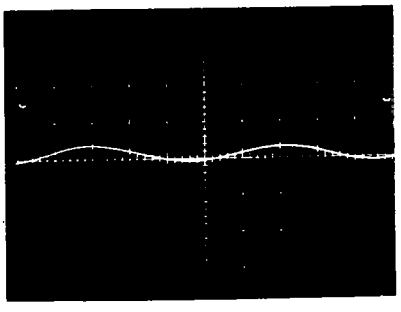

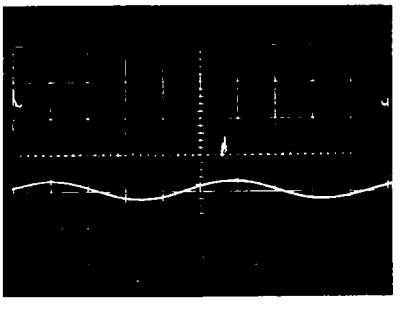

dc force plus 200 cps component

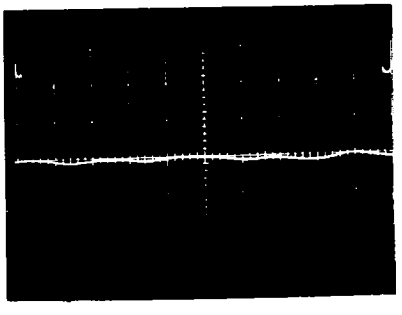

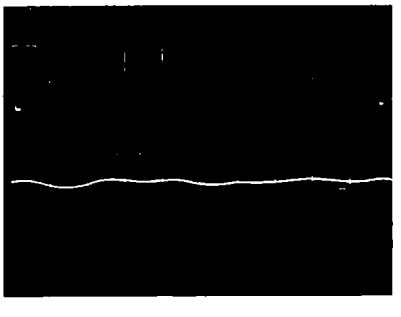

dc force plus 300 cps component

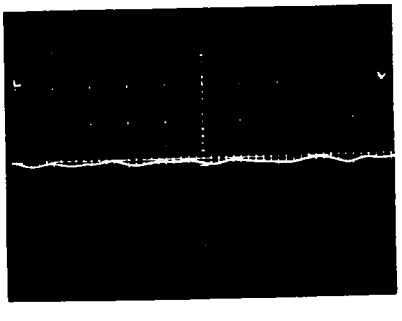

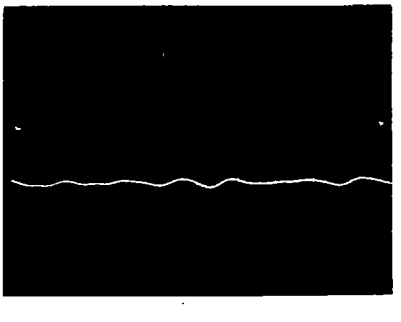

FORCES EXERTED ON THE BEARINGS OF THE BRAYTON CYCLE ALTERNATOR

Eccentricity: .006 in. toward bottom of generator

Equivalent Load Condition: 11.25 KVA 1.0 P.F. 3ϕ

Location: DE bearing

RPM: 3000

Force Scale: 5 pounds per centimeter radial or vertical

Time Scale: One revolution between timing marks

Top of Alternator

Left Side of Alternator

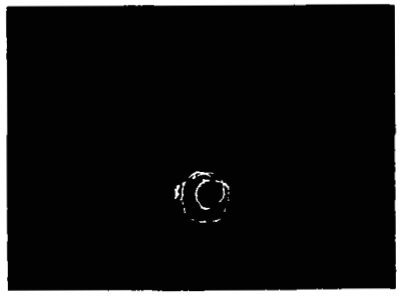

+Y↑

+X→

Polar Plot of Bearing Forces

X Forces vs. Time

Y Forces vs. Time

+X↑

+Y↑

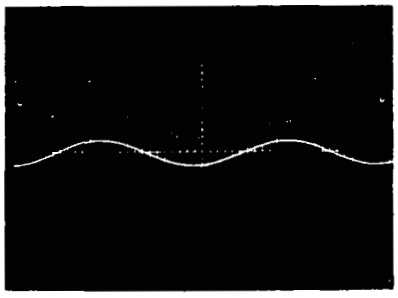

dc force plus 100 cps component

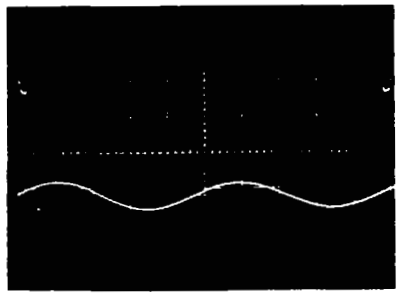

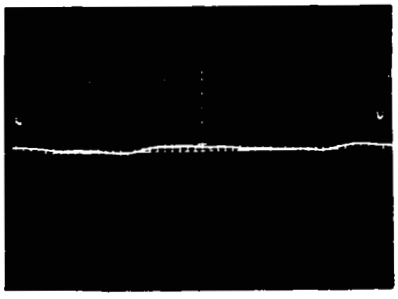

dc force plus 200 cps component

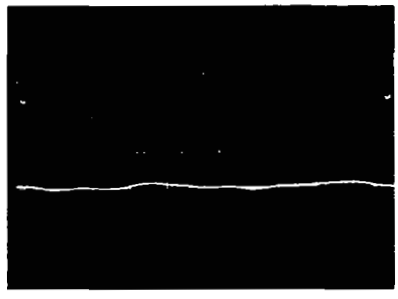

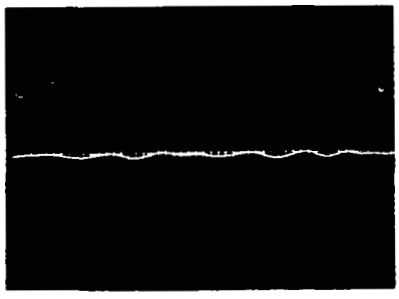

dc force plus 300 cps component

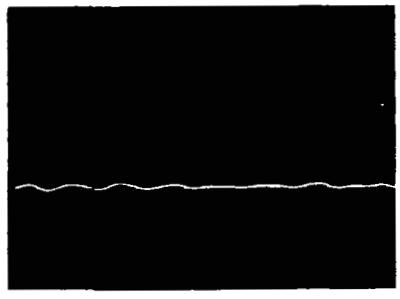

FORCES EXERTED ON THE BEARINGS OF THE BRAYTON CYCLE ALTERNATOR

Eccentricity: .006 in. toward bottom of generator

Equivalent Load Condition: 11.25 KVA 0.8 P.F. 3ϕ

Location: DE bearing

RPM: 3000

Force Scale: 5 pounds per centimeter radial or vertical

Time Scale: One revolution between timing marks

Top of Alternator

Left Side of Alternator

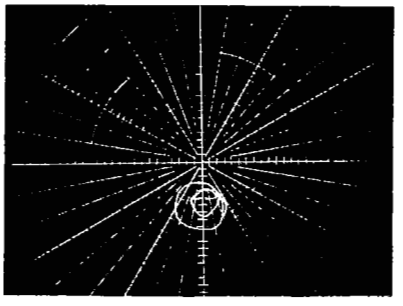

+Y↑

+X→

Polar Plot of Bearing Forces

X Forces vs. Time

Y Forces vs. Time

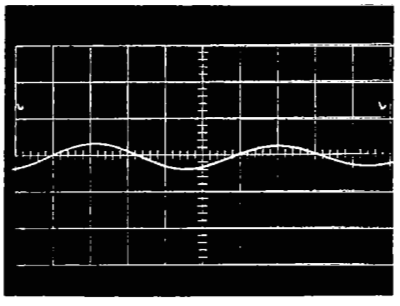

+X↑

dc force plus 100 cps component

+Y↑

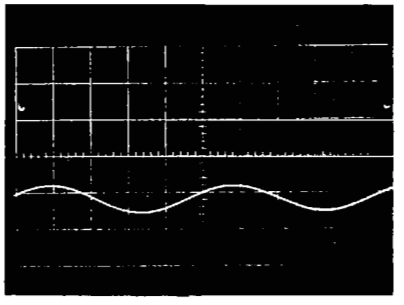

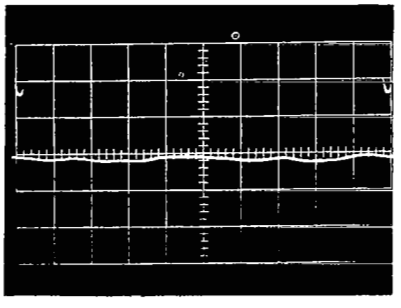

dc force plus 200 cps component

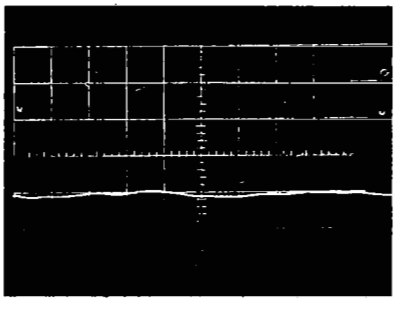

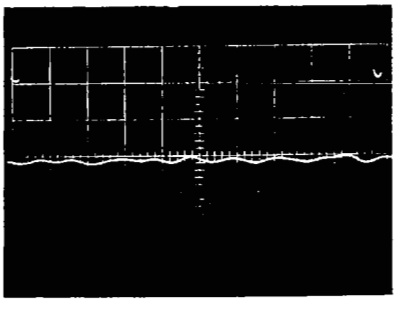

dc force plus 300 cps component

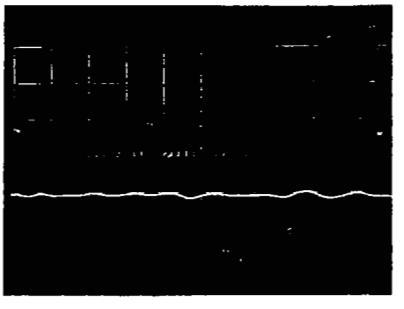

FORCES EXERTED ON THE BEARINGS OF THE BRAYTON CYCLE ALTERNATOR

Eccentricity: .005 in. toward bottom of generator

Equivalent Load Condition: 15 KVA 0.8 P.F. 3 ϕ

Location: DE bearing

RPM: 3000

Force Scale: 5 pounds per centimeter radial or vertical

Time Scale: One revolution between timing marks

Top of Alternator

Left Side of Alternator

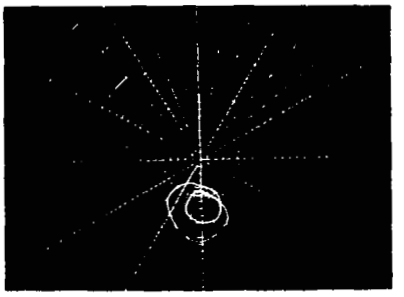

+Y↑

+X→

Polar Plot of Bearing Forces

X Forces vs. Time

Y Forces vs. Time

+X↑

+Y↑

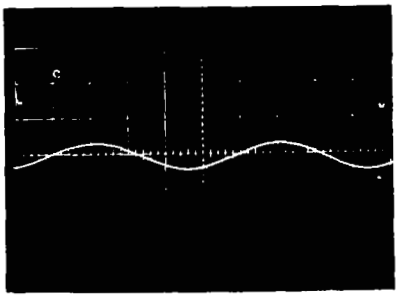

dc force plus 100 cps component

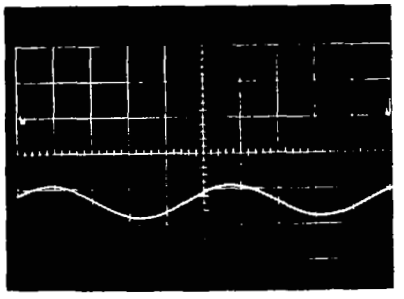

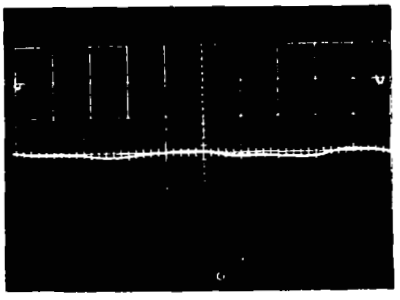

dc force plus 200 cps component

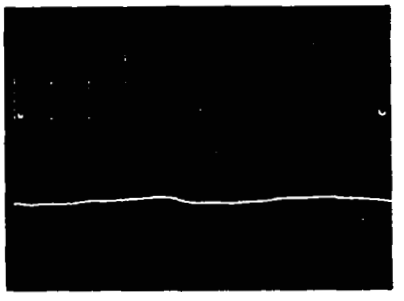

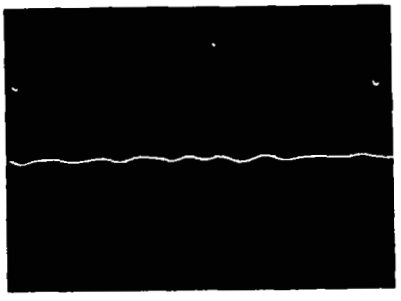

dc force plus 300 cps component

FORCES EXERTED ON THE BEARINGS OF THE BRAYTON CYCLE ALTERNATOR

Eccentricity: .006 in. toward bottom of generator

Equivalent Load Condition: 15 KVA 0.8 P.F. 3ϕ

then 1 ϕ shorted

Location: DE bearing

RPM: 3450

Force Scale: 5 pounds per centimeter radial or vertical

Time Scale: One revolution between timing marks

Top of Alternator

Left Side of Alternator

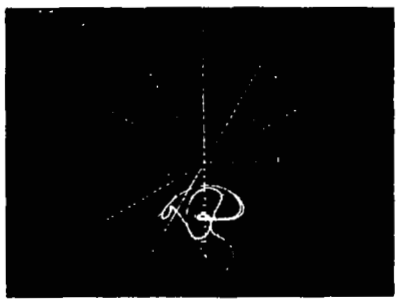

+Y↑

+X→

Polar Plot of Bearing Forces

X Forces vs. Time

Y Forces vs. Time

+X↑

+Y↑

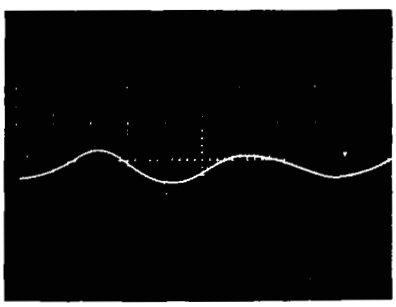

dc force plus 115 cps component

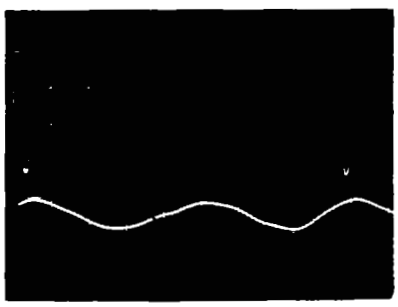

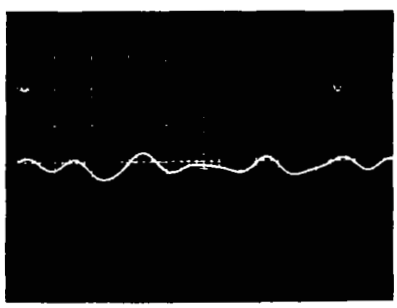

dc force plus 230 cps component

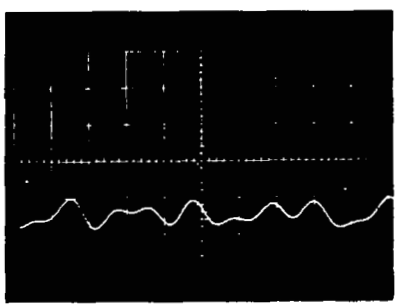

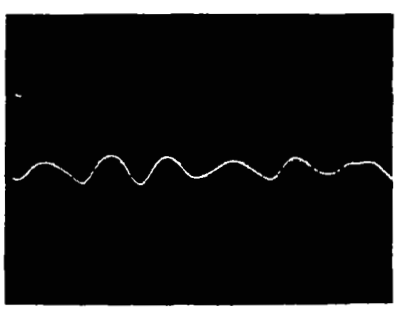

dc force plus 345 cps component

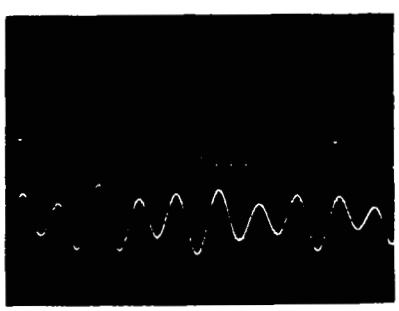

FORCES EXERTED ON THE BEARINGS OF THE BRAYTON CYCLE ALTERNATOR

Eccentricity: .006 in. toward bottom of generator

Equivalent Load Condition: 15 KVA 0.8 P.F. 3 ϕ

then 3 ϕ shorted

Location: DE bearing

RPM: 3000

Force Scale: 5 pounds per centimeter radial or vertical

Time Scale: One revolution between timing marks

Top of Alternator

Left Side of Alternator

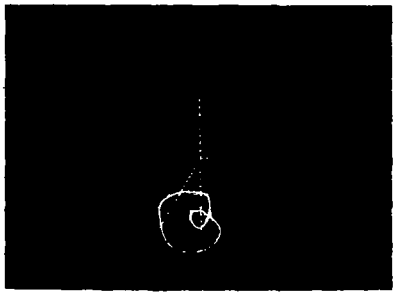

+Y↑

+X→

Polar Plot of Bearing Forces

X Forces vs. Time

Y Forces vs. Time

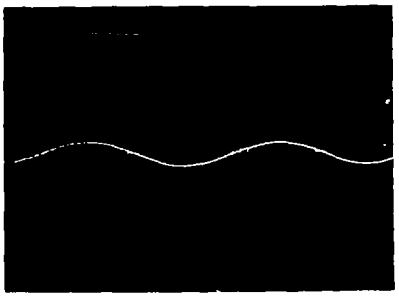

+X↑

+Y↑

dc force plus 100 cps component

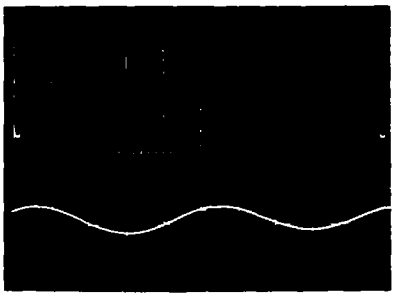

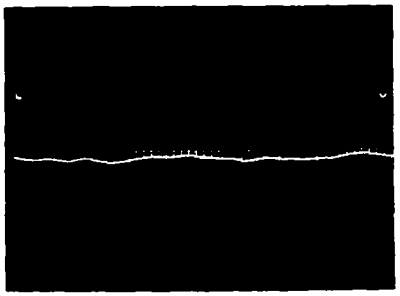

dc force plus 200 cps component

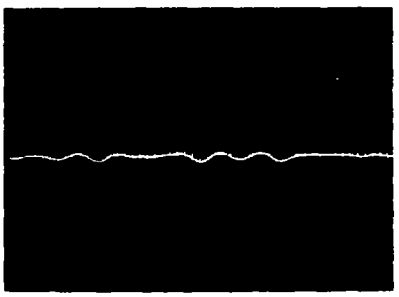

dc force plus 300 cps component

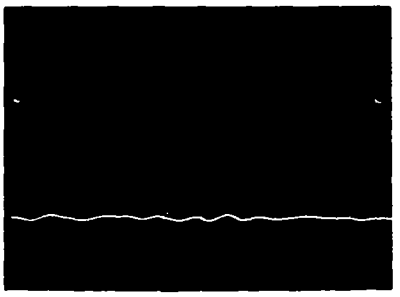

FORCES EXERTED ON THE BEARINGS OF THE BRAYTON CYCLE ALTERNATOR

Eccentricity: Zero

Equivalent Load Condition: No load, no field

Location: ODE bearing

RPM: 3000

Force Scale: 5 pounds per centimeter radial or vertical

Time Scale: One revolution between timing marks

Top of Alternator

Left Side of Alternator

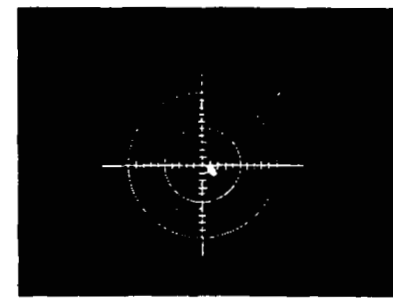

+Y↑

+X→

Polar Plot of Bearing Forces

X Forces vs. Time

Y Forces vs. Time

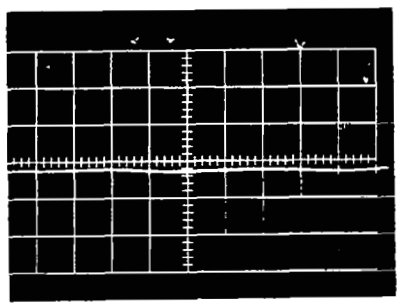

+X↑

dc force plus 100 cps component

+Y↑

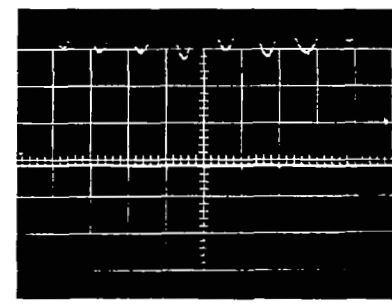

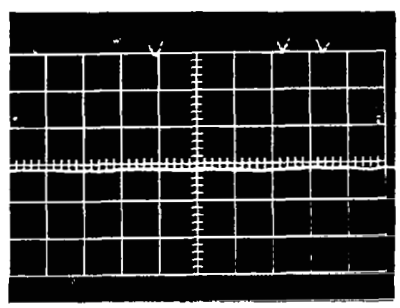

dc force plus 200 cps component

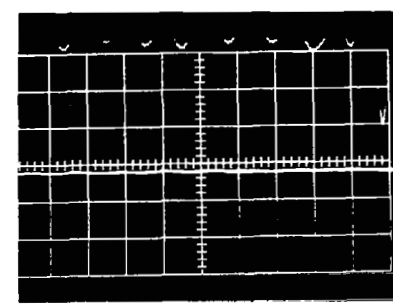

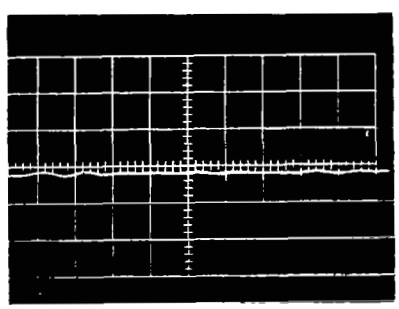

dc force plus 300 cps component

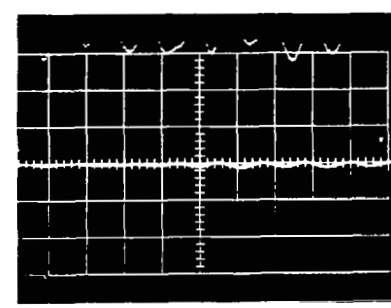

FORCES EXERTED ON THE BEARINGS OF THE BRAYTON CYCLE ALTERNATOR

Eccentricity: Zero

Equivalent Load Condition: 3.33 KVA 1.0 P.F. 1ϕ

Location: ODE bearing

RPM: 3000

Force Scale: 5 pounds per centimeter radial or vertical

Time Scale: One revolution between timing marks

Top of Alternator

Left Side of Alternator

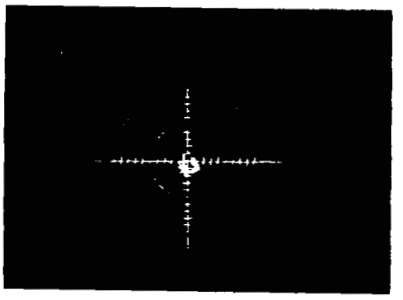

+Y

+X

Polar Plot of Bearing Forces

X Forces vs. Time

Y Forces vs. Time

+X

+Y

dc force plus 100 cps component

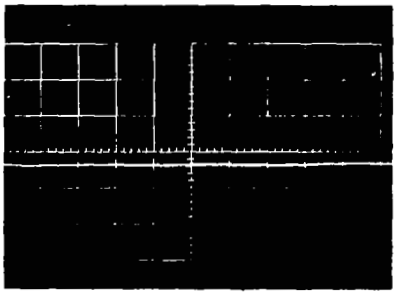

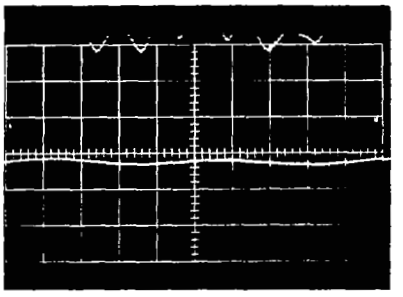

dc force plus 200 cps component

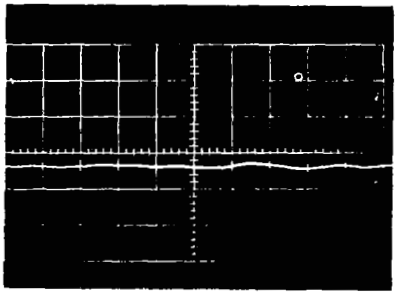

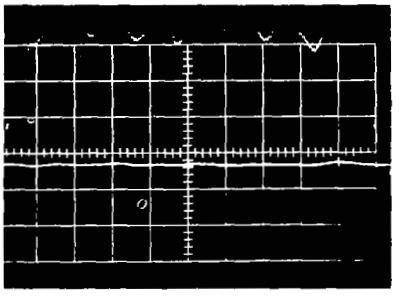

dc force plus 300 cps component

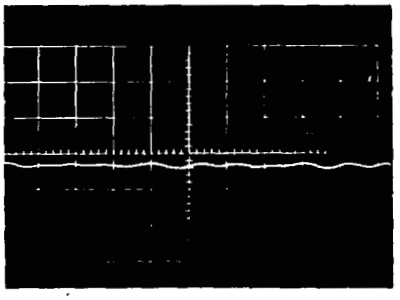

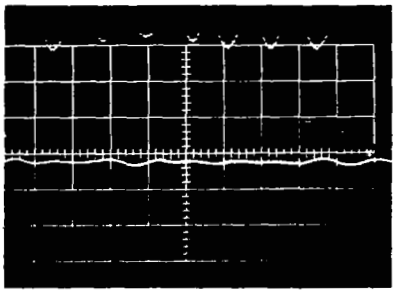

FORCES EXERTED ON THE BEARINGS OF THE BRAYTON CYCLE ALTERNATOR

Eccentricity: Zero

Equivalent Load Condition: 11.25 KVA 1.0 **P.F.** 3ϕ

Location: ODE bearing

RPM: 3000

Force Scale: 5 pounds per centimeter radial or vertical

Time Scale: One revolution between timing marks

Top of Alternator

Left Side of Alternator

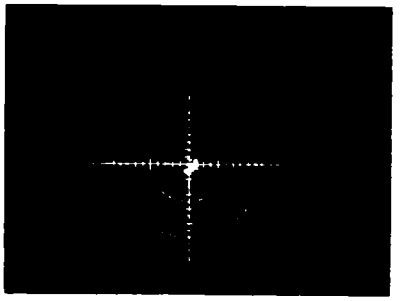

+Y↑

+X→

Polar Plot of Bearing Forces

X Forces vs. Time

Y Forces vs. Time

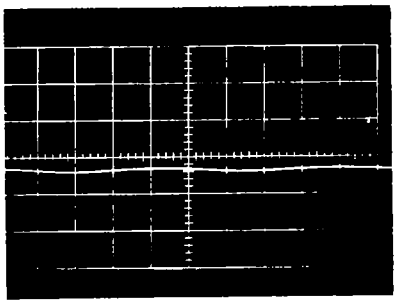

+X↑

+Y↑

dc force plus 100 cps component

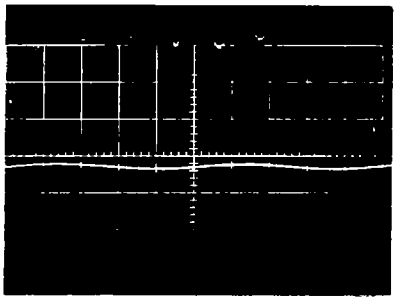

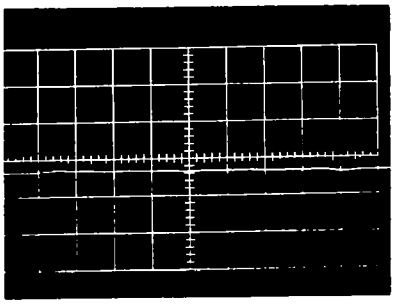

dc force plus 200 cps component

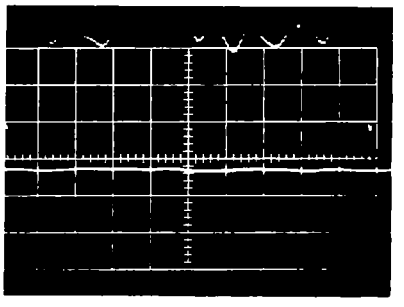

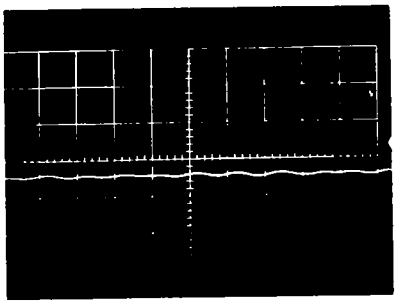

dc force plus 300 cps component

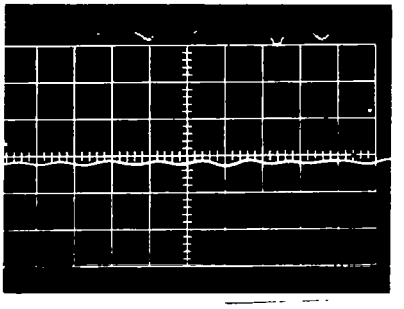

FORCES EXERTED ON THE BEARINGS OF THE BRAYTON CYCLE ALTERNATOR

Eccentricity: .002 in. toward bottom of generator

Equivalent Load Condition: No load, no field

Location: ODE bearing

RPM: 3000

Force Scale: 5 pounds per centimeter radial or vertical

Time Scale: One revolution between timing marks

Top of Alternator

Left Side of Alternator

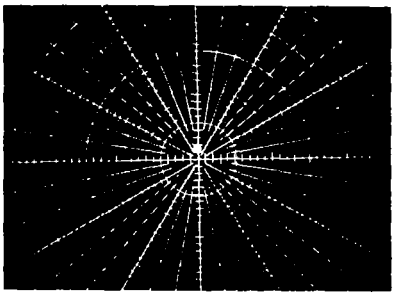

+Y↑

+X→

Polar Plot of Bearing Forces

X Forces vs. Time

Y Forces vs. Time

+X↑

+Y↑

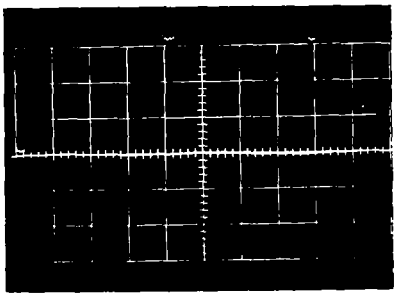

dc force plus 100 cps component

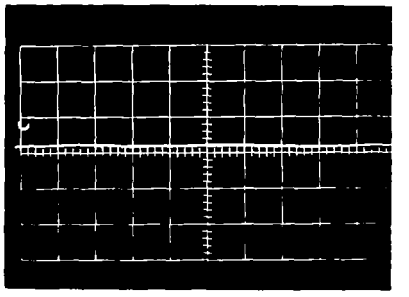

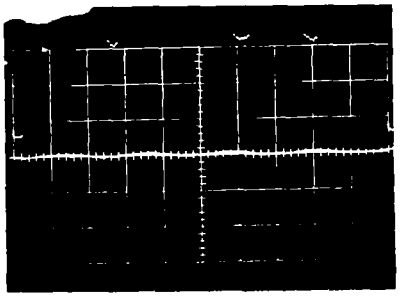

dc force plus 200 cps component

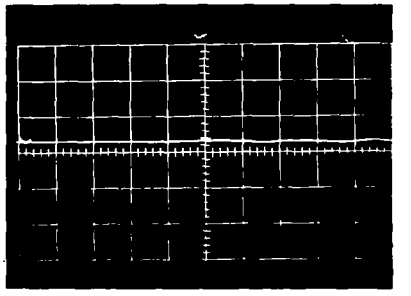

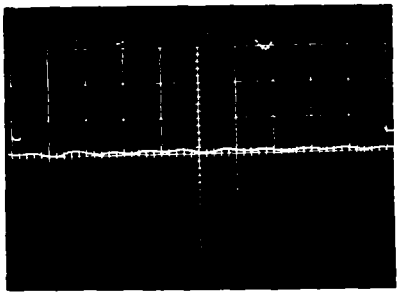

dc force plus 300 cps component

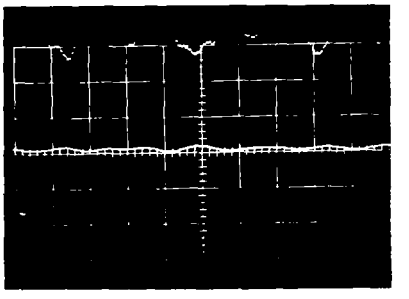

Eccentricity: .002 in. toward bottom of generator

Equivalent Load Condition: 3.33 KVA 1.0 P.F. 1ϕ

Location: ODE bearing

RPM: 3000

Force Scale: 5 pounds per centimeter radial or vertical

Time Scale: One revolution between timing marks

Top of Alternator

Left Side of Alternator

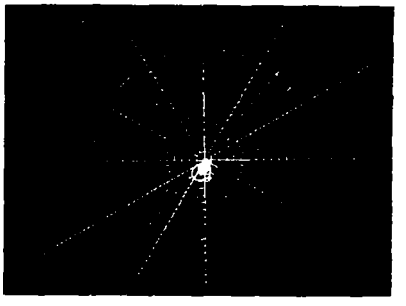

+Y↑

+X→

Polar Plot of Bearing Forces

X Forces vs. Time

Y Forces vs. Time

+X↑

+Y↑

dc force plus 100 cps component

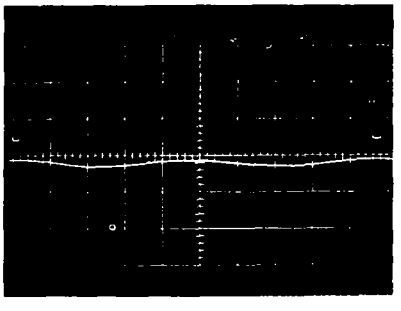

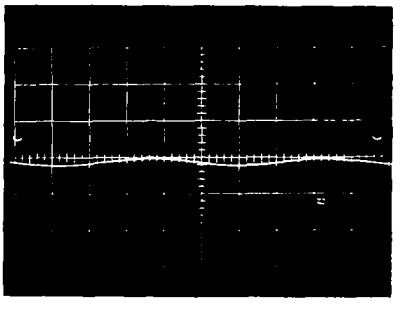

dc force plus 200 cps component

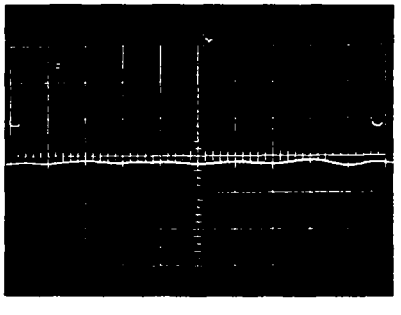

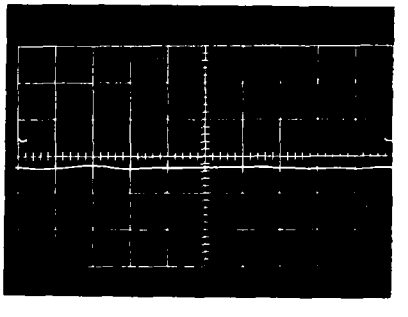

dc force plus 300 cps component

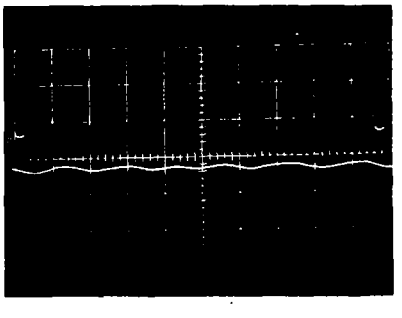

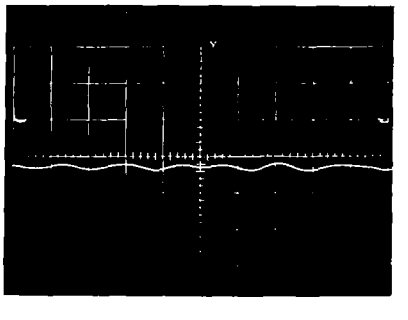

FORCES EXERTED ON THE BEARINGS OF THE BRAYTON CYCLE ALTERNATOR

Eccentricity: .002 in. toward bottom of generator

Equivalent Load Condition: 11.25 KVA 1.0 P.F. 1ϕ

Location: ODE bearing

RPM: 3000

Force Scale: 5 pounds per centimeter radial or vertical

Time Scale: One revolution between timing marks

Top of Alternator

Left Side of Alternator

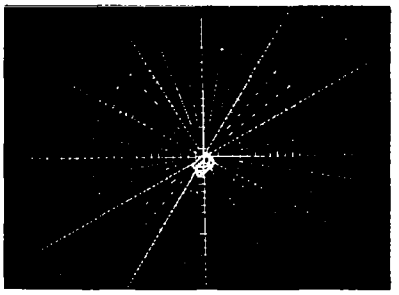

+Y↑

+X→

Polar Plot of Bearing Forces

X Forces vs. Time

Y Forces vs. Time

+X↑

+Y↑

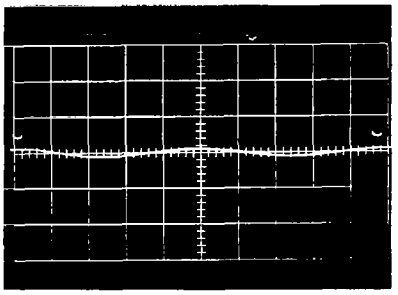

dc force plus 100 cps component

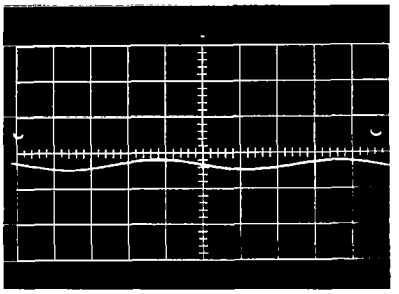

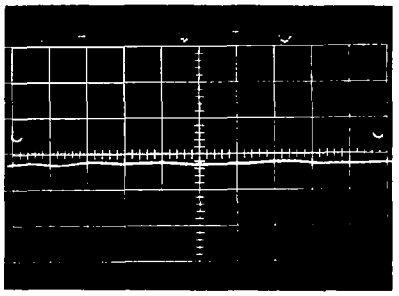

dc force plus 200 cps component

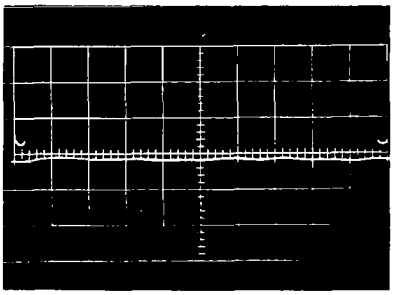

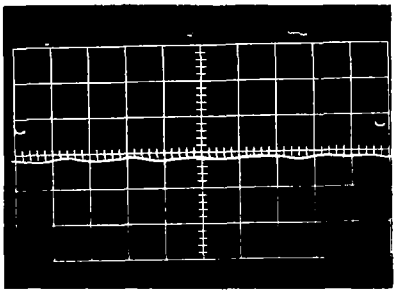

dc force plus 300 cps component

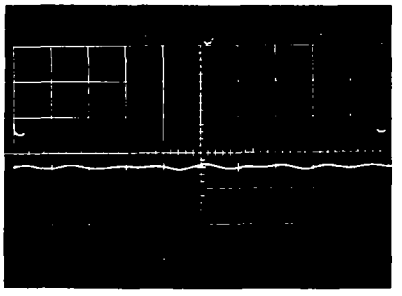

FORCES EXERTED ON THE BEARINGS OF THE BRAYTON CYCLE ALTERNATOR

Eccentricity: .002 in. toward bottom of generator

Equivalent Load Condition: 11.25 KVA 0.8 P.F. 3 ϕ

Location: ODE bearing

RPM: 3000

Force Scale: 5 pounds per centimeter radial or vertical

Time Scale: One revolution between timing marks

Top of Alternator

Left Side of Alternator

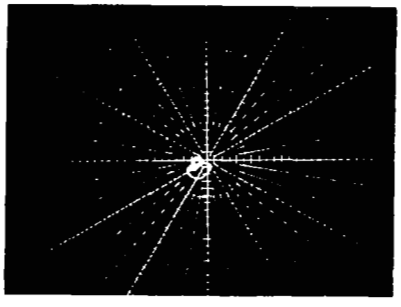

+Y↑

+X→

Polar Plot of Bearing Forces

X Forces vs. Time

Y Forces vs. Time

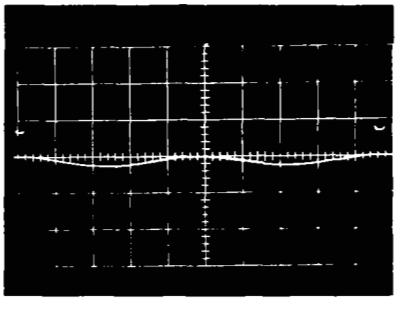

+X↑

dc force plus 100 cps component

+Y↑

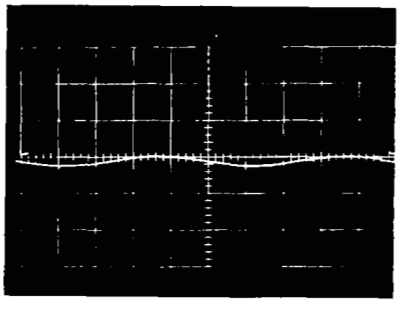

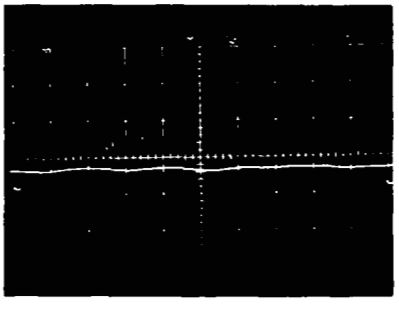

dc force plus 200 cps component

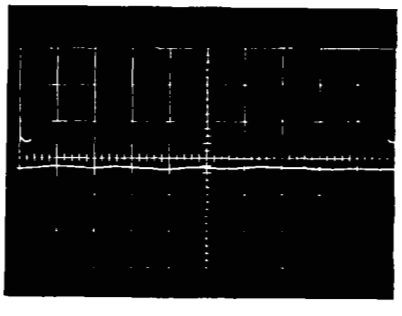

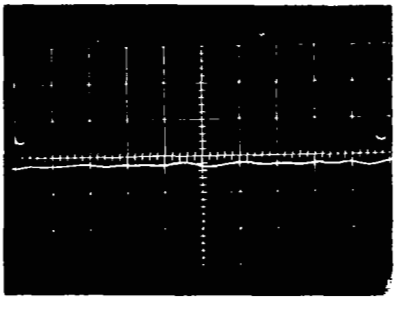

dc force plus 300 cps component

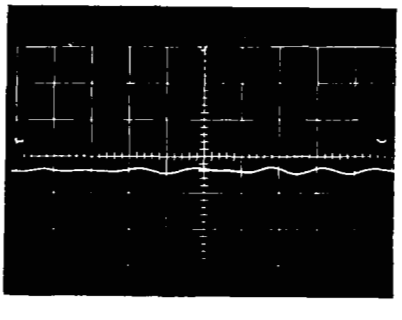

FORCES EXERTED ON THE BEARINGS OF THE BRAYTON CYCLE ALTERNATOR

Eccentricity: .002 in. toward bottom of generator

Equivalent Load Condition: 15 KVA 0.8 P.F. 3 ϕ

Location: ODE bearing

RPM: 3000

Force Scale: 5 pounds per centimeter radial or vertical

Time Scale: One revolution between timing marks

Top of Alternator

Left Side of Alternator

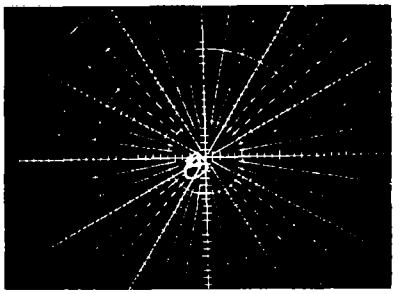

+Y↑

+X→

Polar Plot of Bearing Forces

X Forces vs. Time

Y Forces vs. Time

+X↑

+Y↑

dc force plus 100 cps component

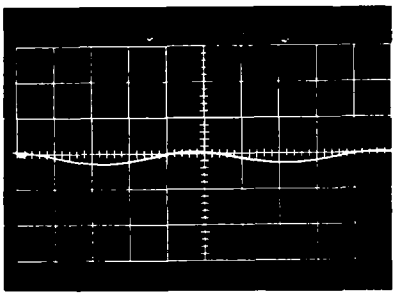

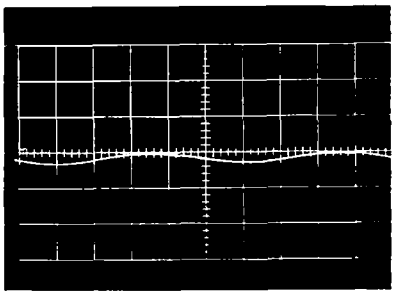

dc force plus 200 cps component

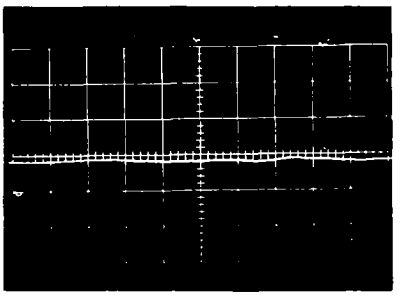

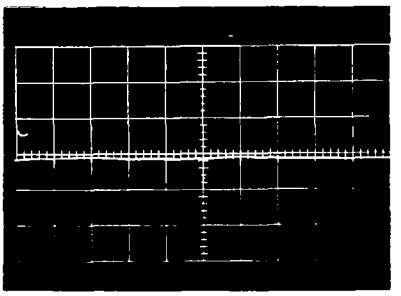

dc force plus 300 cps component

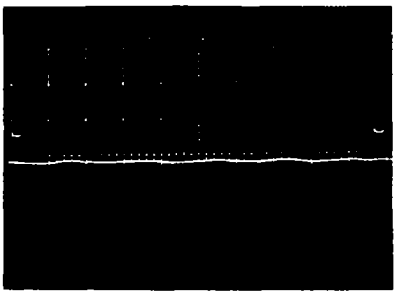

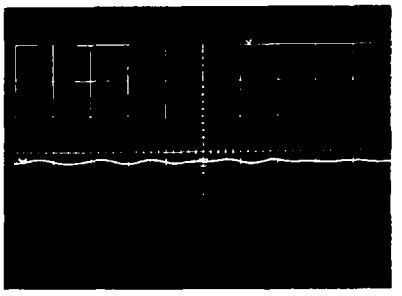

FORCES EXERTED ON THE BEARINGS OF THE BRAYTON CYCLE ALTERNATOR

Eccentricity: .002 in. toward bottom of generator

Equivalent Load Condition: 15 KVA 0.8 P.F. 3 ϕ

then 1 ϕ shorted

Location: ODE bearing

RPM: 3450

Force Scale: 5 pounds per centimeter radial or vertical

Time Scale: One revolution between timing marks

Top of Alternator

Left Side of Alternator

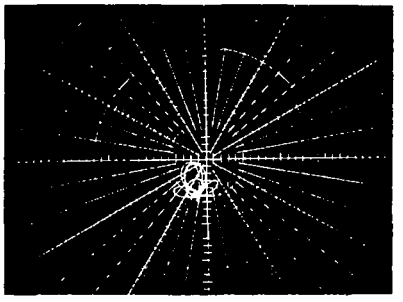

+Y

+X

Polar Plot of Bearing Forces

X Forces vs. Time

Y Forces vs. Time

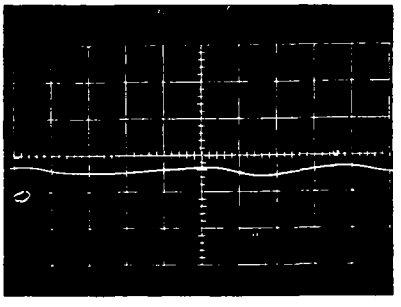

+X

dc force plus 115 cps component

+Y

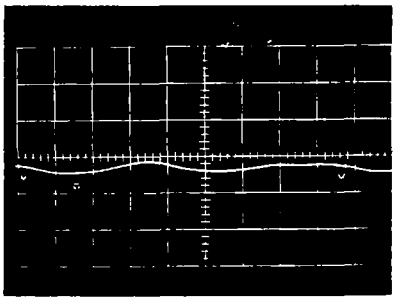

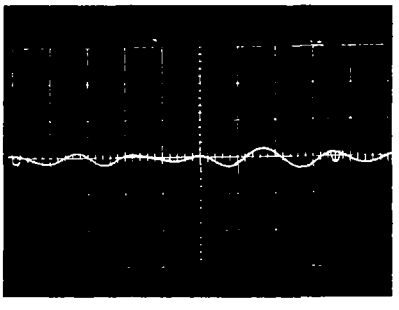

dc force plus 230 cps component

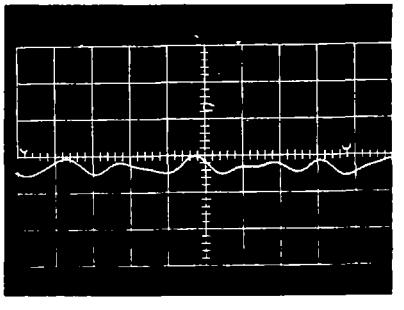

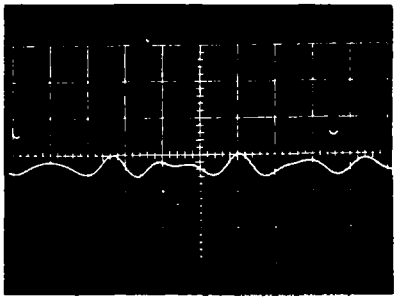

dc force plus 345 cps component

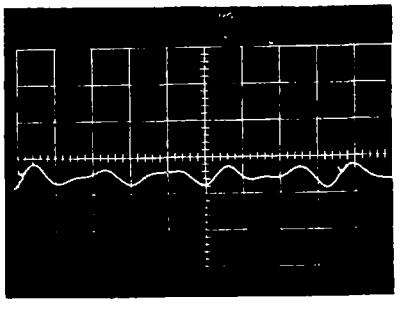

FORCES EXERTED ON THE BEARINGS OF THE BRAYTON CYCLE ALTERNATOR

Eccentricity: .002 in. toward bottom of generator

Equivalent Load Condition: 15 KVA 0.8 P.F. 3 ϕ

then 3 ϕ shorted

Location: ODE bearing

RPM: 3000

Force Scale: 5 pounds per centimeter radial or vertical

Time Scale: One revolution between timing marks

Top of Alternator

Left Side of Alternator

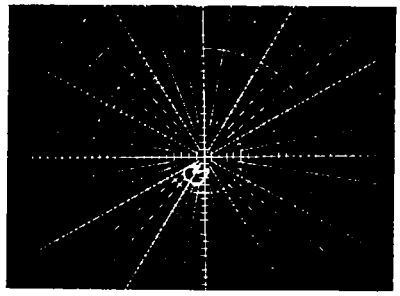

+Y

+X

Polar Plot of Bearing Forces

X Forces vs. Time

Y Forces vs. Time

+X

+Y

dc force plus 100 cps component

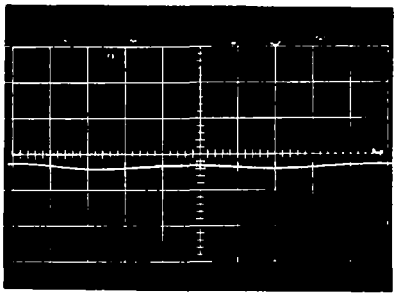

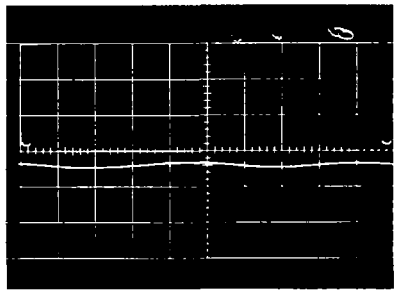

dc force plus 200 cps component

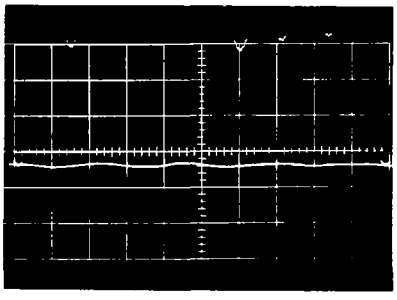

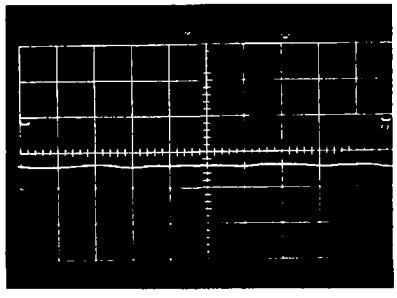

dc force plus 300 cps component

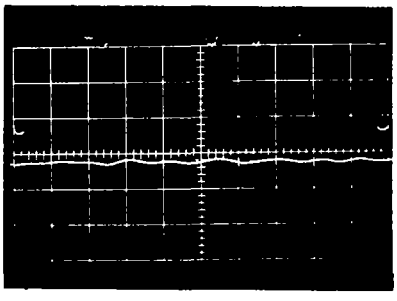

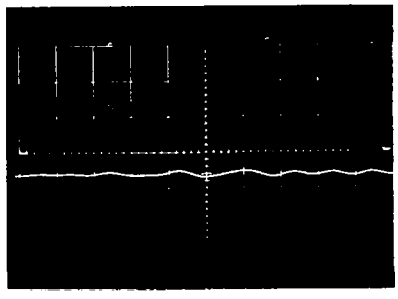

FORCES EXERTED ON THE BEARINGS OF THE BRAYTON CYCLE ALTERNATOR

Eccentricity: .004 in. toward bottom of generator

Equivalent Load Condition: No load, no field

Location: ODE bearing

RPM: 3000

Force Scale: 5 pounds per centimeter radial or vertical

Time Scale: One revolution between timing marks

Top of Alternator

Left Side of Alternator

+Y↑

+X→

Polar Plot of Bearing Forces

X Forces vs. Time

Y Forces vs. Time

+X↑

+Y↑

dc force plus 100 cps component

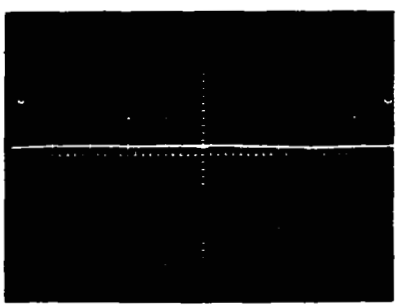

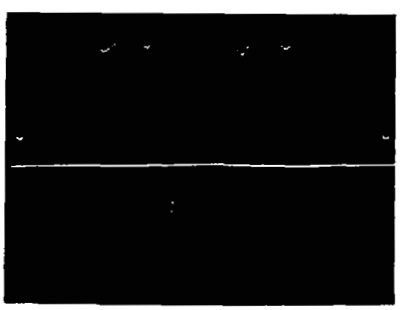

dc force plus 200 cps component

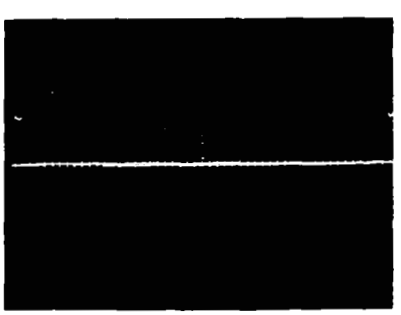

dc force plus 300 cps component

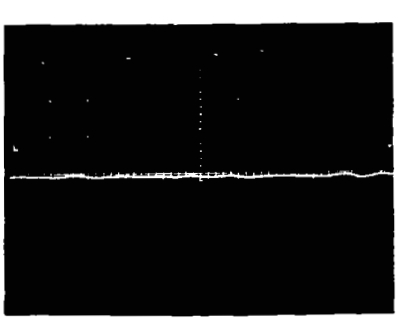

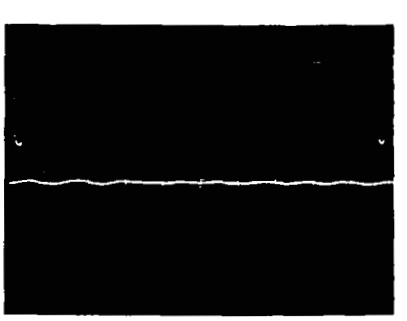

FORCES EXERTED ON THE BEARINGS OF THE BRAYTON CYCLE ALTERNATOR

Eccentricity: .004 in. toward bottom of generator

Equivalent Load Condition: 3.33 KVA 1.0 P.F. 1 ϕ

Location: ODE bearing

RPM: 3000

Force Scale: 5 pounds per centimeter radial or vertical

Time Scale: One revolution between timing marks

Top of Alternator

Left Side of Alternator

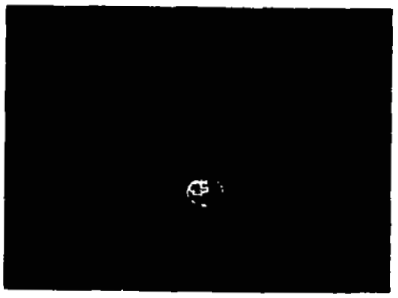

+Y↑

+X→

Polar Plot of Bearing Forces

X Forces vs. Time

Y Forces vs. Time

+X↑

+Y↑

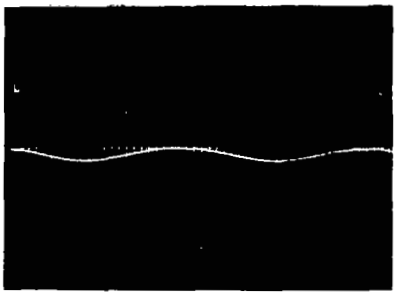

dc force plus 100 cps component

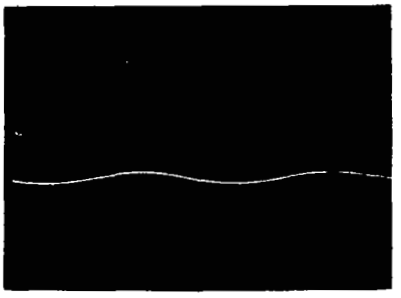

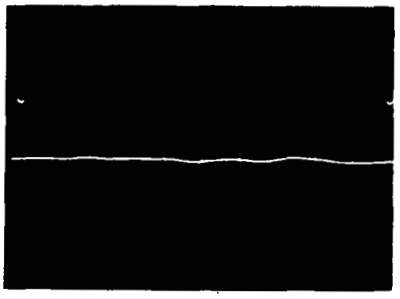

dc force plus 200 cps component

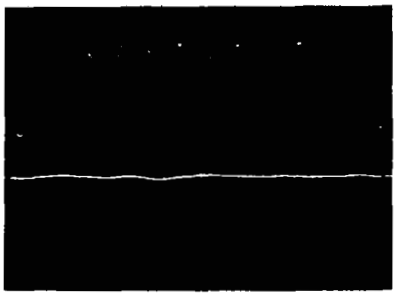

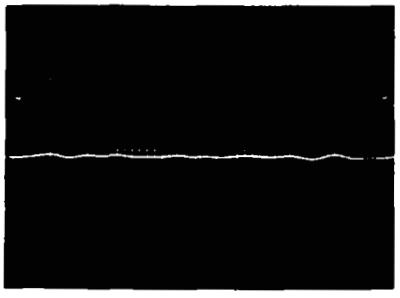

dc force plus 300 cps component

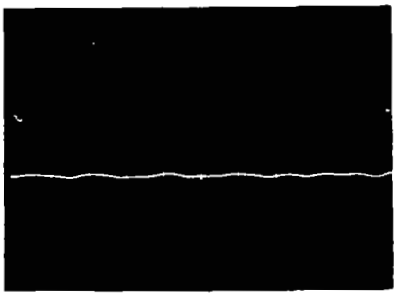

FORCES EXERTED ON THE BEARINGS OF THE BRAYTON CYCLE ALTERNATOR

Eccentricity: .004 in. toward bottom of generator

Equivalent Load Condition: 11.25 KVA 1.0 P.F. 3φ

Location: ODE bearing

RPM: 3000

Force Scale: 5 pounds per centimeter radial or vertical

Time Scale: One revolution between timing marks

Top of Alternator

Left Side of Alternator

+Y↑

+X→

Polar Plot of Bearing Forces

X Forces vs. Time

Y Forces vs. Time

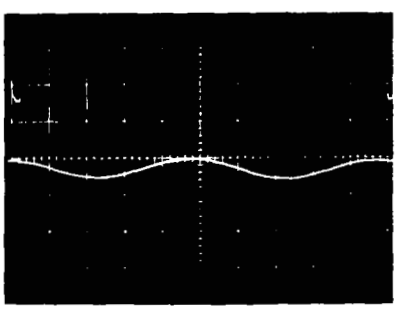

+X↑

dc force plus 100 cps component

+Y↑

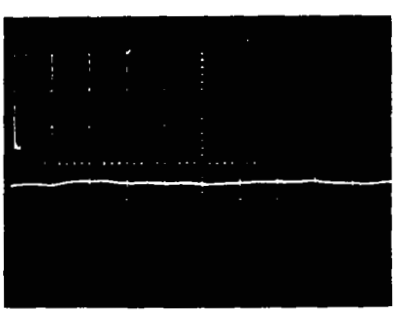

dc force plus 200 cps component

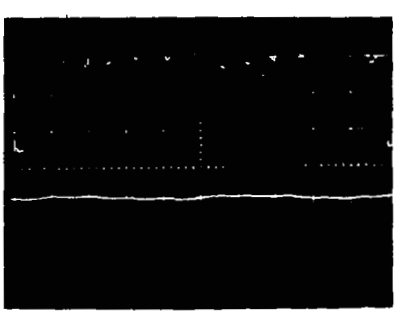

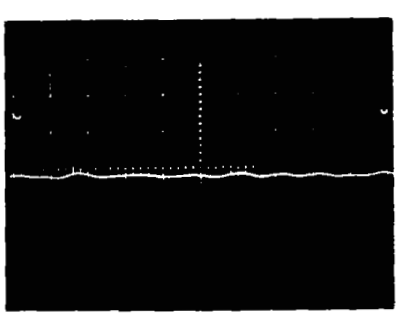

dc force plus 300 cps component

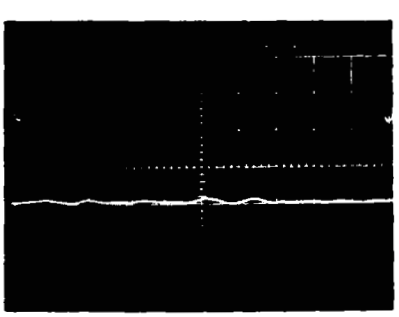

FORCES EXERTED ON THE BEARINGS OF THE BRAYTON CYCLE ALTERNATOR

Eccentricity: .004 in. toward bottom of generator

Equivalent Load Condition: 11.25 KVA 0.8 P.F. 3 ϕ

Location: ODE bearing

RPM: 3000

Force Scale: 5 pounds per centimeter radial or vertical

Time Scale: One revolution between timing marks

Top of Alternator

Left Side of Alternator

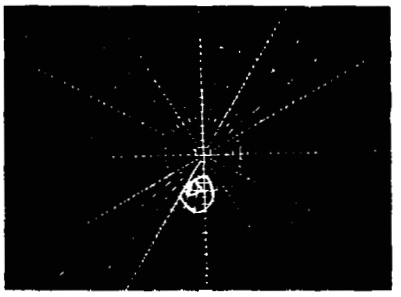

+Y↑

+X→

Polar Plot of Bearing Forces

X Forces vs. Time

Y Forces vs. Time

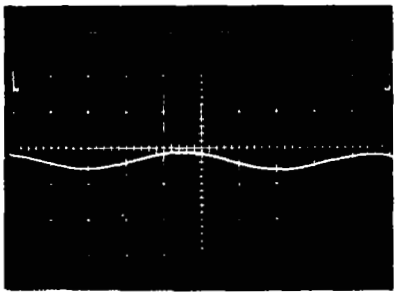

+X↑

+Y↑

dc force plus 100 cps component

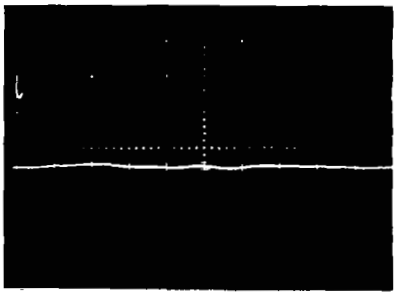

dc force plus 200 cps component

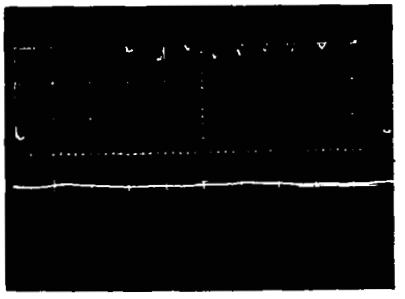

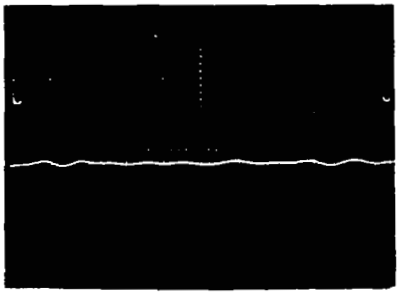

dc force plus 300 cps component

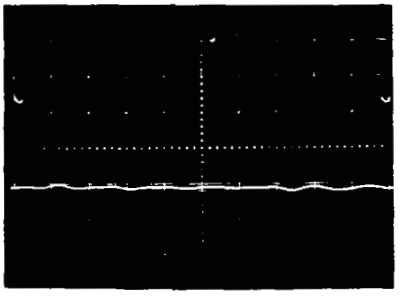

FORCES EXERTED ON THE BEARINGS OF THE BRAYTON CYCLE ALTERNATOR

Eccentricity: .004 in. toward bottom of generator

Equivalent Load Condition: 15 KVA 0.8 P.F. 3ϕ

Location: ODE bearing

RPM: 3000

Force Scale: 5 pounds per centimeter radial or vertical

Time Scale: One revolution between timing marks

Top of Alternator

Left Side of Alternator

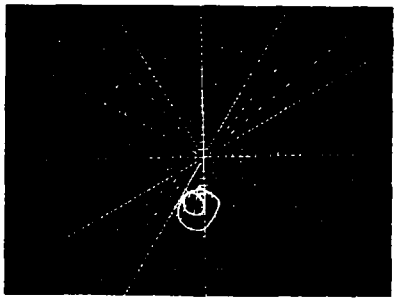

+Y

+X

Polar Plot of Bearing Forces

X Forces vs. Time

Y Forces vs. Time

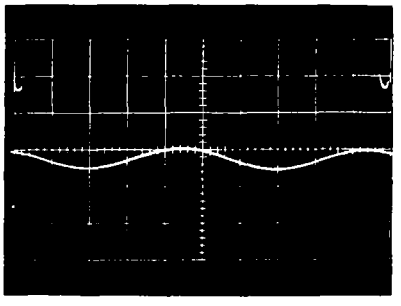

+X

+Y

dc force plus 100 cps component

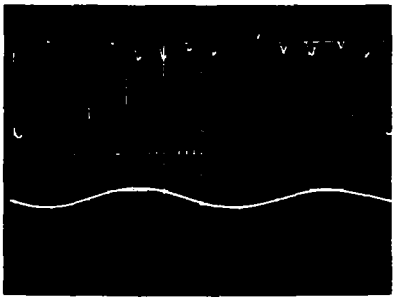

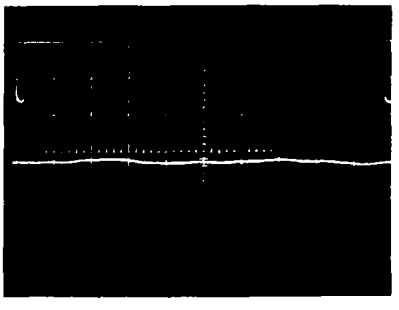

dc force plus 200 cps component

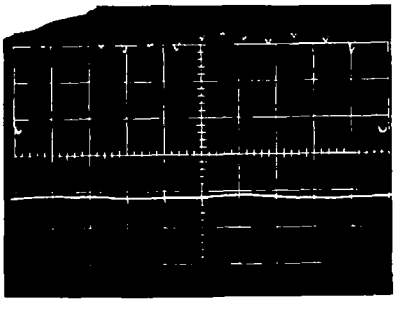

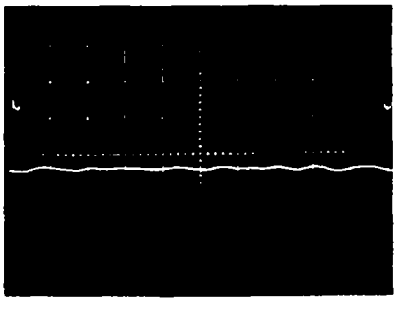

dc force plus 300 cps component

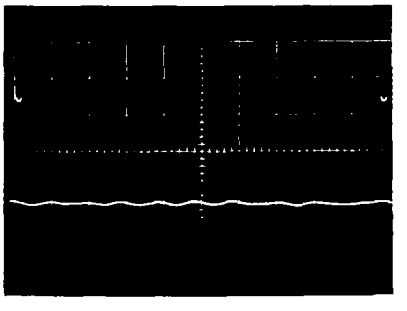

FORCES EXERTED ON THE BEARINGS OF THE BRAYTON CYCLE ALTERNATOR

Eccentricity: .004 in. toward bottom of generator

Equivalent Load Condition: 15 KVA 0.8 P.F. 3ϕ

then 1 ϕ shorted

Location: ODE bearing

RPM: 3450

Force Scale: 5 pounds per centimeter radial or vertical

Time Scale: One revolution between timing marks

Top of Alternator

Left Side of Alternator

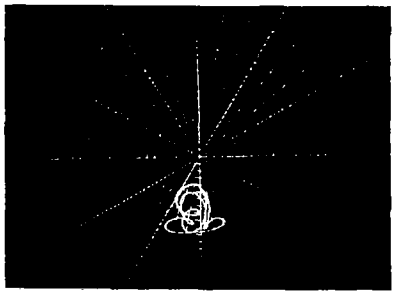

+Y↑

+X→

Polar Plot of Bearing Forces

X Forces vs. Time

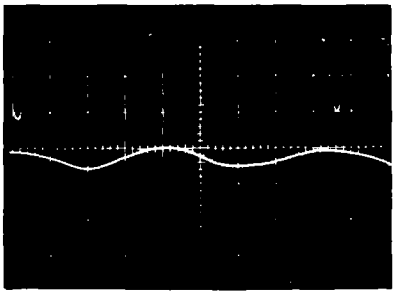

+X↑

dc force plus 115 cps component

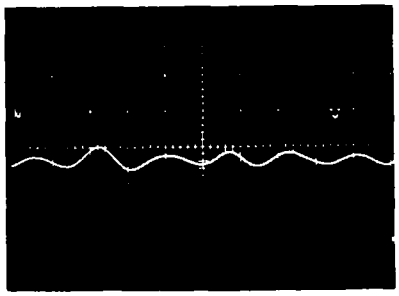

dc force plus 230 cps component

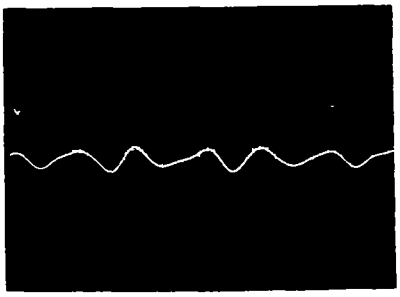

dc force plus 345 cps component

Y Forces vs. Time

+Y↑

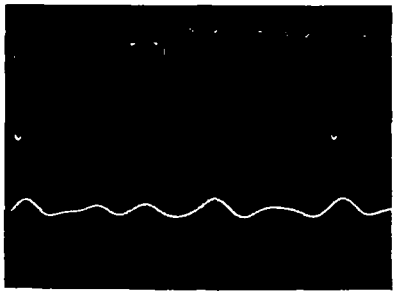

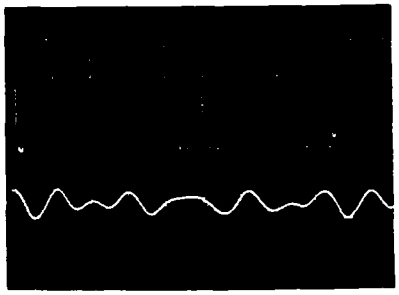

FORCES EXERTED ON THE BEARINGS OF THE BRAYTON CYCLE ALTERNATOR

Eccentricity: .004 in. toward bottom of generator

Equivalent Load Condition: 15 KVA 0.8 P.F. 3ϕ

then 3 ϕ shorted

Location: ODE bearing

RPM: 3000

Force Scale: 5 pounds per centimeter radial or vertical

Time Scale: One revolution between timing marks

Top of Alternator

Left Side of Alternator

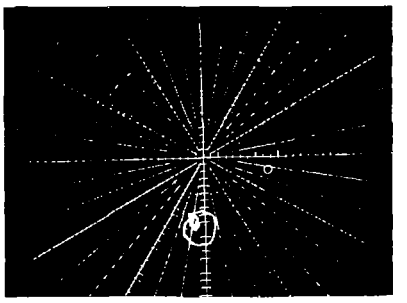

+Y

+X

Polar Plot of Bearing Forces

X Forces vs. Time

Y Forces vs. Time

+X

+Y

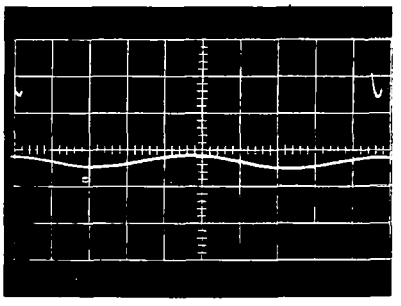

dc force plus 100 cps component

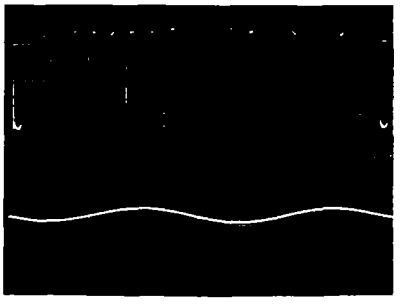

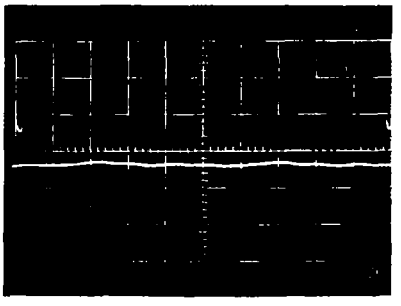

dc force plus 200 cps component

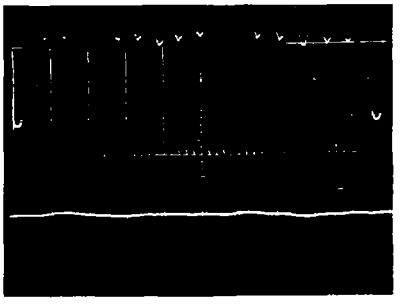

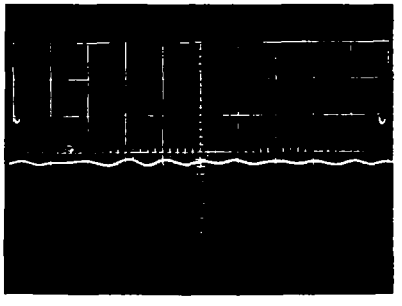

dc force plus 300 cps component

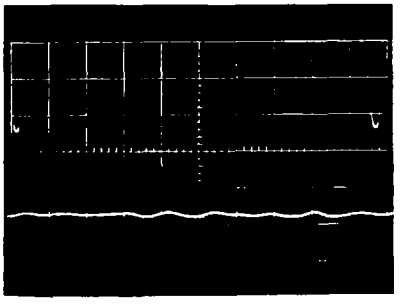

Eccentricity: .006 in. toward bottom of generator

Equivalent Load Condition: No load, no field

Location: ODE bearing

RPM: 3000

Force Scale: 5 pounds per centimeter radial or vertical

Time Scale: One revolution between timing marks

Top of Alternator

Left Side of Alternator

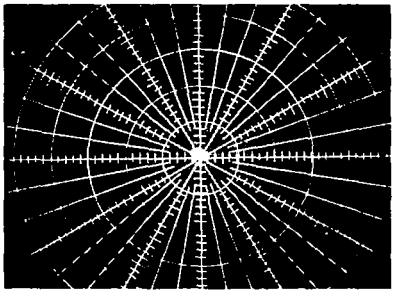

+Y↑

+X→

Polar Plot of Bearing Forces

X Forces vs. Time

Y Forces vs. Time

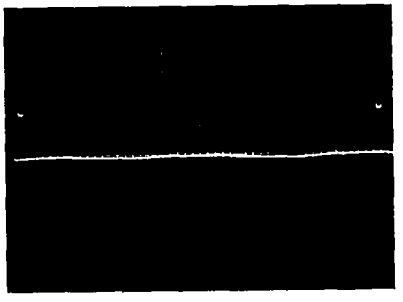

+X↑

+Y↑

dc force plus 100 cps component

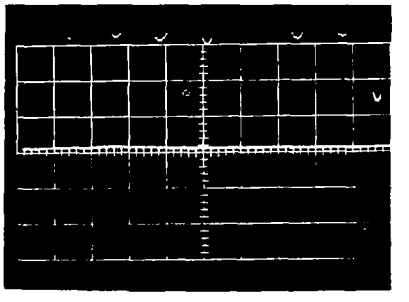

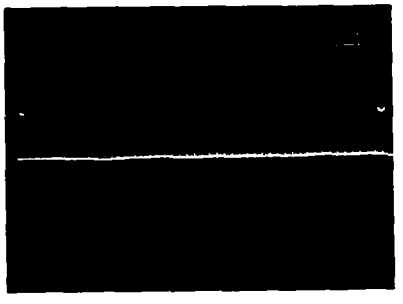

dc force plus 200 cps component

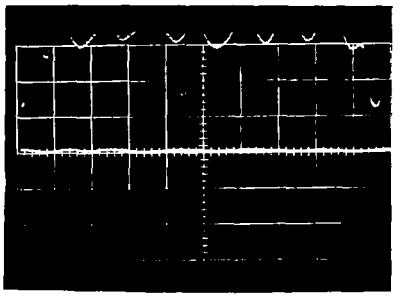

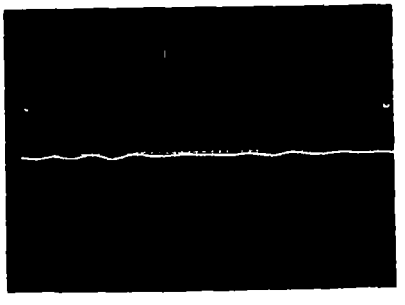

dc force plus 300 cps component

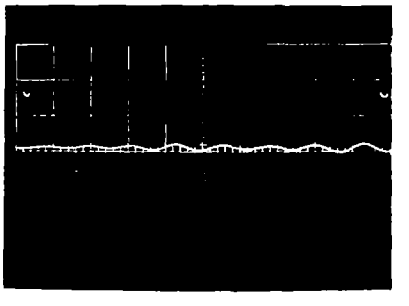

FORCES EXERTED ON THE BEARINGS OF THE BRAYTON CYCLE ALTERNATOR

Eccentricity: .006 in. toward bottom of generator

Equivalent Load Condition: 3.33 KVA 1.0 P.F. 1 ϕ

Location: ODE bearing

RPM: 3600

Force Scale: 5 pounds per centimeter radial or vertical

Time Scale: One revolution between timing marks

Top of Alternator

Left Side of Alternator

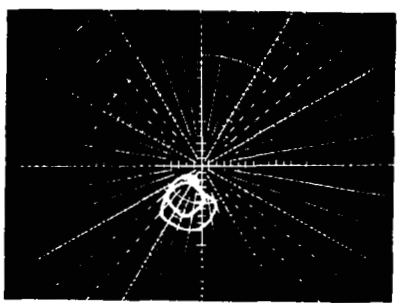

+Y↑

+X→

Polar Plot of Bearing Forces

X Forces vs. Time

Y Forces vs. Time

+X↑

+Y↑

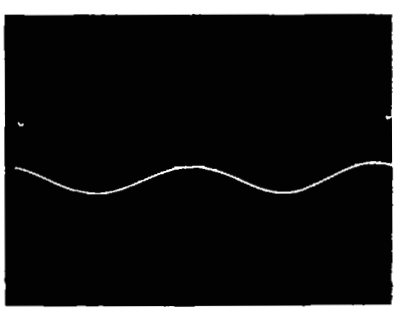

dc force plus 100 cps component

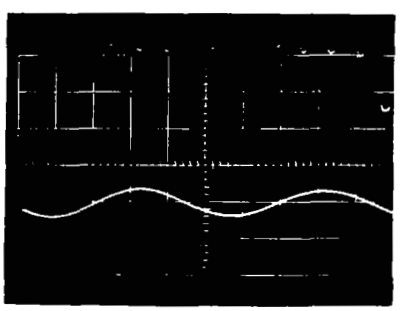

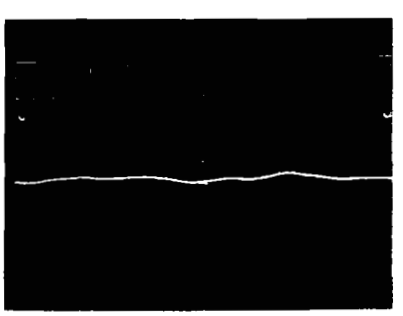

dc force plus 200 cps component

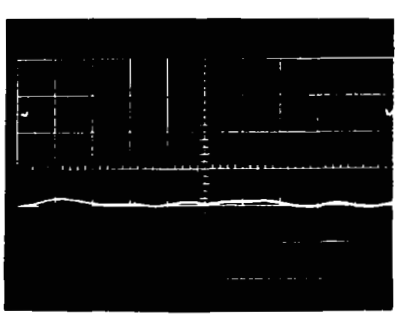

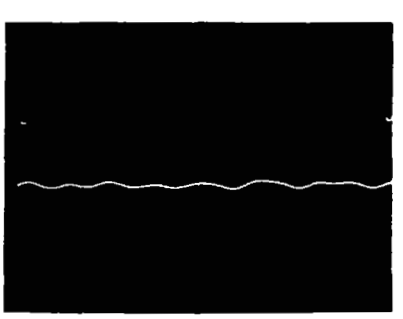

dc force plus 300 cps component

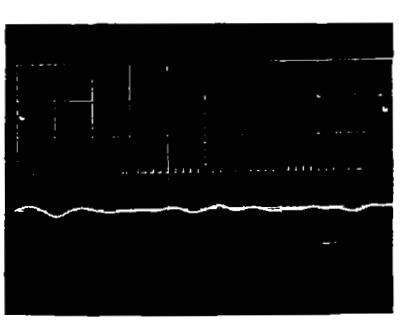

FORCES EXERTED ON THE BEARINGS OF THE BRAYTON CYCLE ALTERNATOR

Eccentricity: .006 in. toward bottom of generator

Equivalent Load Condition: 11.25 KVA 1.0 P.F. 3 ϕ

Location: OD^{2} bearing

RPM: 3000

Force Scale: 5 pounds per centimeter radial or vertical

Time Scale: One revolution between timing marks

Top of Alternator

Left Side of Alternator

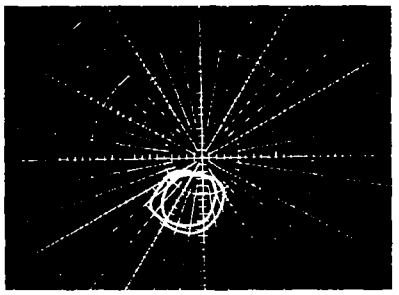

+Y↑

+X→

Polar Plot of Bearing Forces

X Forces vs. Time

Y Forces vs. Time

+X↑

+Y↑

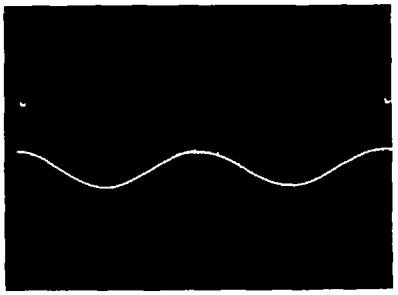

dc force plus 100 cps component

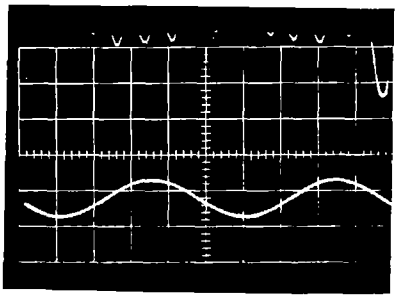

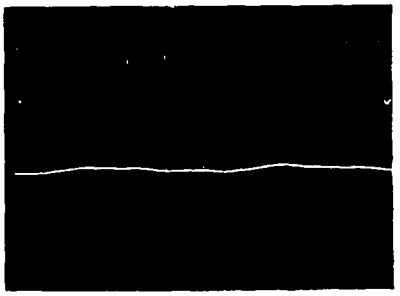

dc force plus 200 cps component

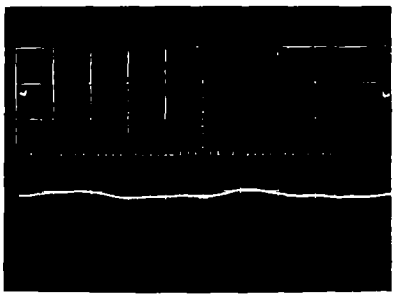

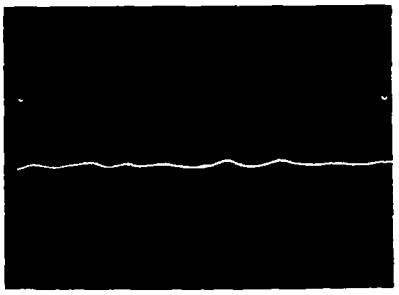

dc force plus 300 cps component

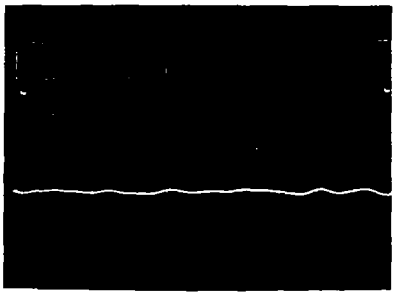

Eccentricity: .006 in. toward bottom of generator

Equivalent Load Condition: 11.25 KVA 0.8 P.F. 3ϕ

Location: ODE bearing

RPM: 3000

Force Scale: 5 pounds per centimeter radial or vertical

Time Scale: One revolution between timing marks

Top of Alternator

Left Side of Alternator

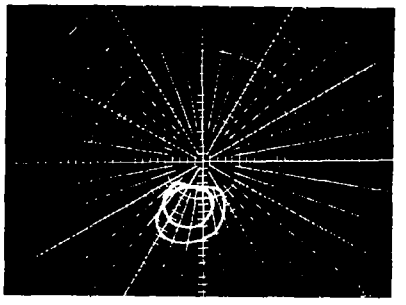

Polar Plot of Bearing Forces

X Forces vs. Time

Y Forces vs. Time

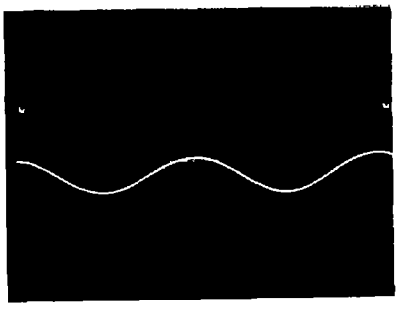

dc force plus 100 cps component

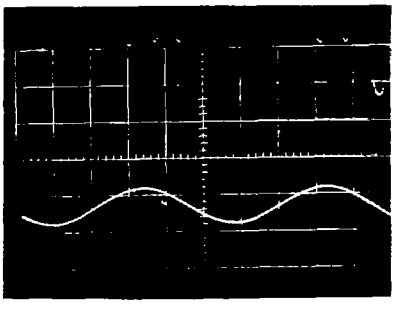

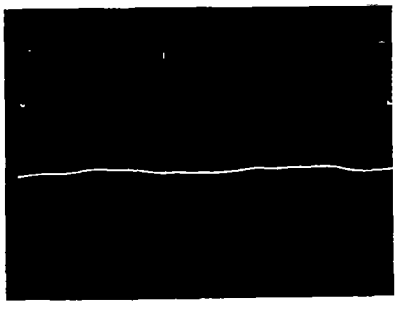

dc force plus 200 cps component

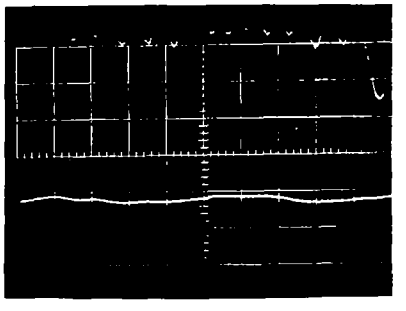

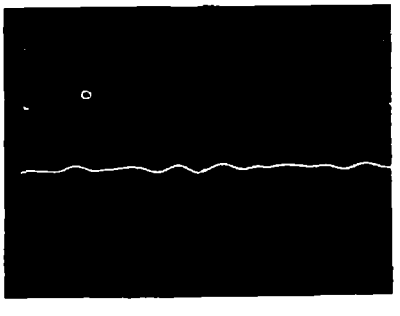

dc force plus 300 cps component

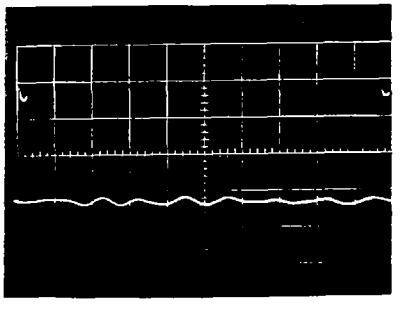

FORCES EXERTED ON THE BEARINGS OF THE BRAYTON CYCLE ALTERNATOR

Eccentricity: .006 in. toward bottom of generator

Equivalent Load Condition: 15 KVA 0.8 P.F. 3ϕ

Location: ODE bearing

RPM: 3000

Force Scale: 5 pounds per centimeter radial or vertical

Time Scale: One revolution between timing marks

Top of Alternator

Left Side of Alternator

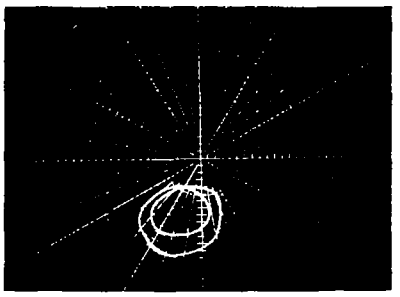

+Y↑

+X→

Polar Plot of Bearing Forces

X Forces vs. Time

Y Forces vs. Time

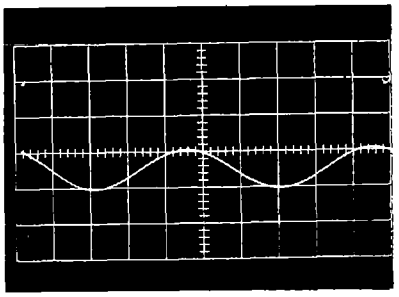

+X↑

dc force plus 100 cps component

+Y↑

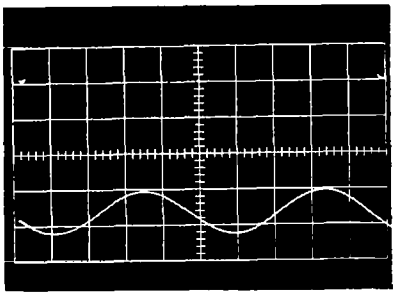

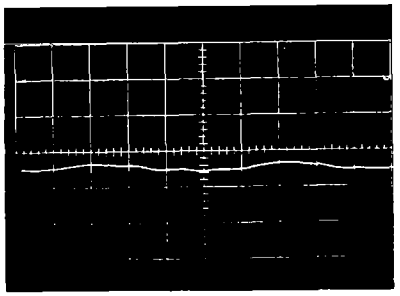

dc force plus 200 cps component

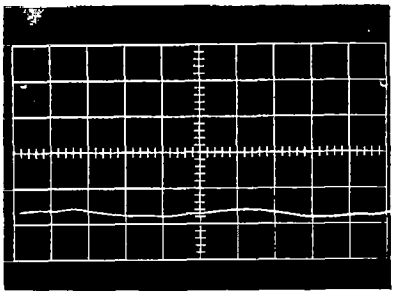

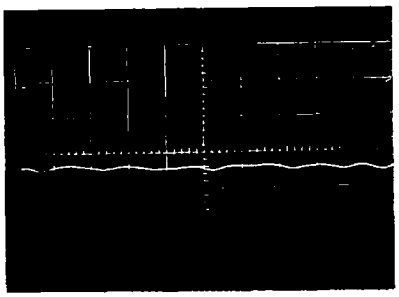

dc force plus 300 cps component

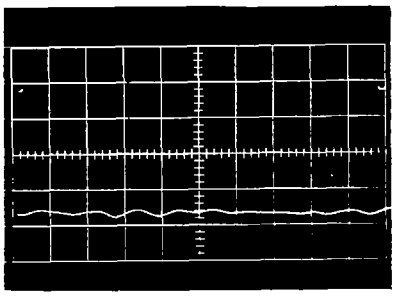

FORCES EXERTED ON THE BEARINGS OF THE BRAYTON CYCLE ALTERNATOR

Eccentricity: .006 in. toward bottom of generator

Equivalent Load Condition: 15 KVA 0.8 P.F. 3 ϕ

then 1 ϕ shorted

Location: CDE bearing

RPM: [illegible]

Force Scale: 5 pounds per centimeter radial or vertical

Time Scale: One revolution between timing marks

Top of Alternator

Left Side of Alternator

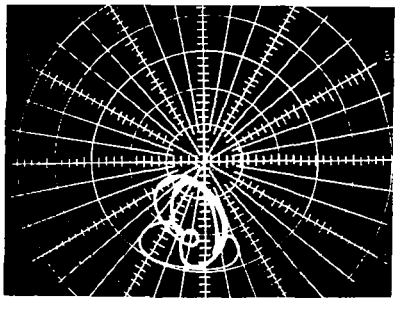

+Y↑

+X→

Polar Plot of Bearing Forces

X Forces vs. Time

Y Forces vs. Time

+X↑

+Y↑

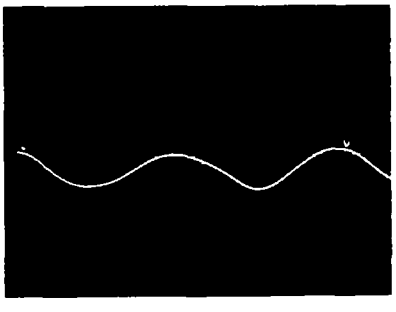

dc force plus 115 cps component

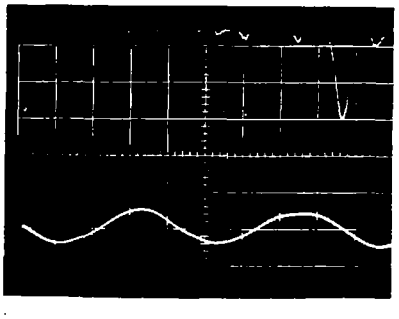

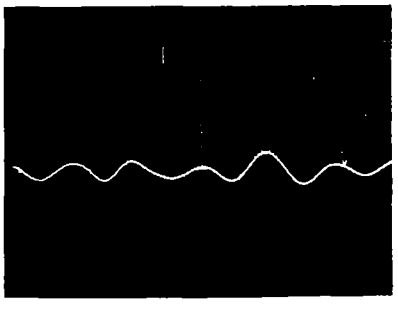

dc force plus [illegible] cps component

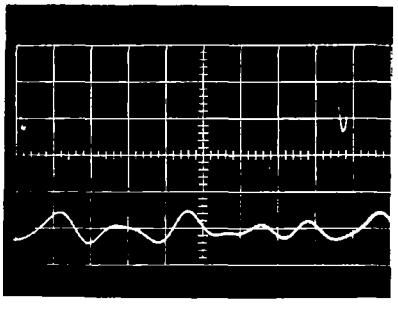

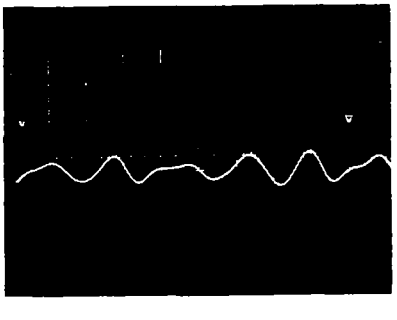

dc force plus [illegible] cps component

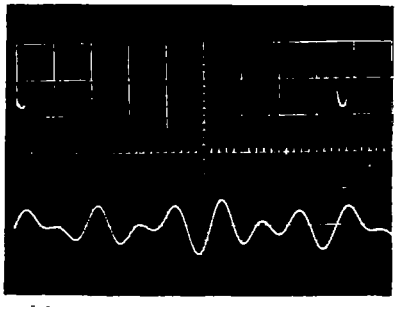

FORCES EXERTED ON THE BEARINGS OF THE BRAYTON CYCLE ALTERNATOR

Eccentricity: .006 in. toward bottom of generator

Equivalent Load Condition: 15 KVA 0.8 P.F. 3ϕ

then 3 ϕ shorted

Location: ODE bearing

RPM: 3000

Force Scale: 5 pounds per centimeter radial or vertical

Time Scale: One revolution between timing marks

Top of Alternator

Left Side of Alternator

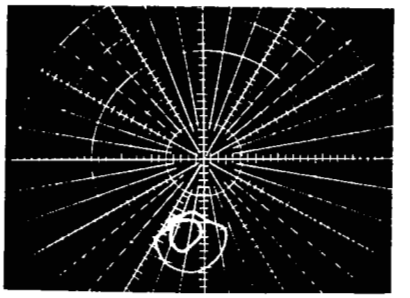

+Y↑

+X→

Polar Plot of Bearing Forces

X Forces vs. Time

Y Forces vs. Time

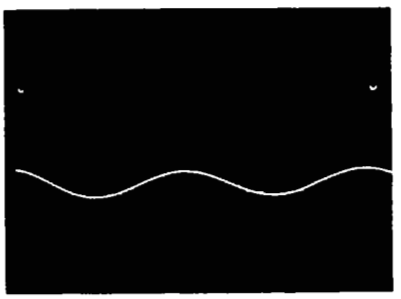

+X↑

+Y↑

dc force plus 100 cps component

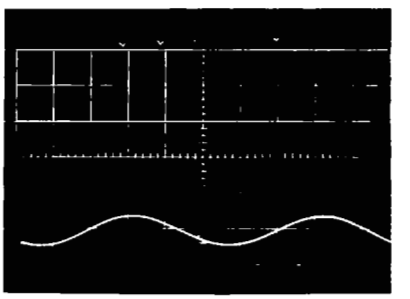

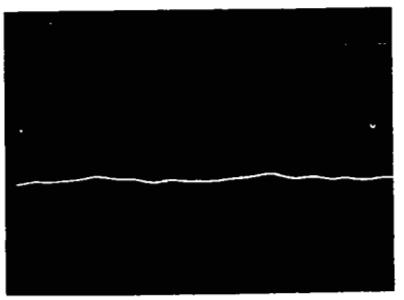

dc force plus 200 cps component

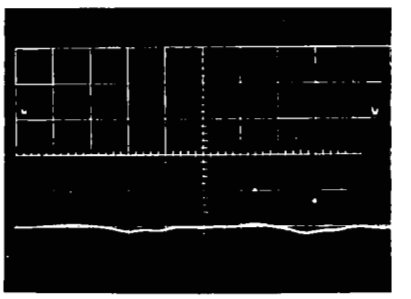

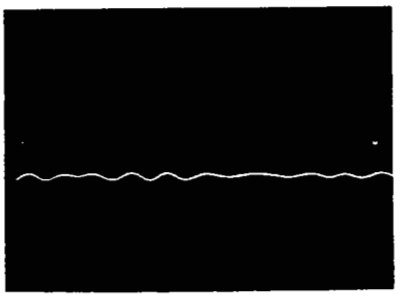

dc force plus 300 cps component

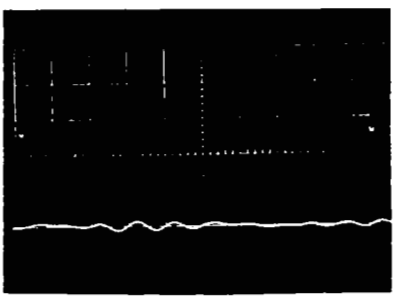

Eccentricity: .006 inches toward bottom of alternator

Equivalent Load Condition: No load, 2.7 field amperes

Location: O.D.E. bearing

RPM: 3000

Force Scale: 10 pounds per centimeter radial or vertical

Top of Alternator

left side of alternator

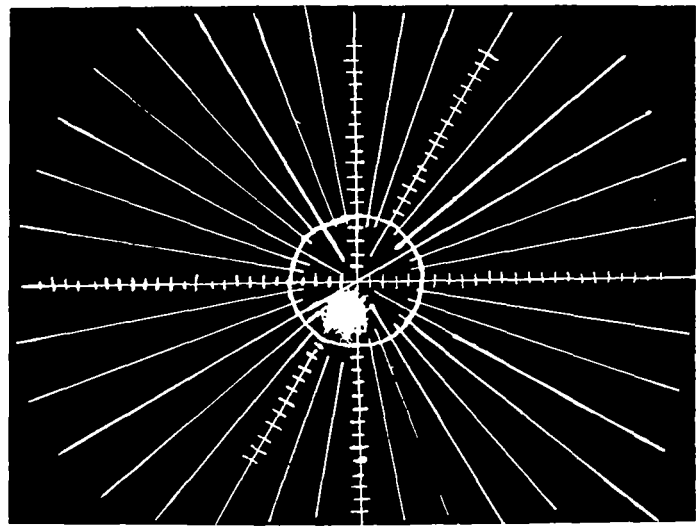

+Y

+X

Polar Plot of Bearing Force

(Unfiltered)

SECTION XI

ECCENTRICITY MEASUREMENTS

The eccentricity of the rotor with respect to the stator was varied by changing from one to another set of specially made bearing housings. These bearing housings had their bores ground eccentric to their OD's by .000", .002", .004", and .006". Even though these housings were made quite accurately, tolerance stack-up in the various parts resulted in eccentricities differing from those desired.

The actual eccentricity of rotor to stator was determined by measuring the air gap between rotor and stator at each end of the alternator. The rotor (see Figure 23) had a "windage" shield or disc at each end of the poles that has the same OD as the rotor. A specially modified taper gage was inserted between this disc and the bore of the stator (at a stator tooth) to measure the gap. This was done at four equally spaced locations around the bore. The differences in the gaps indicated rotor displacement in the "X" and "Y" directions. The X and Y displacements were combined vectorially to determine the total displacement and the ratio of X and Y displacements determined the direction.

The results of these measurements are shown in Figure 24.

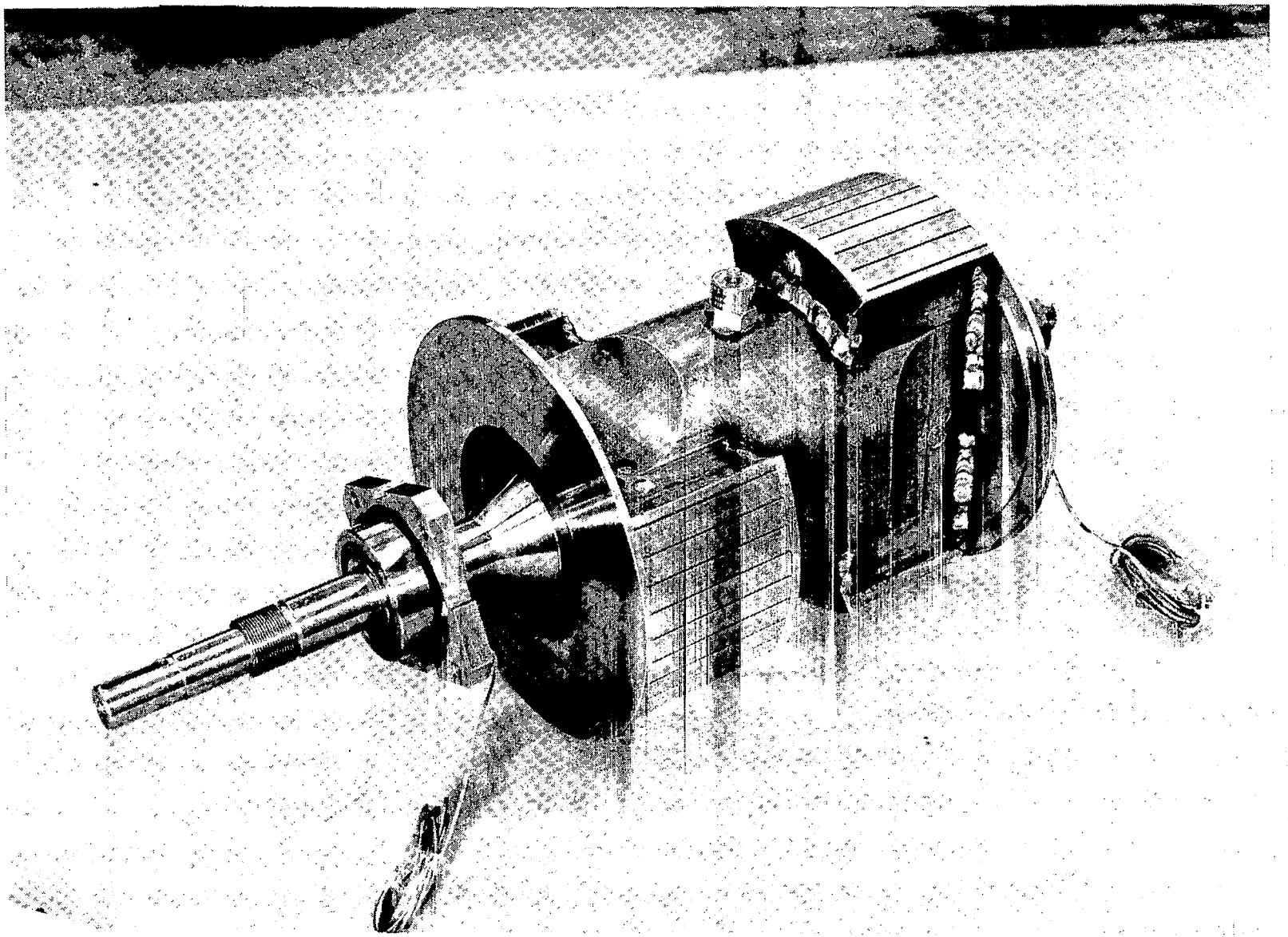

ARP BEARING FORCE TEST ROTOR

FIGURE 23

Measured Rotor Eccentricity As Viewed From The Opposite Drive End

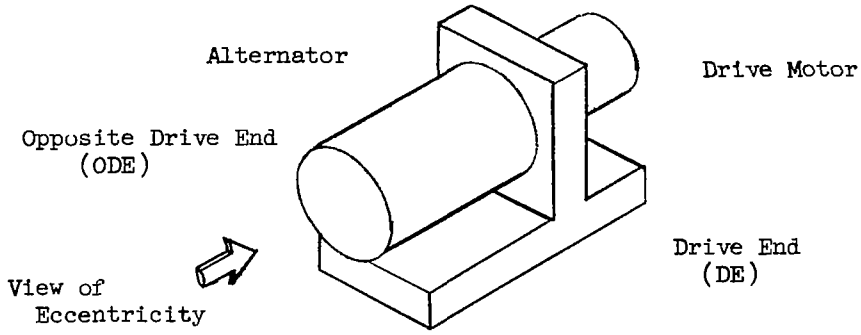

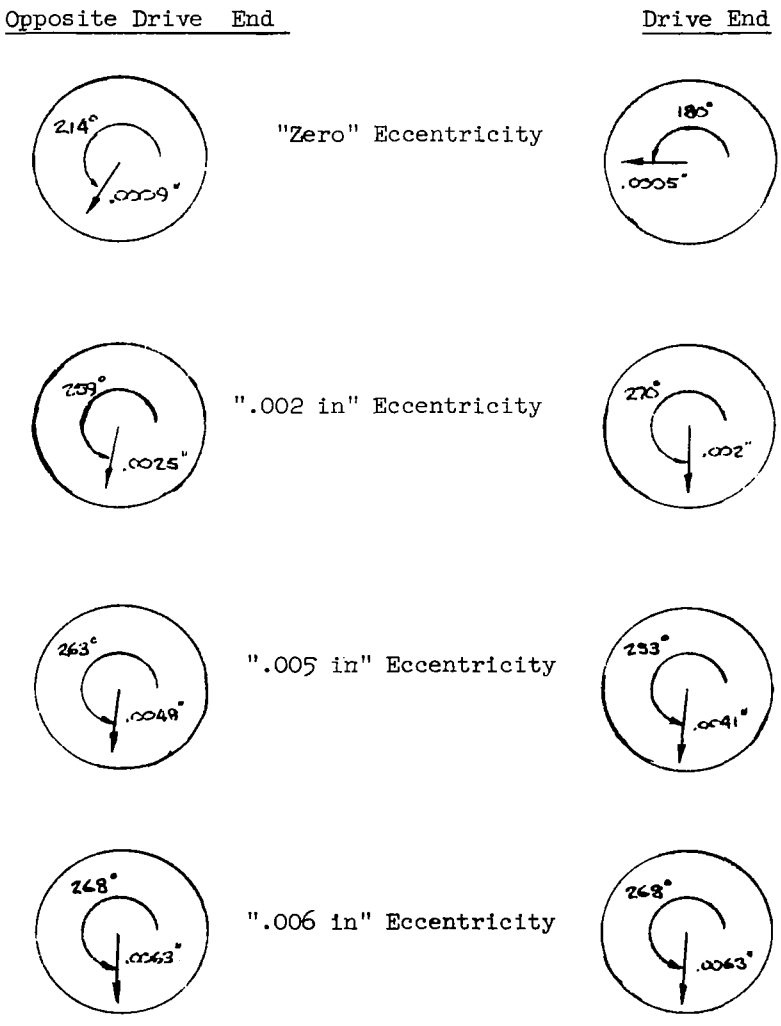

Figure 24

SECTION XII

TRANSDUCER DESIGN AND CALIBRATION

It was decided early in the program that the forces imposed on the bearings of the Brayton Cycle alternator would be determined by measuring the bearing reactions. Special end shields were designed which supported each bearing housing (and, consequently, the rotor) on four thin arms. These arms were instrumented with strain gages. The arms were spaced at 90^{o} intervals and were arranged to be sensitive to the "X" (horizontal) and "Y" (vertical) components of force exerted by the bearing housing on the alternator stator. Figures 25, 26 and 27 show the special end shields with the transducer arms both separately and as installed in the alternator.

One goal in the design of the force measuring system was to have a simple and clean system with inherently good accuracy and freedom from various troubles. The gages and bridge circuits were laid out to be self-canceling and self-compensating for most predictable sources of error. Conventional foil gages were used rather than semi-conductor gages to escape the temperature dependent properties of gage factor and linearity of the latter. A schematic of the gage arrangement is shown below:

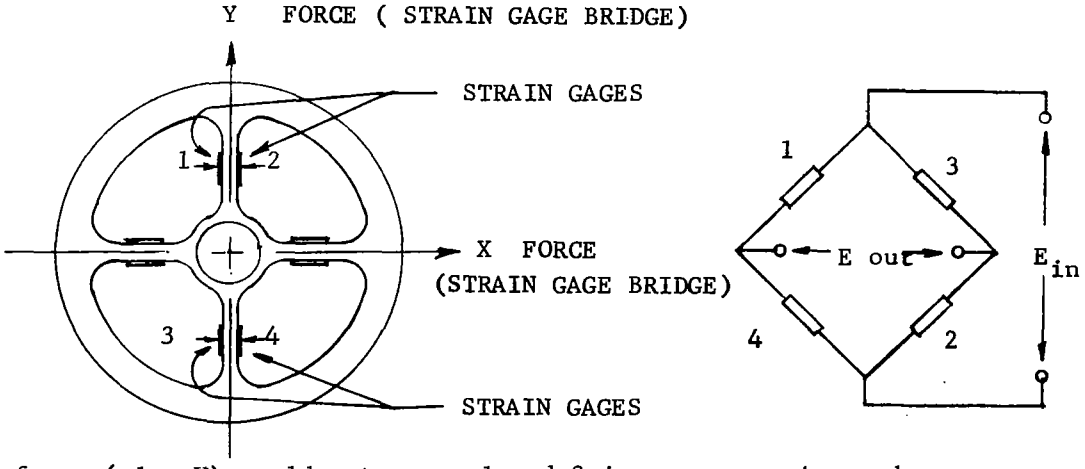

An upward force (plus Y) would put gages 1 and 2 in a compression and gages 3 and 4 in tension allowing maximum output with a four active arm bridge.

The transducer arms were proportioned and arranged as shown below:

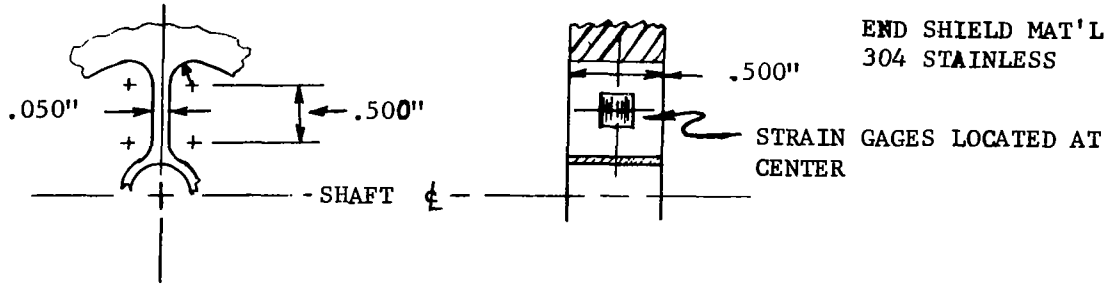

These arms are very stiff in the axial direction to withstand the thrust forces due to bearing axial preload. The gages are relatively insensitive to axial forces since the gages are mounted on the neutral axis of the transducer for bending in that direction.

The .050 thickness is great enough compared to the .5 in. length that the transducers act like stiff columns and there is no danger of buckling from compression loads.

The arms are not stiff for bending occurring in the plane of the end shield but the gages are arranged so that these strains tend to cancel. If the arm of the Y axis containing gages 1 and 2 were bent, the strain in gage 1 would be cancelled by the strain of opposite sign in gage 2 because they are in diagonally opposite legs of the bridge.

Since gages 1 and 2 are physically removed from gages 3 and 4, there was some possibility of their seeing slightly different temperatures. A four active arm bridge with all four arms at the same temperature is self-temperature compensating. The temperatures of the transducer arms were stabilized and equalized by passing water through tubes located at each end of the arms. The intent of the water flow was not to cool the arms but to overcome, by brute force, any temperature differences resulting from differences in heat flow in each arm. These tubes were fed in parallel from a header (a copper doughnut) that can be seen in Figure 27. Water was also passed through a loop of tubing on the face of each bearing housing to remove bearing losses.

The strain gages, which can be clearly seen in the close up of the transducer arm in Figure 28, are actually a double or "sandwich" gage. Two identical gages are placed one on top of the other and wired in series in such a way that any voltage induced in one gage by stray magnetic flux is cancelled by the voltage induced in the other gage.

Expected forces exerted at each bearing ranged from zero to 60 pounds and the transducer system was designed around these figures. The actual forces measured were much less than this but the system worked well enough that this did not prove to be a problem. Tektronix "Q Unit" strain gage amplifiers were used because of their extremely high output and their adaptability to oscilloscope display. The sensitivity of the "Q Unit" is such that a scope beam deflection of one centimeter results for 2.5 μ strain (2.5×10^6 in/in.) in each strain gage. This relates to the load in the transducer arms as follows:

$$\text{Strain} = \frac{\text{Stress}}{\text{Modulus of Elasticity}} = \frac{\text{Force/Area}}{E}$$

$$\text{area per force component} = \text{2 arm x .05 thk x .5 deep}$$

$$\text{area} = .05 \text{ in.}^2$$

$$\text{for a force of 10 lb., strain} = \frac{10 \text{ lb}/.05 \text{ in.}^2}{29 \times 10^6 \text{ lb/in}^2} = 6.9 \times 10^{-6} \text{ in/in.}$$

beam deflection for 10 lb. force per bearing:

$$\text{deflection} = \frac{1 \text{ cm}}{2.5 \times 10^{-6} \text{ in/in.}} \times 6.9 \times 10^{-6} \text{ in/in.} = \underline{2.76} \text{ cm/10 lb}$$

or 3.52 lb/cm

(The system was later used at a setting of 5 pounds per centimeter to make the data more readable).

The stress level in the arms with a force on the bearing of 10 lbs. is:

$$\text{stress} = \frac{10 \text{ lb.}}{.05 \text{ in.}} = 200 \text{ psi}$$

The transducers were calibrated by using the device pictured in Figures 29 and 30. This dummy frame, shaft and the test end shields were set up in a tensile testing machine. Loads were applied to the axial center of the shaft in steps of 10 lbs. per end from zero to 100 lbs. per end. The holes around the periphery of the frame allowed the load to be applied in line with the transducers and in 30° increments between the axes of the transducers. The system resolved the "X" and "Y" components of off axis forces well enough that the maximum difference between indicated and measured force was 3 lbs. at 100 lbs. with a maximum 3° error in direction of indicated force. The Q Unit settings used to get a calibrated output are shown in the table below.

Set Q Unit sensitivity at 200$\mu\epsilon$/division (cm)
Press "Calibrate" button
Adjust scope beam deflection to following values to get indicated force calibrations

Drive End	X axis	2.64 cm
	Y axis	2.70 cm

Opposite Drive End	X axis	3.04 cm
	Y axis	3.04 cm

Resulting Force Calibrations (DE & ODE)

Sensitivity Setting	10	20	50	100	200	500
Force (lb) per cm of beam deflection	5	10	25	50	100	250

Although the transducer system worked very well for static loads, the system was required to perform dynamically. The rotor and its transducers comprised a mass-spring system which had resonant frequencies. The ratio of force transmitted through the spring to force applied (transmissibility) to the mass is a function of the ratio of exciting frequency to natural frequency of the system as shown in the sketch below.

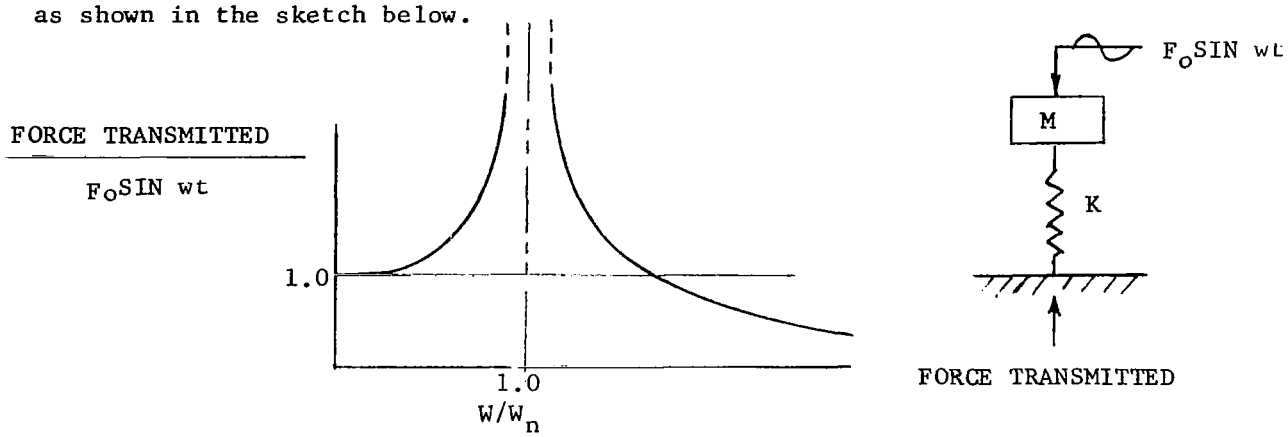

The transmissibility of the system was determined experimentally and the results are shown in Figure 31. An accelerometer was mounted at the center of the rotor as pictured in Figure 32 and the assembly of rotor and stator was placed in the vibration test fixture shown in Figure 33. Other accelerometers were placed on the stator in line with the transducers. The output of the rotor accelerometer divided by the average of the output of the stator accelerometers at each end of the alternator was taken as the transmissibility of the system.

The translational resonant frequency of the rotor turned out to be about 400 cps, very close to the pole frequency. The principle contributor to the system having this resonant frequency was the ball bearing. The transducers had a spring rate of about 2.4×10^6 lb/in. while the bearing had calculated radial spring constants in the range of 4×10^5 lb/in. to 8×10^5 lb/in. depending on radial load, axial load and rotational speed. Since these two "springs" (the bearing and the transducer arms) were in series, changing the stiffness of the transducer arms could not have changed the resonant frequency of the rotor system by any appreciable amount. The axial bearing load of 80 lbs. was chosen as a compromise between bearing capacity limitations, heating, and resonant frequency.

Section XIII presents some of the effects of these resonant frequencies and the resultant changes in test procedure.

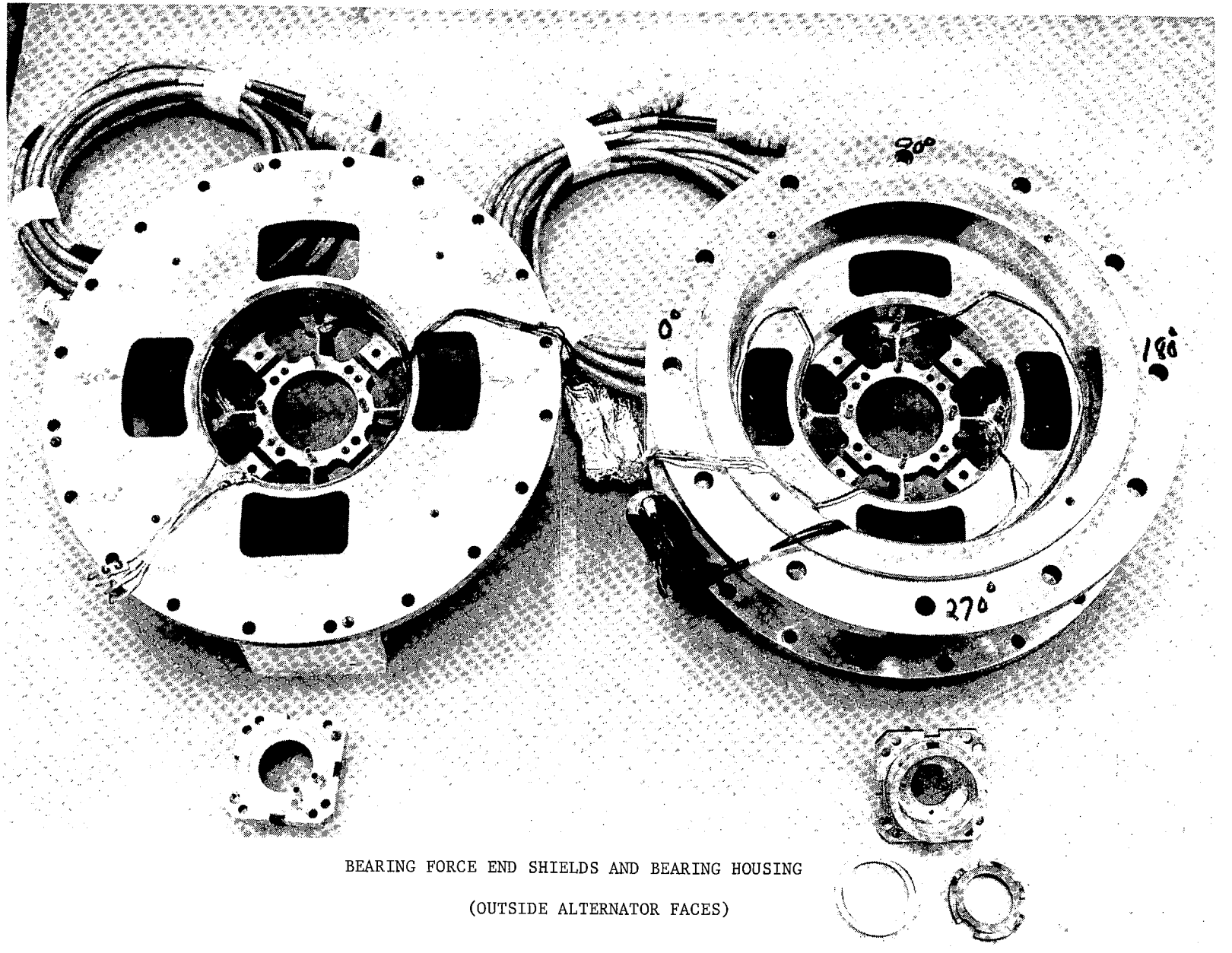

BEARING FORCE END SHIELDS AND BEARING HOUSING

(OUTSIDE ALTERNATOR FACES)

FIGURE 25

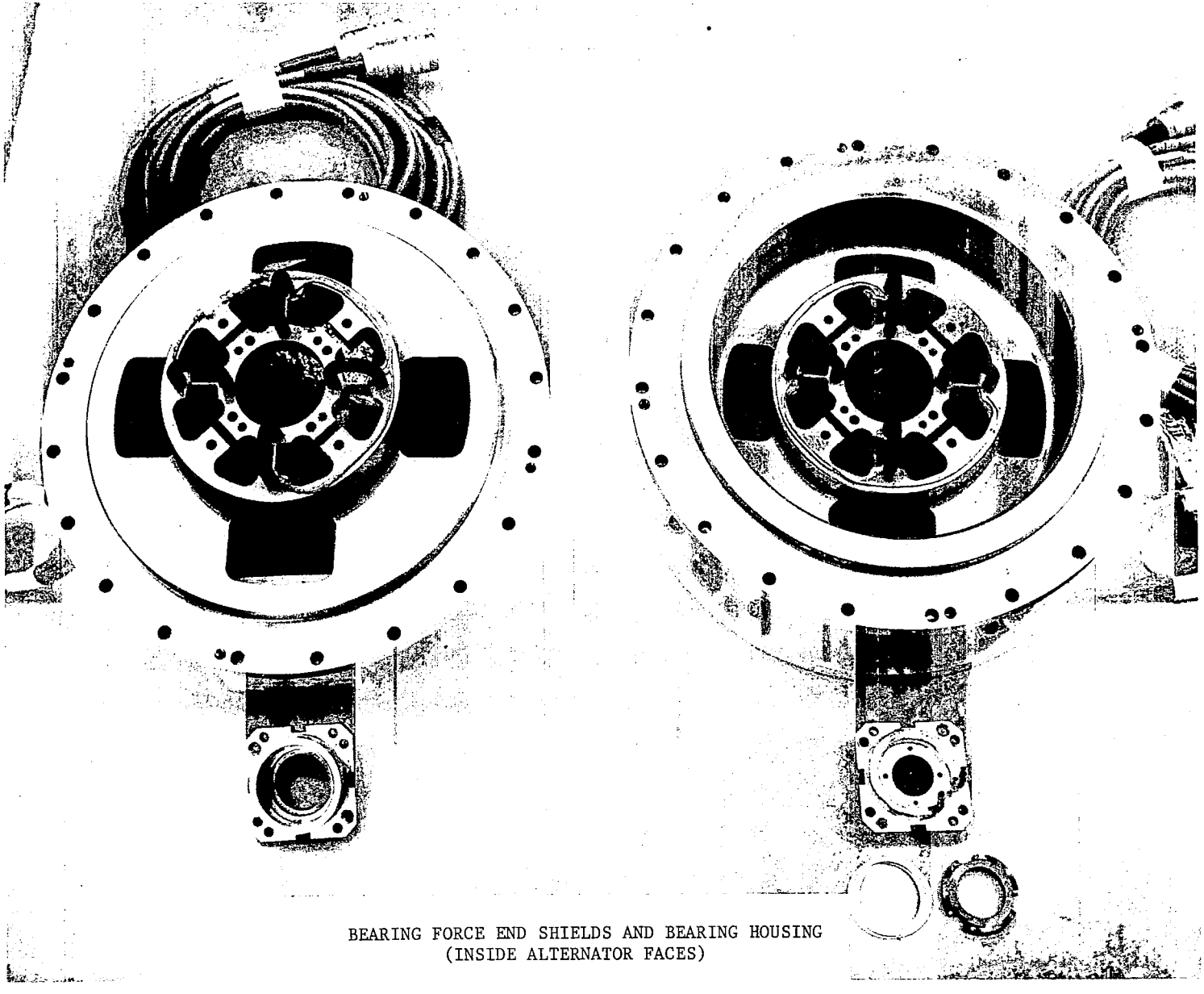

BEARING FORCE END SHIELDS AND BEARING HOUSING
(INSIDE ALTERNATOR FACES)

FIGURE 26

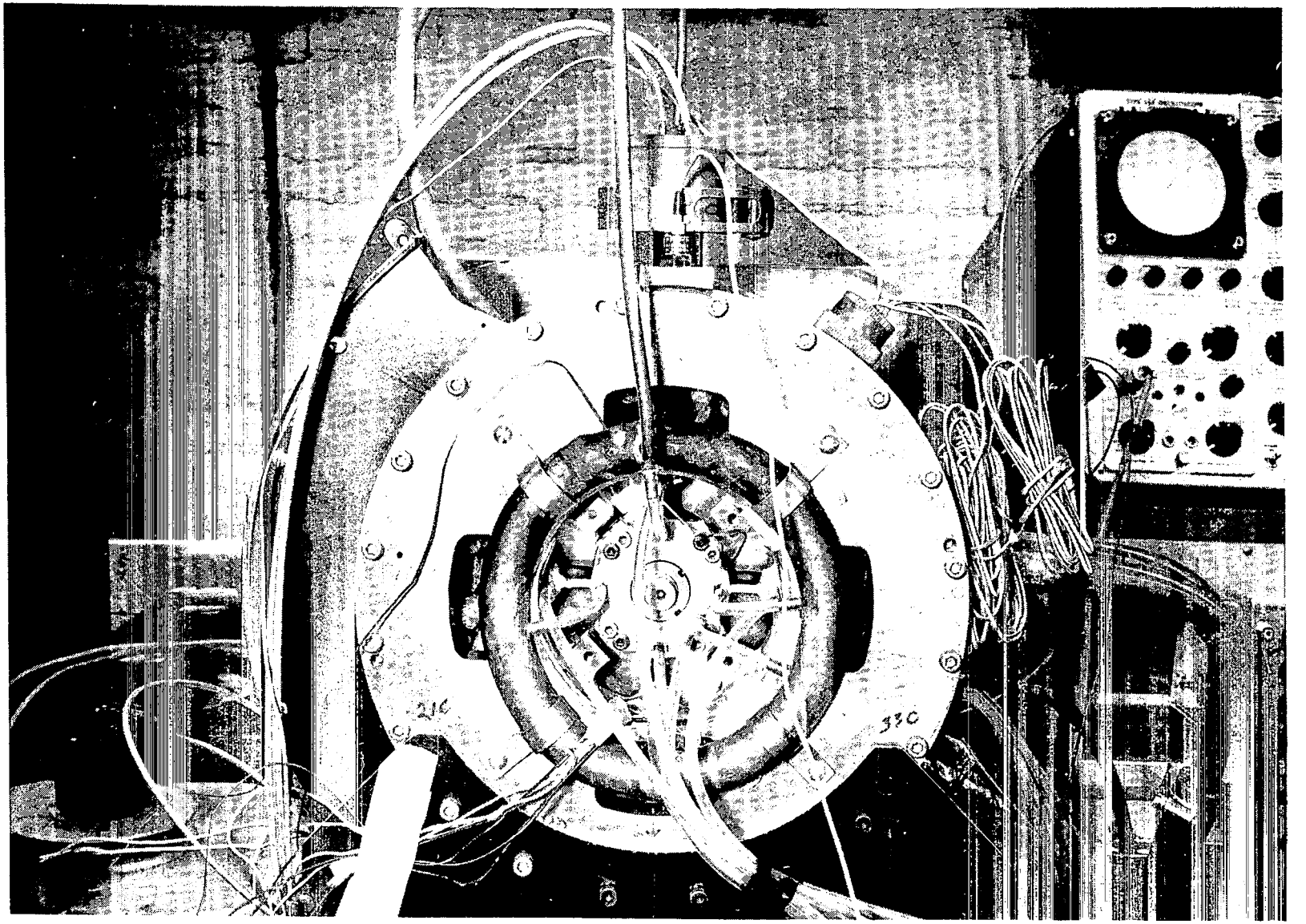

BEARING FORCE TESTS A.D.E. OF ALTERNATOR

FIGURE 27

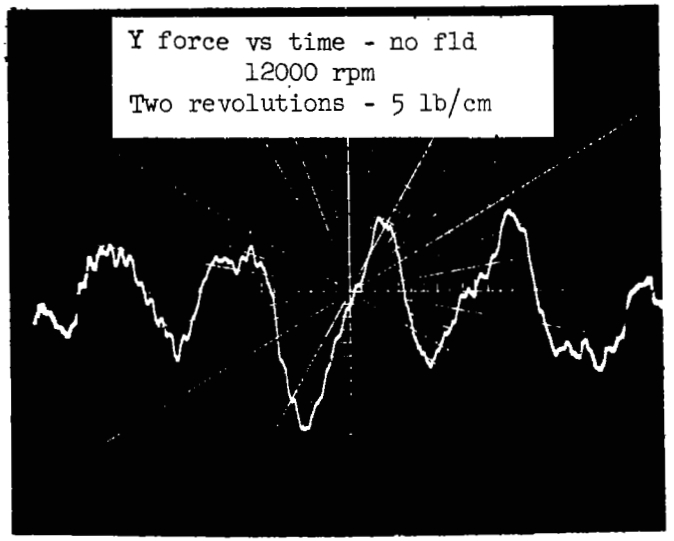
Y force vs time - no fld
12000 rpm
Two revolutions - 5 lb/cm

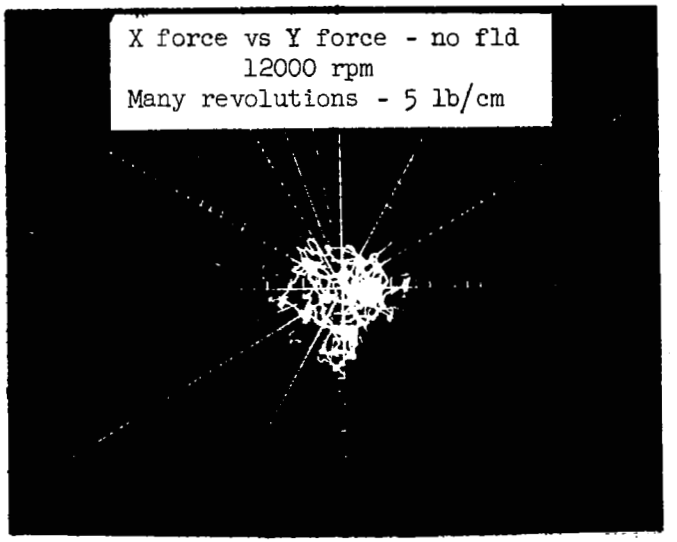
X force vs Y force - no fld
12000 rpm
Many revolutions - 5 lb/cm

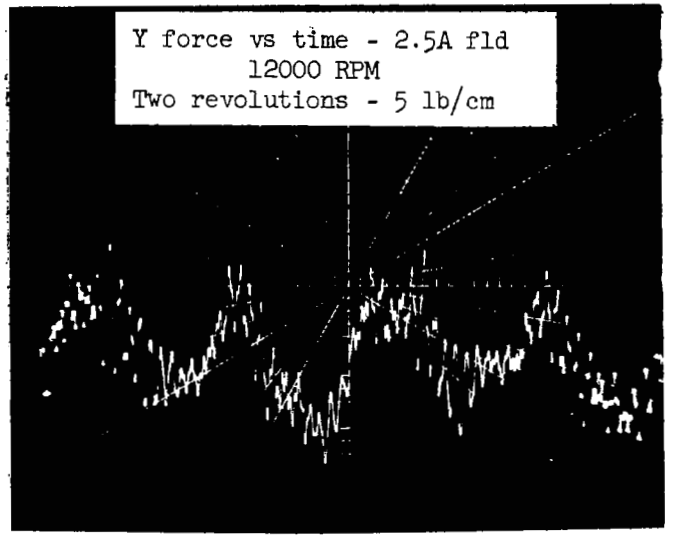
Y force vs time - 2.5A fld
12000 RPM
Two revolutions - 5 lb/cm

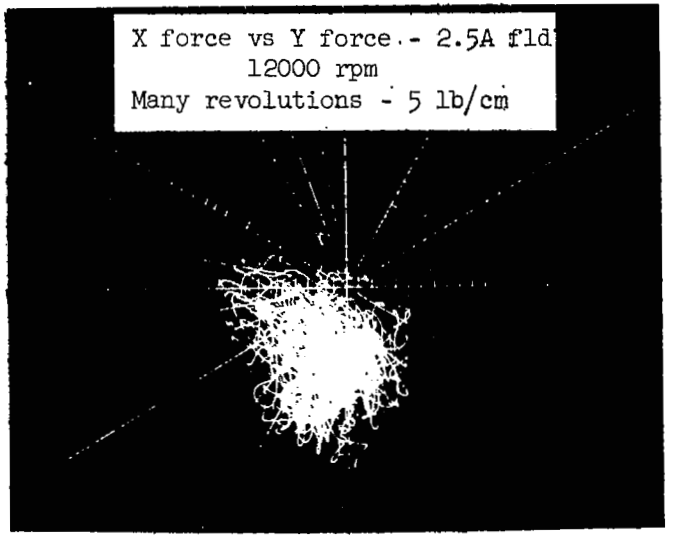
X force vs Y force - 2.5A fld
12000 rpm
Many revolutions - 5 lb/cm

FIGURE 33

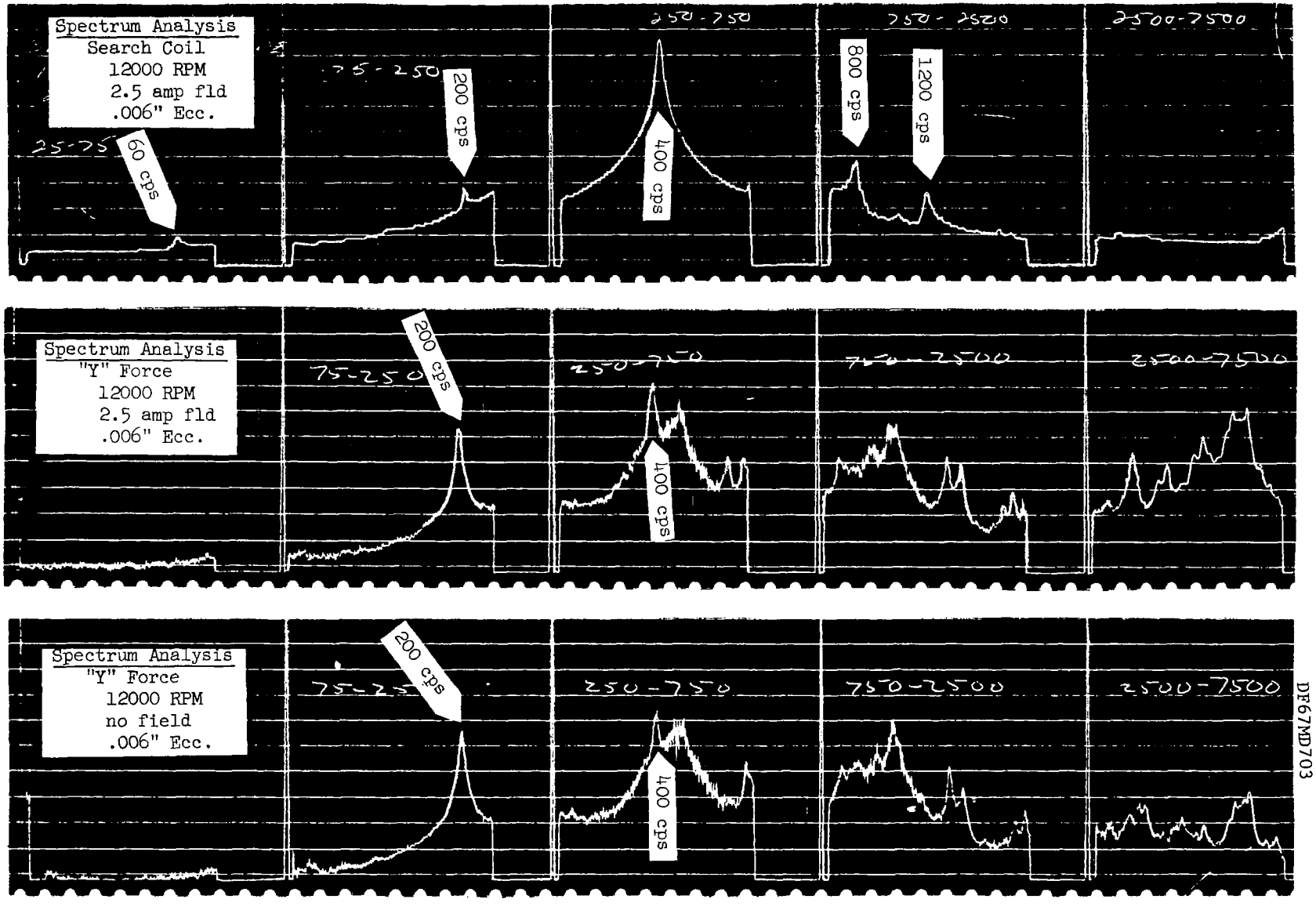

FIGURE 34

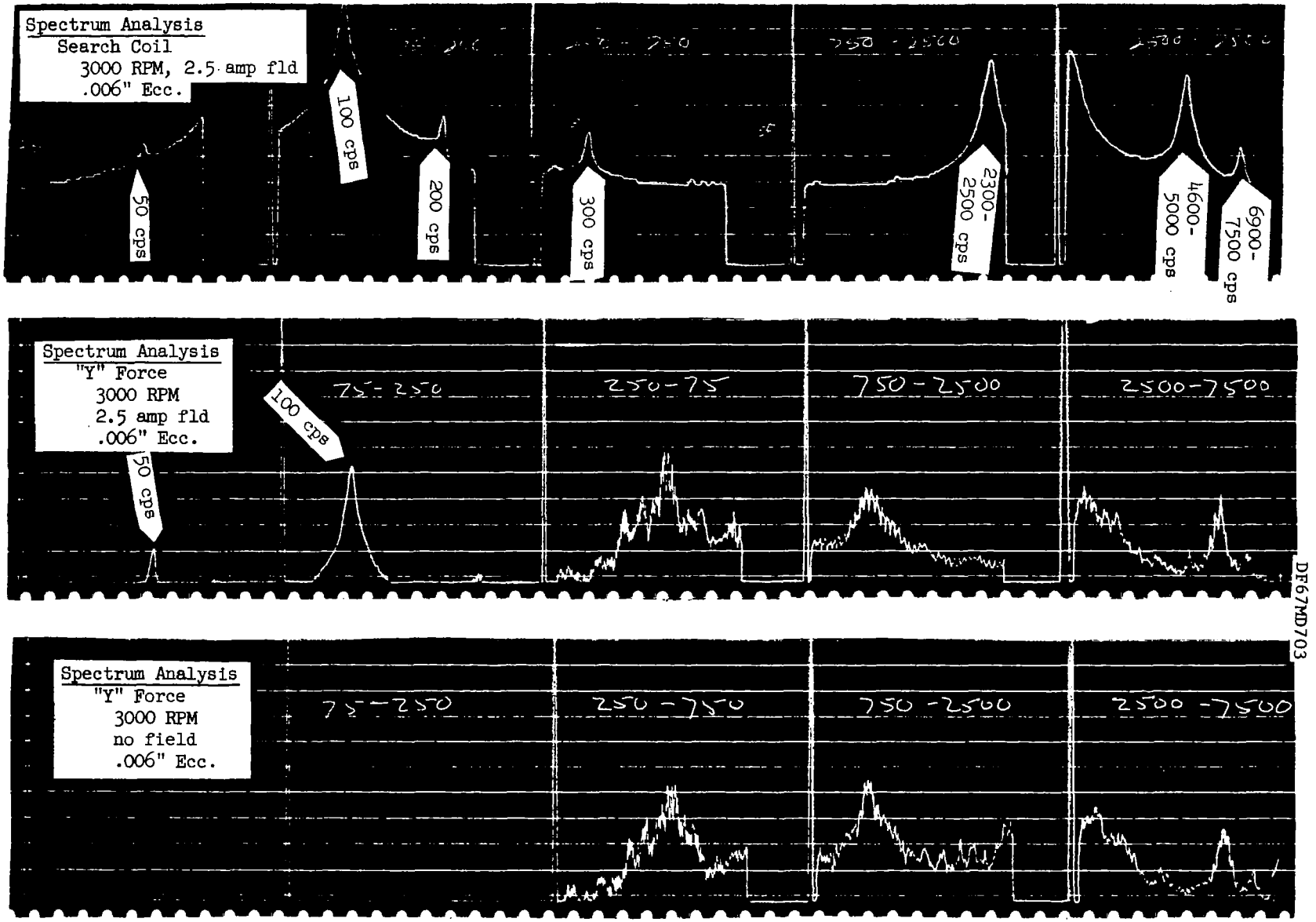

FIGURE 35

SECTION XIV

Analytical and Experimental Correlation

Referring air gap force to bearings.

The unbalanced magnetic force occurring in the air gap can be reflected to the bearings by moment summation. Consider the following diagram of the rotor:

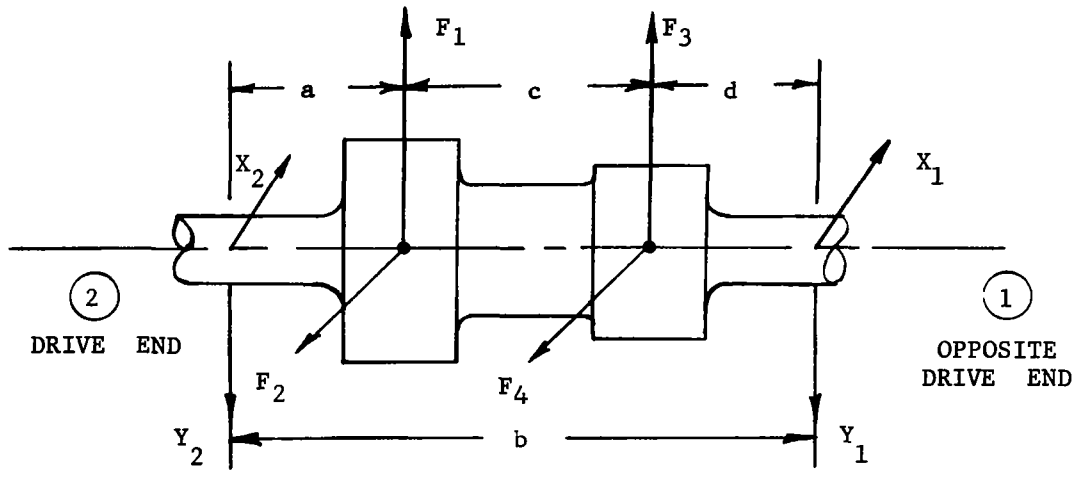

Taking moments about the drive end bearing yields the following reactions at the opposite drive end bearing:

$$Y_1 = \frac{a}{b} F_1 + \frac{(a+c)}{b} F_3$$

$$X_1 = \frac{a}{b} F_2 + \frac{(a+c)}{b} F_4$$

A similar procedure gives the reactions at the drive end.

$$Y_2 = \frac{d}{b} F_3 + \frac{(c+d)}{b} F_1$$

$$X_2 = \frac{d}{b} F_4 + \frac{(c+d)}{b} F_2$$

Since the eccentricity angle, B, was zero for the experimental results, the equations for no load as given in Section VII reduce to the following:

$$F_1 = 7.6 + 6.16 \cos 2 wt$$

$$F_2 = 6.16 \sin 2 wt$$

The forces F_3 and F_4 are displaced 90 mechanical degrees from F_1 and F_2 due to rotor construction and thus become:

$$F_3 = 7.6 - 6.16 \cos 2 wt$$

$$F_4 = - 6.16 \sin 2 wt$$

The reactions can now be determined and thus the resultant bearing force and its angle are as follows:

$$Z_1 = \sqrt{Y_1^2 + X_1^2}$$

$$\theta = \text{Arc Tan } \frac{X_1}{Y_1}$$

$$Z_2 = \sqrt{Y_2^2 + X_2^2}$$

$$\theta_2 = \text{Arc Tan } \frac{X_2}{Y_2}$$

The above equations were programmed on the General Electric time sharing computer and resulted in the Lissajous pattern shown in Figure 36. The maximum value of the force is about 10.6 pounds which when multiplied by 3 to reflect a 0.006" eccentricity yields the 32 pounds of Table IV. A similar procedure was used to determine the 15 KVA, .8 PF case and the single phase loading case.

DIFFERENTIAL SATURATION

Saturation occurring in either the stator or rotor teeth will result in a lower magnetic unbalance force than the unsaturated case for a given field excitation. The saturation ampere turns are normally considered as an increase in air gap thus giving decreased flux density and consequently force. Table I of Section III shows the effect of saturation on the full load case for the condition where the saturation is identical for opposing rotor poles. However, for an eccentric rotor the flux density at one rotor pole is greater than at the opposing pole due to different air gap lengths, andthis gives rise to a differential saturation effect, which further reduces the force. As a means of analyzing this effect, the no load case at zero speed was investigated in some detail. The zero speed no load case was chosen since it eliminates the effects of stator circuits and amortisseur windings, as well as armature reaction. Since the inclusion of differential saturation in the established computer programs would entail considerable reprogramming, a small time sharing computer program was written that produced only the total force magnitude at one rotor position. This was quite adequate for the purpose at hand and resulted in the following data:

NO LOAD - ZERO SPEED

0.006" Eccentricity

Condition	Maximum F_y Force (pounds)
Unsaturated	84.0
Differential Saturation	65.7
Differential Saturation + Different Carter's Coefficients	61.5

Note that the unsaturated force compares very well with the maximum F_y force of Figure 5 after eliminating the circuit effect and ratioing from 0.002" to 0.006" eccentricity. The comparison is good because very little saturation occurs at rated no load voltage. Differential saturation shows a very marked effect on the force and some reduction also occurs due to different Carter's coefficients (slot fringing) arising from the different air gap lengths. The ratio of 61.5/84.0 was used to arrive at the 11.7 pound figure given in Table IV. The computer program could have been expanded to include armature reaction, but to avoid this effort the above ratio was also applied to the load condition and probably represents a conservative approach due to the somewhat greater saturation under load conditions.

BRAYTON CYCLE ALTERNATOR
CALCULATED LISSAJOUS PATTERN
NO LOAD - OPPOSITE DRIVE END BEARING

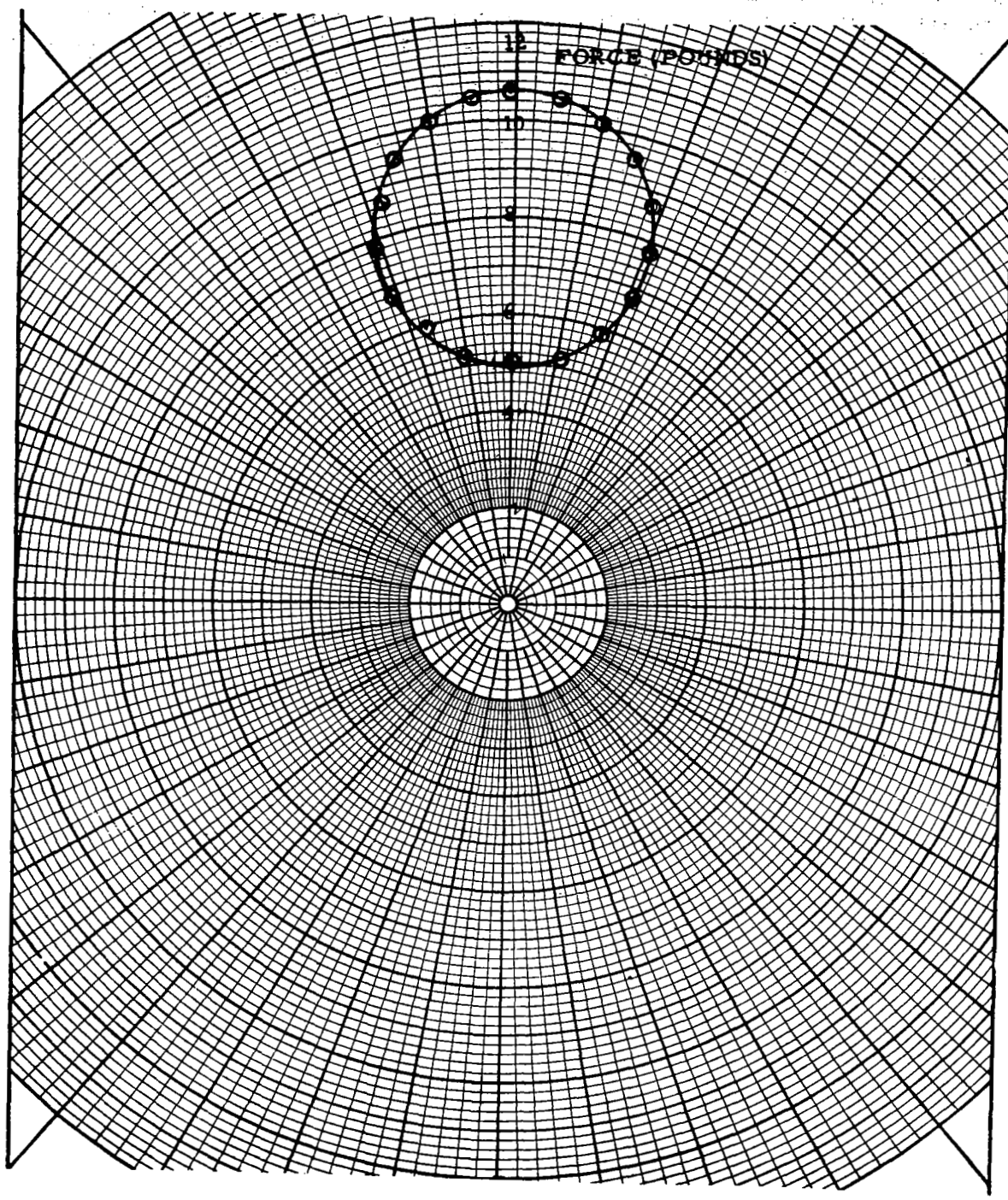

FIGURE 36

SECTION XV

REFERENCES

1. "Alternating Current Machinery," By L.V.Bewley, The Macmillan Company, New York, 1949.

2. "The Nature of Polyphase Induction-Machines," By Philip L. Alger, John Wiley and Sons, Inc., New York, 1951.

3. "Synchronous Machines, " By Charles Concordia, John Wiley and Sons., Inc., New York , 1951.

4. "Electric Machinery," By A.E.Fitzgerald and C. Kingsley, McGraw-Hill Book Company, Inc., New York, 2nd Edition, 1961.

5. "The Calculation of Harmonics Due to Slotting in the Flux Density Waveform in Dynamo Electric Machines," By Dr. E.M.Freeman, IEE Paper #523U, June 1962.

6. "Unbalanced Magnetic Pull in Induction Motors with Eccentric Rotors," By A. Covo, AIEE Paper #54-413, December 1954.

7. " A Guide to Fortran Programming," By Daniel D. McCracken, John Wiley and Sons, Inc., New York,1961.

8. "Mechanical Engineers' Handbook," Edited by Lionel S. Marks, McGraw-Hill Book Company, Inc., New York, 1951.

9. "Transverse Magnetic-Attraction in Rotating Machines," By L. Centurioni, Ansaldo-San Giorgio Bulletin, October, 1962.

NASA-Langley, 1970 — 3 E-5152